

Design and Synthesis of Dendrimers for Multipurpose Tasks

by

Rami Hourani

October 2009

Department of Chemistry, McGill University

Montréal, Québec, Canada

A thesis submitted to McGill University in partial fulfilment of the requirements of the degree of Doctor of Philosophy

© Rami Hourani, 2009

*This thesis is dedicated to my Parents
Fayez Hourani and Farha Al-Mutlaq*

Acknowledgements

I would like to thank my supervisor, Dr. Ashok Kakkar, for his help, guidance, and mentorship throughout the years. He has been a great advisor, supporter, and mostly a friend. I thank him from the bottom of my heart for his understanding, trust, and encouragement through the difficult period of time I went through while doing my Ph.D. Without his trust and support, I would never be writing these very lines.

I am greatly thankful to Dr. M. A. Whitehead for all his help and guidance through the theoretical work included in this thesis. He has been indeed a great supporter throughout all these years. I thank him for the coffee, and tea time in the middle of hard-working days, and sharing all his incredible knowledge with me. I thank him for not only teaching me science, but also about life in general.

Doing a Ph.D. requires hard work and commitment. During that time a Ph.D. candidate needs support, help, some fun time and friendship. I have been lucky to work with amazing people throughout these years. They have been there for me through the bad and good times. I thank all my previous and current colleagues at Dr. Kakkar's lab for all the help, love, and fun they provided. I would like to thank specifically Jessica Douglas, Anjali Sharma, and Gregory Franc for their help with my chemistry, through sharing ideas, remaking of some compounds. I would like to thank Annie Castonguay for translating my abstract, and taking over responsibilities in the lab. For Kunal Khanna, Liz Ladd, and Rishi Sharma, thank you for all your help and fun times we have spent together. I also would like to thank all previous students I worked with; Olivier Bourrier, Tatiana Vassilieff, Xiaojun Liu, Cecile Malardier-Jugroot, Roger Gaudeault, Olivier Rolland, Renaud Gillet, Arnaud Vieyres Tina Lam, Ye Tian, Tyler Ye and others. Special thanks go to Florence Quist and Thomas Lazzara, for their unique and unconditional support, help, and love. I would also like to thank Dr. Aradhana Bachher, for her direct and indirect help and support.

I gratefully acknowledge the assistance provided by the following contributors: Dr. Nadim Saadeh for mass and MALDI-TOF spectroscopy analysis, Dr. Antisar Hlil for MALDI-TOF analysis, Fred Morin for NMR analysis, Petr Fiurasek for UV-Vis, and Fluorescence measurements, Katerina Krumova and Matthew Hassler for their help, and Dr. Dusica Maysinger, and Manasi Jain, for their help, sharing ideas, and hard work in carrying out the pharmacological studies through the collaboration process.

I would like to thank NSERC, FQRNT, CSACS, Sigma Xi, Chemistry Department, and McGill University for all the financial assistance, and in particular I thank FQRNT for granting me postgraduate scholarship for my Ph.D. and a postdoc fellowship for the coming two years.

Special thanks go to the incredible people behind the scenes in the chemistry department, Sandra, Karen, Alison, Fay, and Chantal. They make the life of a graduate student easier. I thank them from the bottom of my heart. I would like to extend this gratitude to Chantal Marotte for going over the call of duty in helping me and other grad students, and for her friendship.

I would like to thank all my friends outside the department of chemistry and McGill University in general for all their support and love. Without sharing those moments outside the lab, I could not have pulled through. All my friends have touched my life in a way or another, and I thank them for all the love and encouragement they have given me. I thank Zeid Khasawneh, Yazan Tamimi, Khaled Abu Sheikha, and specially my long-time friend and supporter Ghassan Abidi, for all the great support and fun time they offered.

The unconditional love and blind support of the most important people in my life, my family, have been and will always be the main drive force in my life. I am lucky to have the most wonderful family in the world. I thank my brothers and sisters Rad, Dema, Odi, Rawan, and Razan Hourani for all they have given me. Finally, I thank my parents Fayez Hourani, Farha Al-Mutlaq for their love, devotion, and hard work for me and my siblings. They have always made me proud, and been my motivation for success in this life. I hope to make them proud every moment of my life.

Abstract

Monodisperse macromolecules with tailored architecture constitute the key to designing efficient and smart nanomaterials. They offer real potential to achieve this goal, and one of the earlier challenges faced by this novel class of macromolecules has been addressed by the evolutions in their synthetic methodologies. In this thesis, i) inorganic, organometallic, and organic synthetic routes are employed to construct mono- and bi-functional dendrimers; and ii) a detailed study including an evaluation of their structure-property relationships using a combination of experiment with theoretical calculations, and their applications in molecular encapsulations and drug delivery, are reported. Geometric characterization of 3,5-dihydroxybenzyl alcohol (DHBA)-based dendrimers, using aminosilanes as linkers was achieved using molecular mechanics MM+ method and the PM3 semi-empirical molecular orbital theory. Optimization of DHBA-based dendrimer generations 1–5 (DG1–5) suggested that DG1–3 have a relatively open structure with no internal spaces of any particular size or shape, while DG4 and 5 assume a more globular structure with well-defined internal cavities. Encapsulation of disperse red 1 (DR1) into the cavities of these dimethylsilyl linked DHBA-based dendrimers led to a blue shift in the λ_{max} of DR1, and transmission electron microscopy (TEM) showed a rectangular shape of dendritic aggregates containing DR1. Catalytic activity of (COD)RhCl(PPh₂(CH₂)₃OH) encapsulated in dendritic aggregates of generations 1–4, indicated a significant decrease in catalytic conversion of 1-decene to decane in dendrimer generation 4 upon going from a concentration below critical aggregation concentration (*cac*) to above *cac*. Subsequently, a simple divergent methodology to synthesize 1,3,5-triethynylbenzene (TEB)-based dendrimers, using amino stannanes as linkers, was developed. A theoretical evaluation of their structure suggested that they evolve into a turbine shape with benzene rings arranged in a fashion to create sandwich type cavities. Our results show that the inorganic entities (Me₃Sn) in these dendrimers act as electron donors, and can significantly influence their photophysical properties. The versatility of these

dendrimers in introducing transition metal centers directly into the backbone is demonstrated by substitution of dimethyltin links with square planar platinum centers, upon reaction with $(^n\text{Bu}_3\text{P})_2\text{PtCl}_2$. This eliminates the need to add a catalyst in the synthesis of such organometallic dendrimers. In an attempt to streamline the synthesis of dendrimers that incorporate organic backbones, we report the synthesis of molecular building blocks that contain azide and alkyne terminated functionalities, suitable for carrying out Cu^{I} catalyzed cycloaddition between alkynes and azides (CuAAC) “click” reaction. We show the versatility of these building blocks in constructing dendritic frameworks with 4, 6 or 12 peripheral acetylene groups, using either the convergent or divergent methodologies. Using the same protocol, we devised an efficient iterative methodology using CuAAC “click” chemistry to construct bifunctional dendrimers which combine imaging and therapeutic functions, and can specifically target lipid droplets. BODIPY, a tracer dye, and the drug, α -lipoic acid, are covalently linked in these dendrimers. A detailed evaluation of subcellular distribution of these dendrimers clearly demonstrates that i) they do not induce marked metabolic abnormalities in human liver cells; ii) the rate and extent of internalization of dendrimers containing either only the BODIPY or both BODIPY and α -lipoic acid, are different from the free dye and drug.

Résumé

Les macromolécules hyperbranchées et monodisperses possédant une architecture modulée constituent la clé au design de nanomatériaux efficaces et intelligents. Elles offrent un réel potentiel pour atteindre ce but, et un des défis précédemment rencontrés par cette nouvelle classe de macromolécules a été adressé par l'évolution de leurs méthodologies synthétiques. Dans cette thèse, i) des routes synthétiques inorganiques, organométalliques et organiques sont employées pour construire des dendrimères mono-et bi-fonctionnels; et ii) une étude détaillée incluant une évaluation de leurs relations structure-propriété, utilisant une combinaison d'expériences incluant des calculs théoriques, ainsi que leurs applications en encapsulation moléculaire et en libération de médicaments, sont rapportées. La caractérisation géométrique de dendrimères composés d'unités d'alcool 3,5-dihydroxybenzyle (DHBA), pontées par des aminosilanes a été accomplie utilisant la méthode de mécanique moléculaire MM+ ainsi que la théorie des orbitales moléculaires semi-empirique PM3. L'optimisation des dendrimères DHBA de génération 1-5 (DG1-5) a suggéré que DG1-3 possèdent une structure relativement ouverte sans espaces internes de grandeur ou de forme particulière, tandis que DG4 et 5 possèdent une structure plus globulaire caractérisée par des cavités internes bien définies. L'encapsulation de *disperse red 1* (DR1) dans les cavités des dendrimères composés d'unités DHBA pontés par des diméthylsilyles a mené à un déplacement vers le bleu du λ_{\max} de DR1, et la microscopie électronique en transmission (TEM) a démontré une forme rectangulaire pour les agrégats dendritiques comprenant DR1. L'activité catalytique de (COD)RhCl(PPh₂(CH₂)₃OH encapsulé dans les agrégats dendritiques des générations 1-4, a indiqué une diminution significative dans la conversion catalytique de 1-décène à décane pour le dendrimère de génération 4 en partant d'une concentration sous celle de la concentration d'agrégation critique (*cac*) jusqu'à une concentration plus élevée que cette dernière. Subséquemment, une

simple méthodologie divergente pour synthétiser des dendrimères composés d'unités 1,3,5-triéthynylbenzene (TEB) pontées par des aminostannanes a été développée. Une évaluation théorique de leur structure a suggéré qu'ils évoluent en une forme turbine, les cycles benzènes étant arrangés de façon à créer des cavités de type sandwich. Nos résultats démontrent que les entités inorganiques (Me_3Sn) dans ces dendrimères agissent comme donneurs d'électrons, et peuvent influencer de façon significative leurs propriétés photophysiques. La versatilité de ces dendrimères pour l'introduction directe de centres métalliques dans la structure est démontrée par la substitution des liens Me_2Sn par des centres de platine plans carrés, lorsque réagis avec $(^n\text{Bu}_3\text{P})_2\text{PtCl}_2$. Ceci élimine le besoin d'ajouter un catalyseur dans la synthèse de tels dendrimères organométalliques. De façon à faciliter la synthèse de dendrimères possédant des structures organiques, nous rapportons la synthèse de blocks moléculaires comprenant des fonctionnalités terminales azides et alcynes, pouvant subir une réaction de cycloaddition "click" catalysée par le Cu^{I} (CuAAC). Nous démontrons la versatilité de ces blocks moléculaires dans la construction de structures dendritiques comprenant 4, 6 ou 12 groupes périphériques acétylènes, utilisant des méthodologies soit convergentes ou divergentes. Faisant usage du même protocole, nous avons créé une méthodologie itérative utilisant la chimie "click" CuAAC pour la construction de dendrimères bifonctionnels qui combinent des fonctions d'imagerie et des fonctions thérapeutiques, et qui peuvent viser spécifiquement des gouttes lipidiques. Le BODIPY, un colorant traceur, et un médicament, l'acide α -lipoïque, sont liés de façon covalente dans ces dendrimères. Une évaluation détaillée de la distribution sous-cellulaire de ces dendrimères démontre clairement que i) ils n'induisent pas d'anomalies métaboliques marquées dans les cellules de foie humain; et que ii) la vitesse et l'étendue de l'internalisation des dendrimères comprenant soit seulement le BODIPY ou bien le BODIPY et l'acide α -lipoïque, sont différentes de celles du colorant et du médicament libres.

Table of Contents

	Page
Preface	
Dedication	<i>ii</i>
Acknowledgements	<i>iii</i>
Abstract	<i>v</i>
Résumé	<i>vii</i>
Table of Contents	<i>ix</i>
List of Tables	<i>xiii</i>
List of Schemes	<i>xiv</i>
List of Figures	<i>xv</i>
List of Abbreviations and acronyms	<i>xix</i>
Contributions of Authors	<i>xxii</i>
Chapter 1: Introduction and Scope of Thesis	1
1.1 Dendritic polymers: an overview	2
1.2 Synthesis of dendrimers	6
1.3 Core-functionalized dendrimers	11
1.4 Encapsulation of Guests in the Internal Cavities	13
1.5 Functionalizing the periphery	19
1.5.1 Monofunctional dendrimers	20
1.5.2 Multifunctional dendrimers	25
1.6 Dendrimers containing heteroatoms and transition metal centers	30
1.7 Multiblock dendrimers	35
1.8 Dendrimers decorated with polymers	41
1.9 Dendronized Polymers	46
1.10 Summary and outlook	48
1.11 Scope of the thesis	49
	ix

1.12	References	50
Chapter 2: 3,5-Dihydroxybenzylalcohol Based Dendrimers: Structure		
Evaluation and Molecular Encapsulation in Generations 1-5		
		61
2.1	Introduction	62
2.2	Theoretical methods for the investigation of the structure of DHBA-based dendrimers	63
2.3.	Results and discussion	66
2.3.1	Shapes of dendrimer generations 1-5	67
2.3.2	Sizes of the dendrimer generations 1-5	68
2.3.3	Internal cavities of dendrimer generations 4 and 5	69
2.3.4	Encapsulation of DR1	70
2.3.5	Transmission electron microscopy (TEM) study of the encapsulation of DR1 into dendrimers	72
2.3.6	Encapsulation of active transition metal centers in dendritic aggregates	73
2.4	Conclusions	74
2.5	Experimental Section	75
2.5.1	General procedures	75
2.5.2	Materials	75
2.5.3	Inclusion of disperse red 1 in dendrimer generation 4 and 5 (DG4 and DG5)	76
2.5.4	Transmission electron microscopy (TEM) analysis	77
2.5.5	Dialysis experiments	77
2.5.6	Interaction of 3,5-dihydroxybenzyl alcohol (DHBA) with DR1	78
2.5.7	Inclusion of (COD)RhCl(PPh ₂ (CH ₂) ₃ OH) in dendrimer generations 1-4 (DG1-DG4)	78
2.6	References	79
Chapter 3: Turbine Shape Organotin Dendrimers: Photophysical Properties and Direct Replacement of Sn with Pt		
		82

3.1 Introduction	83
3.2 Results and discussion	83
3.3 Conclusions	87
3.4 General procedure for the dendrimers synthesis	88
3.5 Theoretical methods	89
3.6 Experimental section	89
3.6.1 Synthesis of 1,3,5-triethynylbenzene (TEB) based dendrimers	91
3.6.2 Synthesis of capped dendrimers with SnMe ₃ groups	91
3.6.3 Replacement of Sn in 1 st Generation Dendrimer with Pt (DG4 and DG5)	92
3.6.4 Spectroscopic data for 1,3,5-triethynylbenzene (TEB) based compounds	92
3.7 References	93
Chapter 4: Designing Dendritic Frameworks with Versatile Building Blocks Suitable for Cu^I Catalyzed Alkyne Azide “Click” Chemistry	96
4.1 Introduction	97
4.2 Results and discussion	97
4.3 Conclusions	102
4.4 Experimental section	102
4.4.1 Materials	102
4.4.2 Instruments	103
4.4.3 Synthesis and characterization	103
4.5 References	111
Chapter 5: Multi-tasking with Single Scaffold Dendrimers for Targeting Sub-Cellular Microenvironment	113
5.1 Introduction	114
5.2 Results and discussion	116
5.3 Conclusions	128

5.4 Methods	128
5.5 Experimental section	131
5.6 References	142
Chapter 6: Conclusions, Contributions to Original Knowledge, and Suggestions for Future Work	145
6.1 Conclusions and contribution to general knowledge	146
6.2 Suggestions for future work	148
6.2.1 Using the acetylene-terminated dendrimers as unimolecular micelles	148
6.2.2 Using the acetylene-terminated dendrimers as frameworks for larger multifunctional dendrimers	149
6.2.3 Incorporating solubilizing agents and other therapeutic molecules	149
6.2.4 Incorporating solubilizing agents, therapeutic molecules, and Imaging dye	150
Appendix I: Theoretical Investigation of 3,5-Dihydroxybenzyl Alcohol Based Dendrimer Generations 1–5 Using Molecular Mechanics (MM+) Method and the PM3 Semi-Empirical Molecular Orbital Theory	151

List of Tables

	Page
Table 2.1: Summary of the relative sizes of DG1-5 determined by the MM+ method.	69
Table 2.2: Conversion (%) of 1-decene to decane using generations 1-4 dendrimer encapsulated CODRhCl(PPh ₂ (CH ₂) ₃ OH).	73
Table 2.3: Quantities of DG4 and DR1 that were used in preparing solutions.	76
Table 2.4: Quantities of DG5 and DR1 that were used in preparing solutions.	76
Table 2.5: Quantities of DG1-4 that were used in catalysis applications.	78
Table 3.1: Photophysical Data of DG0-3 and their Capped forms (DG0-SnMe ₃ to DG3-SnMe ₃) in benzene at room temperature.	86

List of Schemes

	Page
Scheme 1.1: A schematic summary of the different routes used to construct globular dendrimers.	7
Scheme 1.2: A schematic summary of the different routes used to construct multiblock dendrimers.	36
Scheme 3.1: Synthesis of the first generation dendrimer (DG1), capping with Me ₃ Sn, and replacement of Sn with Pt.	84
Scheme 3.2: Synthesis of TEB-based dendrimers, their Me ₃ Sn-terminated analogs, and replacement of Sn with Pt in DG1.	91
Scheme 4.1: Synthesis of building blocks.	98
Scheme 4.2: Synthesis using CuAAC “click” reaction.	99
Scheme 4.3: Synthesis of dendrons for convergent synthesis.	100
Scheme 4.4: Convergent and divergent synthetic routes of dendrimers.	101
Scheme 5.1: The synthesis of the azide functionalized red BODIPY dye (PM-N ₃) using the alcohol form of the commercial PM605 dye (PM) and 6-azidohexanoic acid.	116
Scheme 5.2: Synthetic scheme for the ABB’ building block, and its functionalization with 11-Azido-undecan-1-ol, and the azide moiety.	117
Scheme 5.3: Synthesis of bifunctional dendrimer (D-PM-LA) with PM dye and α -lipoic acid at the periphery.	118
Scheme 5.4: Synthesis of D-PM by the reaction of three PM-N ₃ dye molecules with a three arm core (1,3,5-triethynylbenzene) (TEB).	119
Scheme 5.5: Synthetic scheme for the linear analog (PM-LA) containing covalently linked PM dye and α -lipoic acid.	120

List of Figures

	Page
Figure 1.1: Classification of “dendritic polymers”.	2
Figure 1.2: The dendrimer structure and its composition.	4
Figure 1.3: Tomalia’s amine-terminated PAMAM dendrimer.	8
Figure 1.4: Fréchet-type generation 4 poly(benzyl ether) dendron with brominated focal point.	10
Figure 1.5: Dendrimer with porphyrin core functionalized with Frechet-type dendrons.	11
Figure 1.6: Helms’s catalytic pump dendrimer with DMAP molecules anchored to the core.	12
Figure 1.7: Carbosilane dendrimer containing catalytically active Ni complex.	13
Figure 1.8: Rose bengal molecules encapsulated in a dendritic box.	14
Figure 1.9: Dendrimer with 3'-azido-3'-deoxythymidine (AZT) encapsulated via hydrogen bonding.	16
Figure 1.10: Hahn’s Light harvesting dendrimer with eosin fluorescent dye inside.	17
Figure 1.11: Ford’s PPI dendrimer based unimolecular micelle.	19
Figure 1.12: PPI dendrimer generation 4 functionalized with dansyl groups.	20
Figure 1.13: van Koten’s polysilane dendrimers with peripheral diaminoarylnickel(II) complexes.	22
Figure 1.14: Astruc’s dendrimer containing triazole rings and peripheral ferrocenyl groups.	23
Figure 1.15: Water soluble PAMAM dendrimer with glucosamine at the periphery.	24
Figure 1.16: Fréchet’s PEG-cholesterol-dendrimer conjugate dendrimers.	25
Figure 1.17: Bifunctional dendrimer for orthogonal functionalization.	27
Figure 1.18: PPI dendrimer generation 3 with both ferrocene and	

cobaltocenium at the periphery.	28
Figure 1.19: 5 th Generation PAMAM dendrimer functionalized with folic acid (FA), methotrexate (MTX), and fluorescein-5-thiosemicarbazide (FITC) at the periphery.	29
Figure 1.20: Morikawa's Silicoxane-carbosilane dendrimer.	31
Figure 1.21: An organo-platinum dendrimer.	32
Figure 1.22: Humphrey's ruthenium containing dendrimer.	34
Figure 1.23: Majoral's phosphorus containing dendrimer with fluorescein-5-thiosemicarbazide (FITC) at the periphery.	35
Figure 1.24: A diblock dendrimer containing both Frechet type and PAMAM dendrons.	36
Figure 1.25: Dipolar dendrimer based on Frechet's dendrons.	37
Figure 1.26: Miller's dumb-bell shape dendritic macromolecule.	38
Figure 1.27: Hawker's bifunctional dendrimer containing coumarin dyes and protein-binding mannose molecules.	39
Figure 1.28: Triblock dendrimer containing Frechet's and Newkome's dendrons and a redox active ferrocene molecule.	40
Figure 1.29: Examples of dendrimers decorated with linear polymer chains.	41
Figure 1.30: Hydrophilic PEO linear polymer attached to the 3 rd generation polyester dendron with cyclic hydrophobic acetals of 2,4,6-trimethoxybenzaldehyde at the periphery, and encapsulated doxorubicin (DOX) molecules.	42
Figure 1.31: Gillies' "bow-tie" polyester dendrimer containing PEO linear polymer chains and covalently attached doxorubicin (DOX) molecules.	44
Figure 1.32: Frechet's dendritic unimolecular micelle with PEG polymer chains at the periphery and encapsulated indomethacin drug molecules.	46
Figure 1.33: Examples of linear polymers decorated with dendrons.	47
Figure 1.34: Frechet type dendrons attached to the ends of a long linear	

PEG polymer chain.	48
Figure 2.1: Dendrimer generations 4 and 5 (DG4 and 5) of DHBA-based dendrimers.	64
Figure 2.2: The lowest unoccupied molecular orbitals (LUMO) of DG1 along with their numbers and energies.	65
Figure 2.3: The optimized structures of dendrimer generation 1-5 using the molecular modelling MM+ method shown as overlapping spheres.	67
Figure 2.4: The relationship between the dendrimer generation number and its relative diameter (Å).	69
Figure 2.5: The optimized molecular structure of DR1 calculated by MM+ method.	70
Figure 2.6: UV-Vis spectra of free DR1, and encapsulated DR1 in DG4.	70
Figure 2.7: a) TEM micrographs of dendrimer generation 4 (DG4) with DR1 a) and b), and without DR1 c) and d) at concentration of 5mg.mL ⁻¹ .	72
Figure 3.1: PM3-optimized structures of TEB dendrimer generations 1-3.	85
Figure 3.2: Structures of dendrimer generation 2, and 3 (DG2 & DG3).	89
Figure 5.1: Structures of dendrimers containing the red BODIPY dye (D-PM), BODIPY dye and the lipoic acid (D-PM-LA), and its linear analogue (PM-LA).	121
Figure 5.2: The absorption and emission spectra of the commercial PM605 red BODIPY dye (PM), and the bifunctional dendrimer (D-PM-LA).	121
Figure 5.3: Cellular internalization, distribution, cytotoxicity, and cytoprotectivity of the linear and dendritic compounds.	122
Figure 5.4: Time course of cellular uptake and subcellular distribution of dendrimers, PM-linear analog and PM alone.	125
Figure 5.5: Intracellular localization of fluorescent linear and dendritic structures.	127
Figure 6.1: Dendritic unimolecular micelles.	149

Figure 6.2: Covalent attachment of drugs and solubilizing polymers to the dendrimer.	150
Figure 6.3: covalent attachments of drugs, dyes and solubilizing polymers to the dendrimer.	150

List of Abbreviations

BODIPY	8-Acetoxymethyl-2,6-diethyl -1,3,5,7-tetramethyl pyrromethene fluoroborate
<i>cac</i>	<i>Critical aggregation concentration</i>
COD	Cyclooctadiene
CuAAC	Cu(I)-catalyzed cycloaddition between primary alkynes and azides
D-PM	Dendrimer containing BODIPY dyes
D-PM-LA	Dendrimer containing BODIPY dyes and α -lipoic acid molecules
DCC	<i>N,N</i> -dicyclohexylcarbodiimide
DEA	Diethyl amine
DEB	1,4-Diethynylbenzene
DHBA	3,5-Dihydroxybenzyl alcohol
DLMO	Delocalized molecular orbitals
DMF	Dimethylformamide
DMSO	Dimethylsulfoxide
DR1	Disperse red 1
DMAP	4-(dimethylamino)pyridine
EI-MS	Electron impact-mass spectroscopy
ES-MS	Electro-spray-mass spectroscopy
FT-IR	Fourier transform-infra red
GC-MS	Gas chromatography-mass spectroscopy
DG _n	Dendrimer Generation number
e	Electron charge
LA	α -Lipoic acid
LD	Lipid droplet
LMO	Localized molecular orbital
LUMO	Lowest unoccupied molecular orbital
HOMO	Highest occupied molecular orbital
H-bonding	Hydrogen bonding

Hz	Hertz
J	Coupling constant
MALDI-TOF	Matrix assisted laser desorption ionization-time of flight
MCF-7	Human breast cancer cells
MM+	HyperChem Molecular Mechanics force field
MO	Molecular orbital
MS	Mass spectroscopy
NaAsc	Sodium Ascorbate
NMR	Nuclear magnetic resonance
NSAID	Non-steroidal anti-inflammatory drugs
<i>p</i> -	Para
PAMAM	Poly(amido amine)
PM	Pyromethene fluoroborate
PM-LA	Linear compound containing a BODIPY dye and α -lipoic acid
PM3	Parametric method 3
ppm	Part per million
RMS	Root mean square
TBAF	Tetrabutylammonium fluoride
<i>t</i> -Bu	Tert-butyl
TEA	triethylamine
TEB	1,3,5-triethynylbenzene
TEM	Transmission electron microscopy
THF	Tetrahydrofuran
TIPS	Triisopropylsilyl
TMS	Trimethylsilyl
TPP	Triphenylphosphine
UV-Vis	Ultra violet-visible
%	Percentage
ν	Frequency (stretching)
δ	Chemical shift
π	Bonding pi orbital

π^* Antibonding pi orbital
 Φ_f Fluorescence quantum yield

Contribution of Authors

“The Faculty of Graduate Studies and Research at McGill University allows, as an alternative to the traditional thesis format, a manuscript-based thesis, where the candidate has the option of including, as part of the thesis, the text of one or more papers submitted, or to be submitted, for publication, or the clearly-duplicated text (not the reprints) of one or more published papers. The thesis must be more than a collection of manuscripts. All components must be integrated into a cohesive unit with a logical progression from one chapter to the next. In order to ensure that the thesis has continuity, connecting texts that provide logical bridges preceding and following each manuscript are mandatory.”

“when co-authored papers are included in a thesis, the candidate must be the primary author (the author who has made the most substantial contribution) for all papers included in the thesis. In addition, the candidate is required to make an explicit statement in the thesis as to who contributed to such work and to what extent.”

Chapters 2 and 3 of this thesis are reproduced, in part, from published manuscripts, while Chapters 1, 4 and 5 of this thesis are reproduced, in part, from submitted for publication manuscripts as the following:

Chapter 1: Hourani R., and Kakkar A., *Macromol. Rapid Commun.* **2009**, in press, DOI: 10.1002/marc.200900712.

This manuscript is a review article written by the author. The co-author, Dr. Ashok Kakkar, gave advice, guidance and edited the text of the manuscript.

Chapter 2: Hourani R., Kakkar A., and Whitehead M. A., *J. Mater. Chem.*, **2005**, 15, 2106.

Chapter 3: Hourani R., Whitehead M. A., and Kakkar A., *Macromolecules*, **2008**, *41*, 508.

These two manuscripts are co-authored by Dr. Ashok Kakkar, who supervised the experimental studies, and Dr. M. A. Whitehead, who supervised the theoretical studies. Other than advice and guidance, all work in these two chapters was performed by the author.

Chapter 4 : Hourani R., Sharma A., and Kakkar A., **2009**, submitted.

This manuscript is co-authored by Anjali Sharma, a new Ph.D. student, who synthesized the 3 dendrons used for the convergent synthesis, and helped writing their experimental sections. All starting materials, building blocks, and the final dendritic structure other than these 3 compounds were synthesized by the author. The other co-author is Dr. Ashok Kakkar, who gave advice and guidance throughout the work.

Chapter 5: Hourani R., Jain M., Maysinger D., and Kakkar A., **2009**, submitted.

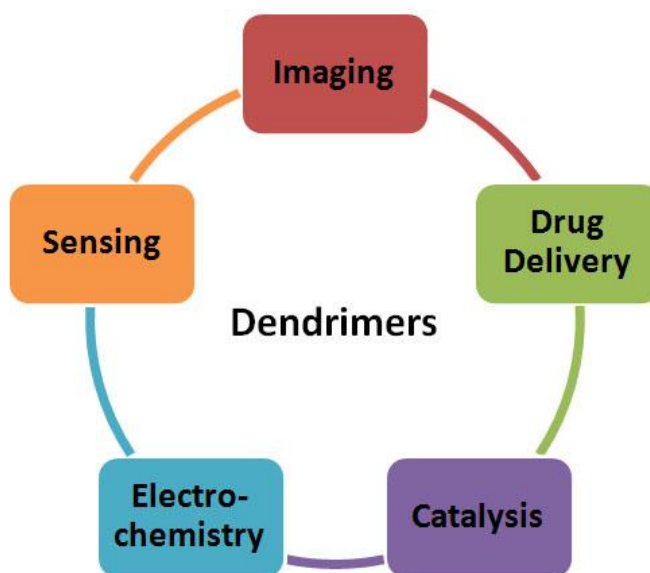
This manuscript is co-authored by Manasi Jain, a Ph.D. Student in the Department of Pharmacology & Therapeutics, who performed all experiments related to the pharmacological studies of the dendritic compounds. All the original compounds in this manuscript were synthesized and characterized by the author. The other co-authors, Dr. Ashok Kakkar and Dr. Dusica Maysinger, gave advice and guidance as research advisors.

Appendix I: Hourani R., Kakkar A., and Whitehead M. A., *J. Mol. Struct. (Theochem.)*, **2007**, 807, 101.

This manuscript is co-authored by Dr. Ashok Kakkar, and Dr. M. A. Whitehead. Other than advice and guidance, all work in this appendix was performed by the author.

Chapter 1

Introduction and Scope of the Thesis:



Recent Advances in the Elegance of Chemistry in Designing Dendrimers

Hyperbranched and monodisperse macromolecules with tailored architecture constitute the key to designing efficient and smart nanomaterials. Dendrimers offer real potential to achieve this goal, and one of the earlier challenges faced by this novel class of polymers has been addressed by the evolutions in the synthetic methodologies.

Reproduced in part with permission from:

Hourani R., and Kakkar A., *Macromol. Rapid Commun.* **2009**, in press, DOI: 10.1002/marc.200900712.

Copyright, 2009, Wiley-VCH Verlag.

1.1 Dendritic polymers: an overview

Over the past century, polymers have revolutionized our daily life by providing essential materials needed for our survival in the modern world. The synthesis of linear, branched, or cross-linked polymers is now well established, and the individual polymeric architecture can be tailored for specific applications in a diverse range of fields. Functionalized polymers continue to be key candidates for advances in technology, and increasingly nowadays, in biology.^[1] It is well understood that the macromolecular architecture and its self-assembly in different media greatly influence their overall properties.^[2] The increasing demand for more sophisticated applications, especially in medicine, has shifted the focus to much less polydisperse, and more highly branched polymeric materials, commonly referred to as “dendritic polymers” (Figure 1.1).^[3] The latter can be sub-divided into two categories: structure-controlled polymers such as dendrons, dendrimers and dendrigrafts, and the random structure hyperbranched polymers. This new class of polymeric materials exhibit different properties than their linear analogues which one could take advantage of, in designing efficient and smart nanomaterials.

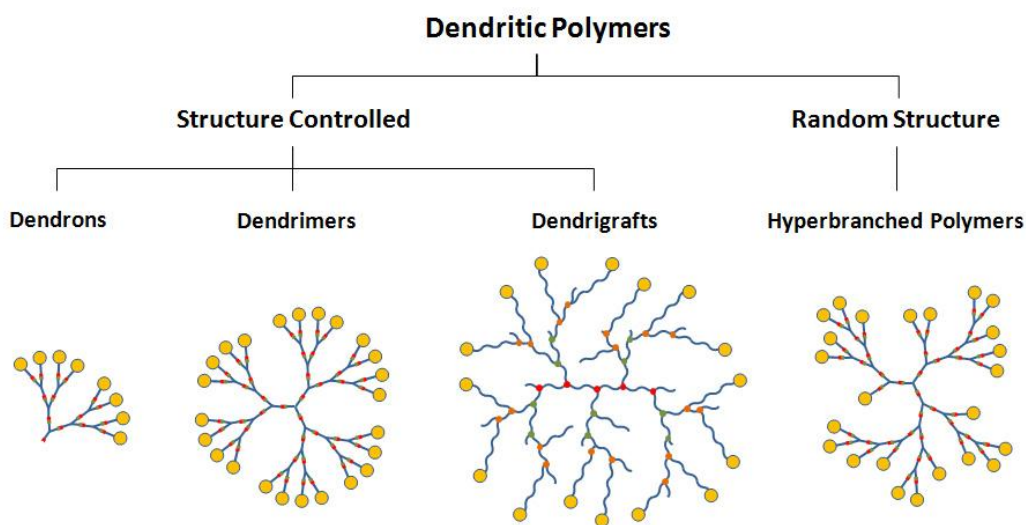


Figure 1.1. Classification of “dendritic polymers”.

Dendrons and dendrimers are commonly synthesized in a layer-by-layer fashion with a high degree of control over the synthesis of each layer, known as

a generation.^[4] This iterative approach provides macromolecules that are monodisperse, and contain a large number of peripheral functional groups. A dendron is typically a tree branch that has a focal point which allows it to react with a multi-arm core upon activation, and the assembly of two or more dendrons onto a core leads to the formation of a dendrimer. Dendrimers have unique structural properties that are influenced by their composition, and are dependent on their overall size, shape and surface groups.^[5] There is a large library of dendrimers with polydispersity of ≈ 1.0005 that has been synthesized using a variety of organic reagents and building blocks.^[6]

Dendrigrfts are akin to dendrimers because they are constructed using a similar divergent methodology.^[7] However, each layer is a polymer chain instead of a typical well-defined organic monomer, as is the case for dendrimers. Since a random polymerization process is used in the construction of each generation, dendrigrfts also depict resemblance to hyperbranched polymers.^[8] The synthesis of these high molecular weight branched macromolecules that combines layer-by-layer build-up with random polymerization, is much easier and more rapid than dendrimer synthesis. As expected, the polydispersity of dendrigrfts is higher than dendrimers (≈ 1.1), but it is still lower than hyperbranched polymers due to the added degree of control during synthesis.^[9]

Hyperbranched polymers are considered as the fourth class of polymer architectures, and are generally synthesized using traditional polymerization methods including the most common condensation reactions.^[10] Their one-pot synthetic process that does not necessitate protection/activation processes, is much simpler compared to the synthesis of dendrimers. The high degree of branching in hyperbranched polymers makes them similar to dendrimers in many respects, and this is the reason they are generally considered as a sub-class of dendritic polymers with unique and different properties than their linear, branched, and cross-linked analogues.^[11] However, they contain structural defects because of the one-pot random polymerization procedure used to synthesize them, and display polydispersity of ≈ 2 .^[12] Although, the degree and distribution of branching in hyperbranched polymers is uncontrolled in contrast

to dendrimers, they do share many properties with dendrimers such as the globular shape, amplified surface group effect, and higher solubility than their linear analogues.^[13]

Even though hyperbranched polymers and dendrigrafts are attractive candidates for industrial scale applications, there is continued and well deserved interest in dendrimers, especially for applications in biology and medicine, due to their monodisperse nature that is desired for therapeutics and related applications.^[14] In addition, the higher degree of control over the dendrimer structure, especially the peripheries, can lead to tailored biocompatibility and cytotoxicity for these macromolecules. Thus, dendrimers are compact macromolecules, the overall properties of which can be tailored using variables including the type of core, building blocks, and the functional groups at the peripheries (Figure 1.2). The latter have a tremendous effect on the evolving three dimensional macromolecular structure and the inherent development of internal cavities, which can be used to encapsulate guest molecules. The core can serve merely as a branching unit with multiple arms, or it can also be of a specific function such as a catalytic center for selective catalysis, imaging probe for labelling *etc.*

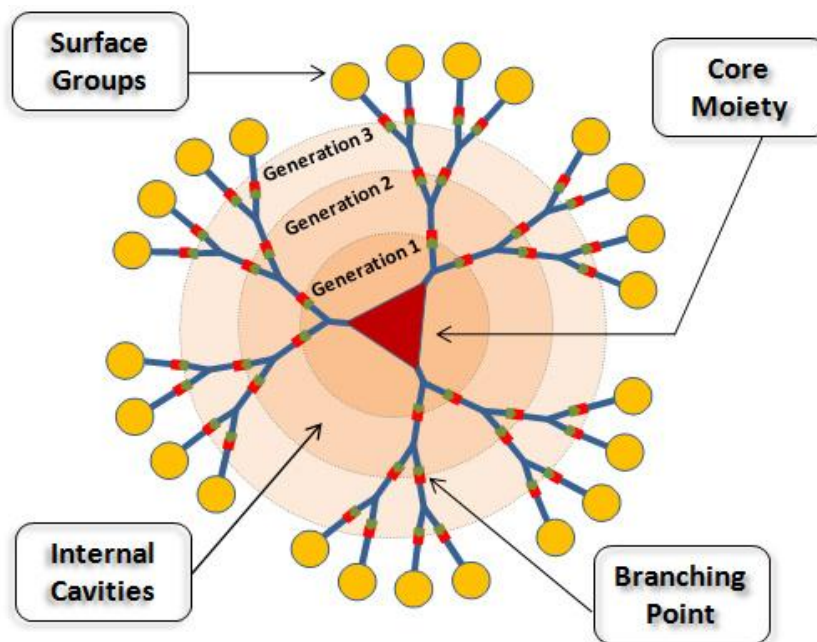


Figure 1.2. The dendrimer structure and its composition.

The choice of the functional groups at the periphery of the dendrimers can influence their physical properties, and thus allow for tailoring their interactions with the surrounding environment. The surface groups can also allow the attachment of various therapeutic drugs,^[15] imaging probes,^[16] and targeting molecules.^[17] Dendrimers have also been used to anchor transition metal centers,^[18] catalysts,^[19] and metal nanoparticles.^[20] This has allowed one to exploit what is now known as the “dendritic effect” in numerous applications. Despite the fact that the layer-by-layer construction of dendrimers makes them tedious and costly to synthesize, each dendrimer generation can be part of a large library. For certain applications, higher generations are more desired for their relatively large size and sufficient amplification of the peripheral functionalities, while others take advantage of the smaller size of lower generations.

The synthetic chemistry world has evolved over the years, and the dynamics have changed from making of small molecules from single atoms, to the art of making macromolecules at the nanoscale size using molecules, commonly referred to nowadays as the building blocks. Dendrimer synthesis has been challenging in the past due to the need for making suitable building blocks and performing clean chemistry that reduces, or completely eliminates, the formation of side products. The protection/activation and the purification associated with each step, made it even more tedious, time consuming, and costly.^[21] It is important to note that other significant issues also emerge as the generation number increases in terms of solubility, back-folding, coiling, and structural defects due to steric hindrance at the periphery.^[22] There has been a tremendous effort to overcome these challenges, and it has led to the construction of a diverse range of dendritic macromolecules. In fact, the synthesis of dendrimers is constantly evolving and new methodologies and mild chemical reactions such as Diels-Alder,^[23] Cu(I)-catalyzed cycloaddition between primary alkynes and azides (CuAAC)^[24] “click” reactions have been developed to address key synthetic issues in dendrimer synthesis.

Introducing multiple functions into the same dendrimer scaffold is more complex and difficult than building a monofunctional dendrimer.^[25] Dendrimers

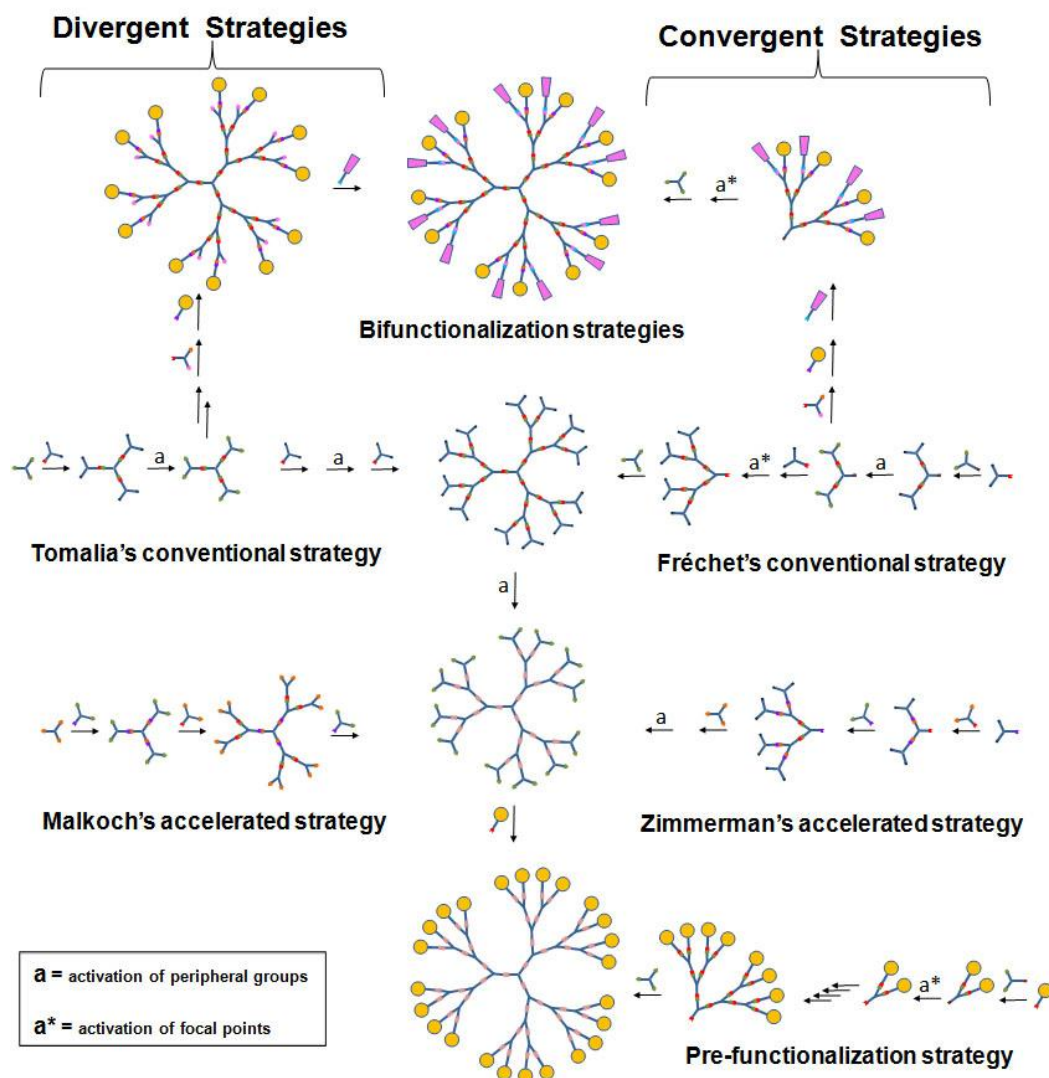
containing only one type of active molecule at the peripheries require similar reactive groups for the final attachment. On the other hand, introducing two or more active molecules into the dendrimer structure for multitasking creates an extra challenge, since it requires developing appropriate functional groups at the periphery that will react in sequence, using different chemical reactions. The latter must be independent, and should not interfere with each other for a complete control on the number of molecules covalently linked and their precise location. Anchoring different molecules using the similar reactive sites is also possible; however, it leads to a statistical distribution of the products that is dependent on the number of equivalents of each reactant used in the mixture. The synthesis of multifunctional dendrimers is fascinating and it constitutes an art on its own. In this chapter, examples of monofunctional as well as multifunctional dendrimers are presented that demonstrate high elegance of chemistry in putting together monodisperse macromolecules that have started to play a key role in designing novel nanomaterials.

1.2 Synthesis of dendrimers

The history of the synthesis of dendrimers goes back to the late seventies, when Vögtle and coworkers constructed the so called “cascade” molecules that allowed the use of repetitive units to form branched molecules.^[26] In the early 1980s, Tomalia and coworkers achieved the first divergent synthesis of these monodisperse hyperbranched macromolecules, and coined the term dendrimer,^[27] in parallel with the development of Newkome’s “arborol” systems.^[28]

The divergent methodology is also known as the inside-out approach, and it allows the growth from a suitable core molecule to a desired higher generation using the same building block, an AB_2 monomer, by reacting it with the peripheral groups of the previous generation. The B moieties are generally protected, and subsequently activated by deprotection prior to the addition of the next layer of AB_2 units. Once the desired generation is achieved, a functional

group or molecule of interest can be attached to the activated sites to obtain a monofunctional dendrimer (Scheme 1.1).



Scheme 1.1. A schematic summary of the different routes used to construct globular dendrimers.

This method provides maximum control on the growth of the dendrimer, and allows the building of higher generations until the peripheries get too crowded and prevent the complete reaction of all branches involved in the build-up of the next generation.

Tomalia and coworkers achieved the synthesis of PAMAM dendrimers (Figure 1.3) using a repetitive Michael addition of methyl acrylate to amines,

followed by amidation of the resulting esters with an excess of ethylenediamine (EDA).^[27] The most commonly used initiator cores for the synthesis were ammonia and ethylenediamine, and a seventh generation PAMAM dendrimer was successfully prepared following this procedure. PAMAM dendrimers are now commercially available, and extensively used in the literature for different applications in medicine and industry via various surface modifications of the original structure.

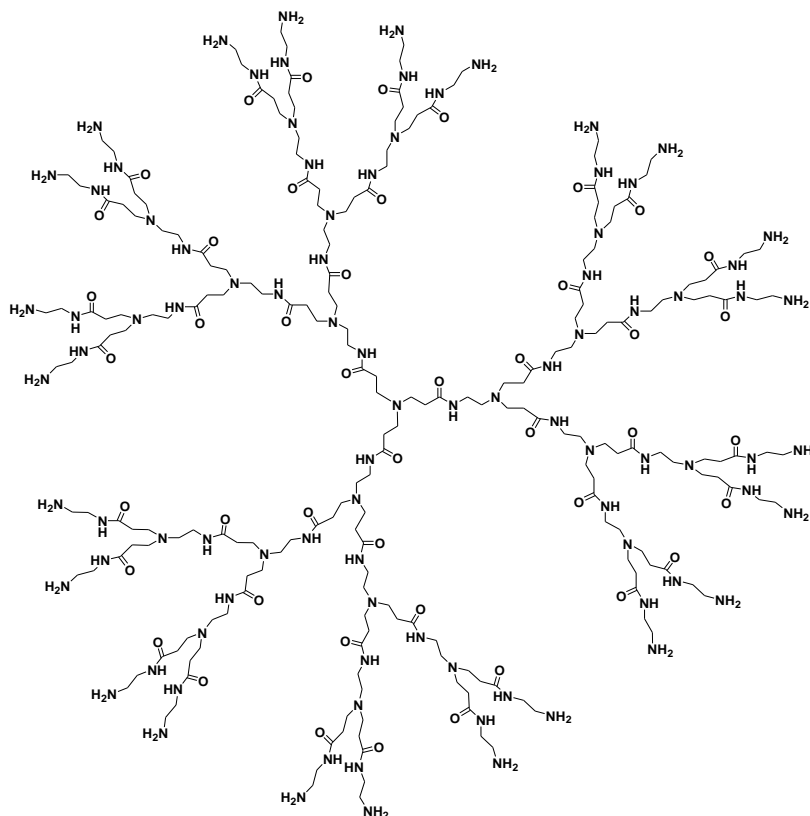


Figure 1.3. Tomalia's amine-terminated PAMAM dendrimer.

The possibility of having incomplete reactions during the build-up of dendrimers especially at higher generations, leads to what is known as the “structure defect”, and it is one of the disadvantages in this methodology.^[29] The latter also include the need to use molar excess of the building block, and the possible complications associated with their removal during purification. Moreover, it is difficult to incorporate many functions in the dendrimer using the divergent methodology. To overcome this challenge, it is possible to attach a

multifunctional building block of ABC type as the last layer, which will allow the addition of two different molecules of interest by activating the B and C arms in a consecutive fashion. This leads to a bifunctional dendrimer with alternating functions at the periphery (Scheme 1.1).

In a traditional divergent dendrimer build-up, an activation (deprotection) step is required after the construction of each generation, and it certainly adds to the number of synthetic steps required for each generation growth. Malkoch and coworkers have recently developed a divergent synthetic technique that overcomes the activation step, and it can be considered a step closer towards commercialization and reduction of cost in the synthesis of dendrimers.^[30] Their methodology involves the use of two different monomers, AB₂ and CD₂ and eliminates the deprotection step completely (Scheme 1.1). Even though this methodology requires the synthesis of an additional small building unit, it does offer substantial advantages, especially when it comes to avoiding additional purification of a much larger molecule after each step of activation.

In 1990, Hawker and Fréchet achieved the synthesis of dendrimers using the convergent approach, which overcame some of the disadvantages of the divergent methodology.^[31] The convergent method allows one to build different dendrons separately, and then as a final step, link them to a suitable core, through their activated focal point (Scheme 1.1). Using this approach, dendrons can be pre-functionalized with a desired molecule, or their periphery is kept protected until they are linked to the core, and then decorated with functional molecules in the same fashion as the divergent methodology (Scheme 1.1).

The first Fréchet-type convergent synthesis was achieved by forming benzyl ethers from phenols and benzylic halides in quantitative yields.^[31] The monomer used for the synthetic elaboration was 3,5-dihydroxybenzyl alcohol (DHBA), which has two alcohol groups with different reactivities towards benzylic halides. Starting with the desired benzyl bromide, which will become the periphery of the dendrimer, 2 equivalents of it were condensed with the two phenolic groups of the 3,5-dihydroxybenzyl alcohol. The unreacted benzylic alcohol was then activated by transforming it to a bromide to repeat the

condensation reaction with another DHBA molecule. Subsequent iteration of bromination and condensation is used to synthesize higher dendron generations. The resulting brominated dendron of any desired generation (Figure 1.4) can then be coupled to a multiphenolic core such as 1,1,1-tris(4'-hydroxyphenyl)ethane to obtain the first convergently synthesized dendrimer. Fréchet's dendrons have been widely modified with different groups, and have been attached to a wide variety of cores including porphyrins^[32] and polymeric cores.^[33]

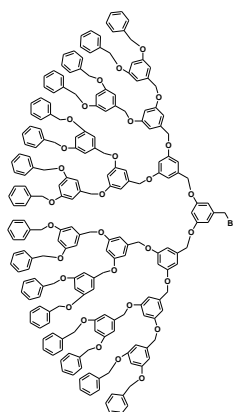


Figure 1.4. Fréchet-type generation 4 poly(benzyl ether) dendron with brominated focal point.

Since dendrons are relatively smaller than their dendrimer analogues, they are generally easier to synthesize and purify, as well as ensuring complete reaction in the build-up up to each generation. The convergent method can also be used to develop alternating bifunctional peripheries, as in the case of the divergent method, by functionalization of each dendron separately using the ABC block, as described above, and then group them onto a suitable core (Scheme 1.1). The main disadvantage of the convergent synthesis is that the steric constraints can prevent the access of the focal point of the dendron to the polyfunctional core at higher generations.^[29] As in the case of the divergent methodology, rapid synthesis using orthogonal coupling strategies were attempted to speed up the convergent synthesis. Zeng and Zimmerman achieved the synthesis of a sixth generation dendrimer using orthogonal reactions with

AB₂ and CD₂ building blocks to build the dendrons involved in the convergent synthesis (Scheme 1.1).^[34]

1.3 Core-functionalized dendrimers

Many examples have appeared in the literature that demonstrate designing systems which mimic naturally existing hemoproteins by capping, crowning, or strapping metalloporphyrin cores.^[32] Various studies have indicated the importance of shielding the porphyrin core by steric isolation in order to achieve certain biological functions, and in this regard building a dendritic structure around the porphyrin core by attaching dendrons to the arms of a pre-synthesized core has been achieved by numerous groups including the pioneering work of Aida,^[35] Suslick,^[36] and Diedrich.^[37]

Using the convergent methodology, Aida and coworkers managed to covalently attach Fréchet-type dendrons, via an alkali-mediated coupling reaction, to the 5,10,15,20-tetrakis(3',5'-dihydroxyphenyl)porphyrin core, that contained different metals including Zinc and Iron (Figure 1.5).^[35]

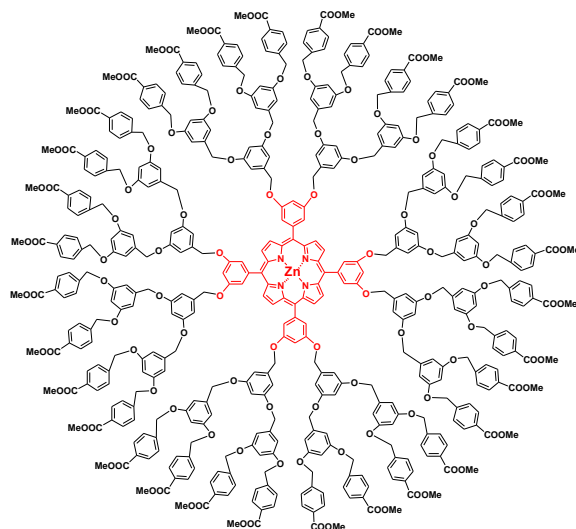


Figure 1.5. Dendrimer with porphyrin core functionalized with Fréchet-type dendrons.

The periphery of the dendrons have been modified with esters, ethers, positively charged, or negatively charged moieties, to provide water solubility, electron-transfer, O₂-binding or interactions with other media. They

demonstrated the use of a functional molecule of interest as the core of the dendrimer, and the feasibility of taking advantage of the dendritic arms in shielding it to attain desired applications similar to biological systems. The hydrophobic dendritic arms provided protection to the dioxygen adduct that forms at the active site (the core), which increased its half life.

The effect of the dendrimer architecture and nanoenvironment of the internal cavities, on the catalytic properties was first investigated by Helms and coworkers.^[38] They synthesized a trivalent core containing three 4-(dimethylamino) pyridine (DMAP) analogues, which was used to construct the well-known Fréchet-type benzyl ether and aliphatic ester dendrimer of generation 3 (Figure 1.6).

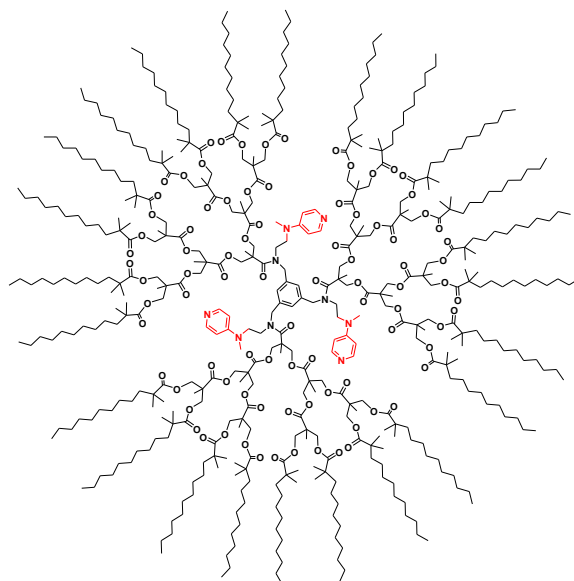


Figure 1.6. Helms's catalytic pump dendrimer with DMAP molecules anchored to the core.

The catalytic activity of DMAP for the esterification of sterically hindered tertiary alcohols was investigated, and results from the catalysis experiments indicated that the nanoenvironment had a substantial effect on the catalytic activity. The amphiphilic nature of the polyester platform created a radial gradient of polarity, which facilitated the entry and accumulation of the alcohol substrate into the more polar core of the dendrimer to be in proximity to the catalysts, while the less polar acetylated product was driven out towards the non-

polar reaction medium (cyclohexane). Interestingly, catalytic experiments using DMAP alone, under the same reaction conditions, showed that it is only marginally effective in transformation reactions. This example demonstrated the potential of using dendrimer architecture as a free-energy driven catalytic pump that prevents product inhibition.

Dendritic scaffolds have also been incorporated into the design of catalysts,^[39] and the presence of such bulky architectures around the catalytically active sites can provide site isolation, or create a microenvironment that alters the catalytic properties of the active sites. van Leeuwen and co-workers have successfully constructed two second generation carbosilane-based dendrons which contain bidentate P, O ligands that form complexes with nickel for important industrial reactions (Figure 1.7).^[40]

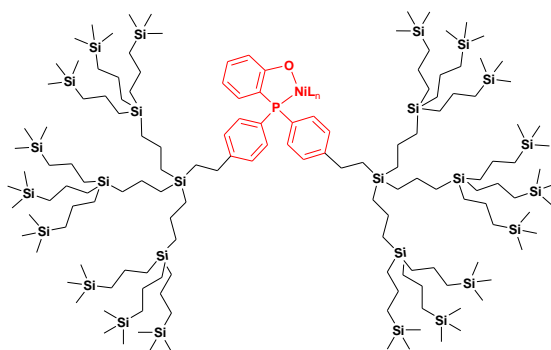


Figure 1.7. Carbosilane dendrimer containing catalytically active Ni complex.

The unfunctionalized parent (P, O)Ni compound forms bis(P, O)Ni complexes that causes deactivation of the catalytic complex. In comparison, the presence of the dendritic framework around this complex prevented the formation of the undesirable bis(P, O)Ni complexes in toluene, and thus enhanced the productivity of the parent complex. This work demonstrates a general example that can be applied to other transition metal catalysts, for which the formation of bimetallic complexes can cause deactivation.

1.4 Encapsulation of Guests in the Internal Cavities

The poly(propylene imine) (PPI) dendrimer developed by Meijer *et al* was one of the first dendrimers to be synthesized in high purity for the large-

scale production.^[41] Even though the reaction sequence used was similar to that used by Vögtle *et al.*,^[26] it overcame the drawbacks related to the restrictions of the latter in synthesizing higher generations due to low yields. The divergent methodology was based on a double Michael addition of acrylonitrile to primary amines followed by hydrogenation of nitriles groups, and it was used to prepare up to the fifth generation of PPI dendrimers in quantitative yields. 1,4-Diaminobutane, with two primary amines, was used as a core, and an excess of acrylonitrile was added in two steps. The first equivalent was added at room temperature, and the second equivalent at an elevated temperature to ensure full conversion of all available arms of each layer. The terminated nitriles were then converted to primary amines using heterogeneously catalyzed hydrogenation yielding twice the number of primary amines. PPI dendrimers have been modified and used extensively in a variety of applications related to encapsulation of guest molecules.^[42]

Meijer and coworkers took advantage of the internal cavities in a generation 5 PPI dendrimer to permanently encapsulate up to 4 rose bengal molecules in their “dendritic box” (Figure 1.8).^[42]

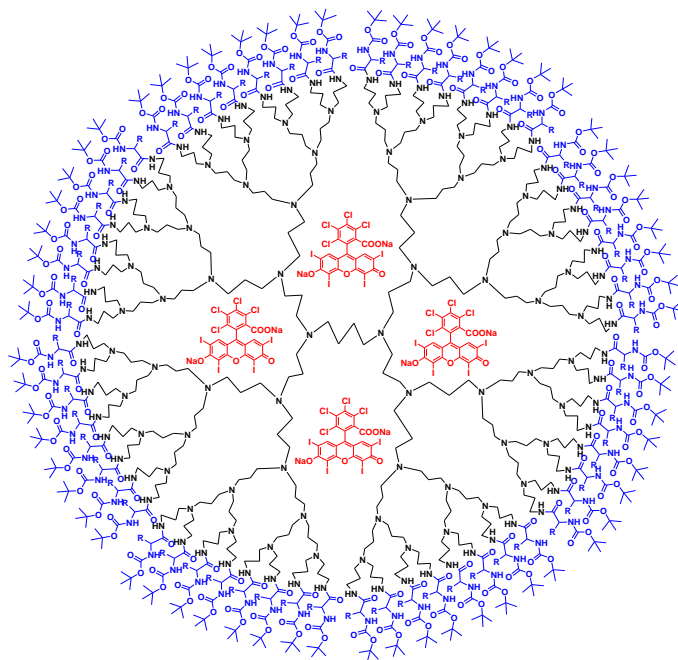


Figure 1.8. Rose bengal molecules encapsulated in a dendritic box.

The permanent encapsulation was made possible by forming a rigid shell around the PPI dendrimer by modifying the terminal groups with a bulky amino acid derivative such as N-hydroxy-succinimide ester of a tert-butyloxycarbonyl (tBOC)-protected amino acid. The presence of the rose bengal molecules inside the “dendritic box” was confirmed using dialysis and other spectroscopic techniques including UV-Vis and fluorescence spectroscopy. This unique example demonstrates the usefulness of dendrimers in physically entrapping guest molecules within a confined environment. The shape and size-selective release of encapsulated molecules from the “dendritic box” was also examined using two guest molecules; rose Bengal, and *p*-nitrobenzoic acid as a smaller guest. The shell was partially perforated, liberating the smaller guest, and the subsequent removal of the shell liberated the larger rose Bengal guest molecules. This further demonstrates the potential of dendrimers in delivery and controlled release of therapeutic molecules. It is worth mentioning here that attempts to encapsulate guest molecules in generation two of PPI dendrimers were not successful due to their relatively open structure. Other guest molecules including free radicals such as 3-carboxy-proxyl radicals have also been entrapped in the “dendritic box”, which showed that intermolecular ferromagnetic exchange interactions can take place in such guest-host systems.

Newkome and coworkers took the idea of physical encapsulation a step further by introducing chemical units capable of specific binding of molecules of interest via hydrogen bonding (Figure 1.9).^[43] For this purpose, 2,6-diaminopyridine was incorporated in the backbone of the dendrimer. Encapsulation of 3'-azido-3'-deoxythymidine (AZT) via hydrogen bonding to binding sites of the dendritic host was confirmed using ¹H NMR titration experiments. This study has demonstrated a clear example of the possibility of using dendrimers as drug carriers via the recognition and encapsulation of selected guest drug molecules.

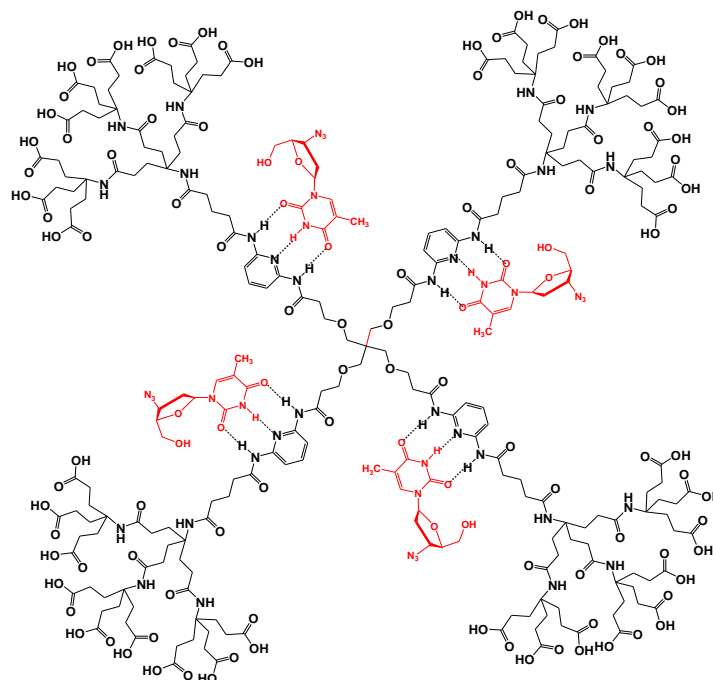


Figure 1.9. Dendrimer with 3'-azido-3'-deoxythymidine (AZT) encapsulated *via* hydrogen bonding.

Dendrimers have also attracted considerable attention as light harvesting systems,^[44] since high degree of order and control over the layer-by-layer build up of the dendrimer structure allows the incorporation of a variety of chromophoric molecules at predetermined and well-arranged sites in the structure, to construct an efficient light harvesting device. The multivancy at the periphery, and the relatively short distance between the relevant donor/acceptor units allows efficient energy transfer. Moreover, the presence of internal cavities can facilitate energy transfer from numerous dendrimer chromophoric units to ionic or neutral luminescent guest molecules. This can also help tune the wavelength of the sensitized emission by changing the luminescent guest molecule in the same dendrimer.

Hahn and coworkers have prepared a fascinating light harvesting dendritic system with a total of 64 chromophoric units of three different types (Figure 1.10).^[45] Upon introducing a suitable guest molecule to the internal cavity, electronic energy was successfully collected from all chromophoric units with high efficiency. The synthesis was achieved using PPI dendrimer generation

2 that was functionalized with eight 5-dimethylamino-1-naphthalenesulfonyl (dansyl) chromophoric groups, followed by the attachment of dendrons containing 24 dimethoxybenzene units in their backbone, and 32 naphthalene-type units at the periphery.

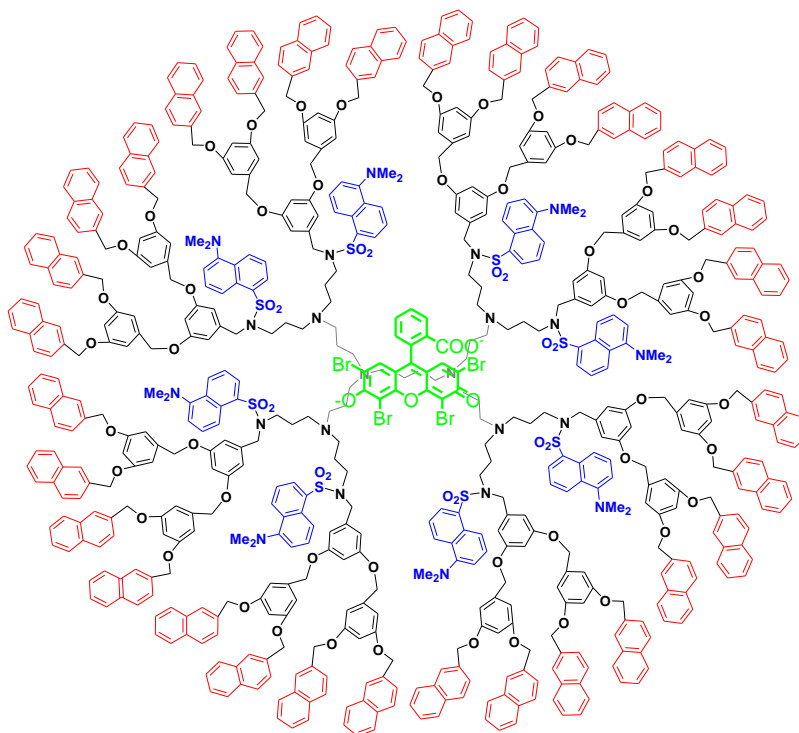


Figure 1.10. Hahn's Light harvesting dendrimer with eosin fluorescent dye inside.

Quantitative measurements showed that the energy transfer from the peripheral dimethoxybenzene and naphthalene chromophores to the fluorescent dansyl units (intramolecular process) occurs with over 90% efficiency. When the eosin fluorescent dye was encapsulated, due to its affinity to the PPI backbone, the dansyl fluorescence was quenched and that of the eosin guest was sensitized. Quantitative measurements showed that the eosin molecule harvested the electronic energy (intermolecular process) from all 64 chromophoric units of the dendrimer structure with an efficiency of over 80%. This example demonstrated that both intramolecular and intermolecular energy transfer processes can take place very efficiently using dendrimers via a resonance mechanism, if the donor/acceptor units of the dendrimers are chosen carefully to have a strong overlap

between their emission and absorption spectra respectively. This opens the door for further applications of dendrimers in solar energy conversion, and signal amplification for luminescence sensors.

In the mid 1990s, several groups realized that the interior tertiary amines and also the peripheral groups of PAMAM and PPI dendrimers can complex metal ions such as Cu^{2+} , Co^{2+} , Pt^{2+} , and Pd^{2+} .^[46] Since then, PAMAM dendrimers have been extensively used as templates for the formation of metallic nanoparticles (NPs). Pioneering work in this area has been carried out by the groups of Rempel,^[47] Esumi,^[48] and Crooks.^[49] The presence of tertiary amines and the ease of modifying the peripheral groups of PAMAM dendrimers made them ideal candidates for controlling the shape and size of metallic nanoparticles, while providing them with a stabilizing environment. Moreover, the presence of well defined internal cavities at higher generations provides protection, and selective access to the NPs. Crooks' group in particular, has focused on the synthesis of metal nanoparticles within the internal cavities of dendrimer by functionalizing the periphery of the dendrimer with non-complexing functional moieties such as hydroxyl groups. The latter allowed the metal ions to be complexed exclusively in the interior backbone of the dendrimer structure. Upon reduction, the dendrimer-encapsulated nanoparticles (DENs) are formed. The use of dendrimers has provided tremendous advantages for the design and synthesis of stable metal NPs with tremendous potential in designing novel materials for diverse applications in biomedicine, catalysis, and optoelectronics.

The peripheries of dendrimers can be modified to construct dendritic unimolecular micelles, first introduced by Newkome's group. The latter are superior to traditional micelles because of their ability to retain the colloidal structure regardless of the concentration, ionic strength, or temperature.^[50] The backbone of the dendrimer can also be utilized to bring in and encapsulate certain guests. Pan and Ford attached hydrophobic octyl arms to a 4th generation PPI dendrimer via amidation of octanoyl chloride with the primary amine groups at the periphery.^[51] Reduction of the resulting amide using LiAlH_4 afforded the

secondary amine, which was used to attach the hydrophilic triethylene glycol (triethylenoxy methyl ether) via the amidation of its acid chloride form. The reduction step was then repeated to yield the bifunctionalized polyamine dendrimer (Figure 1.11).

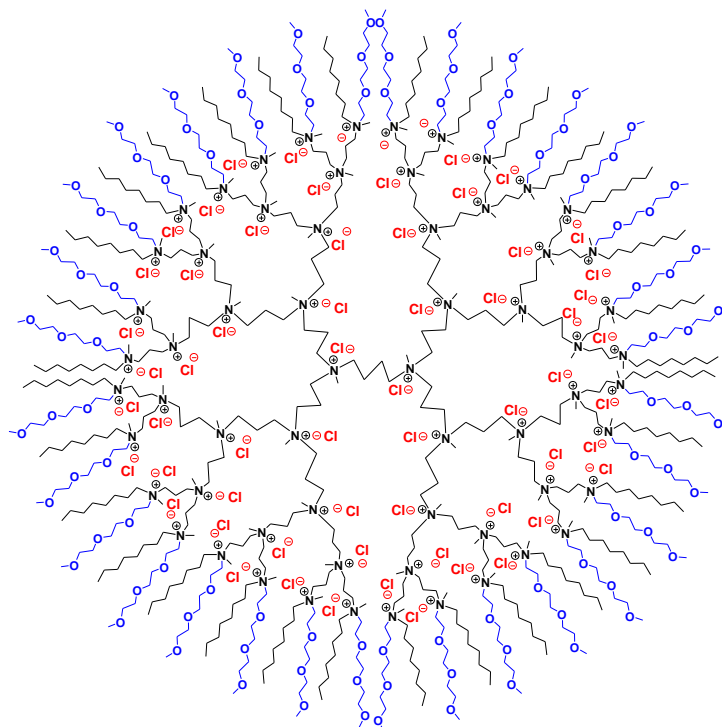


Figure 1.11. Ford's PPI dendrimer based unimolecular micelle.

The tertiary amines in the backbone of the dendrimer were quaternized with methyl iodide, and subsequently converted to the corresponding ammonium chloride by a simple ion exchange. These ammonium chloride dendrimers were found to be soluble in both organic solvents as well as in water, and provided aqueous solubility for the encapsulated lipophilic compounds such as pyrene and Reichardt's dye. They showed remarkable increase in the rates of catalytic decarboxylation of 6-nitrobenzoxazole-3-carboxylic acid in water, in comparison to their hydrophilic dendrimer counterparts. Moreover, evaluation of the binding constants of these dendrimers has shown positive dependence on the generation number, depicting the synergistic dendrimer generation effect. This example constitutes a clear demonstration of the effectiveness in tuning the

periphery of the dendrimers in order to manipulate or enhance their catalytic activity.

1.5 Functionalizing the periphery

1.5.1 Monofunctional dendrimers

The periphery of PPI dendrimers has been successfully functionalized with different types of fluorescent molecules including fluorescent dansyl units.^[52] The attachment of 32 dansyl units was achieved by reacting dansyl chloride with the commercially available PPI dendrimer generation 4 (Figure 1.12).^[53] The interaction of Co^{2+} ions, as nitrate salt, with the dendrimer backbone caused a strong quenching of all the dansyl units at the periphery.^[54] It was shown that the quenching occurs upon coordination of the metal ions to the aliphatic amine groups in the interior of the PPI dendrimer.

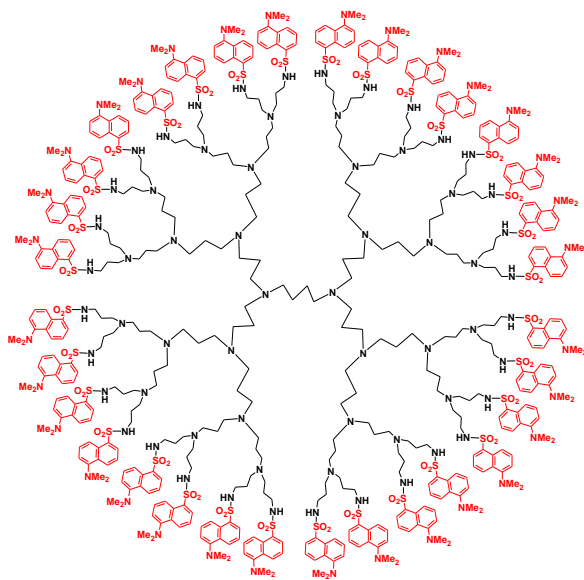


Figure 1.12. PPI dendrimer generation 4 functionalized with dansyl groups.

Interestingly, at higher dendrimer generations, the presence of only one Co^{2+} ion guest was sufficient to quench every dansyl unit at the periphery. This represented a 32 times increase in sensitivity, in comparison to a normal single dansyl unit, and it demonstrates the use of the dendrimer backbone as a platform for coordinating guest molecules which allows them to interact with the

periphery groups. There is a significant potential for the use of such dendrimers as fluorescent sensors for metal ions, with signal amplification and enhanced sensitivity, since the metal analyte can interact with a large number of fluorescent units.

Incorporating catalytic metal centers into the core or at the periphery have attracted the attention of many scientific groups because of the advantages including providing extra thermal and mechanical stability, to improved solubility.^[55] If the catalytic center is incorporated at the core or in the cavities of the dendrimer, selective catalysis can be achieved based on the size of the reactants and the opening to the internal cavities. Moreover, due to their relatively larger size, catalytic dendrimers can be removed or separated from the reaction mixture using different separation techniques, such as nanofiltration, membrane separation, and precipitation.^[56]

The first dendrimer based catalytic system was reported by van Koten and coworkers, where they functionalized the periphery of polysilane dendrimers (Figure 1.13) with diaminoarylnickel(II) complexes (pincer species).^[57] These metallodendrimers were found to successfully catalyze the Kharasch addition of polyhaloalkanes to alkenes. Moreover, the use of such a system for continuous catalytic processes, using a membrane reactor, showed promising results. In their original work, van Koten and coworkers have attached a carbamate unit to the carbosilane framework to allow the rapid attachment of the pincer species. Since this could potentially limit further reactivity with different reagents such as alkyl lithium, they changed that link between the aryl ring and the pincer to silyl groups, which gave a library of dendrimers with tunable crowding at the periphery.

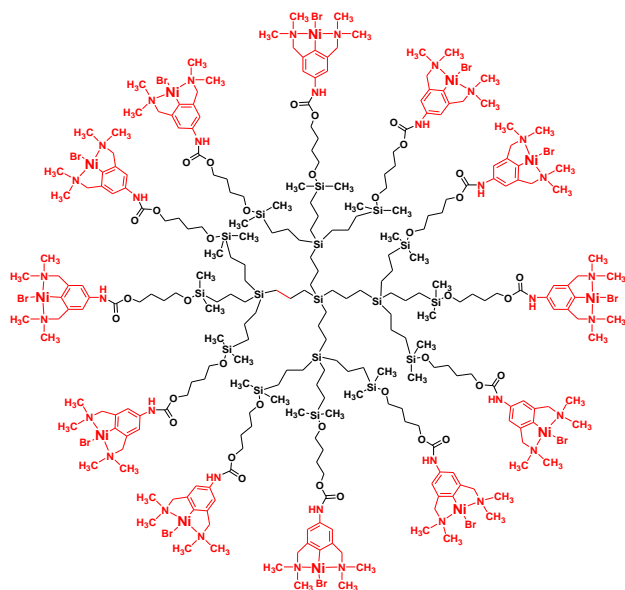


Figure 1.13. van Koten's polysilane dendrimers with peripheral diaminoarylnickel(II) complexes.

Polycationic metallodendrimers have been used as redox sensors for the recognition of inorganic anions. The incorporation of redox centers in a dendritic platform provided extra stability and enhanced redox potentials. Moreover, the dendrimer generation effect was apparent when cyclic voltammetric studies showed improved sensing and recognition as the dendrimer generation gets higher. Pioneering work in this field includes that of van Koten,^[58] Keifer,^[59] and Astruc^[60] groups.

For example, Astruc's group presented the synthesis of various stable polycationic metallodendrimers using condensation reactions of a nona-amine and chlorocarbonyl cyclopentadienyl-iron and cobalt sandwich type complexes, and other dendritic backbones containing peripheral amide-linked ferrocenyl units.^[60] More recently, Astruc and coworkers have reported a faster and more efficient synthesis of dendrimers linked by 1,2,3-triazole rings using Cu(I) catalyzed cycloaddition between azides and alkynes (CuAAC) click reaction, which was further used to click ferrocenyl groups functionalized with azide groups at the peripheries of the dendrimer (Figure 1.14).^[61]

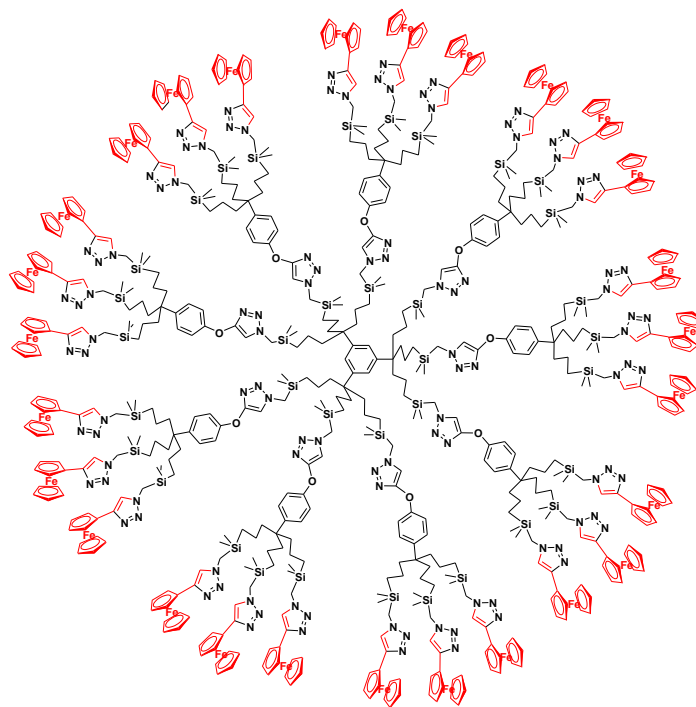


Figure 1.14. Astruc's dendrimer containing triazole rings and peripheral ferrocenyl groups.

The ability of the triazole rings to recognize and bind oxo anions and metal cations was investigated while using the ferrocenyl groups at the periphery as redox monitors. The results showed selective recognition of oxo anions such as H_2PO_4^- and ATP_2^- , and transition metal cations such as Pd^{2+} and Pt^{2+} . This example demonstrated the use of metallodendrimers with internal recognition sites for potential encapsulation, transport, and catalysis applications.

Dendrimers have been investigated for various potential applications in medicine such as drug delivery and organelle targeting *via* the attachment of therapeutic or receptor molecules to the periphery.^[62] Due to their homogenous polyvalent structure, dendrimers constitute excellent candidates for cooperative interactions involved in immuno-regulation *via* cell-surface interactions, which makes them superior to their structurally heterogeneous linear polymer counterparts.^[63]

Shaunak *et al* have used the carboxylic acid-terminated PAMAM dendrimer to covalently attach glucosamine and glucosamine 6-sulfate to the

periphery using 1-ethyl-3-(3-dimethylaminopropyl) carbodiimide hydrochloride (EDCI) (Figure 1.15).^[64]

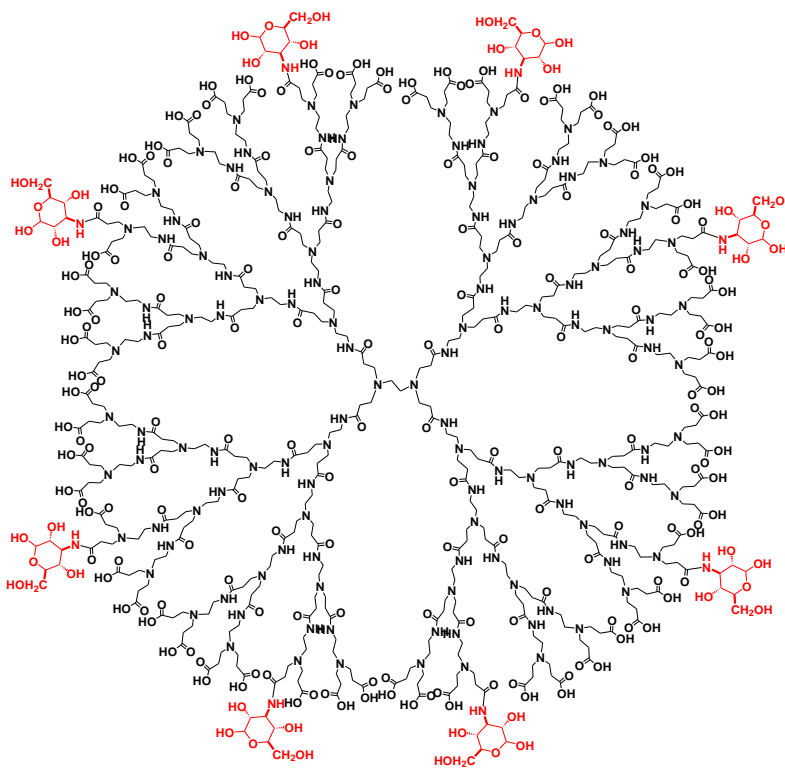


Figure 1.15. Water soluble PAMAM dendrimer with glucosamine at the periphery.

The dendrimer-glucosamine and the sulphated dendrimer-glucosamine were found to have immuno-modulatory and anti-angiogenic properties, respectively. The water soluble conjugates were then used in combination, to prevent scar tissue formation after glaucoma filtration surgery, synergistically, which increased the long term success of this surgery from 30% to 80%. This work has shown that the anionic carboxylic acid-terminated PAMAM dendrimers are neither toxic nor immunogenic, and can be used to target pro-inflammatory mediators and neovascularization to prevent scar tissue formation. Furthermore, since the two receptors involved in this healing mechanism are involved with other diseases, these conjugates could have potential applications in other diseases, and surgical procedures.

1.5.2 Multifunctional dendrimers

Hydrophobic drug molecules can also be attached covalently to dendrimers through hydrolytically labile linkages. However, the dendritic structure must provide the aqueous solubility at the same time. Synthetically this implies a more difficult approach to introduce different functional groups, and consequently different molecules including drugs and solubilising agents, to the periphery of the dendrimer.^[65] Fréchet's group has achieved this goal by using a polyether dendrimer that contains two different types of chain end functionalities. One of these functionalities was used to attach short PEG chains to bring in water solubility, and the other chain ends were used to link model drugs such as cholesterol, phenylalanine, and tryptophan *via* carbonate, ester, and carbamate linkages respectively (Figure 1.16).^[66]

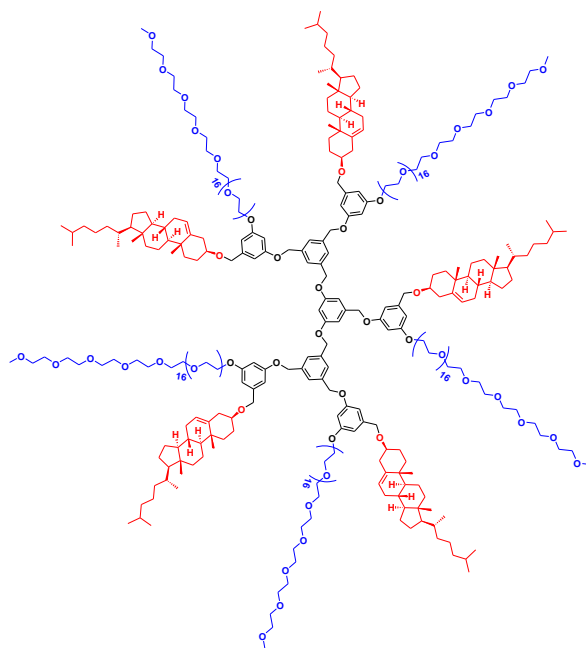


Figure 1.16. Fréchet's PEG-cholesterol-dendrimer conjugate.

The introduction of the two functionalities on the surface of the dendrimer was made possible using a clever way of constructing a dendrimer with a polyether framework that contains 5 free benzylic alcohols and five protected phenols with *tert*-butylchlorodiphenyl silyl (TBDPS) groups. Upon removal of the TBDPS protective groups, the coupling of the mesylate-

terminated PEG chains *via* Williamson ether synthesis was achieved. The remaining hydroxyl groups were utilized to attach the model drug molecules. For example, cholesterol was attached by activating its hydroxyl group with carbonyl diimidazole, and subsequently coupling it to the dendrimer's hydroxyl groups using a catalytic amount of sodium hydride to afford the PEG-cholesterol-dendrimer conjugate. It is worth noting here that even with the extreme hydrophobicity of cholesterol, the conjugate system was still water soluble, which indicates that this model can be valid for other types of drug molecules. Despite the fact that such systems are meant for testing the design features of dendrimers, they indeed show the possibility of multi-functionalization of the surface of the dendrimer to include drug molecules together with other functionalities to provide solubility and eventually targeting.

More recently, Fréchet and coworkers demonstrated a rapid and scalable synthesis of bifunctional dendrimers containing both alkynes and protected aldehydes on the periphery for orthogonal functionalization reactions.^[67] The synthesis involved building aliphatic polyester dendrimer based on 2,2-bis(hydroxymethyl)propanoic acid (bis-HMPA) using pentaerythritol as a core (Figure 1.17). The symmetric cyclic carbonate periphery was reacted efficiently and cleanly with aminoacetaldehyde-dimethylacetal to yield a dendrimer with eight acetal groups, and eight primary alcohols. Subsequent activation of the free alcohols with 1,1'-carbonyldiimidazole and reaction with propargylamine gave the desired product. This example offers potential as a platform for drug delivery applications, because attachment of therapeutic molecules can be combined with solubilising agents or imaging probes at the periphery of such dendrimers. The acetal groups can be deprotected to be used in aldehyde involving reactions, which are orthogonal to subsequent click reactions that can be performed using the free acetylene groups.

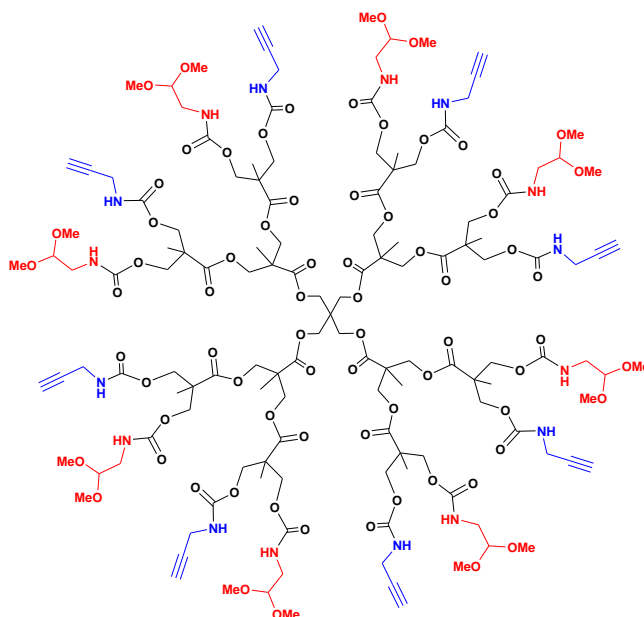


Figure 1.17. Bifunctional dendrimer for orthogonal functionalization.

Organometallic moieties, such as ferrocene and cobaltocenium, have also been incorporated separately at the periphery of the PPI dendrimers, and shown to create multi-site redox-active guests in a soluble supramolecular assembly.^[68] Later on, Casado and coworkers have successfully incorporated both redox active moieties into the periphery of the same dendritic structure.^[69] The bifunctionalized dendrimers depicted the reversible properties of the neutral ferrocenes as oxidation and the cationic cobaltoceniums as reduction sites in the same dendritic structure (Figure 1.18). As expected, the ratio of the two active units at the periphery had an interesting effect on the solubility of such a macromolecular assembly. The higher the loading of cobaltocenium, the more soluble the assembly was in water, and less soluble in dichloromethane. The ratio could be varied by changing the stoichiometry of the metallocene starting materials. The synthesis was achieved by reacting the primary amines of PPI dendrimer generations 1-4 with equimolar amounts of chlorocarbonylferrocene and the hexafluorophosphate salt of chlorocarbonylcobaltocenium. The desired products were isolated as air-stable solids.

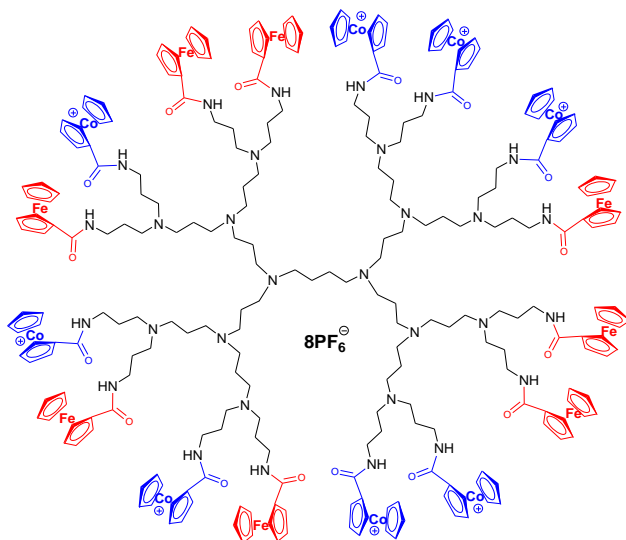


Figure 1.18. PPI dendrimer generation 3 with both ferrocene and cobaltocenium at the periphery.

The goal was to obtain same number of two different metallocene units at the periphery. However, in reality the presence of two different molecules competing for the same reactive groups at the periphery would not allow that, and a mixture of different compounds with different ratios of the two metal centers were obtained and isolated. These bifunctional dendrimers were used to modify electrode surfaces, and were successfully used as glucose sensors. The ferrocene units mediated the enzymatic process under anaerobic conditions, and the cobaltocenium units participated in the electrocatalytic process in the presence of oxygen. These bifunctionalized dendrimers demonstrated the possibility of tuning the surface charge density of dendrimers, and thus changing their solubility.

An ideal targeted drug delivery system consists of a uniform, stable and nontoxic material that can accommodate multiple components such as a therapeutic drug, a targeting agent, and a fluorescent sensor.^[70] Such drug delivery systems can be extremely beneficial in cancer therapy for enhancing drug efficacy, and eliminating side effects due to the ability to deliver the therapeutic cytotoxic agents to specific cell type or tissue without affecting the healthy tissues.^[71] Dendrimers constitute highly suitable candidates for such

systems due to their monodispersity and their modifiable multivalent peripheries. Dendrimer-drug conjugates have been shown to increase the aqueous solubility of the drug and its plasma half life.^[72] Moreover, dendritic systems can be used to target tumors via the enhanced permeability and retention (EPR) phenomenon that is characteristic of tumor tissues.^[73] PAMAM dendrimers have been widely used for delivering drugs, DNA and MRI contrast agents.^[74]

In their pioneering work for designing drug delivery systems using PAMAM dendrimers, Baker and coworkers have prepared a trifunctional dendrimer conjugate containing folic acid (FA) as a targeting agent, methotrexate (MTX) as a therapeutic drug, and fluorescein-5-thiosemicarbazide (FITC) as a sensing agent (Figure 1.19).^[75] The cellular internalization and cytotoxicity of the trifunctional system were evaluated in vitro. For this purpose, PAMAM dendrimer generation 5 was used to covalently attach the FITC using thiourea linkages, followed by the attachment of FA via an amide link, and finally the anchoring of MTX through an ester linkage.

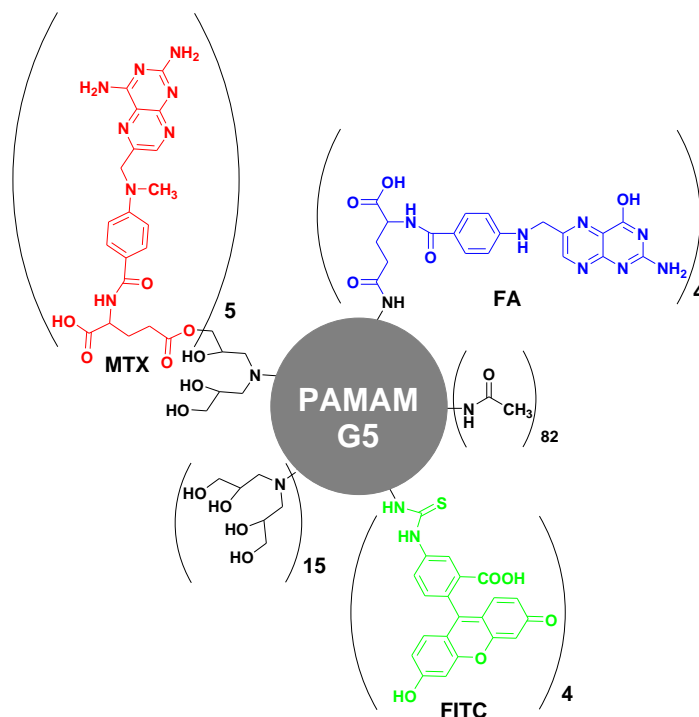


Figure 1.19. 5th Generation PAMAM dendrimer functionalized with folic acid (FA), methotrexate (MTX), and fluorescein-5-thiosemicarbazide (FITC) at the periphery.

It is worth mentioning here that the terminal amine groups of the dendrimer had been neutralized by partial acetylation to prevent non-specific binding with cell membrane, increase aqueous solubility, and reduce toxicity. In-vitro experiments have confirmed that this trifunctional device does indeed bind and induce cytotoxicity in FA receptor-expressing KB cells, thus inhibiting their growth. It was demonstrated that this process took place in a receptor specific manner because conjugates of MTX with the dendrimer, without FA, had failed to inhibit the cell growth. Furthermore, cytotoxicity studies have shown that the covalent attachment of MTX to the dendritic platform is better suited for specific targeting in comparison to the dendrimer encapsulated MTX, which had similar activity to the free drug. This engineered device has demonstrated the use of dendrimers in cancer targeting and imaging, which can potentially be used to overcome the side effects of chemotherapy and some types of drug resistance when using the free drug.

1.6 Dendrimers containing heteroatoms and transition metal centers

Even though most of the initial work involving the synthesis of dendrimers used organic chemistry, inorganic and organometallic chemists have also kept up with the concept, and have employed their skills to the development of unique inorganic and organometallic dendrimers for applications in electrochemistry, catalysis, imaging, and even therapeutics.^[68] Examples of dendrimers containing heteroatoms such as bismuth, boron, silicon, phosphorous, and germanium have also been reported.^[76] The introduction of latter into dendrimers has yielded dendrimers with intriguing properties and applications. For example, phosphorous containing dendrimers reported by Majoral's group have shown potential significant potential in biomedical applications.

The first example of dendrimers containing heteroelements was reported by Rebrov and coworkers in 1989, in which they synthesized a silicon based fourth generation dendrimer that had siloxane linkages in the backbone and forty

eight ethoxy groups at its periphery.^[77] Since then, several examples of dendrimers having siloxane, carbosilane or silane linkages at the branching points have appeared in the literature through the work of various groups including Masamune,^[78] Imae,^[79] Dubois,^[80] Kakkar,^[81] Mollen^[82] and others. While most syntheses of silicon-containing dendrimers followed the divergent methodology, Morikawa and co-workers prepared the first silicoxane-carbosilane dendrimer using the convergent methodology (Figure 1.20).^[83] The branching points in this methodology were carbosilane, while the siloxane units were used to attach the linear components in all branches.

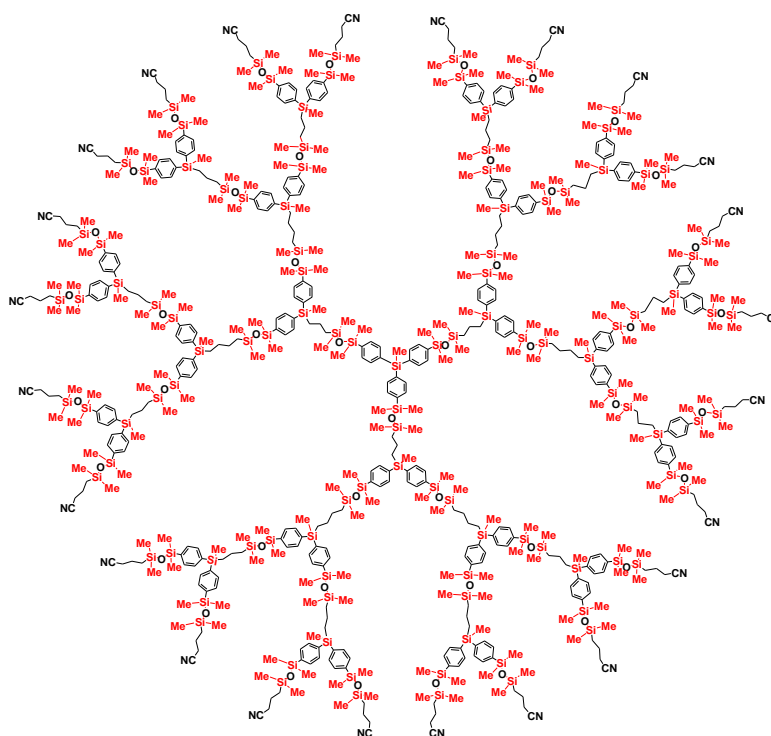


Figure 1.20. Morikawa's Silicoxane-carbosilane dendrimer.

Their synthetic methodology involved three sequential steps to build dendrons up to the third generation. The starting allyl cyanide monomers were first hydrosilylated with chlorodimethylsilane to afford a silane containing intermediate, followed by amination with diethylamine. The resulting structure was reacted with the building block, 4-(hydroxydimethylsilyl) phenylmethylsilane, to yield the first-generation dendron with two peripheral cyanide groups and an olefin. The repetition of the synthetic steps allowed the

construction of up to the fourth generation dendron. Dendron generation 3 was then reacted with a suitable trivalent core containing Si-OH groups to yield the third generation dendrimer.

The introduction of organometallic centers into dendrimers provides unique properties and different reactivity patterns.^[18,84] In 1994, Puddephatt and coworkers reported the first synthesis of dendrimers containing Pt centers as an integral part of the dendritic skeleton.^[85] Since then, several examples in the literature have been presented by the groups of Takahashi,^[86] Leininger,^[87] Humphrey^[88] and others.

Takahashi and coworkers reported the synthesis of organo-platinum dendrimers of different sizes based on the Pt-acetylide linkages using convergent, divergent, or a combination of the two synthetic methodologies (Figure 1.21).^[86] In general, the procedure relied on using Cu(I)-catalyzed coupling reaction of Pt-Cl groups and terminal acetylenes.

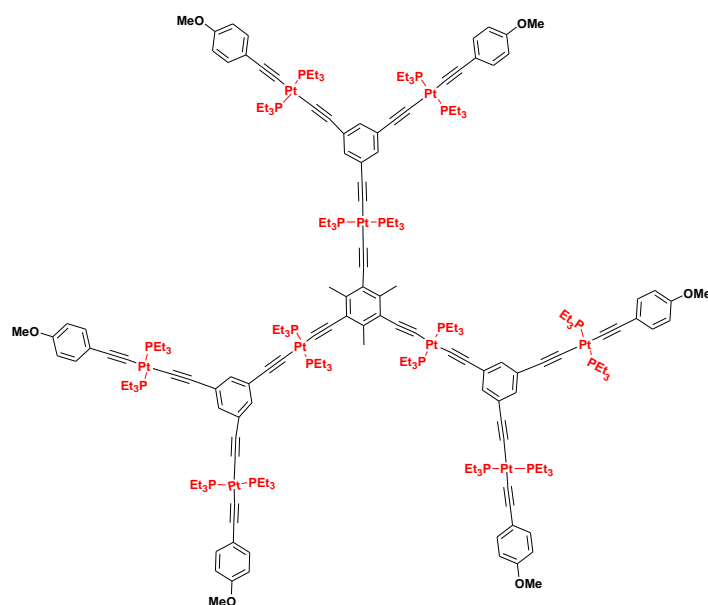


Figure 1.21. An organo-platinum dendrimer.

In their recent work, large platinum-acetylide dendrimers containing up to sixty platinum atoms were synthesized using the convergent methodology.^[89] The synthesis of dendrons up to the third generation was achieved by the smart design of a building block containing three acetylene arms protected with two

different trialkylsilyl groups: two arms protected with trimethylsilyl groups, and the other arm was protected with triisopropylsilyl. Upon deprotection of the trimethylsilyl groups selectively with K_2CO_3 , two free acetylene groups were available for reaction with terminal *p*-methoxyphenyl)ethynylplatinum moieties in the presence of Cu(I) catalyst. The removal of the triisopropylsilyl group using a stronger reagent (Bu_4NF) afforded the first dendron generation containing one free acetylene group. Separately, another building unit can also be functionalized with Pt-Cl groups by a coupling reaction to the free acetylenes, the reaction of which with 2 equivalents of the first dendron, followed by another deprotection step, allows the construction of the second generation dendron. Reiteration of these 2 synthetic steps gave the 3rd generation dendron. Each of these dendrons was then complexed to a trivalent chloroplatinum-acetylide complex to yield the corresponding dendrimer. Even though steric hinderance prevented the construction of dendrimer generations higher than the 3rd, this synthetic route has demonstrated a very versatile method for construction of organometallic nanomaterials.

The introduction of bulky ruthenium metal centers into a dendritic skeleton have been studied by Humphrey's group, and they used a coupling reaction between Ru-Cl groups with terminal acetylene groups to build the dendritic structure (Figure 1.22).^[88] In contrast to the Pt centers described above, the bulkier $Ru(1,2\text{-bis(diphenyl phosphino)ethane})_2$ required a more open core and building units with larger distance between the arms. For that purpose, arylethynyl spacer (1-iodo-4-trimethylsilylethynylbenzene) was linked to the 1,3,5-triethynylbenzene using the Sonogashira coupling, followed by removal of the trimethylsilyl groups. The acetylene arms were then reacted with the bulky Ru complex, to give a trivalent core complex containing three Rh-Cl groups available for further reaction with the previously synthesized dendrons. The resulting dendrimer with 9 bulky Ru centers was shown to be stable under different oxidative and thermal conditions. Furthermore, it was shown to exhibit interesting non-linear optical (NLO) properties that can be switched on and off using electrochemical stimuli.

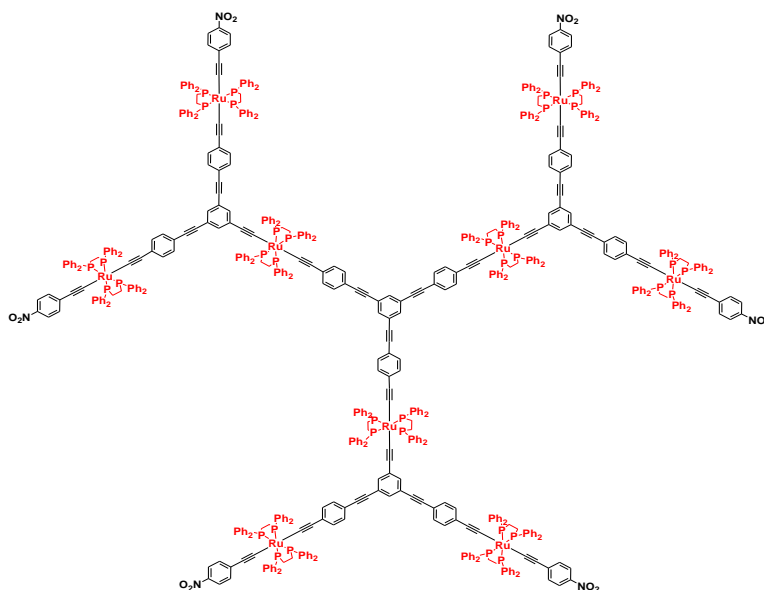


Figure 1.22. Humphrey's ruthenium containing dendrimer.

This showed the possibility to synthetically modify certain building blocks to create a suitable platform for the inclusion of bulky metallic centers in an electron rich dendritic structure. This methodology can be further extended to construct higher dendrimer generations for tailored materials applications.

In 1990, Rengan and Engel synthesized the charged dendrimers containing phosphorus at the core and in the branching points of the backbones.^[90] A few years later, the synthesis of neutral phosphorus-containing dendrimers appeared in the literature. Since then, the modification and functionalization of phosphorous-containing dendrimers has blossomed for various applications in catalysis and pharmacology. For example, incorporation of Pt, Pd, Ni metallic centers in some of these dendrimers gave rise to complexes with catalytic functions including electrochemical reduction of carbon dioxide.^[91] Majoral's group has synthesized a library of phosphorous-containing dendrimers via reiterative methodology using two reactions involving nucleophilic substitution and condensation in a sequential fashion starting from cyclotriphosphazene (P_3N_3) core to yield different dendrimer generations (Figure 1.23).^[92] Surface modification of these dendrimers gave rise to monosubstituted, symmetrically disubstituted, and asymmetrically substituted phosphorous

containing dendrimers with phosphonic or carboxylate groups. It was demonstrated that their phosphonic acid capped dendrimers selectively target and activate human monocytes. To prove the biological role of this bio-tool, one of the surface azabisphosphonic groups of the dendrimer was replaced statistically with fluorescein-5-thiosemicarbazide (FITC) using a synthetic methodology that involved orthogonal reactivity. This revealed the details of the interactions between dendrimers and cells, and emphasized the importance of dendrimers as tunable biomaterials for therapeutic applications.

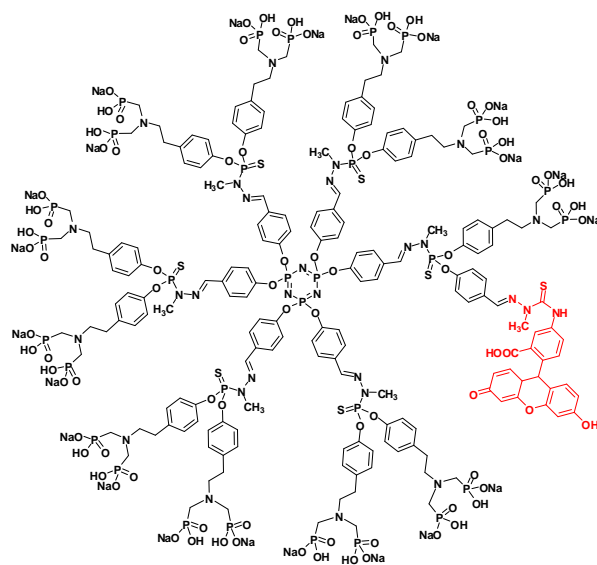
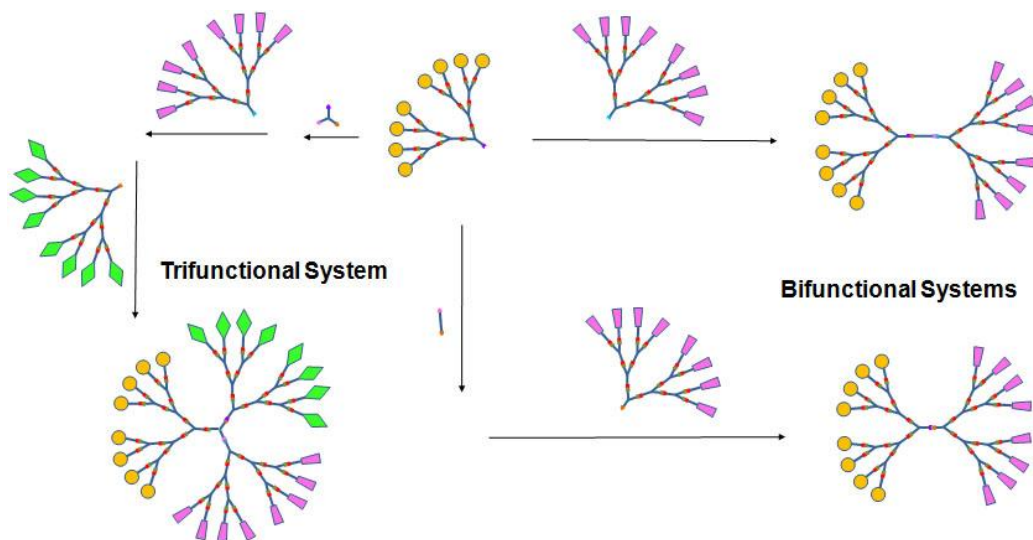


Figure 1.23. Majoral's phosphorus containing dendrimer with fluorescein-5-thiosemicarbazide (FITC) at the periphery.

1.7 Multiblock dendrimers

Because dendrons are built and functionalized independently, different functions can be incorporated into separate dendrons before converging them onto a common core, leading to a multifunctional block-type dendrimer (Scheme 1.2). Diblock or triblock dendrimers can be constructed using this methodology. The triblock dendrimer is structurally similar to that of the traditional globular shape. However, using different types of cores, new morphologies can be obtained. Focally activated dendrons have been widely used in a variety of macromolecular dendritic systems by capping the end groups of small bridging units, or attached to another dendron with different surface groups directly.



Scheme 1.2. A schematic summary of the different routes used to construct multiblock dendrimers.

Lee and coworkers reported the synthesis of a diblock dendrimer containing both Fréchet type and PAMAM dendrons (Figure 1.24).^[93] Their general procedure involved the modification of the focal point of the former to include an azide functional group, and the modification of the latter's focal point with a free alkyne group. The efficient CuAAC click reaction was then used to stitch the two componently differentiated dendrons together.

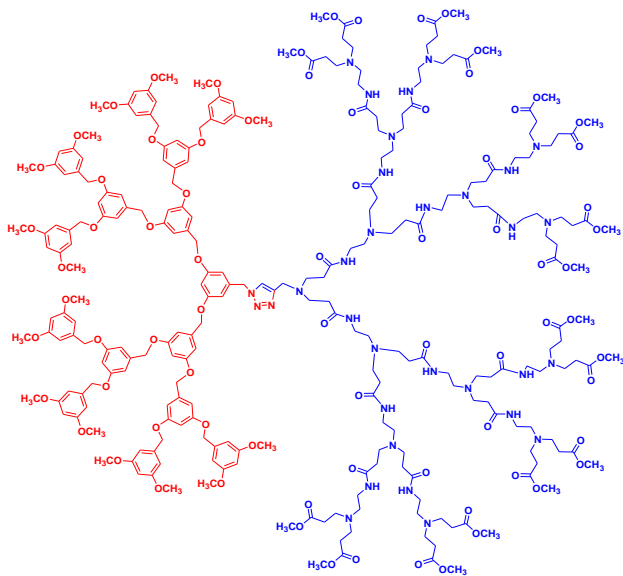


Figure 1.24. A diblock dendrimer containing both Fréchet-type and PAMAM dendrons.

The use of click chemistry in this case is believed to be a key factor in allowing such combination, especially for the synthesis of higher dendrimer generations. Using this general strategy, the synthesis of diblock dendrimers of different sizes was achieved. The latter allowed tunable applications of these macromolecules, by taking advantage of the amphiphilicity of the system for encapsulation, and combining multiple functionalities.

Another example of using poly(aryl ether) Fréchet-type dendrons was achieved by his own group by combining two dendrons with two different functional groups at their peripheries using a small divalent linking unit as a core, and it led to a series of dendrimers with enhanced dipole moments (Figure 1.25).^[94] Both dendrons contained benzylbromide as the active focal point, however, one was pre-functionalized with electron-withdrawing cyano groups and the other with electron-donating benzyloxy groups. The two dendrons were then covalently attached to 4,4'-dihydroxybiphenyl via its phenolic groups.

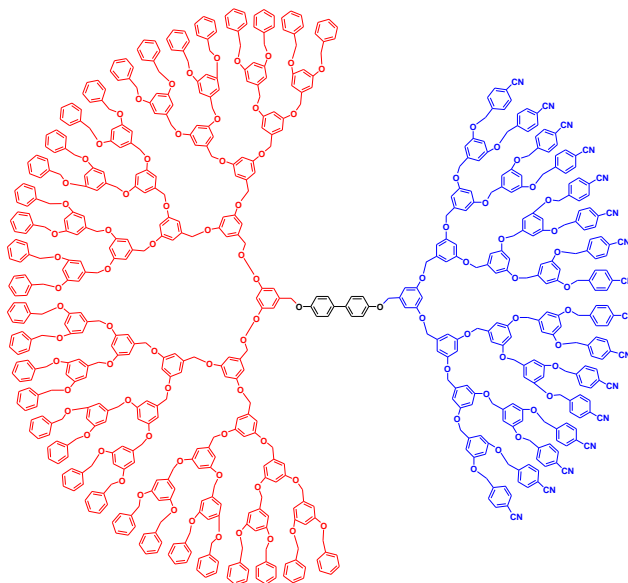


Figure 1.25. Dipolar dendrimer based on Fréchet's dendrons.

The placement of two dendrons at opposing sites created a dipole moment that became stronger as the generation number used was increased. This work demonstrated the possibility of combining different dendrons to create a polarity gradient that can be very useful for applications in nanotechnology such

as designing molecular machines or switches, and macromolecular nonlinear optics.

In their efforts to synthesize and design unusual nanoscopic structures for applications in materials science, Miller and coworkers prepared dumbbell-shape macromolecules by attaching flexible bulky dendrons at the ends of rigid rods (Figure 1.26).^[95] In their work, poly(aryl ether) dendrons of generations 1-4, were connected to either naphthalene diimides or rigid rod naphthalene diimide-benzidine oligomers to make the dumbbells. Since the imide groups of the rigid-rod core can be reduced, and the peripheries of the dendrons can be modified, this system provides a good example for building materials for electrical and optical properties. Electrochemical reduction experiments in DMF demonstrated the apparent effect of the dendrons on the reduction process with the larger dendron being more effective in slowing the electrochemical reaction.

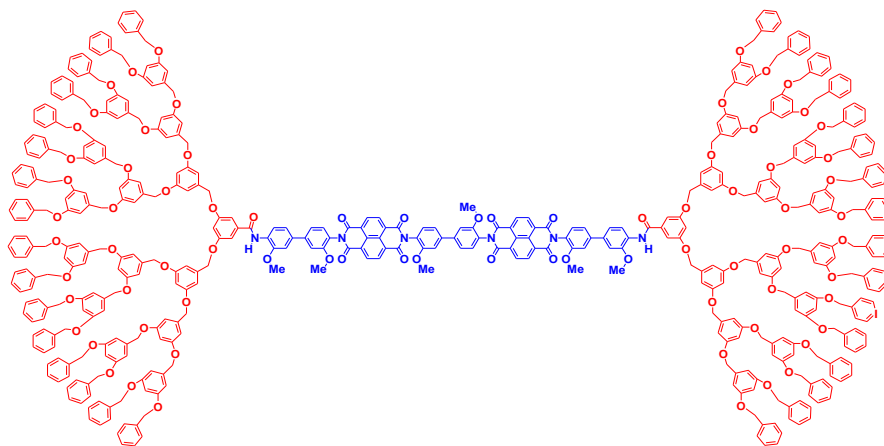


Figure 1.26. Miller's dumb-bell shape dendritic macromolecule.

In 2004, Fokin, Hawker and coworkers introduced the copper(I)-catalyzed azide-alkyne cycloaddition (CuAAC) click chemistry to the dendrimer field.^[96] Since then several groups have utilized this elegant reaction not only to decorate the dendrimer framework, but also to construct the dendrimer skeleton itself.^[97] Hawker and coworkers demonstrated how the efficient and versatile CuAAC click chemistry can be employed to build bifunctional dendrimers by employing a general synthetic strategy that allowed the construction of dendrimers containing orthogonal reactive blocks for the introduction of multiple

functions in the same framework (Figure 1.27).^[98] The synthesis of the backbone of the dendrons was based on the biocompatible 2,2-bis(hydroxymethyl)propionic acid (bis-MPA) building block to construct two dendrons: one that included hydroxyl groups at the periphery and an azide focal point, and the other one containing acetonide groups at the periphery with an alkyne at the focal point. Generations 1-4 of each of these dendrons were synthesized, and upon performing the CuAAC click reaction between the two dendrons, a library of amphiphilic dendrimers was put together.

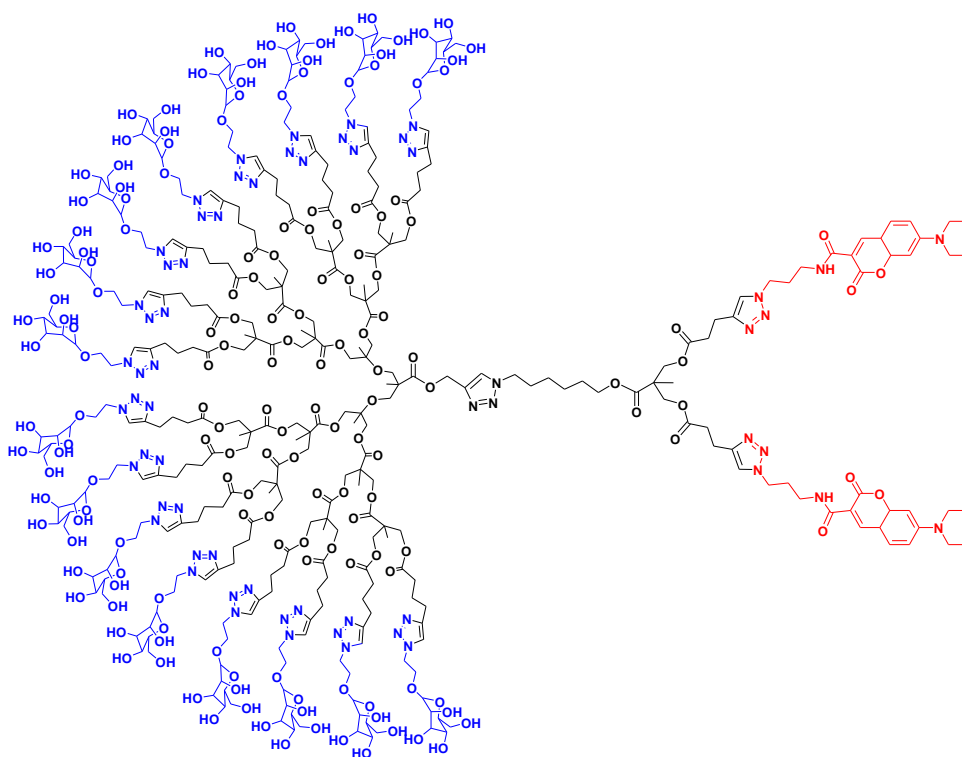


Figure 1.27. Hawker's bifunctional dendrimer containing coumarin dyes and protein-binding mannose molecules.

This novel design allowed the introduction of varied functional groups at different stages, and in this specific example, both peripheral sides were functionalized with alkyne groups to be used in further CuAAC click reactions. Using this platform, fluorescent coumarin dyes were successfully attached to one side, and 16 surface-active mannose groups on the 4th generation dendron on the other side. This unsymmetric bifunctional system combined recognition and

detection functions for the inhibition of hemagglutination. In fact, this unique dendritic structure proved to be 240 times more effective than the monomeric mannose in standard hemagglutination assay, and demonstrated the power of CuAAC click chemistry in constructing and introducing different functionalities to the dendrimer in a very efficient and easy fashion. This general synthetic strategy can be easily applied for the design and synthesis of various types of dendrimers for different applications.

Linking different entities onto a common core can be achieved using sequential reactive steps to introduce multiple functionalities in a multi-block fashion. It has been shown that trichlorotriazine (cyanuric chloride) can be sequentially decorated with one, two or three substituents by controlling the temperature of the reaction.^[99] Kaifer and coworkers have successfully combined three different entities in the same dendrimer using the triazine core (Figure 1.28).^[100] Two different dendron types (Fréchet and Newkome) and a redox active entity (ferrocene) were anchored on the same core, and combinations of different generation numbers of the two dendrons were tested for their effect on the redox activity of ferrocene.

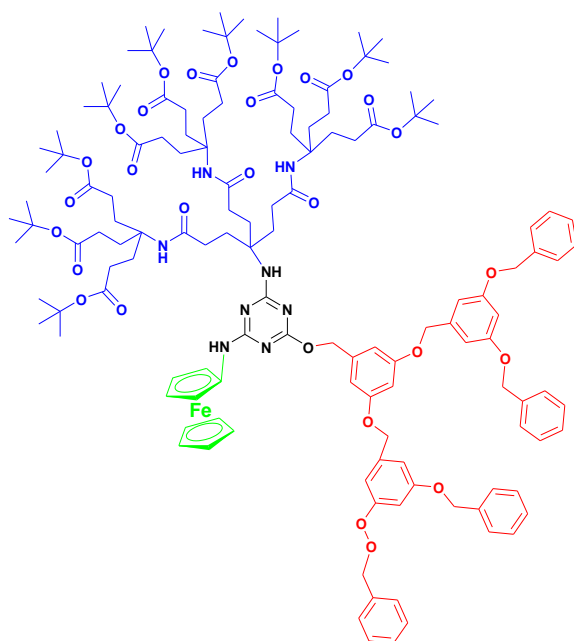


Figure 1.28. Triblock dendrimer containing Fréchet's and Newkome's dendrons and a redox active ferrocene molecule.

The anchoring of Fréchet-type dendrons of generations one, two or three to benzyl alcohol at the focal point, was followed by the attachment of Newkome-type dendron (up to the third generation) at room temperature. Finally the redox active amino ferrocene was covalently attached in refluxing THF, and the effect of different generation combinations on the microenvironment of the ferrocene active center was studied. Results showed that the Newkome-type dendrons are considerably more effective than the Fréchet-type dendrons in changing the half-wave potential for the one-electron oxidation of the ferrocenyl moiety. The latter can be justified by the fact that Newkome dendrons are more flexible and multivalent, and are thus capable of wrapping around the active center and altering its microenvironment more effectively, while Fréchet-type dendrons seem to grow away from the core. This example demonstrated the feasibility of building a multi-block dendrimer from a common core, and the fine tuning of the properties of redox active units by changing the type and generation number of the adjacent dendrons.

1.8 Dendrimers decorated with polymers

Dendrimers have also been periphery functionalized with linear polymers (Figure 1.29), and it has resulted in novel properties that combine the dendritic effect with the properties of linear polymers.

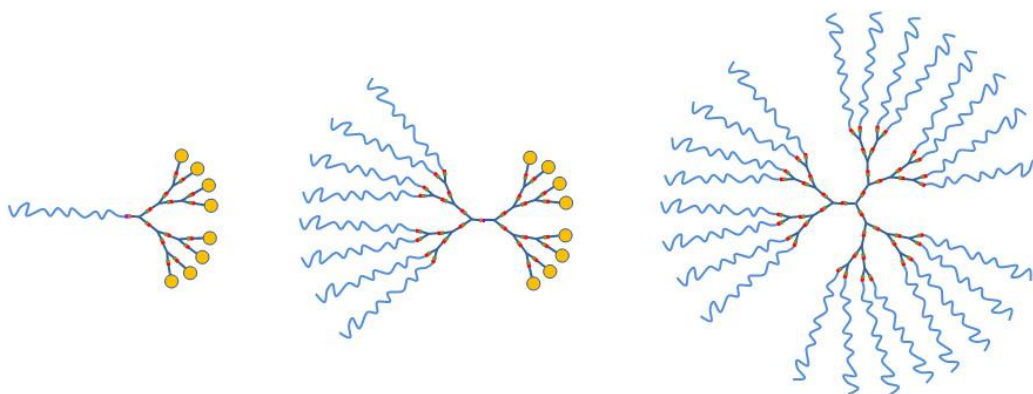


Figure 1.29. Examples of dendrimers decorated with linear polymer chains.

As mentioned above, a successful and efficient drug delivery system must combine a few characteristics including low polydispersity, water

solubility, no cytotoxicity, and the multivalent sites for the attachment of number of drug molecules.^[101] Currently only a few commercially available conventional polymers match all of these characteristics.^[65] The big challenge in this domain remains in combining the drug molecules with other solubilizing or targeting moieties in the same dendritic structure. Amphiphilic block copolymers have been studied extensively for their potential as drug delivery systems in aqueous solution by encapsulating drug molecules in their core which provides water solubility. Moreover, the relatively larger size has been shown to be very effective in avoiding rapid renal exclusion. Dendrimers and dendrons have also been functionalized with long polymer chains to prepare micelles based on the polymer-dendrimer conjugate.^[33] The presence of the dendritic structure at one end allows for further types of applications including encapsulation of the drug molecules in the dendritic cavities.

Gillies and Fréchet demonstrated the practicality of this design in delivering doxorubicin (DOX) as an anticancer drug (Figure 1.30).^[102] The system consisted of a hydrophilic PEO linear polymer attached to third generation polyester dendron containing cyclic hydrophobic acetals of 2,4,6-trimethoxybenzaldehyde at the periphery.

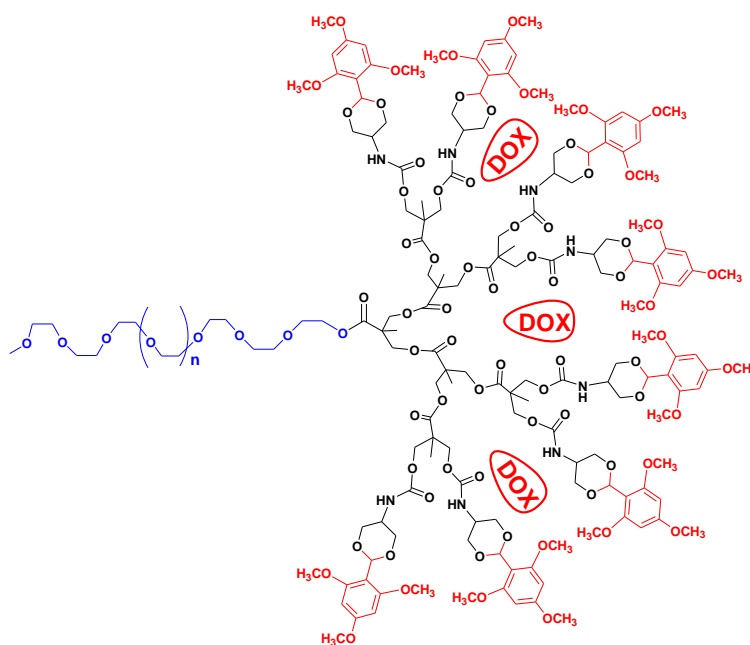


Figure 1.30. Hydrophilic PEO linear polymer attached to the 3rd generation polyester dendron with cyclic hydrophobic acetals of 2,4,6-trimethoxybenzaldehyde at the periphery, and encapsulated doxorubicin (DOX) molecules.

The dendritic wedge was capable of encapsulating the DOX molecules to be delivered. The acetal linkages were acid sensitive, and upon dropping the pH similar to that of the endosomes and lysosomes, the hydrophobic protective groups were removed. This cleavage step exposes the hydrophilic hydroxyl groups of the third generation in the core, thus destabilizing the micelle and causing the release of the therapeutic drug. It demonstrated the possibility of forming block copolymers containing dendrimers, and showed the unique advantages that emerge as a result of tailoring the dendritic structure.

Gillies and Fréchet successfully achieved the synthesis of a “bow-tie” type polyester dendrimer by covalently linking two polyester dendrons (Figure 1.31).^[25,103] One of the two dendrons has free hydroxyl groups available for attaching solubilising agents, while the other dendron has orthogonally protected hydroxyl groups at the periphery, which can be later deprotected and used for attaching drug molecules.

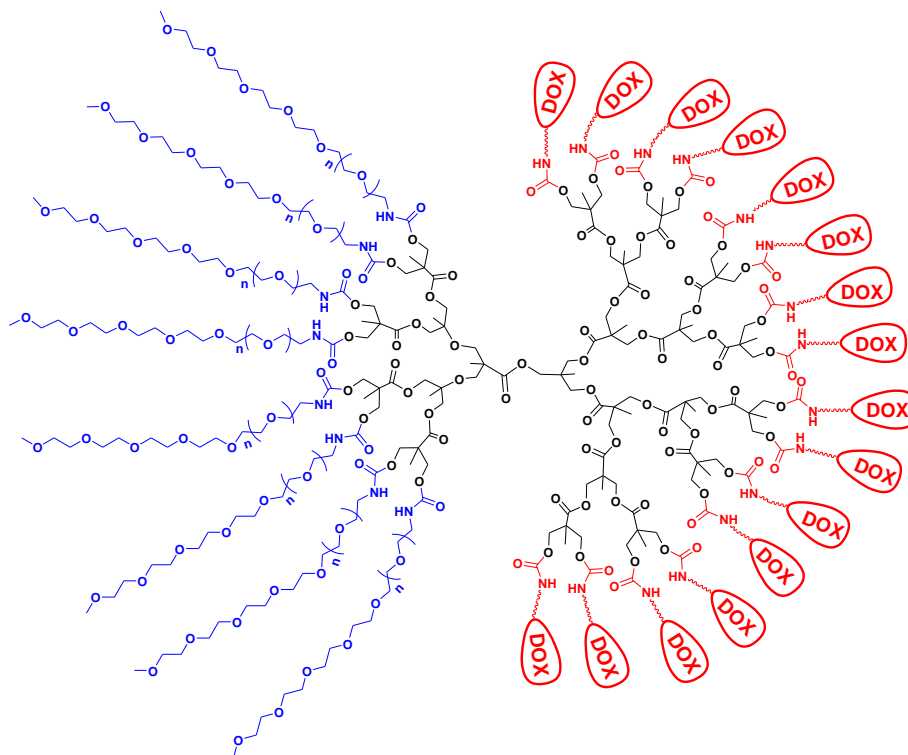


Figure 1.31. Gillies' "bow-tie" polyester dendrimer containing PEO linear polymer chains and covalently attached doxorubicin (DOX) molecules.

The synthetic strategy involved the preparation of a polyester dendron using 2,2-bis(hydroxymethyl)propionic acid as a building block with protected peripheral groups, in a convergent way. The focal point of this dendron was then activated, and used for the divergent synthesis of the second dendron with free hydroxyl groups at the periphery. It is essential to mention here that the protective groups used in the divergent synthesis were benzylidene acetals, which can be selectively removed without affecting the isopropylidene acetal groups at the periphery of the other side of the "bow-tie". The two dendrons were coupled convergently, but the yields were low due to steric factors. Poly(ethylene oxide) (PEO) chains were then attached to the side that contains the free hydroxyl groups, and then covalently attaching the amine-functionalized PEO chains. Consequently the acetonide protective groups in the other side were removed to give hydroxyl terminated side, which was eventually used to attach hydrophobic therapeutic drugs such as doxorubicin as shown in Figure 1.30. As

a matter of fact, the bow-tie system containing doxorubicin attached to the 4th generation dendron was found to cure mice bearing C-26 colon carcinomas. The generation number from each side and the size of the PEO chain used were varied, and a variety of combinations have shown different results with regard to the plasma circulation time and the tumour uptake. This study demonstrates a high degree of control in the number of peripheral groups available for drug loading, as well as the combination of solubilising agents such as polymer chains with therapeutic drugs in the same dendrimer.

Several research groups have demonstrated the possibility of providing aqueous solubility to drugs by entrapping them inside the hydrophobic core of conventional micelles made from amphiphilic block copolymers.^[104] The layer-by-layer build up of dendrimers, and the possibility of covalently attaching hydrophilic peripheral layer to a hydrophobic core, allows the build up of what is commonly referred to as unimolecular micelle.

Fréchet's group have demonstrated an elegant example of dendritic unimolecular micelle by coupling the phenolic periphery of their hydrophobic dendrimers with poly(ethylene glycol) (PEG) mesylate chains via nucleophilic displacement to provide aqueous solubility, while being biocompatible for potential pharmaceutical applications (Figure 1.32).^[105]

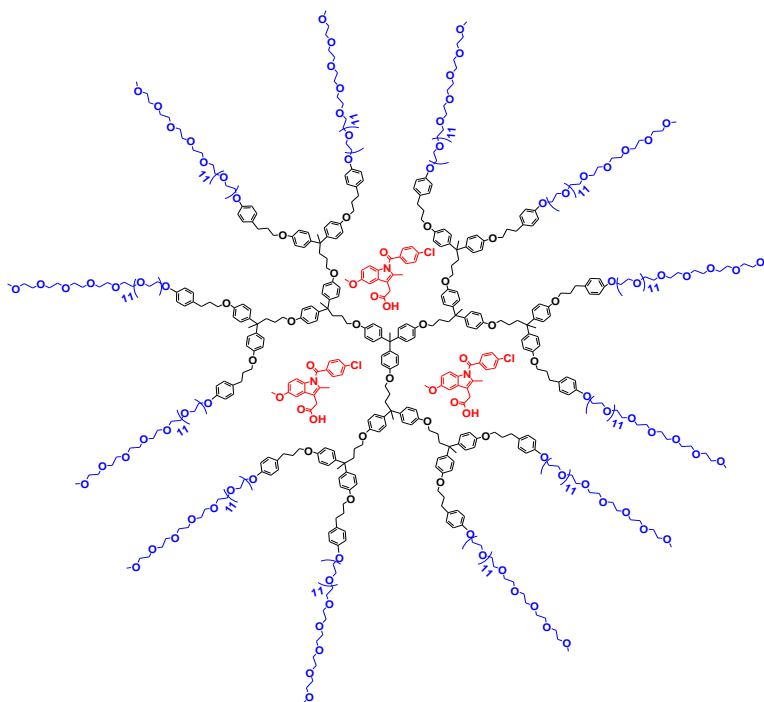


Figure 1.32. Fréchet's dendritic unimolecular micelle with PEG polymer chains at the periphery and encapsulated indomethacin drug molecules.

The choice of the building unit (4,4-bis(4'-hydroxyphenyl) pentanol) of the hydrophobic dendritic core was particularly interesting. It provided more flexibility than the commonly used 3,5-dihydroxybenzyl alcohol (DHBA) to the hydrophobic core, thus increasing its loading capacity for guest molecules. For example, 11% w/w loading of the model drug (indomethacin) into the generation 3 unimolecular micelles was achieved. The release of the drug is a critical factor in drug delivery, and the indomethacene model drug release from the dendrimer unimolecular micelle was sustained over 30 hours as opposed to the rapid release over 4 hours using conventional micelles. It demonstrated the feasibility of using dendrimers to encapsulate and deliver drug molecules, while providing extra stability as a unimolecular micelle, for pharmacological applications in drug delivery.

1.9 Dendronized Polymers

Dendrons can also be grafted onto conventional polymers of different types in order to modify their chemophysical properties (Figure 1.33). Examples

in the literature range from peripheral modifications of multi-arm polymers, or attaching dendrons to multiple locations on the backbone of linear and cyclic polymers.^[5,22]

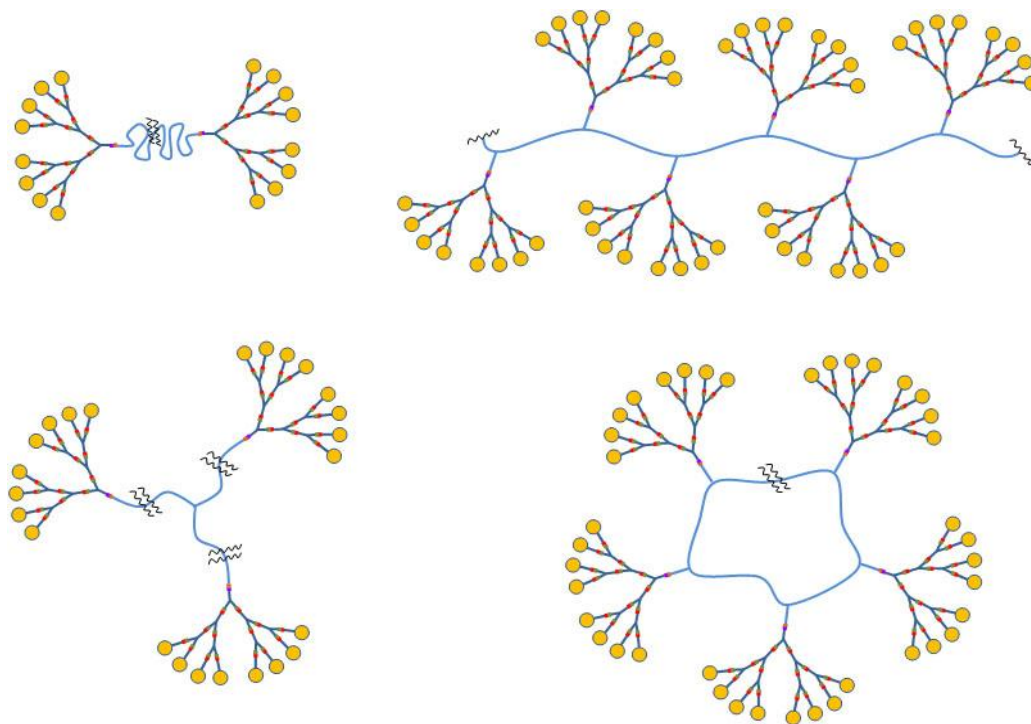


Figure 1.33. Examples of linear polymers decorated with dendrons.

In most cases, the convergent methodology is used to establish multiple focal points on the backbone of the polymers suitable for attaching the desired dendrons through their activated focal points.^[106] However, there are examples of using the divergent methodology as well in such a design by building the dendrons from specific branching points in the polymer backbone.^[107]

The incorporation of Fréchet-type dendrons with linear divalent polymeric units including poly(ethylene oxide) (PEO), poly(ethylene glycol) (PEG), polyester and polystyrene chains were the first to appear in the literature.^[108] Eventually, multivalent polymeric chains were also employed for the same purpose.^[109] One of the earliest examples of such systems was that reported by Gitsov and coworkers, in which two highly hydrophobic aromatic polyether Fréchet-type dendrons were attached to a linear PEO or PEG chain by coupling the ends of the linear chain to the focal points of the dendrons (Figure

1.34).^[110] The incorporation of dendritic wedges into polymer chains affords new properties that can expand the scope of applications of such materials.

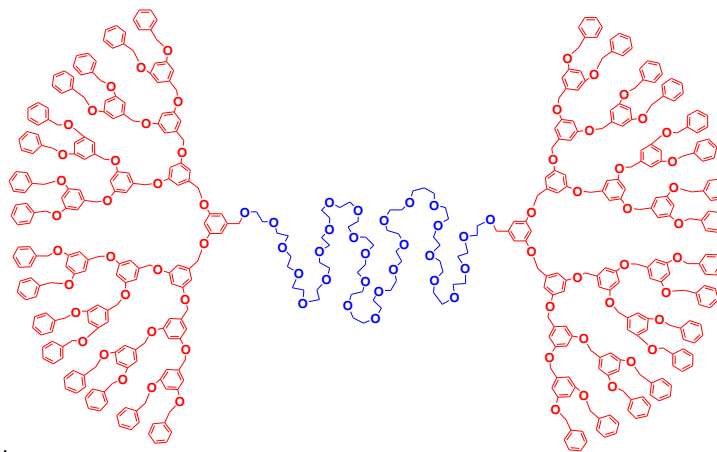


Figure 1.34. Fréchet-type dendrons attached to the ends of a long linear PEG polymer chain.

The other examples shown in the Figure 1.33 are from the work of several groups, in particular of Schlüter and Percec, in the design and development of dendron grafted polymeric materials using several polymerization techniques including ring-opening metathesis,^[111] radical polymerization of styrenes,^[112] Suzuki polycondensation,^[113] *etc.* More recently, examples of macrocyclic polymers functionalized with dendrons have appeared, including the pioneering work of Grayson and coworkers.^[114] Macrocyclic polymers have interesting properties, and have been shown to be more monodisperse than their linear analogs, and the macrocyclization process provides a more well-defined shape and size for the polymer. However, the synthesis of macrocyclic polymers is more challenging, especially in terms of preparing functionalized macrocycles.^[115]

1.10 Summary and outlook

This review had aimed at highlighting the developments in the synthesis of dendrimers which is now an art in itself, in the design of such nanomaterials with varied shapes and sizes, including the combination of dendrimers with conventional linear polymers. Dendrimers have been demonstrated to invoke

novel applications in a variety of fields, and some of these are expected to lead to actual commercialization in the very near future. The key to such an achievement is to introduce multiple functions into the same dendritic framework. We made an attempt here to depict the elegance of synthetic methodologies that has led to the design of a variety of such mono- and multi-functional dendrimers. In particular, the introduction of the so called “click” reactions has certainly paved the way to overcome daunting challenges that were faced previously. Considering the relatively young age of such macromolecules, the potential offered and demonstrated applications of such systems, can offer novel solutions to challenging issues especially in the medical field. It is apparent that an important factor in designing multi-tasking dendrimers is the development of important building blocks that would facilitate their synthesis through orthogonal functionalization. “Click” chemistry has indeed revolutionized the synthesis, and the dendrimer field is definitely on the right track towards their inclusion into industrial applications for applications in numerous fields.

1.11 Scope of the thesis

Although the synthesis of dendrimers has advanced since the first report of such macromolecules almost 3 decades ago, only a few dendrimers have found their way into actual practical industrial and medical applications. Therefore, there is still need for more efficient and quantitative synthetic strategies, and a detailed understanding of the structure-property relationships in dendrimers, to enhance their feasibility into practical applications. It is also well understood now that it is essential to introduce multiple functions into the same dendritic scaffold for complex applications in the medical field. The key to achieve this goal lies in the smart design of versatile building blocks suitable for the construction of these macromolecules. This thesis presents efficient and quantitative synthetic strategies for the synthesis of such intriguing nanostructures, an evaluation of their structure using a combination of experiment with theory, and demonstrates the ease with which multi-tasking can

be introduced into dendrimers by covalently linking therapeutic and imaging agents.

Chapter 2 describes detailed theoretical and experimental studies to understand the structure of 3,5-dihydroxybenzyl alcohol based dendrimers, evolution of internal cavities in them, and their potential in encapsulating guest molecules.

Chapter 3 describes an inorganic synthetic route, which is developed to construct rigid-rod type dendrimers that depict intriguing photophysical properties. A detailed theoretical study is used to evaluate the structure of such dendrimers that adopt a turbine type shape, and a model reaction is then presented to exploit their potential to incorporate metallic centers into the backbone of these dendrimers by direct substitution of dimethyltin centers with square planar platinum moieties.

Chapter 4 describes an elegant synthesis of building blocks that can be used to construct dendritic frameworks using the efficient Cu^{I} catalysed alkyne azide coupling (“click”) chemistry.

Chapter 5 contains synthetic details of novel and versatile building blocks capable of introducing multiple functions into the same dendritic scaffold using “click” chemistry, and the actual utilization of these building blocks to construct dendrimers containing covalently linked fluorescent dyes and drug molecules, and a detailed pharmacological evaluation of their effects in biological systems.

Chapter 6 provides a summary of our findings in the field of dendrimers, and a future outlook in this topical area of research.

Appendix I provides more details about the theoretical investigation of the structure of DHBA-based dendrimer generations 1-5.

1.12 References

- [1] [1a] K. L. Kiick, *Science* **2007**, *317*, 1182; [1b] R. Langer and D. A. Tirrell, *Nature* **2004**, *428*, 487.
- [2] [2a] C. Fischbach, D. J. Mooney, *Biomaterials* **2007**, *28*, 2069; [2b] M. P. Lutolf, J. A. Hubbell, *Nat. Biotech.* **2005**, *23*, 47; [2c] C. Fischbach, D. J. Mooney, *Biomaterials* **2007**, *28*, 2069; [2d] R. Dancun, *Nature* **2003**, *2*, 347.
- [3] J. M. J. Fréchet, D. A. Tomalia, *Dendrimers and Other Dendritic Polymers*, John Wiley & Sons, Chichester, **2001**.
- [4] [4a] J.R. Baker, A. Quintana, L. Piehler, M. Banazak-Holl, D. A. Tomalia, *Biomed. Microdevices* **2001**, *3*, 61; [4b] D. A. Tomalia, I. J. Majoros, *Supramol. Polym. J. Macromol. Sci. C-Polym. Rev.* **2003**, *43(3)*, 441; [4c] D. Bhadra, S. Bhadra, S. Jain, N. K. Jain, *Int. J. Pharm.* **2003**, *257*, 111.
- [5] [5a] F. Zeng, S. C. Zimmerman, *Chem. Rev.* **1997**, *97*, 1681; [5b] A. Carlmark, C. Hawker, A. Hult, M. Malkoch, *Chem. Soc. Rev.* **2009**, *38*, 352.
- [6] G. R. Newkome, C. N. Moorefield, F. Vögtle, *Dendrimers and Dendrons: Concepts, Syntheses, Applications*, Wiley-VCH, Weinheim, **2001**.
- [7] [7a] D. A. Tomalia, D. M. Hedstrand, M. S. Ferritto, *Macromolecules* **1991**, *24*, 1435; [7b] M. Gauthier, M. Möller, *Macromolecules* **1991**, *24*, 4548.
- [8] S. T. Teertstra, M. Gauthier, *Prog. Polym. Sci.* **2004**, *29*, 277.
- [9] M. Gauthier, *J. Polym. Sci., Part A: Polym. Chem.* **2007**, *45*, 3803.
- [10] [10a] A. Hult, M. Johansson, E. Malmström, *Adv. Polym. Sci.* **1999**, *1*, 143; [10b] A. Garcia-Bernaby, M. Kramer, B. Olah, R. Haag, *Chem. Eur. J.* **2004**, *10*, 2822; [10c] A. Hirao, K. Sugiyama, A. Matsuo, Y. Tsunoda, T. Watanabe, *Polym. Int.* **2008**, *57*, 554.
- [11] M. Kramer, J.F. Stumby, G. Grimm, B. Kaufmann, U. Kruger, M. Weber; R. Haag, *Chem. Bio. Chem.* **2004**, *5*, 1081.
- [12] [12a] Y. H. Kim, *J. Polym. Sci., Part A: Polym. Chem.* **1998**, *36*, 1685; [12b] R. Haag, *Angew. Chem.* **2004**, *116*, 280.
- [13] [13a] M. W. P. L. Baars, E. W. Meijer, *Top. Curr. Chem.* **2000**, *210*, 131; [13b] S. E. Stiriba, H. Frey, R. Haag, *Angew. Chem.* **2002**, *114*, 1385.
- [14] B. Helms, E. W. Meijer, *Science* **2006**, *313*, 929.

-
- [15] A. K. Patri, I. J. Majoros, J. R. Baker, *Current Opinion in Chemical Biology* **2002**, *6*, 466.
- [16] S. Langereis, A. Dirksen, T. M. Hackeng, M. H. P. van Genderena, E. W. Meijer, *New J. Chem.* **2007**, *31*, 1152.
- [17] S. Svenson, D. A. Tomalia, *Advanced Drug Delivery Reviews* **2005**, *57*, 2106.
- [18] P. A. Chase, R. J. M. Klein Gebbink, G. van Koten, *J. Organomet. Chem.* **2004**, *689*, 4016.
- [19] B. Helms and J. M. J. Fréchet, *Adv. Synth. Catal.* **2006**, *348*, 1125.
- [20] R. M. Crooks, M. Zhao, L. Sun, V. Chechik, L. K. Yeung, *Acc. Chem. Res.* **2001**, *34*(3), 181.
- [21] A. W. Bosman, H. M. Janssen, E. W. Meijer, *Chem. Rev.* **1999**, *99*, 1665.
- [22] S. M. Grayson, J. M. J. Fréchet, *Chem. Rev.* **2001**, *101*, 3819.
- [23] G. Franc, A. K. Kakkar, *Chem. Eur. J.* **2009**, *15*, 5630.
- [24] [24a] H. C. Kolb, M. G. Finn, K. B. Sharpless, *Angew. Chem. Int. Ed.* **2001**, *40*, 2004; [24b] G. Franc, A. Kakkar, *Chem. Commun.* **2008**, 5267.
- [25] E. R. Gillies, J. M. J. Fréchet, *J. Am. Chem. Soc.* **2002**, *124*, 14137.
- [26] E. Buhleier, W. Wehner, F. Vögtle, *Synthesis* **1978**, 155.
- [27] D. A. Tomalia, H. Baker, J. R. Dewald, M. Hall, G. Kallos, S. Martin, J. Roeck, J. Ryder, P. Smith, *Polym. J.* **1985**, *17*, 117.
- [28] G. R. Newkome, Z.-Q. Yao, G. R. Baker and V. K. Gupta, *J. Org. Chem.* **1985**, *50*, 2004.
- [29] G. R. Newkome, C. N. Moorefield, E. He, *Chem. Rev.* **1999**, 1689.
- [30] P. Antoni, D. Nystrom, C. J. Hawker, A. Hult, M. Malkoch, *Chem. Commun.* **2007**, 2249.
- [31] C. J. Hawker, J. M. J. Fréchet, *J. Chem. Soc., Chem. Comm.* **1990**, 1010.
- [32] W. Maes, W. Dehaen, *Eur. J. Org. Chem.*, 2009, 4719.
- [33] I. Gitsov, *J. Polym. Sci. Part A: Polym. Chem.* **2008**, *46*, 5295.
- [34] F. Zeng, S. C. Zimmerman, *J. Am. Chem. Soc.* **1996**, *118*, 5326.
- [35] [35a] R. H. Jin, T. Aida, S. Inoue, *J. Chem. Soc., Chem. Commun.* **1993**, 1260; [35b] D. L. Jiang, T. Aida, *Chem. Commun.* **1996**, 1523; [35c] R.

Sadamoto, N. Tomioka, T. Aida, *J. Am. Chem. Soc.* **1996**, *118*, 3978; [35d] D. L. Jiang, T. Aida, *J. Macromol. Sci., Pure Appl. Chem.* **1997**, *A34*, 2047; [35e] D. L. Jiang, T. Aida, *J. Am. Chem. Soc.* **1998**, *120*, 10895; [35f] S. Machida, K. Sugihara, I. Takahashi, K. Horie, D. L. Jiang, T. Aida, *J. Polym. Sci., Part B: Polym. Phys.* **2002**, *40*, 210; [35g] Y. J. Mo, D. L. Jiang, M. Uyemura, T. Aida, T. Kitagawa, *J. Am. Chem. Soc.* **2005**, *127*, 10020.

[36] [36a] P. Bhyrappa, J. K. Young, J. S. Moore, K. S. Suslick, *J. Am. Chem. Soc.* **1996**, *118*, 5708; [36b] P. Bhyrappa, G. Vaijyanthimala, K. S. Suslick, *J. Am. Chem. Soc.* **1999**, *121*, 262.

[37] [37a] P. J. Dandliker, F. Diederich, M. Gross, C. B. Knobler, A. Louati, E. M. Sanford, *Angew. Chem. Int. Ed. Engl.* **1994**, *33*, 1739; [37b] J. P. Collman, L. Fu, A. Zingg, F. Diederich, *Chem. Commun.* **1997**, 193; [37c] A. Zingg, B. Felber, V. Gramlich, L. Fu, J. P. Collman, F. Diederich, *Helv. Chim. Acta.* **2002**, *85*, 333; [37d] S. van Doorslaer, A. Zingg, A. Schweiger, F. Diederich, *Chem. Phys. Chem.* **2002**, *3*, 659.

[38] B. Helms, C. O. Liang, C. J. Hawker, J. M. J. Fréchet, *Macromolecules* **2005**, *38*, 5411.

[39] G. E. Oosterom, J. N. H. Reek, P. C. J. Kamer, P. W. N. M. van Leeuwen, *Angew. Chem. Int. Ed.* **2001**, *40*, 1828.

[40] C. Muller, L. J. Ackerman, J. N. H. Reek, P. C. J. Kamer, P. W. N. M. van Leeuwen, *J. Am. Chem. Soc.* **2004**, *126*, 14960.

[41] E. M. M. de Brabander-van den Berg, E. W. Meijer, *Angew. Chem. Int. Ed.* **1993**, *32*, 1308.

[42] [42a] J. F. G. A. Jansen, E. M. M. de Brabander-van den Berg, E. W. Meijer, *Science* **1994**, *266*, 1226; [42b] J. F. G. A. Jansen, E. M. M. de Brabander-van den Berg, E. W. Meijer, *Rec. Trav. Chim. Pays-Bas* **1995**, *114*, 225; [42c] J. F. G. A. Jansen, R. A. J. Janssen, E. M. M. de Brabander-van den Berg, E. W. Meijer, *Adv. Mater.* **1995**, *7*, 561; [42d] J. F. G. A. Jansen, E. W. Meijer, E. M. M. de Brabander-van den Berg, *Macromol. Symp.* **1996**, *102*, 27.

-
- [43] [43a] G. R. Newkome, B. D. Woosley, E. He, C. N. Moorefield, R. Guther, G. R. Baker, G. H. Escamilla, J. Merrill, H. Luftmann, *Chem. Commun.* **1996**, 2737; [43b] G. R. Newkome, *J. Het. Chem.* **1996**, 33:1445.
- [44] [44a] S. Jordens, G. De Belder, M. Lor, G. Schweitzer, M. Van der Auweraer, T. Weil, E. Reuther, K. Müllen, F. C. De Schryver, *Photochem. Photobiol. Sci.*, **2003**, 2, 177; [44b] V. Balzani, P. Ceroni, M. Maestri, V. Vicinelli, *Current Opinion in Chemical Biology* **2003**, 7, 657.
- [45] U. Hahn, M. Gorka, F. Vögtle, V. Vicinelli, P. Ceroni, M. Maestri, V. Balzani, *Angew. Chem. Int. Ed.* **2002**, 41, 19.
- [46] [46a] L. Balogh, D.A. Tomalia, *J. Am. Chem. Soc.* **1998**, 120, 7355; [46b] R. M. Crooks, M. Zhao, L. Sun, V. Chechik, L. K. Yeung, *Acc. Chem. Res.* **2001**, 34(3), 181.
- [47] X. Peng, Q. Pan, G. L. Rempel, *Chem. Soc. Rev.* **2008**, 37, 1619.
- [48] K. Esumi, A. Suzuki, N. Aihara, K. Usui, K. Torigoe, *Langmuir* **1998**, 14, 3157.
- [49] [49a] M. Zhao, L. Sun, R. M. Crooks, *J. Am. Chem. Soc.* **1998**, 120, 4877; [49b] R. W. J. Scott, O. M. Wilson, R. M. Crooks, *J. Phys. Chem. B* **2005**, 109, 692.
- [50] G. R. Newkome, C. N. Moorefield, G. R. Baker, M. J. Saunders, S. H. Grossman, *Angew. Chem., Int. Ed. Engl.* **1991**, 30, 1178.
- [51] Y. Pan, W. T. Ford, *Macromolecules* **2000**, 33, 3731.
- [52] P. Ceroni, G. Bergamini, F. Marchioni, V. Balzani, *Prog. Polym. Sci.* **2005**, 30, 453.
- [53] V. Balzani, P. Ceroni, S. Gestermann, C. Kauffmann, M. Gorka, F. Vögtle, *Chem. Commun.* **2000**, 10, 853.
- [54] F. Vögtle, S. Gestermann, C. Kauffmann, P. Ceroni, V. Vicinelli, V. Balzani, *J. Am. Chem. Soc.* **2000**, 122, 10398.
- [55] I. Cuadrado, M. Moran, C. M. Casado, B. Alonso, J. Losada, *Coord. Chem. Rev.* **1999**, 395, 193.
- [56] E. de Jesus, J. C. Flores, *Ind. Eng. Chem. Res.* **2008**, 47, 7968.

-
- [57] [57a] J. W. J. Knapen, A. W. van der Made, J. C. de Wilde, P. W. N. M. van Leeuwen, P. Wijkens, D. M. Grove, G. van Koten, *Nature* **1994**, 372, 659; [57b] R. A. Gossage, L. A. van de Kuil, G. van Koten, *Acc. Chem. Res.* **1998**, 31, 423.
- [58] [58a] L. A. van de Kuil, D. M. Grove, J. W. Zwikker, L. W. Jenneskens, W. Drenth, G. van Koten, *Chem. Mater.* **1994**, 6, 1675; [58b] A. W. Kleij, R. A. Gossage, J. T. B. H. Jastrzebski, J. Boersma, G. van Koten, *Angew. Chem., Int. Ed.* **2000**, 39, 176.
- [59] [59a] C. M. Cardona, T. D. McCarley, A. E. Kaifer, *J. Org. Chem.* **2000**, 65, 1857; [59b] W. Ong, J. Grindstaff, D. Sobransingh, R. Toba, J. M. Quintela, C. Peinador, A. E. Kaifer, *J. Am. Chem. Soc.* **2005**, 127, 3353; [59c] D. Sobransingh, A. E. Kaifer, *Langmuir* **2006**, 22, 10540.
- [60] [60a] D. Astruc, F. Chardac, *Chem. Rev.* **2001**, 101, 2991; [60b] C. ValKrio, J. L. Fillaut, J. Ruiz, J. Guittard, J.C. Blais, D. Astruc, *J. Am. Chem. Soc.* **1997**, 119, 2588.
- [61] C. Ornelas, J. Ruiz Aranzaes, E. Cloutet, S. Alves, D. Astruc, *Angew. Chem. Int. Ed.* **2007**, 46, 872.
- [62] M. Islam, I. J. Majoros, J. R. Baker Jr., *J. Chromat. B Analyt. Technol. Biomed. Life Sci.* **2005**, 822, 21.
- [63] [63a] T. P. Thomas, I. J. Majoros, A. Kotlyar, J. F. Kukowska-Latallo, A. Bielinksa, *J. Med. Chem.* **2005**, 48(11), 3729; [63b] D. A. Tomalia, I. J. Majoros, *Supramol. Polym. J. Macromol. Sci. C-Polym. Rev.* **2003**, C43(3), 441.
- [64] S. Shaunak, S. Thomas, E. Gianasi, A. Godwin, E. Jones, I. Teo, K. Mireskandari, P. Luthert, R. Duncan, S. Patterson, P. Khaw, S. Brocchini, *Nature* **2004**, 22(8), 977.
- [65] E. R. Gillies, J. M. J. Fréchet, *D.D.T.* **2005**, 10(1), 35.
- [66] M. Liu, K. Kono, J. M. J. Fréchet, *J. of Pol. Sci.: Part A: Poly. Chem.* **1999**, 37, 3492.
- [67] A. P. Goodwin, S. S. Lam, J. M. J. Fréchet, *J. Am. Chem. Soc.* **2007**, 129, 6994.
- [68] D. Astruc, C. Ornelas, J. Ruiz, *Acc. Chem. Res.* **2008**, 41(7), 841.

-
- [69] C.M. Casado, B. Gonzaález, I. Cuadrado, B. Alonso, M. Moran, J. Losada, *Angew. Chem. Int. Ed.* **2000**, *39*, 2135.
- [70] A. D'Emanuele, D. Attwood, *Advanced Drug Delivery Reviews* **2005**, *57*, 2147.
- [71] E. C. Wiener, S. Konda, A. Shadron, M. Brechbiel, O. Gansow. *Invest. Radiol.* **1997**, *32*, 748.
- [72] A. K. Patri, J. F. Kukowska-Latallo, J. R. Baker Jr., *Advanced Drug Delivery Reviews* **2005**, *57*, 2203.
- [73] [73a] N. Malik, E. G. Evagorou, R. Duncan. *Anticancer Drugs* **1999**, *10*, 767; [73b] N. Malik, R. Wiwattanapatapee, R. Klopsch, K. Lorenz, H. Frey, J. W. Weener, E. W. Meijer, W. Paulus, R. Duncan, *J. Control. Release* **2000**, *65*, 133; [73c] R. Duncan, *Nat. Rev. Drug Discov.* **2003**, *2*, 347; [73d] H. Maeda, J. Wu, T. Sawa, Y. Matsumura, K. Hori, *J. Control. Release* **2000**, *65*, 271.
- [74] [74a] U. Boas, P. M. H. Heegaard, *Chem. Soc. Rev.* **2004**, *65*, 3343; [74b] J. F. Kukowska-Latallo, A. U. Bielinska, J. Johnson, R. Spindler, D. A. Tomalia, J. R. Baker Jr., *Proc. Natl. Acad. Sci.* **1996**, *93*, 4897; [74c] S. D. Konda, M. Aref, S. Wang, M. Brechbiel, E.C. Wiener, *Magma* **2001**, *12*, 104; [74d] E. C. Wiener, M. W. Brechbiel, H. Brothers, R. L. Magin, O. A. Gansow, D. A. Tomalia, P. C. Lauterbur, *Magn. Reson. Med.* **1994**, *31*, 1; [74e] C. R. DeMattei, B. Huang, D. A. Tomalia, *Nano Lett.* **2004**, *4(5)*, 771.
- [75] [75a] T. P. Thomas, I. J. Majoros, A. Kotlyar, J. F. Kukowska-Latallo, A. Bielinska, A. Myc, J. R. Baker Jr., *J. Med. Chem.* **2005**, *48*, 3729; [75b] I. J. Majoros, C. R. Williams, A. Becker, J. R. Baker Jr., *Nanomedicine and Nanobiotechnology*, **2009**, *1*, 502.
- [76] [76a] J.-P. Majoral, A.-M. Caminade, *Chem. Rev.* **1999**, *99(3)*, 845; [76b] V. G. Krasovskii, G. Ignateva, V. D. Myakushev, N. A. Sadovskii, T. V. Strelkova, A. M. Muzafarov, *Polym. Sci., Ser. A* **1996**, *38*, 1070; [76c] A. G. Vitukhnovsky, M. I. Sluch, V. G. Krasovskii, A. M. Muzafarov, *Synth. Methods* **1997**, *91*, 375.
- [77] E. A. Rebrov, A. M. Mazafarov, V. S. Papkov, A. A. Zhdanov, *Dokl. Akad. Nauk. SSSR* **1989**, *309*, 376.

-
- [78] H. Uchida, Y. Kabe, K. Yoshino, A. Kawamata, T. Tsumuraya, S. Masamune, *J. Am. Chem. Soc.* **1990**, *112*, 7077.
- [79] [79a] A. Morikawa, M. A. Kakimoto, Y. Imai, *Macromolecules* **1992**, *25*, 3247; [79b] A. Morikawa, M. A. Kakimoto, Y. Imai, *Macromolecules* **1991**, *24*, 3469; [79c] A. Morikawa, M. A. Kakimoto, Y. Imai, *Polym. J.* **1992**, *24*, 573.
- [80] A. Miedaner, C. J. Curtis, R. M. Barkley, D. L. DuBois, *Inorg. Chem.* **1994**, *33*, 5482.
- [81] [81a] O. Bourrier and A. K. Kakkar, *J. Mater. Chem.* **2003**, *6*, 1306; [81b] O. Bourrier, J. Butlin, R. Hourani, A. K. Kakkar, *Inorg. Chim. Acta* **2004**, *357*, 3836; [81c] R. Hourani, A. K. Kakkar, M. A. Whitehead, *J. Mater. Chem.* **2005**, *15*, 2106; [81d] R. Hourani, A. K. Kakkar, M. A. Whitehead, *J. Mol. Struct. (THEOCHEM)* **2007**, *807*, 101; [81e] A. K. Kakkar, *Chem. Rev.* **2002**, *102(10)*, 3579; [81f] M. Petrucci-Samija, V. Guillemette, M. Dasgupta and A. K. Kakkar, *J. Am. Chem. Soc.* **1999**, *121*, 1968.
- [82] S. S. Sheiko, G. Eckert, G. Ignateva, A. M. Muzafarov, J. Spikermann, H. J. Räder, M. Möller, *Macromol. Rapid Comm.* **1996**, *17*, 283.
- [83] A. Morikawa, M. A. Kakimoto, Y. Imai, *Macromolecules* **1992**, *25*, 3247.
- [84] R. Hourani, M. A. Whitehead, A. K. Kakkar, *Macromolecules* **2008**, *41*, 508.
- [85] [85a] S. Achar, R. J. Puddephatt, *Angew. Chem. Int. Ed. Engl.* **1994**, *33*, 847; [85b] S. Achar, R. J. Puddephatt, *J. Chem. Soc., Chem. Commun.* **1994**, 1895; [85c] S. Achar, J. J. Vittal, R. J. Puddephatt, *Organometallics* **1996**, *15*, 43.
- [86] [86a] N. Ohshiro, F. Takei, K. Onitsuka, S. Takahashi, *Chem. Lett.* **1996**, 871; [86b] N. Ohshiro, F. Takei, K. Onitsuka, S. Takahashi, *J. Organomet. Chem.* **1998**, *569*, 195; [86c] K. Onitsuka, A. Shimizu, S. Takahashi, *Chem. Commun.* **2003**, 280.
- [87] S. Leininger, P. J. Stang, S. Huang, *Organometallics* **1998**, *17*, 3981.

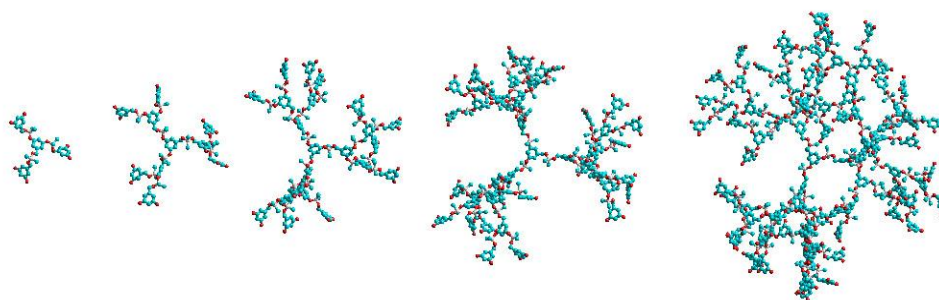
-
- [88] [88a] S. K. Hurst, M. P. Cifuentes, M. G. Humphrey, *Organometallics* **2002**, *21*, 2353; [88b] A. M. McDonagh, C. E. Powell, J. P. Morrall, M. P. Cifuentes, M. G. Humphrey, *Organometallics*, **2003**, *22*, 1402.
- [89] K. Onitsuka, M. Fujimoto, H. Kitajima, N. Ohshiro, F. Takei, S. Takahashi, *Chem. Eur. J.* **2004**, *10*, 6433.
- [90] [90a] K. Rengan, R. Engel, *J. Chem. Soc. Chem. Commun.* **1990**, 1084; [90b] K. Rengan, R. Engel, *J. Chem. Soc., Perkin Trans. 1* **1991**, 987.
- [91] [91a] A. Miedaner, C. J. Curtis, R. M. Barkley, D. L. DuBois, *Inorg. Chem.* **1994**, *33*, 5482; [91b] N. Launay, A.-M. Caminade, R. Lahana, J.-P. Majoral, *Angew. Chem., Int. Ed. Engl.* **1994**, *33*, 1589.
- [92] [92a] L. Brauge, G. Magro, A.-M. Caminade and J.-P. Majoral, *J. Am. Chem. Soc.*, **2001**, *123*, 6698; [92b] M. Poupot, L. Griffe, P. Marchand, A. Maraval, O. Rolland, L. Martinet, F.-E. L'Faqihi-Olive, C.-O. Turrin, A.-M. Caminade, J.-J. Fournie, J.-P. Majoral, R. Poupot, *FASEB J.*, **2006**, *20*, 2339.
- [93] J. W. Lee, B.-K. Kim, J. H. Kim, W. S. Shin, S.-H. Jin, *J. Org. Chem.* **2006**, *71*, 4988.
- [94] [a] C. J. Hawker, K. L. Wooley, J. M. J. Fréchet, *Polym. Prepr.* **1999**, *32*, 623; [b] C. J. Hawker, K. L. Wooley, J. M. J. Fréchet, *J. Am. Chem. Soc.* **1993**, *115*, 11496.
- [95] [95a] L. L. Miller, B. Zinger, J. S. Schlechte, *Chem. Mater.* **1999**, *11*, 2313; [95b] L. L. Miller, J. S. Schlechte, B. Zinger, C. J. Burrell, *Chem. Mater.* **2002**, *14*, 5081.
- [96] P. Wu, A. K. Feldman, A. K. Nugent, C. J. Hawker, A. Scheel, B. Voit, J. Pyun, J. M. J. Fréchet, K. B. Sharpless, V. V. Fokin, *Angew. Chem., Int. Ed.* **2004**, *43*, 3928.
- [97] [97a] M. J. Joralemon, R. K. O'Reilly, J. B. Matson, A. K. Nugent, C. J. Hawker, K. L. Wooley, *Macromolecules* **2005**, *38*, 5436; [97b] M. Malkoch, K. Schleicher, E. Drockenmuller, C. J. Hawker, T. P. Russell, P. Wu, V. V. Fokin, *Macromolecules* **2005**, *38*, 3663; [97c] C. J. Arnusch, H. Branderhorst, B. de Kruijff, R. M. J. Liskamp, E. Breukink, R. J. Pieters, *Biochemistry* **2007**, *46*, 13437; [97d] M. Ortega-Munoz, J. Morales-Sanfrutos, F. Perez-Balderas, F.

-
- Hernandez-Mateo, D. Giron-Gonzalez Ma, N. Sevillano- Tripero, R. Salto-Gonzalez, F. Santoyo-Gonzalez, *Org. Biomol. Chem.* **2007**, *5*, 2291; [97e] M. Touaibia, A. Wellens, T. C. Shiao, Q. Wang, S. Sirois, J. Bouckaert, R. Roy, *Chem. Med. Chem.* **2007**, *2*, 1190; [97f] M. J. Joralemon, R. K. O'Reilly, J. B. Matson, A. K. Nugent, C. J. Hawker, K. L. Wooley, *Macromolecules* **2005**, *38*, 5436.
- [98] P. Wu, M. Malkoch, J. N. Hunt, R. Vestberg, E. Kaltgrad, M. G. Finn, V. V. Fokin, K. B. Sharpless, Craig J. Hawker, *Chem. Commun.* **2005**, 5775.
- [99] [99a] M. B. Steffensen, E. E. Simanek, *Angew. Chem., Int. Ed.* **2004**, *43*, 5178; [99b] M.-X. Wang, H.-B. Yang, *J. Am. Chem. Soc.* **2004**, *126*, 15412.
- [100] W. Wang, H. Sun, A. E. Kaifer, *Org. Lett.* **2007**, *9(14)*, 2657.
- [101] R. K. Tekade, P. V. Kumar, N. K. Jain, *Chem. Rev.* **2009**, *109*, 49.
- [102] [102a] E. R. Gillies, Jean M. J. Fréchet, *Bioconjugate Chem.* **2005**, *16*, 361; [102b] M. Gingras, J.-M. Raimundo, Y. M. Chabre, *Angew. Chem. Int. Ed.* **2007**, *46*, 1010.
- [103] E. R. Gillies, E. Dy, J. M. J. Fréchet, F. C. Szoka, *Molecular Pharmaceutics* **2004**, *2(5)*, 129.
- [104] [104a] M. Liu, K. Kono, J. M. J. Fréchet, *J. Polym. Sci. Part A: Polym. Chem. Ed.* **1999**, *37*, 3492; [104b] M. W. Baars, R. Kleppinger, M. H. J. Koch, S.-L. Yeu, E. W. Meijer, *Angew. Chem., Int. Ed.* **2000**, *39*, 1285; [104c] C. Kojima, K. Kono, K. Maruyama, T. Takagishi, *Bioconjug. Chem.* **2000**, *11*, 910.
- [105] M. Liu, K. Kono¹, J. M. J. Fréchet, *Journal of Controlled Release* **2000**, *65*, 121.
- [106] [106a] A. D. Schlüter, J. P. Rabe, *Angew. Chem., Int. Ed.* **2000**, *39*, 864; [106b] H. Frey, *Angew. Chem., Int. Ed. Engl.* **1998**, *37*, 2193; [106c] A. D. Schlüter, *Top. Curr. Chem.* **1998**, *197*, 165.
- [107] [107a] S. M. Grayson, J. M. J. Fréchet, *Macromolecules* **2001**, *34*, 6542; [107b] R. Yin, Y. Zhu, D. A. Tomalia, H. Ibuki, *J. Am. Chem. Soc.* **1998**, *120*, 2678.
- [108] C. J. Hawker, J. M. J. Fréchet, *Polymer* **1992**, *33*, 1507.

-
- [109] [109a] D. Yu, N. Vladimirov, J. M. J. Fréchet, *Macromolecules* **1999**, *32*, 5186; [109b] J. M. J. Fréchet, I. Gitsov, *Macromol. Symp.* **1995**, *98*, 441.
- [110] [110a] I. Gitsov, K. L. Wooley, J. M. J. Fréchet, *Angew. Chem. Int. Ed.* **1992**, *31*, 1200; [110b] I. Gitsov, J. M. J. Fréchet, *Macromolecules* **1993**, *26*, 6536.
- [111] [111a] V. Percec, A. D. Schlüter, J. C. Ronda, G. Johansson, G. Ungar, J. P. Zhou, *Macromolecules* **1996**, *29*, 1464; [111b] V. Percec, A. D. Schlüter, *Macromolecules* **1997**, *30*, 5783; [c] G. M. Stewart, M. A. Fox, *Chem. Mater.* **1998**, *10*, 860.
- [112] [112a] I. Neubert, E. Amoulong-Kirstein, A. D. Schlüter, H. Dautzenberg, *Macromol. Rapid Commun.* **1996**, *17*, 517; [112b] S. Forster, I. Neubert, A. D. Schlüter, P. Lindner, *Macromolecules* **1999**, *32*, 4043; [112c] L. Shu, A. Schafer, A. D. Schlüter, *Macromolecules* **2000**, *33*, 4321.
- [113] [113a] W. Claussen, N. Schulte, A. D. Schlüter, *Macromol. Rapid Commun.* **1995**, *16*, 89; [113b] B. Karakaya, W. Claussen, K. Gessler, W. Saenger, A. D. Schlüter, *J. Am. Chem. Soc.* **1997**, *119*, 3296.
- [114] [114a] B. A. Laurent, S. M. Grayson, *J. Am. Chem. Soc.* **2006**, *128*, 4238; [114b] D. M. Eugene, S. M. Grayson, *Macromolecules* **2008**, *41*, 5082; [114c] M. D. Giles, S. Liu, R. L. Emanuel, B. C. Gibb, S. M. Grayson, *J. Am. Chem. Soc.* **2008**, *130*, 14430; [114d] A. J. Boydston, T. W. Holcombe, D. A. Unruh, J. M. J. Fréchet, R. H. Grubbs, *J. Am. Chem. Soc.* **2009**, *131*, 5388.
- [115] [115a] M. Schappacher, A. Deffieux, *Macromolecules* **2001**, *34*, 5827; [115b] V. V. Rostovtsev, L. G. Green, V. V. Fokin and K. B. Sharpless, *Angew. Chem. Int. Ed.* **2002**, *41*(14), 2596.

Chapter 2

3,5-Dihydroxybenzylalcohol Based Dendrimers: Structure Evaluation and Molecular Encapsulation in Generations 1-5



This chapter describes detailed theoretical and experimental studies to understand the structure-property relationships in dendrimers. It reveals valuable information for the design of these macromolecules for specific applications, and the results are relevant to the whole thesis.

Reproduced in part with permission from:

Hourani R., Kakkar A., & Whitehead M. A., *J. Mater. Chem.*, **2005**, 15, 2106.

Copyright, 2009, The Royal Society of Chemistry.

2.1 Introduction

Monodisperse hyperbranched macromolecules, commonly referred to as dendrimers, have been the subject of intense research activity for many years since they exhibit a distinct structure and properties that can be utilized for a variety of applications.¹⁻⁵ Much work has been done in the past to develop synthetic techniques to prepare a variety of dendritic macromolecules. However, our understanding of their actual shape, size, the environment of the cavities inside these dendrimers, and dendritic intermolecular association, is still limited.⁶⁻¹⁰ Determination of the three-dimensional structure of the dendrimers is an important step in predicting their conformations in intended media, and exploring their potential applications in catalysis, drug delivery, photonics etc. A detailed investigation of the structure of 3,5-dihydroxy-benzyl alcohol (DHBA)-based dendrimers using the molecular mechanics MM+ method, and the PM3 semi-empirical molecular orbital theory¹¹ is reported. Determination of the most stable structure, at its lowest energy, provides vital information about the size, shape, and spatial orientation of dendrimers. These properties are important because they govern the structural characteristics of molecules, which can be encapsulated into their internal cavities, as well as the ability of dendrimers to self-associate.

Dendrimers are compact macromolecules with densely packed peripheral functional groups that can participate in intermolecular association leading to the formation of aggregates. For example, DHBA-based dendrimers contain peripheral OH groups, and the individual dendrimer molecules can interact with each other *via* hydrogen bonds to yield large aggregates.^{12,13} These aggregates are formed in THF when the dendrimer concentration exceeds a certain threshold often referred to as the critical aggregation concentration (*cac*). The *cac* for smaller dendrimer generations 1-3 was found to be much higher than dendrimer generations 4 and 5 that showed some degree of aggregate formation even at a concentration as low as 0.1 mg mL⁻¹.^{12,13} Such self-assembled dendritic aggregates are ideal for investigating molecular loading and their controlled release profile.¹⁴ Inclusion of molecules such as disperse red 1 (DR1) in these dendrimers of generation 1-3 was investigated in a previous study before and after their aggregation.^{12,13} Here, we further examined the encapsulation of DR1 into the larger and more

globular DHBA-based dendrimer generations 4 and 5 before and after aggregation. We have also investigated the accessibility of active transition metal centers present in the internal cavities of DHBA-based dendrimers above and below their *cac* in solution, and have examined their activity in olefin hydrogenation. Such studies can help understand the encapsulating behavior of dendrimers, and provide routes to efficient and tailor-made carriers.

2.2 Theoretical methods for the investigation of the structure of DHBA-based dendrimers

Since dendrimers are macromolecules with increasing size upon addition of each generation, it is necessary to choose a theoretical method capable of geometric characterization of such large structures. In the present study, we used molecular mechanics with MM+ force field to perform calculations. The geometry optimizations were carried out using the Polak-Ribiere conjugate gradient, which was set to terminate at an RMS gradient of $0.01 \text{ kcal } \text{\AA}^{-1} \text{ mol}^{-1}$. The semi-empirical parametrization model 3 (PM3) molecular orbital method developed by Stewart,^{15,16} was used with the Gaussian98 program.¹⁷ Semi-empirical optimizations were carried out under standard convergence criteria (max force = 4.5×10^{-4} hartrees bohr⁻¹; RMS force = 3.0×10^{-4} hartrees bohr⁻¹; max displacement = 1.8×10^{-3} Å; RMS displacement = 1.2×10^{-3} Å). PM3 is a robust, accurate, semi-empirical theory, which is always parallel to experiment and consequently predictive.¹⁸⁻²¹ It is a particularly advantageous method to obtain conformational and chemical information about dendrimers. Molecular dynamics, in addition to being a cumbersome method to build large dendritic macromolecules, does not give any information about dendritic chemical behavior.²² It has been demonstrated that the use of molecular dynamics in studying co-factor interaction with polyethylene oxide (PEO) proved ineffective compared with gas phase results from semi-empirical methods.²³ It was found that the size and shape of the co-factor and the PEO remained unaltered after the molecular dynamics calculations. In addition, the solvent (water), was shown to have no effect on the conformation of either molecule.^{24,25} The application of molecular dynamics to protein denaturation

has also provided no clear conclusion about denaturation,²⁶ whereas the gas phase bond dipole moments²⁷ separated unambiguously the denaturing and non-denaturing solutes.

The molecules were initially drawn in the HyperChem Visualizer program,²⁸ and optimized using molecular mechanics with MM+ force field, followed by the Gaussian98 program¹⁷ for optimization by PM3. The conformations of the dendrimers were found by varying all torsional axes to discover the minimum global energy conformation, which was 8-9 kcal more stable than any other conformer. This minimum was established both by using the program in the PM3 Gaussian package, and also established independently using the tree branch method.²⁹

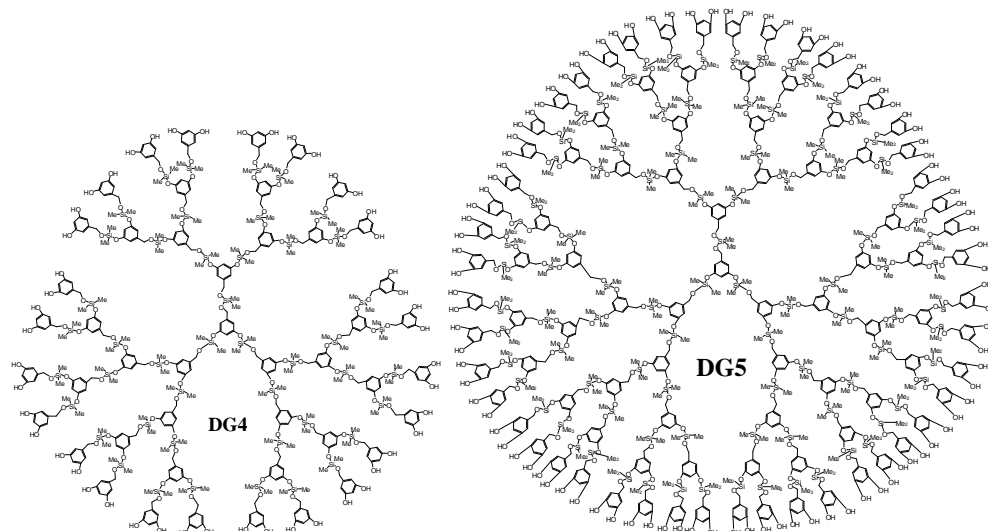


Fig. 2.1 Dendrimer generations 4 and 5 (DG4 and 5) of DHBA-based dendrimers.¹²

DHBA-based dendrimers (**Fig. 2.1** shows generations 4 and 5) have recently become available in large quantities,¹² and their synthesis is based on a simple and highly versatile methodology using acid-base hydrolytic chemistry of commercially available reagents: 3,5-dihydroxybenzyl alcohol and $\text{Me}_2\text{Si}(\text{NMe}_2)_2$.

For the PM3 calculations, the core molecule, 3,5-dihydroxybenzyl alcohol (DHBA), and the linker bis(dimethylamino)-dimethyl silane ($\text{Me}_2\text{Si}(\text{NMe}_2)_2$) were geometrically optimized by PM3. The optimized core molecule was then linked to three $\text{Me}_2\text{Si}(\text{NMe}_2)$ molecules by forming O-Si bonds to give a branched structure. The energetically most stable branched

structure was found by re-optimizing the total system by rotating about the CH₂ group of the core, and then rotating the Me₂Si(NMe₂) around their linkages to the core, followed by the optimization of the whole system. Three additional 3,5-dihydroxybenzyl alcohol molecules were linked to the Me₂Si(NMe₂) branches by forming Si-O bonds at the end of each branch and removing HNMe₂ to give the first dendrimer generation (DG1). In a similar manner, the second and third dendrimer generations (DG2 and DG3) were built and optimized. Initially, the DG(*n* - 1) generation was frozen while DG(*n*) was optimized. The system was then re-optimized with the DG(*n* - 1) unfrozen, and the results were unchanged. As the dendrimer generations number increases, it becomes difficult to study them using PM3, since the surface to be searched for various conformations becomes too large. Dendrimer generations 1-5 were optimized in a similar fashion by the molecular mechanics MM+ in the HyperChem visualizer program.²⁸

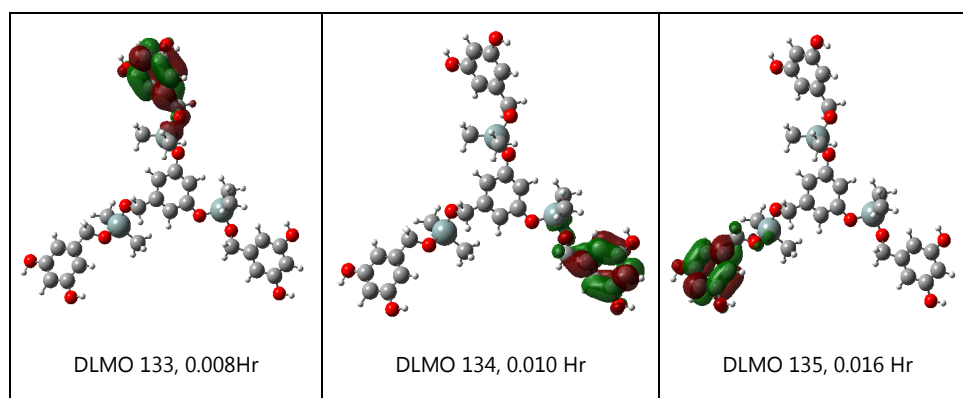


Fig. 2.2 The lowest unoccupied molecular orbitals (LUMO) of DG1 along with their numbers and energies.

By comparison of the results, we established that the MM+ molecular modelling results for DG1-3 were identical in conformation to the PM3 global minimum structures, and hence reliable and predictive for DG4 and 5. Furthermore, single point calculations by PM3 on DG4 and 5 gave identical delocalised molecular orbitals (DLMO) on the periphery atoms to those found by PM3 in DG1-3. **Fig. 2.2** shows the lowest unoccupied molecular orbitals (LUMO) for DG1, which are degenerate, and identical in DG2 and 3 in terms of their locations on the periphery and their energies. Therefore, we can safely conclude that these DLMO do not change as the dendrimer generation number

increases, but they obviously multiply rapidly as the dendrimer grows. This shows that DHBA-based dendrimers would behave in a similar manner, and the reactions that take place at all stages in forming the dendrimers are identical.

Because the dendrimers gradually bend to form more spherical shape, the branches get closer to each other. We were unable to optimize dendrimer generations larger than DG5. This is in agreement with the fact that DG6 could not be synthesized experimentally. A detailed discussion of the wavefunctions and eigenvalues in these dendrimers can be found in **Appendix I**.

2.3 Results and discussion

As mentioned above, DHBA-based dendrimer generations 1-5 were initially studied using the molecular modelling with MM+ force field to estimate their geometric sizes and shapes. Subsequently, molecular orbital semi-empirical PM3 calculations were performed on the smaller dendrimer generations 1-3 to obtain more accurate sizes and shapes, which were found to be almost the same as those obtained from the molecular modelling MM+ results. However, the PM3 analysis yielded additional information including wave-functions, and eigenvalues of the delocalised molecular orbitals (DLMO), and established the validity of using the molecular orbital analysis on the larger dendrimer generations 4 and 5, which cannot be calculated easily because of their size and number of wavefunctions. The DLMO pattern ensures that the charges calculated on the atoms in DG1, 2, and 3 are valid and can be used for DG4 and 5. The peripheral hydroxide groups, which react with the $\text{Me}_2\text{Si}(\text{NMe}_2)_2$ reagent, have a charge of -0.23 on the oxygen atom, and +0.20 on the hydrogen atom, while the silicon atom in the $\text{Me}_2\text{Si}(\text{NMe}_2)_2$ reagent has a charge of +0.54 and the nitrogen atom has a charge of -0.20. On the other hand, in the products of the dendrimer-making reaction, the silicon atom has a charge of +0.94, which is balanced by two oxygen atoms: one oxygen atom attached to benzene group directly and with a charge of -0.55, and the one attached to a CH_2 group has a charge of -0.39. The nitrogen of the side product, HNMe_2 , has a charge of -0.05, and the hydrogen attached to it has a charge of +0.04. This shows that the reaction resulted in the silicon being the more positively charged atom, and the nitrogen, in the side product, is

almost a neutral atom. These values were found to be the same in DG1, 2, and 3, and they can be assumed to be valid for DG4 and 5, which shows that identical reactions occur at all stages in forming the dendrimers.

2.3.1 Shapes of dendrimer generations 1-5

The relative shapes of dendrimer generations 1-5 are shown in **Fig. 2.3**. The structures with the lowest energies were obtained by rotating several bonds in the dendrimers to obtain a more symmetric structure with the least number of unbonded atoms close to each other.

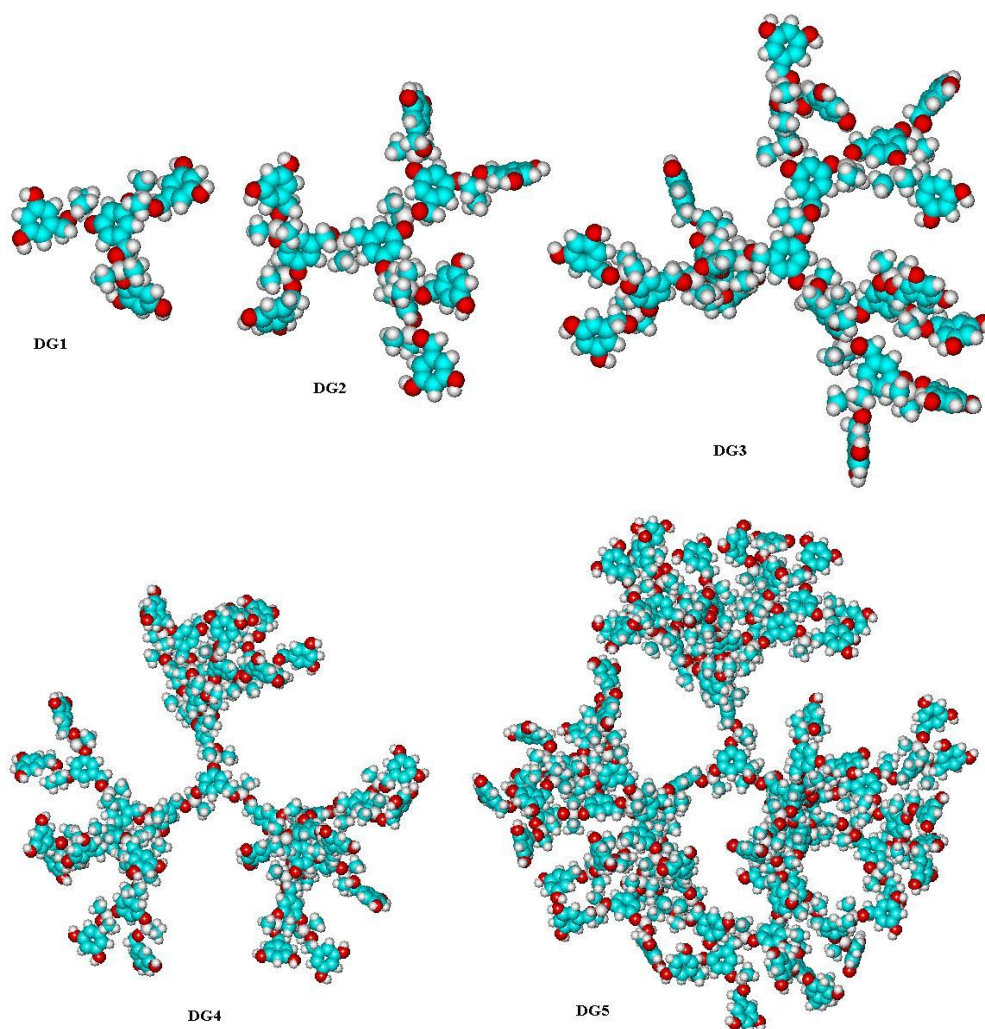


Fig. 2.3 The optimized structures of dendrimer generation 1-5 using the molecular modelling MM+ method shown as overlapping spheres.

The structure of DG1 is very open and planar with the three branches around the core arranged to give the least interaction between the branches. The spaces between the branches do not have any particular shape or size, and

encapsulation of guest molecules is going to be difficult without the formation of aggregates. The structure of DG2 becomes slightly less planar and the branches bend away from the plane but do not give any recognizable internal cavity. Dendrimer generation 3 (DG3) is even more non-planar. However, it also does not contain any recognizable cavities. The optimized structures of DG4 and DG5 have a 3D globular structure, and contain well-defined internal cavities. A change in the 3D structure between DG1 to DG5 shows a clear progress in forming internal cavities in these dendrimers with increasing rigidity and more globular structure. Since the number of peripheral hydroxyl groups in DG4 and DG5 is much larger than that in DG1-3, and the fact that the branches bend and become more spherical, the hydroxyl groups become more available on the surface from all directions. The latter would increase the possibility of hydroxyl groups from two different dendrimers to form hydrogen bonds even at much lower concentrations than those required for DG1-3. This was demonstrated experimentally because the critical aggregation concentration of DG1-3 was found to be around 3.7 mg mL^{-1} , while DG4 and DG5 formed aggregates even at much lower concentrations; as low as 0.1 mg mL^{-1} .^{12,13}

2.3.2 Sizes of the dendrimer generations 1-5

The determination of the average size of dendrimers is an important step in developing nanomaterials for specific applications. The relative diameters of DG1-5, calculated using MM+, are shown in **Table 2.1**. An examination of the size of these dendrimers of generations 1-3 by PM3 gave identical size to the MM+ results. These sizes were obtained by measuring the distance between several pairs of peripheral atoms on opposite sides of the dendrimers. Therefore, the limits in **Table 2.1** are the minimum and maximum measured distances.

Table 2.1 Summary of the relative sizes of DG1-5 determined by the MM+ method.

Dendrimer Generation	Diameter (Å)
1	16-19
2	28-35
3	43-47
4	58-67
5	62-75

The maximum, minimum, and average of the diameters of DG1-5 are plotted against the dendrimer generation number in **Fig. 2.4**. The onset of the globular structure is shown by the decrease in the rate of increase of the diameter (**Fig. 2.4**).

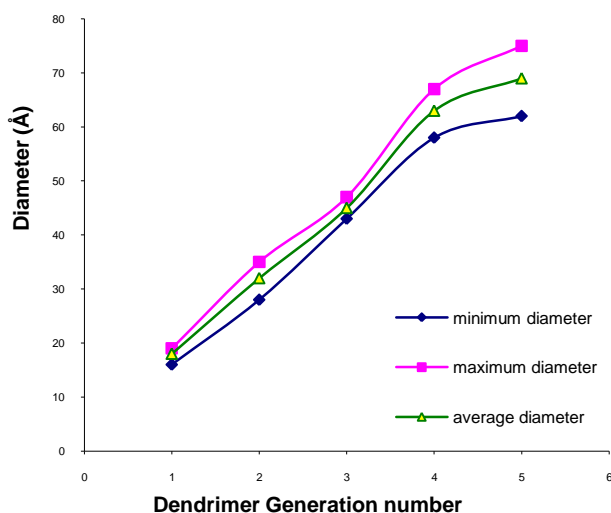


Fig. 2.4 The relationship between the dendrimer generation number and its relative diameter (Å).

2.3.3 Internal cavities of dendrimer generations 4 and 5

The sizes of the internal cavities of DG4 and 5 were estimated from the MM+ calculations, and found to be in the range of 24-35 Å. The size of a guest molecule can be chosen to match that of the internal cavities in these dendrimers. Therefore, disperse red 1 (DR1) dye, shown in **Fig. 2.5**, which has an MM+ estimated length of ~ 16 Å and a width of ~ 3 Å, will obviously fit into the internal cavities of DHBA-based dendrimer generations 4 and 5. Also,

in view of the relative widths, several molecules of DR1 could fit into the cavities.

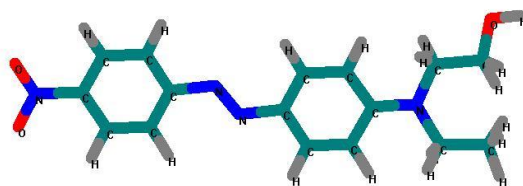


Fig. 2.5 The optimized molecular structure of DR1 calculated by MM+ method.

2.3.4 Encapsulation of DR1

Disperse red 1, shown in **Fig. 2.5**, is an intensely colored molecule that has been shown to exhibit non-linear optical (NLO) properties,^{30,31} and has a strong UV-Vis absorption (λ_{max}) at 485 nm. We have examined its encapsulation into DHBA-based dendrimer generations 1-3^{12,13} and 4-5 (this study) before and after their aggregation using UV-Vis absorption spectroscopy. Upon aggregation, in both DG4 and DG5, there was a blue shift from 486 to 460 nm in the UV-Vis absorption maxima for DR1, as well as a broadening of the absorption maxima (**Fig. 2.6** shows results for DG4).

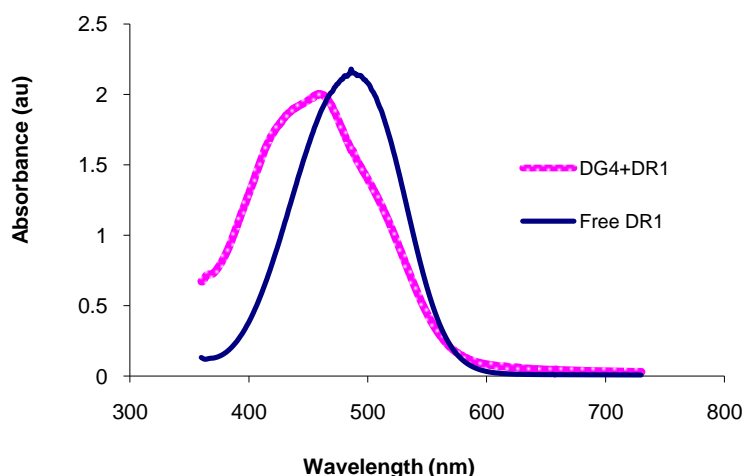


Fig. 2.6 UV-Vis spectra of free DR1, and encapsulated DR1 in DG4.

This was in agreement with our earlier study of encapsulation of DR1 into dendrimer generations 1-3.^{12,13} However, the encapsulation process for DG4 and DG5 had to be done at a much lower concentration of dendrimers in

THF (0.5 mg mL^{-1}) because their *cac* has been shown to be much lower than that of DG1-3 (*cac* = 3.7 mg mL^{-1}).^{12,13} Using very low concentrations of DG4-5 allows DR1 to pass into the interior of the dendrimers. When higher concentrations of DG4 or DG5 ($1\text{-}3 \text{ mg mL}^{-1}$) were used, no change in the λ_{max} at 485 nm for DR1 was observed. The latter clearly depicts that at these concentrations, the dendrimer generations 4 and 5 are substantially aggregated in solution, and the dye molecules are unable to go into their interior. We have also studied the UV-Vis absorption spectra of a mixture of DHBA monomer and DR1 at various concentrations. It did not show any shift in the λ_{max} of DR1. Since DHBA molecule does not form aggregates and has no internal cavities, it demonstrates that the blue shift observed in DR1 encapsulated dendrimers is caused by the entrapment of DR1 molecules, and not by its interaction with the dendrimers at the periphery.

The blue shift in the UV-Vis absorption maxima suggests changes in the surrounding environment (including the solvation micro-environment) of DR1 caused by its encapsulation in the internal cavities of the dendrimers and their aggregates. Encapsulation of DR1 molecules in the internal cavities of the dendrimers may bring them close together, and can allow favorable dipole-dipole interactions to take place. The latter interactions may affect the electronic structure of DR1 and its energy level separations, and create a larger energy gap for the $n\text{-}\pi$ and $\pi\text{-}\pi^*$ transitions in DR1 molecule,³⁰ causing a blue shift to a lower wavelength ($\lambda_{\text{max}} = 460 \text{ nm}$). The broadening of the absorption peak reflects the presence of free DR1 in equilibrium with the encapsulated DR1. Upon reducing the concentration to that of below *cac*, λ_{max} shifted slightly to 468 nm. This suggests that upon dilution, only a small amount of the chromophore is released from the dendrimers, and the majority of the guest molecules are unable to diffuse out.

Introduction of DR1 into dendritic aggregates increased the solubility of dendrimers, and made it difficult to remove any excess dye by simple washing. Dialysis was found to be more useful in this regard. A 50 kDa pore regenerated cellulose membrane dialysis tubing was chosen based on the relative molecular weights of DR1 and the aggregates of DG4 and DG5. The molecular weight cut off (MWCO) of this tubing would allow DR1 to diffuse out of the tube, but not the dendritic aggregates. The solutions of DG4 or DG5

and DR1 were successfully dialyzed after three washings of 500mL THF each. The UV-Vis analysis of the washings showed a similar peak as that for free DR1 at λ_{max} of 485 nm with decreasing absorption intensity from one washing to the next. The UV-vis spectra of the remaining DR1 and dendrimer mixtures showed no clear shift from free DR1. This implies that most of the DR1 molecules had diffused out of the dendritic aggregates upon dialysis.

2.3.5 Transmission electron microscopy (TEM) study of the encapsulation of DR1 into dendrimers

The inclusion of DR1 into dendritic aggregates was examined using TEM, and the micrographs of aggregates of DG4 with DR1 (**Fig. 2.7a-b**) and without DR1 (**Fig. 2.7c-d**) are shown below.

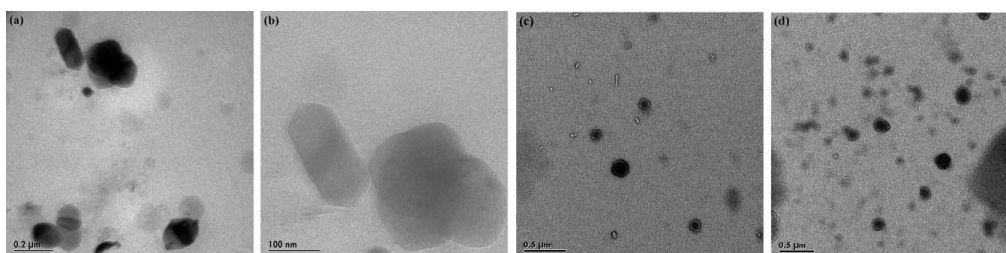


Figure 2.7: a) TEM micrographs of dendrimer generation 4 (DG4) with DR1 a) and b), and without DR1 c) and d) at concentration of 5mg.mL⁻¹.

The majority of the aggregates in DG4 and DG5 with encapsulated DR1 were found to have a unique rectangular shape as shown for DG4 in **Fig. 2.7a-b**. The aggregates of DG4 and DG5 without the presence of DR1 have globular shapes with sizes ranging between 150-210 nm as shown in **Fig. 2.7c-d**. In the presence of DR1, the aggregates adopt the rectangular shape with dimensions of 110 x 240 nm. This change in shape suggests a change in the dendritic aggregate structure upon encapsulation of DR1.

For comparison purposes, TEM studies of DR1 alone, and mixtures of DR1 and DHBA monomer in THF were then carried out. The TEM micrographs did not show any aggregates similar to those observed in the mixtures of dendrimers with DR1. This strongly suggests that inclusion of DR1 into aggregates of dendrimer generations 4 and 5 influences their morphology. Encapsulation of DR1 in the internal cavities of the dendritic

aggregates can strongly affect the rigidity and structural orientation of dendrimers. This could then affect the alignment of the peripheral hydroxyl groups, the number of hydrogen bonds formed, and their strength, therefore, forcing the dendrimers to assemble in a different pattern that can develop into a particular morphology.

2.3.6 Encapsulation of active transition metal centers in dendritic aggregates

Designing supports or carriers for active transition metal catalysts remains a topical area of research. We have studied heterogenization of (COD)RhCl(PR₃) on various media including thin film assemblies and dendrimers.³²⁻⁴¹ Encapsulation of active metallic centers into internal cavities of dendrimers has also attracted much interest recently.^{42,43} We were intrigued to examine the activity of the catalyst (COD)RhCl(PPh₂(CH₂)₃OH) for olefin hydrogenation upon encapsulation into DHBA-based dendritic aggregates. DHBA-based generations 1-4 at concentrations below and above *cac* were used for this study. In a typical experiment, the desired dendrimer was mixed with (COD)RhCl(PPh₂(CH₂)₃OH) in THF, and the solution (below or above *cac*) was allowed to equilibrate for 12 h. The dendrimer encapsulated catalyst solution and 1-decene was then placed in a pressure reactor, and hydrogenation was carried out under a hydrogen pressure of 20 bar at room temperature for a period of 1 h. The results are reported in **Table 2.2**.

Table 2.2 Conversions (%) of 1-decene to decane using generations 1-4 dendrimer encapsulated CODRhCl(PPh₂(CH₂)₃OH).

Dendrimer Generation	% Conversion	
	Below <i>cac</i>	Above <i>cac</i>
1	39	39
2	36	30
3	37	32
4	38	19

For dendrimer generations 1, 2 and 3, the percentage conversions below and above *cac* are quite similar. For DG4, 1-decene to decane

percentage conversion is much higher below *cac*, and in fact almost double that when the dendrimer solution concentration is above *cac*. When the catalyst is mixed with the dendrimer at a concentration below *cac*, the Rh(I) centers in the internal cavities of the dendrimers will be in an equilibrium with the ones that are outside. Upon aggregation, the former will get trapped inside and would have limited access to the olefin. Generations 1, 2, and 3, due to their small size and planar structure, are not able to form densely packed aggregates that can trap the catalytic centers effectively. This is mainly because the large size and bulkiness of the catalyst molecule. This will explain their similarity in percentage conversions below and above *cac*. However, DG4 has well-defined internal cavities, which can host the catalyst and isolate it from the olefin more efficiently. Moreover, DG4 molecules can aggregate more effectively due to their larger surface area and larger number of OH groups that can participate in hydrogen bonding. This creates a more effective trap for the catalytic molecules upon aggregation, and a reduction in catalytic efficiency was observed, as shown in **Table 2.2**.

2.4 Conclusions

3,5-Dihydroxybenzylalcohol-based dendrimers have been optimized using the molecular mechanics MM+ and the semi-empirical PM3 molecular orbital methods, and the sizes of these dendrimers were estimated to be 16-75 Å for generations 1-5 respectively. Generations 1 and 2 show a relatively planar and open structure without any well-defined internal cavities of any particular shape or size. Generation 3 is much less open and non-planar, but there are still no recognizable internal cavities. Generations 4 and 5 are globular in shape with well-defined internal cavities. As the dendrimer generation number increases, the number of peripheral hydroxyl groups increases (6, 12, 24, 48, and 96). Because of the bending of the branches to give a 3D structure, the hydroxyl groups are more densely packed leading to more hydrogen bonds to form aggregates. Encapsulation of DR1 into the interior of these dendrimers had to be carried out using much lower concentrations for generations 4 and 5 since they are aggregated even at a concentration much lower than *cac* of DG1-3. Upon loading DR1 into generations 1-5, a blue shift in the UV-Vis absorption maximum of DR1 was

observed. The change in λ_{max} reflects a change in the environment of DR1 upon entrapment into the dendritic interior. In the dye encapsulated dendritic aggregates, a rectangular morphology was observed using TEM compared with the globular shape of dendrimer aggregates. Encapsulating active transition metal centers above dendrimer *cac* in generations 3 and 4 limits their accessibility, and a lowering of percentage conversion of 1-decene to decane during hydrogenation at a concentration above *cac* was observed. These results demonstrate that DHBA-based dendritic aggregates can provide the desired encapsulating and isolating control on the guest molecules.

2.5 Experimental Section

2.5.1 General procedures

All reactions except for dialysis were performed under a nitrogen atmosphere using either Braun Labmaster MB-150 dry box or standard Schlenk line techniques. All solvents were stored under nitrogen after distillation over sodium. UV-Vis spectra were recorded on a Hewlett Packard 8453 spectrometer using fused silica cuvettes. Dialysis was performed using a 50 kDa pore regenerated cellulose membrane (Spectrum, USA), which was sealed with THF resistant nylon 6,6 clips in wet THF. GC-MS analysis was performed on a Hewlett Packard 6840 and HP 5973 mass spectrometer using He as the carrier gas and an initial temperature of 50°C with a ramp of 10°C min⁻¹ stopping at 250 °C. TEM analysis was carried out on a JEOL 2000FX microscope operating at an acceleration voltage of 80 kV. Copper EM grids (400 mesh) were precoated with carbon. Hydrogenation reactions were carried out using a Parr 4560 Mini-reactor with constant experimental conditions: pH₂ = 20 bar, room temperature, and ratio of n_{catalyst} : n_{decene} = 24 : 200.

2.5.2 Materials

DHBA-based dendrimers were prepared and characterized using the procedure reported earlier.¹² Disperse red 1 (DR1) (Aldrich), chloro(1,5-cyclooctadiene) rhodium(I) dimer [(COD)RhCl]₂ (Pressure Chemicals), and 3-hydroxypropyl-diphenylphosphine (PPh₂(CH₂)₃OH) (Organometallics) were used as received without further purification.

1-Decene was purified by distillation. The catalyst (COD)RhCl(PPh₂(CH₂)₃OH) was prepared by adding two equivalents of PPh₂(CH₂)₃OH to the Rh(I) dimer [(COD)RhCl]₂.³⁴

2.5.3 Inclusion of disperse red 1 in dendrimer generation 4 and 5 (DG4 and DG5)

Solutions of DG4 and DG5 with various concentrations of DR1, as shown in **Tables 2.3** and **2.4**, were prepared. A typical procedure involved dissolving the required amount of the dendrimer in dry THF at a concentration below aggregation (0.5 mg mL⁻¹), and stirred for a period of up to 48 h.

Table 2.3 Quantities of DG4 and DR1 that were used in preparing solutions.

Solution	DG4		DR1	
	mg	μmol	mL	μmol
1	15	1.7	0.3	0.12
2	15	1.7	0.6	0.24
3	15	1.7	1.2	0.48

Table 2.4 Quantities of DG5 and DR1 that were used in preparing solutions.

Solution	DG5		DR1	
	mg	μmol	mL	μmol
1	15	0.81	0.3	0.12
2	15	0.81	0.6	0.24
3	15	0.81	1.0	0.40

The desired amount of DR1 was added to the dendrimer solution, and the mixture was stirred for 24 h. The stirred mixture was then equilibrated without stirring for 24 h, and a UV-Vis spectrum was taken. The solution was evaporated to bring it to a concentration above *cac*, and stirred for 5-6 h. The concentrated solution was equilibrated without stirring for 24 h, and UV-Vis spectra were recorded for these concentrated solutions. The mixtures were

then diluted back to a concentration below *cac*, and stirred for 48 h, and UV-Vis spectra were taken for the diluted solutions.

2.5.4 Transmission electron microscopy (TEM) analysis

Dendrimer generation 4 (30 mg, 3.3×10^{-6} mol), or 5 (30 mg, 1.6×10^{-6} mol) was dissolved in 60 mL of dry THF at a concentration below aggregation (0.5 mg mL^{-1}). The same amount of disperse red 1 (DR1) (2.4×10^{-7} mol) was added to each dendrimer solution, and the mixtures were stirred for 24 h. The latter were then equilibrated without stirring for 24 h. The solutions were evaporated to bring them to aggregation concentration, and were left to stir for several hours. The concentrated solutions were equilibrated without stirring for 24 h. UV-Vis spectra were recorded for the concentrated solutions. The solutions were then evaporated to dryness. Three samples of each dried mixture were prepared at different concentrations of (1 mg, 3 mg, and 5 mg per 1 mL of THF). A drop of each sample was placed on a carbon-coated copper grid, and left to dry. TEM micrographs were taken for the dried samples.

2.5.5 Dialysis experiments

Dendrimer generation 4 (DG4) (50 mg, 5.5×10^{-6} mol), or 5 (DG5) (50 mg, 2.7×10^{-6} mol) was dissolved in 100 mL of dry THF at a concentration below aggregation (0.5 mg mL^{-1}). Disperse red 1 (20 mg, 6.4×10^{-5} mol) and (23 mg, 7.3×10^{-5} mol) was added to DG4 and DG5 solutions respectively, and the mixtures were stirred for 24 h. The latter were then equilibrated without stirring for 24 h. The solutions were evaporated to dryness. The dried samples were diluted with 2 mL of THF, and transferred to a 50 kDa pore regenerated cellulose membranes (Spectrum, USA), which were sealed with THF resistant nylon 6,6 clips. The sealed tubes were placed in 500 mL of THF, with a stirring bar. The washing solutions were changed 3 times every 24 h, and the washings were monitored using UV-Vis spectroscopy. The samples were diluted to a volume of 10 mL of THF, and UV-Vis spectra were taken at 5 mg mL^{-1} .

2.5.6 Interaction of 3,5-dihydroxybenzyl alcohol (DHBA) with DR1

Several solutions of different concentrations of DHBA (100 mg, 7.1×10^{-4} mol) and different amounts of DR1 in THF were prepared with constant stirring. UV-Vis spectra were taken for the solutions. The mixtures were left for one week in separate vials. UV-Vis spectra were recorded again for the mixtures. One mixture was then evaporated to approximately 3 mL, and a UV-Vis spectrum was recorded. TEM micrographs were taken for a sample of DR1 (0.12 mmol) alone in 3 mL of THF, a sample of DR1 (0.12 mmol) with DHBA (30 mg, 2.4×10^{-4} mol) in 3 mL of THF, and a sample of DHBA (30 mg, 2.4×10^{-4} mol) in 3 mL of THF.

2.5.7 Inclusion of (COD)RhCl(PPh₂(CH₂)₃OH) in dendrimer generations 1-4 (DG1-DG4)

Solutions of DG1-4 with Rh(I) catalyst were prepared with various concentrations of the dendrimer above and below *cac* (Table 2.5).

Table 2.5 Quantities of DG1-4 that were used in catalysis applications.

Generation Number	Amount Used (mol)
1	6.2×10^{-5}
2	2.3×10^{-5}
3	2.3×10^{-5}
4	2.6×10^{-6}

A typical procedure is described below: (COD)RhCl(PPh₂(CH₂)₃OH) (34 mg, 6.9×10^{-5} mol) was added to the dendrimer solution, and the mixture was stirred overnight. The mixture was equilibrated without stirring for a few hours. The solution was evaporated to dryness, and the residue was dissolved in THF to a concentration below *cac* and another one to a concentration above *cac*. 1-Decene (2 mL, 1.38×10^{-2} mol) was added to the mixture. The mixture was loaded into a hydrogen pressure reactor. Hydrogenation of 1-decene was carried out at room temperature using 20 bar H₂ pressure for 1 h, and these reaction conditions were used as standard throughout the study. Distillation of

the reaction mixture after catalysis afforded the recovery of the Rh(I) dendritic material as a residue. In Rh(I) catalyzed hydrogenation of olefins, two products can be generally observed *i.e.*, the desired alkane and metathesized olefin (alkene). In our study, both these products were observed by GC-MS analysis.

2.6 References

- ¹ R. van Heerbeek, P. C. J. Kamer, P. W. N. M. van Leeuwen and J. N. H. Reek, *Chem. Rev.*, 2002, **102**, 3717.
- ² A. Andronov and J. M. J. Fréchet, *Chem. Commun.*, 2000, 1701.
- ³ D. Astruc and F. Chardac, *Chem. Rev.*, 2001, **101**, 2991.
- ⁴ F. Vogtle, *Top. Curr. Chem.*, 1998, **197**, 7.
- ⁵ J. M. Lupton, I. D. W. Samuel, P. L. Burn and S. Mukamel, *J. Chem. Phys.*, 2002, **116**, 2, 455.
- ⁶ X. Zhang, K. J. Haxton, L. Ropartz, D. J. Cole-Hamilton and R. E. Morris, *J. Chem. Soc., Dalton Trans.*, 2001, 3261.
- ⁷ A. Herrmann, T. Weil, V. Sinigersky, U.-M. Wiesler, T. Vosch, J. Hofkens, F. C. D. Schryver and K. Mullen, *Chem.-Eur. J.*, 2001, **7**, 22, 4844.
- ⁸ E. N. Govorun, K. B. Zeldovich and A. R. Khokhloy, *Macromol. Theory Simul.*, 2003, **12**, 705.
- ⁹ A. M. Striegel, R. D. Plattner and J. L. Willett, *Anal. Chem.*, 1999, **71**, 978.
- ¹⁰ S. Pricl, M. Fermeglia, M. Ferrone and A. Asquini, *Carbon*, 2003, **41**, 2269.
- ¹¹ G. A. Segal, *Semiempirical Methods of Electronic Structure Calculation, Part A: Techniques*, University of Southern California, Los Angeles, 1997.
- ¹² O. Bourrier and A. K. Kakkar, *J. Mater. Chem.*, 2003, **13**, 1306.
- ¹³ O. Bourrier, J. Butlin, R. Hourani and A. K. Kakkar, *Inorg. Chim. Acta*, 2004, **357**, 3836. Special issue in honor of Tobin J. Marks.
- ¹⁴ F. Hof, S. L. Craig, C. Nuckolls and J. Rubek, *Angew. Chem., Int. Ed.*, 2002, **41**, 1488.
- ¹⁵ J. J. P. Stewart, *J. Comput. Chem.*, 1989, **10**, 2, 209.
- ¹⁶ J. J. P. Stewart, *J. Comput. Chem.*, 1989, **10**, 2, 221.
- ¹⁷ M. J. Frisch, G. W. Trucks, H. B. Schlegel, G. E. Scuseria, M. A. Robb, J. R. Cheeseman, V. G. Zakrzewski, J. A. Montgomery, R. E. Stratmann, J. C. Burant, S. Dapprich, J. M. Millam, A. D. Daniels, K. N. Kudin, M. C. Strain,

O. Farkas, J. Tomasi, V. Barone, M. Cossi, R. Cammi, B. Mennucci, C. Pomelli, C. Adamo, S. Clifford, J. Ochterski, G. A. Petersson, P. Y. Ayala, Q. Cui, K. Morokuma, D. K. Malick, A. D. Rabuck, K. Raghavachari, J. B. Foresman, J. Cioslowski, J. V. Ortiz, B. B. Stefanov, G. Liu, A. Liashenko, P. Piskorz, I. Komaromi, R. Gomperts, R. L. Martin, D. J. Fox, T. Keith, M. A. Al-Laham, C. Y. Peng, A. Nanayakkara, C. Gonzalez, M. Challacombe, P. M. W. Gill, B. G. Johnson, W. Chen, M. W. Wong, J. L. Andres, M. Head-Gordon, E. S. Replogle and J. A. Pople, Gaussian 98W (Revision A.5), Gaussian Inc., Pittsburgh, PA, 1998.

¹⁸ A. Dickie, A. K. Kakkar and M. A. Whitehead, *Langmuir*, 2002, **18**, 5657.

¹⁹ F. Rakotondradany, M. A. Whitehead, A. Lebuis and H. F. Sleiman, *Chem.-Eur. J.*, 2003, **9**, 4771.

²⁰ P. Charbonneau, B. Jean-Claude and M. A. Whitehead, *J. Mol. Struct. (THEOCHEM)*, 2001, **574**, 85.

²¹ C. Malardier-Jugroot, A. C. Spivey and M. A. Whitehead, *J. Mol. Struct. (THEOCHEM)*, 2003, **623**, 263.

²² J. T. Bosko, B. D. Todd and R. J. Sadus, *J. Chem. Phys.*, 2004, **121**, 1091.

²³ R. G. Gaudreault, M. A. Whitehead and T. G. M. van de Ven, *Colloids & Surfaces A*, 2005, **268** (1), 131-146.

²⁴ R. G. Gaudreault, M. A. Whitehead and T. G. M. van de Ven, *J. Phys. Chem. A*, 2006, 3692.

²⁵ C. Malardier-Jugroot, T. G. M. van de Ven and M. A. Whitehead, *J. Mol. Struct. (THEOCHEM)*, 2004, **679**, 171.

²⁶ R. G. A. R. Maclagan, C. Malardier-Jugroot, M. A. Whitehead and M. Lever, *J. Phys. Chem.*, 2004, **108**, 2514.

²⁷ C. Malardier-Jugroot, M. A. Whitehead and M. Lever, *J. Phys. Chem.B.*, 2005, **109**(15), 7022.

²⁸ HyperChem release 5.11. For Windows molecular modelling system, Hypercube Inc., 419 Philip Street, Waterloo, Ont., Canada N2L 3X2, 1999.

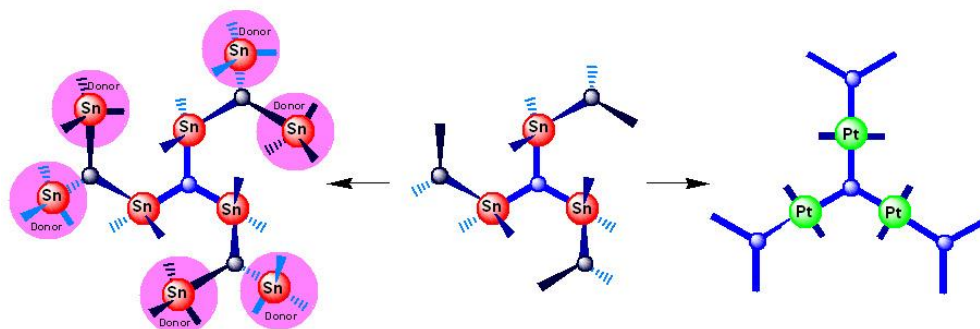
²⁹ F. Villamagna and M. A. Whitehead, *J. Chem. Soc., Faraday Trans.*, 1994, **90**, 1, 47.

³⁰ G. Iftime, L. Fisher, A. Natansohn and P. Rochon, *Can. J. Chem.*, 2000, **78**, 409.

- ³¹ B. Paci, C. Schmidt, C. Fiorini, J.-M. Nunzi, C. Arbez-Gindre and C. G. Screttas, *J. Chem. Phys.*, 1999, **111**, 16, 7486.
- ³² M. G. L. Petrucci and A. K. Kakkar, *J. Chem. Soc., Chem. Commun.*, 1995, 1577.
- ³³ M. G. L. Petrucci and A. K. Kakkar, *Adv. Mater.*, 1996, **8**, 3, 251.
- ³⁴ M. G. L. Petrucci and A. K. Kakkar, *Organometallics*, 1998, **17**, 1798.
- ³⁵ M. G. L. Petrucci and A. K. Kakkar, *Chem. Mater.*, 1999, **11**, 269.
- ³⁶ M. Petrucci-Samija, V. Guillemette, M. Dasgupta and A. K. Kakkar, *J. Am. Chem. Soc.*, 1999, **121**, 1968.
- ³⁷ M. G. L. Petrucci, D. Fenwick and A. K. Kakkar, *J. Mol. Catal. A: Chem.*, 1999, **146**, 309.
- ³⁸ A. K. Kakkar, *Chem. Rev.*, 2002, **102**, 3579.
- ³⁹ M. Dasgupta, M. B. Peori and A. K. Kakkar, *Coord. Chem. Rev.*, 2002, **233-234**, 223.
- ⁴⁰ A. K. Kakkar, *Macromol. Symp.*, 2003, **196**, 145.
- ⁴¹ O. Bourrier and A. K. Kakkar, *Macromol. Symp.*, 2004, **209**, 97.
- ⁴² M. Ooe, M. Murata, T. Mizugaki, K. Ebitani and K. Kaneda, *J. Am. Chem. Soc.*, 2004, **126**, 1604.
- ⁴³ R. M. Crooks, M. Zhao, L. Sun, V. Chechik and L. K. Yeung, *Acc. Chem. Res.*, 2001, **34** (3), 181.

Chapter 3

Turbine Shape Organotin Dendrimers: Photophysical Properties and Direct Replacement of Sn with Pt



This chapter describes a versatile methodology to synthesize dendrimers containing dimethyl tin links in the backbone that can be directly substituted to introduce transition metals moieties in the dendritic structure. It demonstrates the efficacy of acid-base hydrolysis chemistry of amino-stannanes with terminal acetylenes in constructing dendritic backbones, and is in direct relationship to dimethylsilyl linked DHBA dendrimers presented in Chapter 2.

Reproduced in part with permission from:

Hourani R., Whitehead M. A., and Kakkar A., *Macromolecules*, **2008**, *41*, 508.

Copyright, 2009, American Chemical Society.

3.1 Introduction

Designing new dendritic macromolecules continues to be a topical area of research due to their unique properties and the possibility to tailor and control their overall structure using a variety of molecules that constitute their template core and backbone.¹ Hyperbranched architectures containing rigid conjugated organic backbones are of considerable interest due to their potential in designing novel materials by exploiting their photophysical, electronic, and optical properties.^{2,3} We were interested in exploring the structure of dendrimers that will evolve from 1,3,5-triethynylbenzene (TEB) at the template core as well as in the backbone, linked by dimethyltin moieties, and the role of rigid molecular structure and geometrical requirements of the linking unit, in shaping the overall structure of these dendrimers. In this manuscript, we report a simple methodology to synthesize TEB-based dendrimers and an evaluation of their structure that develops into a turbine shape, with benzene rings arranged in a fashion to create sandwich type cavities. Organic donors placed at the periphery of conjugated backbones are known to enhance π -conjugation in their backbone.³ We demonstrate here that inorganic groups such as Me_3Sn provide a similar electronic donating effect and can significantly influence the photophysical properties of these hyperbranched macromolecules. The versatility of these macromolecules in synthesizing dendrimers containing transition metal moieties in the backbone is demonstrated by a direct substitution of dimethyltin links with square planar platinum centers, upon reaction with $(^n\text{Bu}_3\text{P})_2\text{PtCl}_2$. This eliminates the need of a catalyst in the synthesis of such organometallic dendrimers.

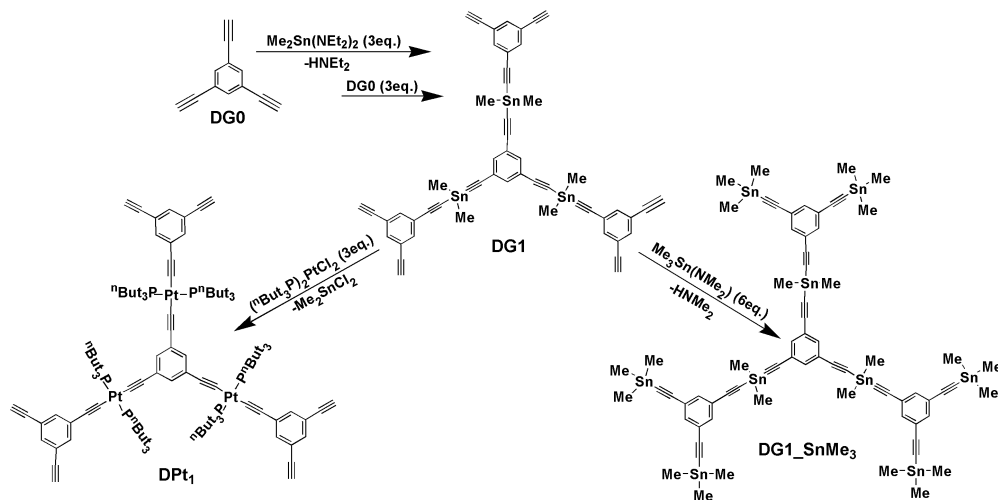
3.2 Results and discussion

The divergent synthetic methodology used to construct TEB based dendrimers is based on acid-base hydrolytic chemistry⁴ of aminostannanes with molecules containing terminal acetylenes. It involved controlled reiterative reaction of molar equivalents of TEB and bis(diethylamino)dimethyltin $[\text{Me}_2\text{Sn}(\text{NEt}_2)_2]$ (**Scheme 3.1**).

The only byproduct in the reaction is a low boiling amine that is removed under vacuum, and the resulting dendrimers are purified by extraction into benzene. The capping of each dendrimer generation with

Me_3Sn can be achieved by reacting with an appropriate amount of $\text{Me}_3\text{Sn}(\text{NMe}_2)$ (**Scheme 3.1**).

Scheme 3.1. Synthesis of the first generation dendrimer (DG1), capping with Me_3Sn , and replacement of Sn with Pt.



A detailed investigation of the structure of these dendrimers, using the molecular mechanics MM+ method and the PM3 semiempirical molecular orbital theory,⁵ shows that the TEB units adopt a completely rigid flat structure and the tin centers are most stable when a tetrahedral structure around them is retained. For the latter arrangement, and to reduce steric hindrance, the TEB units in the upper layers do not stay in the same plane as the TEB unit at the template core. For example, the first generation dendrimer adopts a turbine shape in which the three peripheral TEB arms tilt away from the plane in the same direction, at identical dihedral angles ($\sim 45^\circ$) around the core arms (**Figure 3.1**). In the second generation, the next layer of TEB and Sn centers orient in the same fashion with similar dihedral angles. This leads to an outward growth of each arm away from the center, without back folding in the space between the arms. The additional layer in the third generation dendrimer grows in a similar relationship to DG2. The sustained dihedral angles allow the arms to grow without any crowding that would prevent growth. Because of the larger size of the arms in DG3, a more defined three-dimensional structure develops that resembles a turbine, with the outer benzene ring of an arm coming on top of the arm next to it, at a distance of approximately 20 Å

(**Figure 3.1**). This creates sandwich type cavities in between the turbine arms that could act as potential host sites for molecular encapsulation of small guest molecules, through π - π interactions.

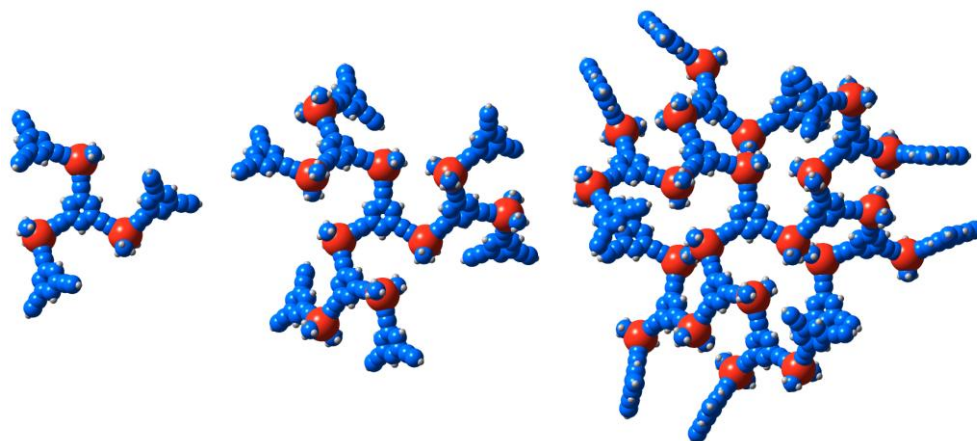


Figure 3.1. PM3-optimized structures of TEB dendrimer generations 1-3.

The average diameters of these dendrimers were found to be 22, 40, and 52 Å for generations 1-3, respectively. Interestingly, these sizes are larger, by an average of 7 Å, than corresponding dendrimers with more flexible backbones, such as 3,5-dihydroxybenzyl alcohol (DHBA).^{6a} This demonstrates that the rigidity of TEB and the reinforced tetrahedral geometry around tin do not permit many options for the TEB arms to move or rotate. In fact, a slight rotation around the tin linkages causes a dramatic increase in the energy of the most stable dendrimer structure. On the other hand, in more flexible dendrimer back bones, the arms can be rotated around the linking unit with only a slight increase in energy.⁶

The photophysical properties of the TEB-based dendrimers were studied using UV-Vis absorption and fluorescence spectroscopies (**Table 3.1**). The absorption spectrum of TEB (DG0) shows λ_{max} at 305 nm, and a fluorescence emission band (λ_{max}) at 336 nm with a quantum yield of 6%. The emission spectrum of the first generation dendrimer (DG1) showed only a small red shift; however, its quantum yield almost doubled (11%). The emission spectrum of the second generation dendrimer (DG2) showed similar emission λ_{max} and a slightly better quantum yield (13%) than the first generation. The same trend was observed for the third generation dendrimer (DG3).

Table 3.1. Photophysical Data of DG0-3 and their Capped forms (DG0-SnMe₃ to DG3-SnMe₃) in benzene at room temperature.

Dendrimer	ϕ_f^a	λ_{abs} (nm)	λ_{em} (nm)
DG0	0.06	305	336
DG1	0.11	308	345
DG2	0.13	308	346
DG3	0.17	308	346
DG0-SnMe₃	0.22	311	346
DG1-SnMe₃	0.30	314	348
DG2-SnMe₃	0.32	314	349
DG3-SnMe₃	0.35	314	349

^aQuantum yield is calculated relative to quinine sulfate ($\phi_f=0.55$ in 0.1M H₂SO₄)

Recent studies have shown that the presence of dipolar units consisting of donor (OMe) and acceptor (C≡C) groups enhances photophysical properties and fluorescence quantum yields of star-shaped oligomers that originate from the TEB core.³ Interestingly, the presence of Me₃Sn groups at the periphery, and symmetrically placed Me₂Sn links in the backbone of the dendrimers reported here, shows a similar effect to that of organic donors. This is demonstrated by the red shift in the absorption/emission spectra and the increase in quantum yields of TEB dendrimers, compared to the TEB molecule. For example, capping of TEB (DG0) with trimethyltin at its periphery (DG0-SnMe₃) led to a red shift in its absorption and emission spectra, and its quantum yield was found to be almost 4 times higher (22%) than that of DG0 (**Table 3.1**). It clearly suggests that the trimethyltin moiety is acting as a donor and enhances n-conjugation in the molecule. These results were further supported by Mulliken charge⁷ calculations on the atoms of the core molecule (DG0) and its trimethyltin capped analogue (DG0-SnMe₃). Mulliken charges provide an estimation of partial atomic charges. For example, in DG0, the terminal carbon in acetylene has a Mulliken charge of -0.158 e, which increases to -0.457 e upon capping with SnMe₃ (DG0-SnMe₃). This indicates that the acetylenic carbon becomes more electron rich upon binding to Sn. Similarly, upon capping the first generation dendrimer with trimethyltin (DG1-SnMe₃), a larger red shift in the absorption maxima and an increase in the quantum yield to about 30% were observed (**Table 3.1**).

Capping of dendrimers of generations 2 and 3 with trimethyltin (DG2-SnMe₃ and DG3-SnMe₃) led to a similar increase in their quantum efficiencies.

The presence of dimethyltin moieties in the backbone of the dendrimers enhances their quantum efficiencies to some extent and causes a red shift in the absorption spectra by about 5 nm. Since a dimethyltin group in the backbone of the dendrimer is placed between two acceptor (C≡C) moieties, its donating effect is shared equally in both directions. On the other hand, when trimethyltin groups are added to the peripheries of the dendrimers, a larger red shift in the absorption spectrum is observed and the quantum yields are enhanced to almost 6-fold, suggesting that terminally substituted Me₃Sn groups have a stronger unidirectional donor effect.

Dendrimers containing transition metal centers in the backbone continue to attract great interest due to their applications in catalysis, photonics, *etc.*⁸ Acetylenic molecules ligated to Sn are known to undergo a metathesis reaction with transition metal halides, and the latter reaction has been demonstrated to be a useful methodology to synthesize linear organometallic polymers.⁹ We were intrigued by the possibility of replacing Sn moieties directly in the backbone with transition metal centers, yielding an attractive route to organometallic dendrimers. In a preliminary investigation, we attempted the reaction of the first generation dendrimer (DG1) with 3 equiv of Cl₂Pt(PⁿBu₃)₂ at room temperature. It led to the replacement of Me₂Sn moieties in the dendrimer with Pt(PⁿBu₃)₂. Such platinum—acetylide dendrimers have been prepared earlier using CuI and NEt₂H base-catalyzed condensation reactions of metal halides with acetylenic compounds.¹⁰ The direct substitution of the Sn moiety in the dendrimers with platinum centers without the need of a catalyst offers potential in tailoring the backbone structure and the resulting properties of the dendrimers described here. We are currently studying the details of this substitution reaction and will subsequently expand the scope of this methodology.

3.3 Conclusions

We have demonstrated that a rigid molecular structure of the repeat unit and the geometric constraints of the linker can significantly influence the evolving hyperbranched structure of the dendrimers. The

1,3,5-triethynylbenzene unit at the template core assumes a flat morphology with the subsequent TEB molecules in the higher generations bending away from each other. It leads to a turbine shape with the benzene rings in a sandwich type structure. The inorganic entities (SnMe_3) present at the periphery of these dendrimers act as donors, which enhances n-conjugation leading to improved quantum yields. The direct metathesis of the Me_2Sn links with $\text{Pt}(\text{P}^n\text{Bu}_3)_2$ can be carried out upon reaction with $\text{Cl}_2\text{Pt}(\text{P}^n\text{Bu}_3)_2$, and it offers a useful synthetic methodology to construct organometallic dendrimers without the need for a catalyst.

3.4 General procedure for the dendrimers synthesis

In a typical iterative reaction sequence, a solution of 1 equivalent of DG0 in dry THF was added dropwise over a period of almost 3 h to an ice-bath cooled solution of 3 equivalents of $\text{Me}_2\text{Sn}(\text{NEt}_2)_2$ in THF. The mixture was left to stir for 1 h, warmed to room temperature, and then added to a solution of 3 equiv of DG0 in THF, in a dropwise fashion over a period of 6 h, and left to stir overnight. After removal of the solvent under vacuum, the first generation dendrimer was extracted into benzene and the removal of solvent yielded a yellowish white solid. The synthesis of the second and third generation dendrimers was done in a similar fashion, by continuing the building over generation 1 and 2, respectively. The structures of generations 2 and 3 are shown in **Figure 3.2**. For capping with SnMe_3 , to a solution of DG0 in THF, 3 molar equiv of $\text{Me}_3\text{Sn}(\text{NMe}_2)$ were added. The solution was left to stir at room temperature overnight. The solvent was subsequently evaporated, and the resulting product was extracted into benzene to yield the desired product in quantitative yields. A similar method was adopted for generations 1, 2, and 3 using 6, 12, and 24 molar equivalents of $\text{Me}_3\text{Sn}(\text{NMe}_2)$, respectively (**Scheme 3.2**). The replacement of Sn by Pt in DG1 was done by mixing 1 equivalent of the dendrimer with 3 equivalents of $(^n\text{Bu}_3\text{P})_2\text{PtCl}_2$ in THF. The mixture was left to stir at room temperature for 48 h. The solvent was evaporated, and the resulting solid was washed several times with hexanes to yield the desired product (DPt1).

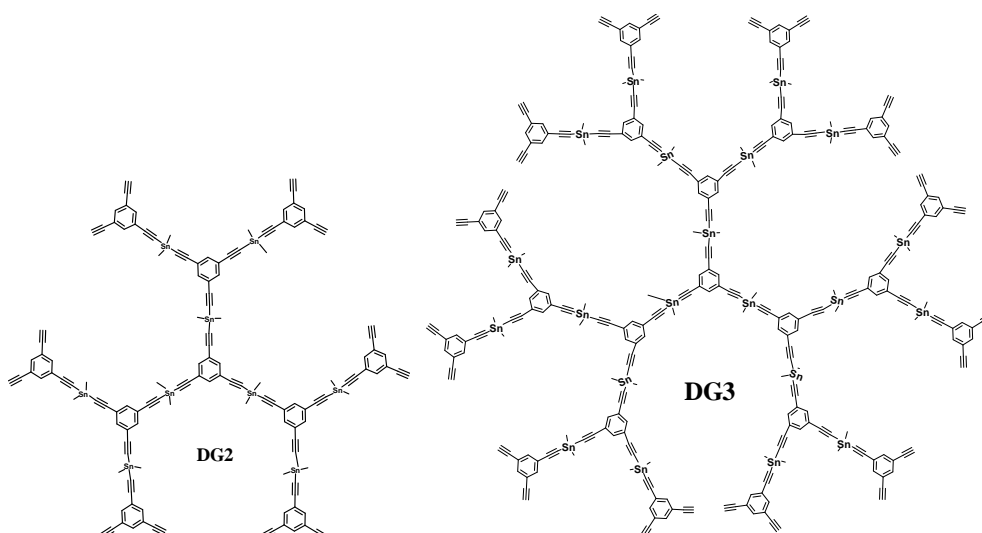


Figure 3.2. Structures of dendrimer generation 2, and 3 (DG2 & DG3).

3.5 Theoretical methods

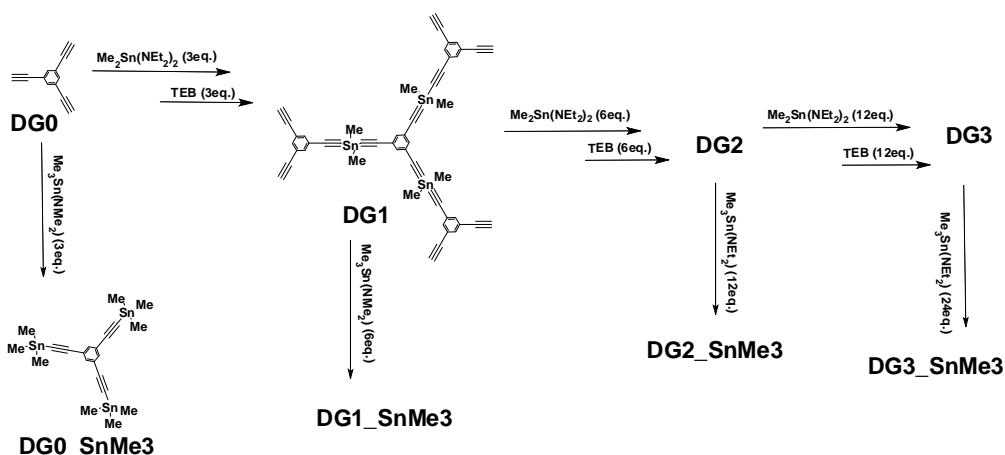
The geometry optimization was carried out using the Polak-Ribiere conjugate gradient, set to terminate at an RMS gradient of $0.01 \text{ kcal. } \text{\AA}^{-1} \cdot \text{mol}^{-1}$. Then, Semi-Empirical Parameterization Model 3 (PM3) Molecular Orbital Method was used with the HyperChem and Gaussian98 programs. Semi-Empirical optimizations were carried out under standard convergence criteria (max force = $4.5 \times 10^{-4} \text{ Hartrees bohr}^{-1}$; RMS force = $3.0 \times 10^{-4} \text{ Hartrees bohr}^{-1}$; max displacement = $1.8 \times 10^{-3} \text{ \AA}$; RMS displacement = $1.2 \times 10^{-3} \text{ \AA}$). The conformations of the dendrimers were found by varying all torsional axes to discover the minimum global energy conformation, which was 8-9 kcal more stable than any other conformer. The energies of the most stable structures of DG1-3 were found to be -10634.9, -27535.2, and -61329.9 kcal/mol respectively. Mulliken charges were calculated using the output file from the Gaussian98 program in the GaussView 3.0 program.

3.6 Experimental section

$\text{Me}_3\text{SnNMe}_2$ was purchased from Aldrich. 1,3,5-triethynylbenzene, $\text{Me}_2\text{Sn}(\text{NEt}_2)_2$ and $(^n\text{Bu}_3\text{P})_2\text{PtCl}_2$ were synthesized using the procedures described in: Weber, E.; Hedur, M.; Koepp, E.; Orlia, W.; Czugler, M. *J. Chem. Soc., Perkin Trans. 2*, 1988, 1251; Jones, K.; Lappert, M. F. *J. Chem. Soc.* **1965**, 1944; and Kauffman, G. B.; Teter, L. A. *Inorg. Synth.* **1963**, 7, 245, respectively. All reactions were carried out under a nitrogen atmosphere using

dry and distilled solvents, and either Braun Labmaster MB-150 dry box or standard Shlenck line techniques. NMR samples were prepared inside the dry box using deuterated solvents, and spectra were measured on a 270 MHz JEOL spectrometer at ambient temperatures. The chemical shifts in ppm are reported relative to tetramethylsilane as an internal standard for ^1H and $^{13}\text{C}\{^1\text{H}\}$ and to H_3PO_3 for $^{31}\text{P}\{^1\text{H}\}$ NMR spectra. Infrared spectra were measured on a Bruker IFS-48 Fourier transform infrared spectrometer using a standard resolution of 4 cm^{-1} for transmission. Mass spectra were recorded on a Hewlett Packard 5973 mass spectrometer, and MALDI-TOF spectra on a Kratos Kompact Maldi 3.v.4.00 spectrometer using LiBr-dithranol as the matrix. UV-Vis spectra were recorded on a Hewlett Packard 8453 with a resolution of 2 nm using quartz cuvettes. Fluorescence measurements were performed on a Photon Technology International (PTI) TimeMaster Model C-720F spectrofluorimeter. An excitation wavelength of 305nm was used for all measurements. The spectra were measured in benzene using concentrations of 0.02 to 0.06 mM in an inert atmosphere at room temperature. The synthesis of 1,3,5-triethynylbenzene based dendrimers involves a layer by layer construction using extremely controlled conditions. The detailed analyses of these dendrimers, using a combination of the characterization techniques, confirmed the structures as shown in **Scheme 3.1**, and eliminated any possibility of constitutional isomers. Details about the synthesis of all compounds, shown in **Scheme 3.2**, are described below.

Scheme 3.2. Synthesis of TEB-based dendrimers, their Me₃Sn-terminated analogs, and replacement of Sn with Pt in DG1.



3.6.1 Synthesis of 1,3,5-triethynylbenzene (TEB) based dendrimers

In a typical iterative reaction sequence to synthesize generation 2 dendrimer, a solution of 1 equivalent of 1,3,5-triethynylbenzene (TEB) (25 mg, 0.167 mmol) in 30 mL of tetrahydrofuran (THF), was added dropwise over a period of almost 3h to an ice-bath cooled solution of 3 equivalents of Me₂Sn(NEt₂)₂ (147 mg, 0.501 mmol) in 5mL of THF. The mixture was left to stir for 1h, warmed to room temperature and transferred to an addition funnel. It was added slowly to a solution of 3 equivalents of TEB (75 mg, 0.501 mmol) in 5mL of THF in a dropwise fashion over a period of 6h, and left to stir overnight. The resulting solution of the first generation dendrimer was then added dropwise, in the same fashion as the first step above, to 6 equivalents of Me₂Sn(NEt₂)₂ (294 mg, 1.002 mmol) in 5 mL of THF, and the solution was stirred overnight. The mixture was added dropwise to 6 equivalents of TEB (150 mg, 1.002 mmol) in 10 mL of THF and left to stir overnight. The solvent was evaporated under vacuum, and the resulting white solid was then purified by extraction into benzene (91% yield).

3.6.2 Synthesis of capped dendrimers with SnMe₃ groups

In a typical reaction, to a solution of DG0 (50 mg, 0.334 mmol) in approximately 10 mL of THF, 3 equivalents of Me₃Sn(NMe₂)₂ (208 mg, 1.002 mmol) were added, and left to stir at room temperature overnight. The solvent

was evaporated, and the resulting product was purified by extraction into benzene resulting in quantitative yield of the desired product.

3.6.3 Replacement of Sn in 1st Generation Dendrimer with Pt

To a solution of DG1 (13 mg, 0.0125 mmol) in approximately 10 mL of THF, 3 equivalents of (ⁿBu₃P)₂PtCl₂ (25 mg, 0.0375 mmol) were added, and left to stir at room temperature for 48 h. The solvent was evaporated, and the resulting solid was washed several times with hexanes (30% yield).

3.6.4 Spectroscopic data for 1,3,5-triethynylbenzene (TEB) based compounds

DG1: ¹H NMR (C₆D₆, 270 MHz): δ (ppm) 0.25 (s, 18 H), 2.58 (s, 6 H), 7.44 (s, 3 H), 7.56 (s, 6 H), 7.73 (s, 3 H). ¹³C{¹H} NMR (C₆D₆, 68 MHz): δ (ppm) -6.9, 78.9, 81.5, 93.4, 109.0, 123.3, 135.3. FT-IR ν_{C≡C}: 2110, 2146 cm⁻¹. MS (MALDI-TOF m/z) Calculated M: 1041.0, found: M⁺ 1041.5.

DG2: ¹H NMR (C₆D₆, 270 MHz): δ (ppm) 0.25 (s, 54 H), 2.54 (s, 12 H), 7.44 (s, 12 H), 7.56 (s, 12 H), 7.73 (s, 6 H). ¹³C{¹H} NMR (C₆D₆, 68 MHz): δ (ppm) -6.9, 78.9, 81.5, 92.5, 107.5, 123.3, 135.4. FT-IR ν_{C≡C}: 2116, 2146 cm⁻¹. MS (MALDI-TOF m/z) Calculated M: 2822.6, found: M⁺ 2823.3.

DG3: ¹H NMR (C₆D₆, 270 MHz): δ (ppm) 0.27 (s, 126 H), 2.54 (s, 24 H), 7.44 (s, 30 H), 7.57 (s, 24 H), 7.69 (s, 12 H). ¹³C{¹H} NMR (C₆D₆, 68 MHz): δ (ppm) -6.8, 78.9, 81.7, 92.5, 108.0, 123.3, 135.3. FT-IR ν_{C≡C}: 2116, 2146 cm⁻¹. MS (MALDI-TOF m/z) Calculated M: 6385.9, found: M+Li⁺ 6396.1.

DG0-SnMe₃: ¹H NMR (C₆D₆, 270 MHz): δ (ppm) 0.15 (s, 27 H), 7.78 (s, 3 H). ¹³C{¹H} NMR (C₆D₆, 68 MHz): δ (ppm) -8.4, 94.9, 107.6, 124.9, 134.7. FT-IR ν_{C≡C}: 2141 cm⁻¹. MS m/z Calculated M: 638.6, found: M⁺ 639.5.

DG1-SnMe₃: ¹H NMR (C₆D₆, 270 MHz): δ (ppm) 0.13 (s, 72 H), 7.75 (s, 12 H). ¹³C{¹H} NMR (C₆D₆, 68 MHz): δ (ppm) -8.4, 94.9, 107.6, 124.9, 134.8. FT-IR ν_{C≡C}: 2142 cm⁻¹. MS (MALDI-TOF m/z) Calculated M: 2017.8, found: M+Li⁺ 2024.6.

DG2-SnMe₃: ¹H NMR (C₆D₆, 270 MHz): δ (ppm) 0.12 (s, 162 H), 7.75 (s, 30 H). ¹³C{¹H} NMR (C₆D₆, 68 MHz): δ (ppm) -8.4, 94.9, 107.6, 124.9, 134.7. FT-IR ν_{C=C}: 2142 cm⁻¹. MS (MALDI-TOF m/z) Calculated M: 4776.3, found: M+Li⁺: 4784.2.

DG3-SnMe₃: ¹H NMR (C₆D₆, 270 MHz): δ (ppm) 0.13 (s, 342 H), 7.77 (s, 66 H). ¹³C{¹H} NMR (C₆D₆, 68 MHz): δ (ppm) -8.5, 94.8, 107.6, 124.9, 134.8. FT-IR ν_{C=C}: 2141 cm⁻¹. MS (MALDI-TOF m/z) Calculated M: 10293.2, found: M⁺: 10293.8.

DPt1: ¹H NMR (C₆D₆, 270 MHz): δ (ppm) 0.89 (t, 54 H), 1.34 (m, 36 H), 1.58 (br m, 36 H), 2.00 (br m, 36 H), 2.58 (s, 6 H), 7.44 (s, 3 H), 7.52 (s, 6 H), 7.78 (s, 3 H). ¹³C{¹H} NMR (C₆D₆, 68MHz): δ (ppm) 11.6, 13.7, 24.5, 26.5, 77.8, 82.6, 92.5, 107.5, 123.1, 134.6. ³¹P{¹H} NMR (C₆D₆, 109MHz): δ (ppm) 4.19 (J_{Pt-P} 2339Hz). FT-IR ν_{C=C}: 2116, 2146 cm⁻¹. MS (MALDI-TOF m/z) Calculated M: 2393.8, found: M⁺ 2394.3.

3.7 References

- ⁽¹⁾ (a) Antoni, P.; Nystrom, D.; Hawker, C. J.; Hulta, A.; Malkoch, M. *Chem. Commun.* **2007**, 2249. (b) Gingras, M.; Raimundo, J.-M.; Chabre, Y. M. *Angew. Chem., Int. Ed.* **2007**, 46, 1010. (c) Helms, B.; Meijer, E. W. *Science* **2006**, 313, 929. (d) van de Coevering, R.; Alfors, A. P.; Meeldijk, J. D.; Martinez-Viviente, E.; Pregosin, P. S.; Klein Gebbink, R. J. M.; van Koten, G. *J. Am. Chem. Soc.* **2006**, 128 (39), 12700. (e) Caminade, A.-M.; Majoral, J.-P. *Acc. Chem. Res.* **2004**, 37, 341. (f) Newkome, G. R.; Moorefield, C. N.; Vogtle, F. *Dendrimers and Dendrons, Concepts, Syntheses and Applications*; Wiley-VCH: Weinheim, Germany, 2002. (g) *Dendrimers and Other Dendritic Polymers*; Frechet, J. M. J., Tomalia, D. A., Eds.; John Wiley & Sons Ltd.: New York, 2001. (h) Grayson, S. M.; Frechet, J. M. J. *Chem. Rev.* **2001**, 101, 3819.
- ⁽²⁾ (a) Wurthner, F.; Stepanenko, V.; Sautter, A. *Angew. Chem., Int. Ed.* **2006**, 45, 1939. (b) Yamaguchi, Y.; Ochi, T.; Wakamiya, T.; Matsubara Y.; Yoshida, Z. *Org. Lett.* **2006**, 8 (4), 717. (c) Gonzalo Rodriguez, J.; Tejedor, J. L. *Eur. J. Org. Chem.* **2005**, 360. (d) Yamaguchi, Y.; Kobayashi, S.; Wakamiya, T.; Matsubara, Y.; Yoshida, Z. *Angew. Chem., Int. Ed.* **2005**, 44, 7040. (e) Barbera,

J.; Gimeno, N.; Monreal, L.; Pinol, R.; Ros, B.; Serrano, J. L. *J. Am. Chem. Soc.* **2004**, *126*, 7190. (f) Qu, J.; Liu, D.; De Feyter, S.; Zhang, J.; De Schryver, F. C.; Mullen, K. *J. Org. Chem.* **2003**, *68*(25), 9802. (g) Kreger, K.; Jandke, M.; Strohmriegl, P. *J. Synth. Met.* **2001**, *119*, 163. (h) Herrmann, A.; Weil, T.; Slinigersky, V.; Wiesler, U.-W.; Vosch, T.; Hofkens, J.; De Schryver, F. C.; Mullen, K. *Chem. Eur. J.* **2001**, *7*, 4844.

⁽³⁾ Yamaguchi, T.; Ochi, S.; Miyamura, T.; Tanaka, S.; Kobayashi, T.; Wakamiya, Y.; Matsubara, Y.; Yoshida, Z.-I. *J. Am. Chem. Soc.* **2006**, *128*, 4504.

⁽⁴⁾ (a) Jones, K.; Lappert, M. F. *J. Organomet. Chem.* **1965**, *3*, 295. (b) Jones, K.; Lappert, M. F. *J. Chem. Soc.* **1965**, 1944. (c) Sawyer, A. K., Ed. *Organotin Compounds*, Vol. 2; M. Dekker: New York, 1971. (d) Davies, A. G. *Organotin Chemistry*, 2nd ed.; Wiley-VCH: Weinheim, Germany, 2004.

⁽⁵⁾ Segal, G. A. *Semiempirical Methods of Electronic Structure Calculation, Part A: Techniques*; Plenum Press: New York, 1997.

⁽⁶⁾ (a) Hourani, R.; Kakkar, A. K.; Whitehead, M. A. *J. Mater. Chem.* **2005**, *15*, 2106. (b) Bosko, J. T.; Todd, B. D.; Sadus, R. J. *J. Chem. Phys.* **2004**, *121*, 1091.

⁽⁷⁾ (a) Mulliken, R. S. *J. Chem. Phys.* **1955**, *23*, 1833. (b) Csizmadia, I. G. *Theory and Practice of MO Calculations on Organic Molecules*; Elsevier: New York, 1976.

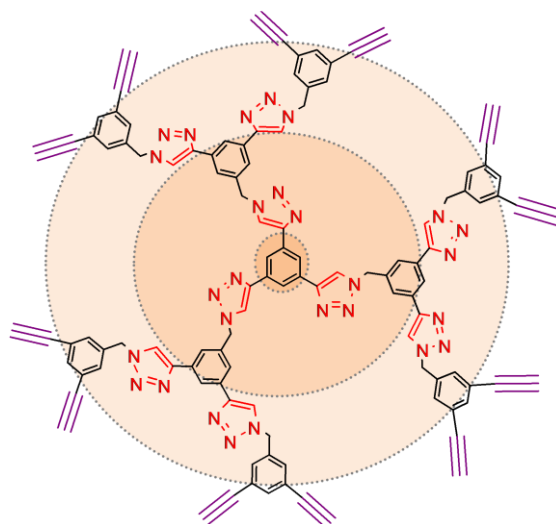
⁽⁸⁾ (a) Kim, M.-J.; MacDonnell, F. M.; Gimon-Kinsel, M. E.; Du Bois, T.; Asgharian, N.; Griener, J. C. *Angew. Chem., Int. Ed.* **2000**, *39*, 615. (b) van Heerbeek, R.; Kamer, P. C. J.; van Leeuwen, P. W. N. M.; Reek, J. N. H. *Chem. Rev.* **2002**, *102*, 3717. (c) Balzani, V.; Ceroni, P.; Juris, A.; Venturi, M.; Campagna, S.; Puntotiero, F.; Serroni, S. *Coord. Chem. Rev.* **2001**, *219*, 545. (d) Leveque, J.; Moucheron, C.; Kirsch-De Mesmaeker, A.; Loiseau, F.; Serroni, S.; Puntoriero, F.; Campagna, S.; Nierengarten, H.; van Dorsselaer, A. *Chem. Commun.* **2004**, 878.

⁽⁹⁾ (a) Johnson, B. F. G.; Kakkar, A. K.; Khan, M. S.; Lewis, J.; Dray, A. E.; Wittmann, F.; Friend, R. H. *J. Mater. Chem.* **1991**, *1*(3), 485. (b) Lewis, J.; Khan, M. S.; Kakkar, A. K.; Johnson, B. F. G. *J. Organomet. Chem.* **1992**, *42*, 165.

⁽¹⁰⁾ (a) Onitsuka, K.; Fujimoto, M.; Kitajima, H.; Ohshiro, N.; Takei, F.; Takahashi, S. *Chem. Eur. J.* **2004**, *10*, 6433. (b) Leininger, S.; Stang, P. J.; Huang, S. *Organometallics* **1998**, *17*, 3981. (c) Khan, M. S.; Schwartz, D. J.; Pasha, N. A.; Kakkar, A. K.; Lin, B.; Raithby, P. R.; Lewis, J. *Anorg. Allg. Chem.* **1992**, 616, 121.

Chapter 4

Designing Dendritic Frameworks with Versatile Building Blocks Suitable for Cu^I Catalyzed Alkyne Azide “Click” Chemistry



In this chapter, building blocks suitable for the construction of dendrimers using Cu^I catalyzed alkyne-azide "click" chemistry are developed. It provides a versatile synthetic methodology that can enable the synthesis of multifunctional dendrimers reported in Chapter 5. Throughout this thesis (Chapters 2-4), the theme of using simple and highly efficient chemistry in the design and synthesis of dendrimers is maintained.

Reproduced in part with permission from:

Hourani R., Sharma A., & Kakkar A., **2009**, submitted for publication.

Unpublished work copyright, 2009.

4.1 Introduction

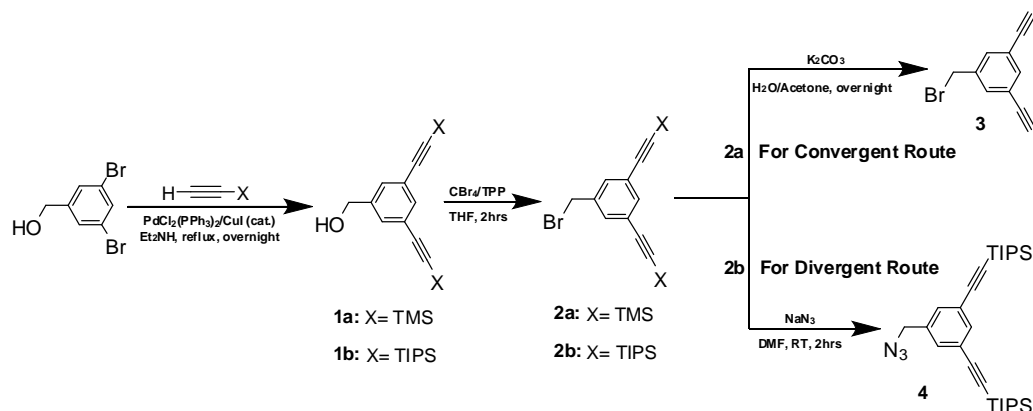
Dendrimers constitute key components in the quest to build smart nanodevices for applications in a diverse range of areas including biology and medicine.¹ The synthesis of these monodisperse macromolecules has attracted the imagination of scientists, and it has already generated a large library with varied backbones.² A major contribution to this renaissance in dendrimer synthesis has been made by one of the highly efficient “click” reactions that involves Cu^I catalyzed coupling of an alkyne with an azide (CuAAC).³ The versatility of this methodology lies in the design of appropriate alkyne and azide terminated molecular units that can then be “clicked” together under a variety of mild reaction conditions. We report here the synthesis of highly versatile AB₂ (A: N₃; and B: C≡CH) building blocks that can be used to perform CuAAC to construct dendrimers using either the divergent or the convergent synthetic methodologies. We demonstrate that the scope and utility of this “greener” approach to the synthesis of dendrimers can be easily elaborated by designing such building blocks. We used these molecular units to construct dendritic frameworks which contain 4, 6 or 12 peripheral alkynes, using “click” chemistry. The surface active acetylene groups in these dendrimers can be used to couple various azide-terminated functional molecules of interest including drugs, fluorescent dyes, metallic centers *etc.*⁴

4.2 Results and Discussion

For the dendrimer synthesis using CuAAC “click” chemistry, we envisioned a molecular unit that will incorporate a primary azide and two protected acetylenes which could be made active at the desired stage. The synthetic elaboration was begun using 3,5-dibromobenzyl alcohol, and to which trimethylsilylacetylene (**1a**) or triisopropylsilylacetylene (**1b**) was linked through bromo position using Sonogashira coupling (Scheme 4.1). It was subsequently followed by bromination of the benzylalcohol group (**2a** and **2b**). The building blocks **2a** and **2b** provide versatile platforms to construct dendrimers using either i) the convergent methodology, in which dendrons are

built separately, and then as a final step their focal point is activated and used to anchor the dendron onto the appropriate core; or ii) the divergent, in-side-out approach that employs an iterative build-up starting from the core molecule.

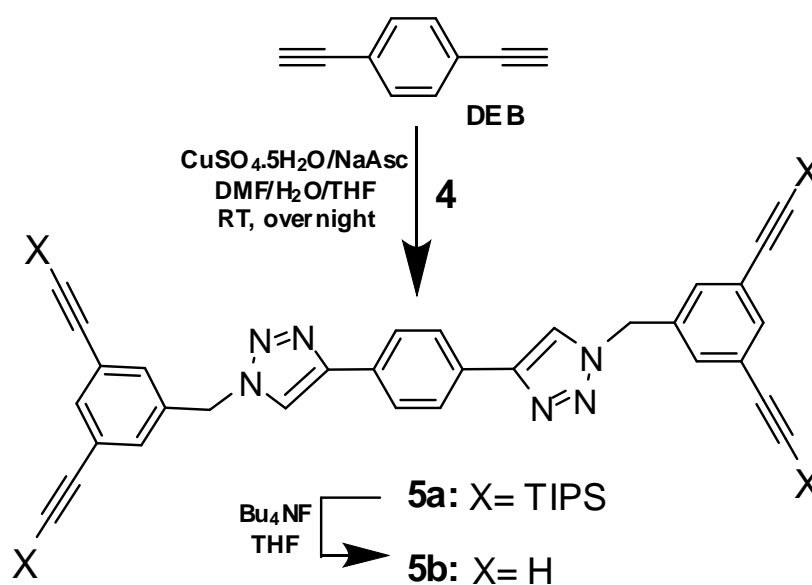
Scheme 4.1. Synthesis of building blocks.



For the convergent construction of dendrimers, the protective (TMS) groups of **2a** were removed using a mild deprotection process with K_2CO_3 . The two acetylene arms in **3** are now available for performing CuAAC click reaction, while the bromo-benzyl constitutes a focal point that can be activated later by converting it to an azide for coupling to core molecules of interest. For divergent synthesis, we converted the bromide arm of **2b** to an azide (**4**) by a simple azidation reaction using NaN_3 in DMF. Compound **4** is used in performing CuAAC click reaction with acetylene terminated core molecules such as 1,4-diacetylenebenzene (**DEB**) with two acetylene arms, and 1,3,5-triethynylbenzene (**TEB**) with three acetylenes, using the divergent methodology, as will be demonstrated below. Interestingly, azidation of **2a**, and its subsequent use in divergent synthesis with CuAAC click reaction, in the presence of the more labile TMS protective groups, did not proceed very well, and yielded a mixture of products. We believe that it was mainly due to a premature deprotection of the TMS groups *in situ* under the CuAAC reaction conditions. It was confirmed by the appearance of the acetylene protons in its 1H NMR. Thus, the TMS protected acetylenes are not ideal silent partners in CuAAC “click” chemistry.

As a model reaction, compound **4**, was first reacted with a divalent core (**DEB**) using the “click” reaction with copper sulfate pentahydrate ($\text{CuSO}_4 \cdot 5\text{H}_2\text{O}$) and sodium ascorbate (Scheme 4.2), to give a four-arm structure with protected acetylene groups (**5a**). The removal of TIPS groups was then achieved using Bu_4NF (**5b**). It should be noted that in this general procedure the sequence of adding the reactants and solvents is highly crucial to ensure a complete reaction. All reactants, except $\text{CuSO}_4 \cdot 5\text{H}_2\text{O}$, were dissolved in a minimal amount of DMF, followed by the addition of $\text{CuSO}_4 \cdot 5\text{H}_2\text{O}$ as an aqueous solution, and then finally THF was added to the mixture. Varying the solvent mixture or the order of addition led to incomplete reactions and lower yields. Thus, we followed the general procedure described above throughout the work reported here for building dendritic frameworks, with only slight variation of temperature and the time of reaction.

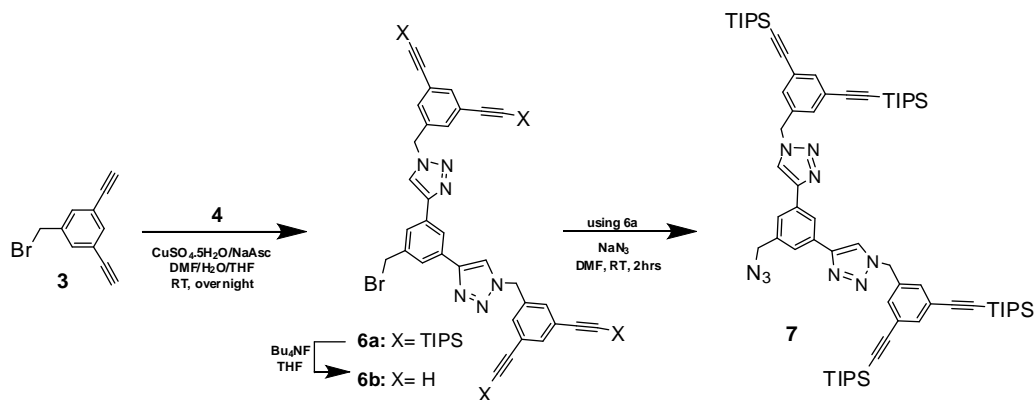
Scheme 4.2. Synthesis using CuAAC “click” reaction.



For the convergent synthesis of dendrimers, dendrons using building blocks **3** and **4** were prepared (Scheme 4.3). The CuAAC click reaction was carried out using a similar procedure as described above for the construction of **5a**, and it yielded a second generation dendron with four TIPS-protected arms

(**6a**). The TIPS protective groups can be easily removed to give free acetylene arms (**6b**), made available for further click reaction, to build higher generation dendrons. Alternatively, the bromine focal point of dendron **6a** can be activated by converting it to an azide, which could be covalently linked to a core molecule while keeping the acetylene peripheries protected. It is important to mention here that the deprotection of **6a** with Bu_4NF gave poor yields. This was due to the fact that Bu_4NF deprotection is also accompanied by the substitution of Br with F at the focal point, as confirmed by ^1H NMR, and mass spectroscopies. The fluoro substituted core does not yield to subsequent azidation.

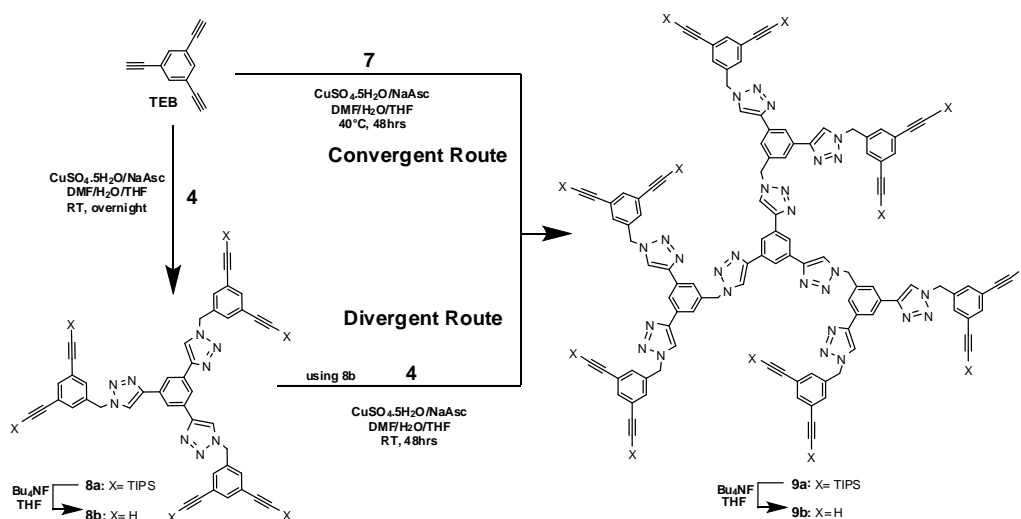
Scheme 4.3. Synthesis of dendrons for convergent synthesis.



The synthesis of the first generation dendrimer with six TIPS-protected acetylenic arms (**8a**) was achieved using the divergent methodology (Scheme 4.4), in which the trivalent core **TEB** was reacted with compound **4**. Subsequent removal of the protective groups using Bu_4NF , yields the first generation dendrimer with six free acetylenes (**8b**) available for functionalization with any azide-terminated molecule of interest. To demonstrate this possibility, and the feasibility of building higher dendrimer generations, **8b** was reacted with compound **4** to give the second generation dendrimer with 12 TIPS-protected acetylene arms (**9a**) as shown in Scheme 4.4. The reaction was performed using the general procedure described in the synthesis of **5a**, however it was left to proceed for 48 hours instead of overnight, to ensure complete reaction of compound **4** with all the available six acetylene arms of the first generation

dendrimer (**8b**). We believe that the increasing polarity of the system with an increase in generation number, and steric crowding at the periphery, slows down the reaction, and thus requires longer time for completion.

Scheme 4.4. Convergent and divergent synthetic routes of dendrimers.



Alternatively, the TIPS-protected second generation dendrimer (**9a**) can also be synthesized using the convergent methodology by reacting the previously prepared dendron **7** with the trivalent **TEB** core (Scheme 4.4). The reaction conditions were similar to those employed in the divergent methodology, however, heating at 40°C was necessary for complete substitution. The TIPS protective groups of the second generation dendrimer, from both convergent or divergent routes, were then removed using Bu_4NF , to give the second generation dendrimer with 12 acetylene peripheral groups (**9b**).

It is worth mentioning that in all the “click” reactions reported here, we used slight excess of azide-terminated molecules to ensure completion to almost quantitative yields (>90%). The removal of excess azide terminated compound was found to be extremely easy *via* flash column chromatography, due to a clear difference in polarity and solubility, as more polar triazole ring containing products are formed. The lower polarity of the starting materials facilitated their removal using low polarity solvent mixtures, except in the case of the protected second generation dendrimer **9a**, in which the presence of 12 triisopropylsilyl

groups enhanced its solubility to a great extent, and it could be flushed down a short column with hexanes, while the excess of the starting material stayed on the column. The synthetic elaboration of the dendrimers was monitored by TLC, ^1H and $^{13}\text{C}\{^1\text{H}\}$ NMR spectroscopy. The latter were found to be diagnostic since there is a clear shift in the ^1H and $^{13}\text{C}\{^1\text{H}\}$ NMR signals as the triazole rings were formed. Interestingly, all compounds reported here were found to be soluble in most organic solvents with the exception of **5b** and **9b**, in which upon removal of the protective TIPS groups the compounds were found to be soluble only in DMF and DMSO. This is intriguing, and we are currently investigating the relationship between the number of triazole rings and free acetylene groups in the structure, on the solubility of these dendrimers.

4.3 Conclusions

In summary, we have demonstrated that by designing appropriate building blocks for highly efficient CuAAC click reaction, one could tailor the synthesis to create a small library of dendritic frameworks with different valencies for further functionalization. Recent reports in the literature have suggested that it is easier and more practical to build the dendritic frameworks, and then introduce suitable surface functionalities as the final step.⁵ The free acetylene groups at the periphery of compounds **5b**, **8b**, and **9b** provide this opportunity, and can be used to couple a diverse range of azide terminated molecules of interest.

4.4 Experimental

4.4.1 Materials

Copper(II) sulfate pentahydrate ($\text{CuSO}_4 \cdot 5\text{H}_2\text{O}$) (>98.0%), Sodium ascorbate (NaAsc) (crystalline, 98%), 1,4-diethynylbenzene (**DEB**) (96%), Tetrabutylammonium fluoride (Bu_4NF) (1.0 M in THF), tetrabromomethane (CBr_4) (99%), K_2CO_3 , Cu^{I} , Bis(triphenylphosphine)palladium(II) dichloride [$\text{PdCl}_2(\text{PPh}_3)_2$], triphenylphosphine (TPP), and sodium azide (NaN_3) (>99.5%)

were purchased from Sigma-Aldrich Canada, and used as received. (Triisopropylsilyl)acetylene, and (trimethylsilyl)acetylene were purchased from Oakwood Products, Inc., and 3,5-Dibromobenzyl alcohol was purchased from Alfa Aesar, and used as purchased. Tetrahydrofuran (THF) was dried over sieves, and diethylamine (DEA) and triethylamine (NEt₃) were distilled over KOH. All other solvents were used as received in their anhydrous forms.

4.4.2 Instruments

NMR spectra were recorded on a 300 or 400MHz (as specified) spectrometer at ambient temperatures. The chemical shifts in ppm are reported relative to tetramethylsilane as an internal standard for ¹H and ¹³C{¹H} NMR spectra. Mass spectra were recorded on Thermo Scientific Orbitrap mass analyzer (ES) and Kratos MS25 (EI) mass spectrometers, and MALDI-TOF spectra on Autoflex III Mass Spectrometer (Bruker) using LiBr-dithranol as the matrix.

4.4.3 Synthesis and Characterization

1,3,5-Triethynylbenzene (TEB): This compound was synthesized using a literature procedure: Weber, E.; Hedur, M.; Koepp, E.; Orlia, W.; Czugler, M. *J. Chem. Soc., Perkin Trans. 2*, 1988, 1251.

¹H NMR (400 MHz, CDCl₃): δ (ppm) 3.11 (s, 3H, -ArCCH), 7.57 (s, 3H, ArH).

Synthesis of 3,5-bis(trimethylsilylethynyl)benzyl alcohol (1a): To a solution of 3,5-dibromo benzyl alcohol (5g, 18.8 mmol) in benzene (70 mL) and triethylamine (130 mL), trimethylsilylacetylene (11.08g, 112.8 mmol) and catalytic amounts (ca. 5 mol%) of [PdCl₂(PPh₃)₂], PPh₃ and CuI were added. The reaction mixture was stirred overnight under reflux, and the solvent was then evaporated and the residue was extracted with diethyl ether. The extract was dried over MgSO₄ and the solvent was evaporated again. The product was purified by silica-gel column chromatography with ethyl acetate/hexane (1:20)

mixture. The solvent was removed under vacuum to yield a pale yellow oil which solidifies upon standing (5.04 g, 89.4%). ^1H NMR (300MHz, CDCl_3): δ (ppm) 0.23 (s, 18H, $-\text{Si}(\text{CH}_3)_3$), 4.63 (d, 2H, $-\text{CH}_2\text{OH}$), 7.40 (s, 2H, $-\text{ArH}$), and 7.50 (s, 1H, ArH). $^{13}\text{C}\{^1\text{H}\}$ NMR (75 MHz, CDCl_3): δ (ppm) 0.1, 64.6, 95.3, 104.1, 123.8, 130.3, 134.7, 141.4. HRMS (EI): Theoretical $M_w = 300.14$ g/mol, found $M_w = 300.10$ g/mol.

Synthesis of 3,5-bis(triisopropylsilylethynyl)benzyl alcohol (1b): To a solution of 3,5-dibromo benzyl alcohol (5g, 18.8 mmol) in benzene (70mL) and triethylamine (130mL), triisopropylsilylacetylene (10.29g, 56.4 mmol) and catalytic amounts (ca. 5 mol%) of $[\text{PdCl}_2(\text{PPh}_3)_2]$, PPh_3 , and CuI were added. The reaction mixture was stirred overnight under reflux. The solvent was then evaporated and the residue was extracted with diethyl ether. The extract was dried over MgSO_4 and the solvent was evaporated again. The product was purified on silica-gel column chromatography with 1:20 (ethylacetate:hexane) mixture. The solvent was removed under vacuum to yield a pale yellow oil (7.97g, 90.5%). ^1H NMR (300MHz, CDCl_3): δ (ppm) 1.13 (br. s, 42H, $-\text{Si}(\text{C}_3\text{H}_7)_3$), 4.65 (d, 2H, $-\text{CH}_2\text{OH}$), 7.42 (s, 2H, ArH), and 7.48 (s, 1H, ArH); $^{13}\text{C}\{^1\text{H}\}$ NMR (75MHz, CDCl_3): δ (ppm) 11.5, 18.9, 64.7, 91.7, 106.1, 124.2, 130.5, 134.5, and 141.3. HRMS (EI): Theoretical $M_w = 468.32$ g/mol. Found $M_w = 468.20$ g/mol.

Synthesis of 3,5-bis(trimethylsilylethynyl)benzyl bromide (2a): To a stirring solution of compound **1a** (5.04g, 16.8 mmol) and carbon tetrabromide (7.23g, 21.8 mmol) in THF (60mL) on an ice bath, PPh_3 (5.71g, 21.8 mmol) was added slowly in small portions. After 15 minutes, the ice bath was removed, and the reaction mixture was left to stir at room temperature for 2 hours. The reaction was then quenched with water and the THF was evaporated. The aqueous phase was then extracted with dichloromethane (DCM, 3x70 mL) and dried with MgSO_4 . The product purified by column chromatography using hexanes. The solvent was evaporated to yield the product as a pale yellow oil (4.37g, 71.9%).

^1H NMR (300MHz, CDCl_3): δ (ppm) 0.24 (s, 18H, $-\text{Si}(\text{CH}_3)_3$), 4.37 (s, 2H, $-\text{CH}_2\text{Br}$), 7.42 (s, 2H, $-\text{ArH}$), and 7.50 (s, 1H, ArH)ppm. $^{13}\text{C}\{^1\text{H}\}$ NMR (75 MHz, CDCl_3): δ (ppm) 0.08, 32.1, 95.8, 103.6, 124.2, 132.5, 135.4, 138.3. HRMS (EI): Theoretical $M_w = 362.05$ g/mol. Found $M_w = 362.10$ g/mol.

Synthesis of 3,5-bis(triisopropylsilylethynyl) benzyl bromide (2b): To a stirring solution of compound **1b** (5.30g, 11.3 mmol) and carbon tetrabromide (4.88g, 0.012 mmol) in THF (60mL) on an ice bath, PPh_3 (3.86g, 14.7 mmol) was added slowly in many portions. After 15 minutes, the ice bath was removed, and the reaction mixture was left to stir at room temperature for 2 hours. The reaction was then quenched with water and the THF was evaporated. The aqueous phase was then extracted with DCM (3x100mL) and dried over MgSO_4 . The product was purified by column chromatography using hexanes. The solvent was evaporated to yield the product as a pale yellow oil (5.20g, 86.7%). ^1H NMR (300MHz, CDCl_3): δ (ppm) 1.14 (br. s, 42H, $-\text{Si}(\text{C}_3\text{H}_7)_3$), 4.41(s, 2H, $-\text{CH}_2\text{Br}$), 7.43 (s, 2H, ArH), and 7.48 (s, 1H, ArH). $^{13}\text{C}\{^1\text{H}\}$ NMR (75MHz, CDCl_3): δ (ppm) 11.5, 18.9, 32.1, 92.3, 105.6, 124.6, 132.5, 135.3, and 138.3. HRMS (EI): Theoretical $M_w = 530.24$ g/mol. Found $M_w = 530.30$ g/mol.

Synthesis of 3,5-diethynylbenzyl bromide (3): To a solution of compound **2a** (4.37g, 12.1 mmol) in acetone (100 mL), an aqueous solution (10 mL) of K_2CO_3 (8.34g, 60.4 mmol) was added. The reaction mixture was stirred overnight at room temperature. Acetone was then evaporated and the residue was extracted with ethylacetate. The organic layer was dried over MgSO_4 , and solvent was evaporated. The product was then flushed down a silica column using hexane to yield a yellowish white solid (2.34g, 89.1%). ^1H NMR (400MHz, CDCl_3): δ (ppm) 3.11 (s, 2H, $-\text{CCH}$), 4.40 (s, 2H, $-\text{CH}_2\text{Br}$), 7.49 (s, 2H, ArH), and 7.53 (s, 1H, ArH). $^{13}\text{C}\{^1\text{H}\}$ NMR (100 MHz, CDCl_3): δ (ppm) 31.6, 81.9, 110.0, 123.1, 132.8, 135.4, and 138.4. HRMS (EI): Theoretical $M_w = 217.97$ g/mol. Found $M_w = 217.90$ g/mol.

Synthesis of 3,5-bis(triisopropylsilylethynyl)benzyl azide (4): To a solution of compound **2b** (5.20 g, 9.81 mmol) in DMF (20 mL), NaN₃ (3.18g, 48.9 mmol) was added. The reaction mixture was left to stir at room temperature for 1hour. The solution was extracted with ethylacetate (3x50 ml). The organic phase was then washed with brine (3x100mL), and dried over MgSO₄, and the solvent was then removed in vacuo. The product was flushed through a short silica-gel column with hexanes to yield a pale yellow oil (3.72g, 96.4%). ¹H NMR (300MHz, CDCl₃): δ (ppm) 1.14 (br. s, 42H, -Si(C₃H₇)), 4.32 (s, 2H, -CH₂N₃), 7.36 (s, 2H, ArH), and 7.52 (s, 1H, ArH). ¹³C{¹H} NMR (75 MHz, CDCl₃): δ (ppm) 11.5, 18.9, 54.2, 92.3, 105.7, 124.6, 131.5, 135.1, and 136.1. HRMS (EI): Theoretical M_w = 493.33 g/mol. Found M_w = 493.30 g/mol.

Synthesis of compound (5a): 1,4-diethynylbenzene (**DEB**) (58mg, 0.46 mmol) and compound **4** (0.50g, 1.01 mmol) were dissolved in 3 mL of DMF, followed by addition of sodium ascorbate (46mg, 0.23 mmol). An aqueous solution (1mL) of CuSO₄.5H₂O (29mg, 0.12 mmol) was then added dropwise, and the solution was left to stir for 30 minutes, followed by the addition of THF (3mL). The reaction mixture was left to stir overnight at room temperature. THF was then evaporated, and the remaining solution was extracted with ethyl acetate (3X20mL), and then the organic layer was washed with brine (3x50mL), and dried over MgSO₄. Silica-gel column chromatography was used to remove the excess of the starting material (compound **4**) using ethyl acetate/hexane (1:20) mixture. After the recovery of the starting materials, the product was flushed down the column with ethyl acetate/Hexane (1:5). The solvent was evaporated to yield the product as a white solid (0.47g, 92.2%). ¹H NMR (400MHz, CDCl₃): δ (ppm) 1.11 (br. s, 84H, -Si(C₃H₇)), 5.51 (s, 4H, -CH₂Ar), 7.37 (s, 4H, ArH), 7.54 (s, 2H, ArH), 7.72 (s, 2H, triazole), and 7.87 (s, 4H, ArH). ¹³C{¹H} NMR (100 MHz, CDCl₃): δ (ppm) 11.2, 18.7, 53.6, 92.9, 104.9, 119.5, 124.8, 126.1, 130.2, 131.4, 134.8, 135.6, and 148.0. HRMS (ES): Theoretical M_w⁺ = 1113.73 g/mol. Found M_w⁺ = 1113.74 g/mol.

Synthesis of compound (5b): To a solution of compound **5a** (0.30g, 0.27 mmol) in THF (3mL) on a dry ice/acetone bath, a solution of Bu₄NF (1.62mL, 1M solution in THF, 1.62mmol) was added in a dropwise fashion. The reaction mixture was allowed to warm to room temperature and left to stir overnight. The solvent was removed under vacuum and the residue was washed with H₂O, and then with ether to yield a white powder (0.12g, 88.9%). ¹H NMR (400 MHz, DMSO-d₆): δ (ppm) 4.33 (s, 4H, CCH), 5.65(s,4H,-CH₂Ar), 7.50 (s, 4H, ArH), 7.53 (s, 2H, ArH), 7.91 (s, 4H, ArH, core), 8.70 (s, 2H, triazoleH). ¹³C{¹H} NMR (100 MHz, (CD₃)₂SO): δ (ppm) 52.4, 82.3, 82.8, 122.3, 123.3, 126.1, 130.5, 132.2, 134.6, 137.7, and 146.8. HRMS (EI): Theoretical M_w = 488.17 g/mol. Found M_w = 488.20 g/mol.

Synthesis of compound (6a): Compound **3** (266 mg, 1.215 mmol) and compound **4** (1.26 g, 2.55 mmol) were dissolved in 3mL of DMF followed by addition of sodium ascorbate (96 mg, 0.48 mmol). An aqueous solution (1mL) of CuSO₄·5H₂O (60 mg, 0.24 mmol) was added dropwise to the solution. The solution was left to stir for 30 minutes, and then THF (3mL) was added. The reaction mixture was left to stir overnight at room temperature. THF was then evaporated, and the remaining solution was extracted with ethyl acetate (3x40mL), and the organic layer was washed with brine (3x50mL). The organic layer was then dried over MgSO₄, and the solvent was evaporated. The crude product was purified by flash chromatography eluting the product with ethyl acetate/hexane (1:10) mixture. The solvent was evaporated to yield the product as white solid (1.72g, 97.0%). ¹H NMR (400MHz, CDCl₃): δ (ppm) 1.11 (br. s, 84H, -Si(C₃H₇), 4.53 (s, 2H, -CH₂Br), 5.51 (s, 4H, -CH₂Ar), 7.37 (s, 4H, -ArH), 7.54 (s, 2H, -ArH), 7.78 (s, 2H, -ArH), 7.85 (s, 2H, -triazoleH), and 8.14 (s, 1H, -ArH). ¹³C{¹H} NMR (75MHz, CDCl₃): δ (ppm) 11.5, 18.9, 33.0 53.9 93.1, 105.2, 120.2, 123.0, 125.1, 126.23, 131.8, 134.9, 135.9, 139.4, and 147.6. HRMS (ES): Theoretical M_w⁺ = 1205.63 g/mol. Found M_w⁺ = 1205.55 g/mol.

Synthesis of compound (6b): To a solution of **6a** (2g, 1.71 mmol) in THF (3mL) in a dry ice/acetone bath, a solution of Bu₄NF (8.22mL, 1M solution in THF, 8.22mmol) was added in a dropwise fashion. The reaction mixture was allowed to warm to room temperature and left to stir overnight. The solvent was removed under vacuum and the residue was extracted with ethyl acetate. The extract was then dried over MgSO₄, and solvent was evaporated. The product was then washed with ether to yield a white powder (0.715g, 72.1%). ¹H NMR (400 MHz, CDCl₃): δ (ppm) 3.12 (s, 4H, -CCH), 4.51 (s, 2H, -CH₂Br), 5.54 (s, 4H, -CH₂Ar), 7.41 (s, 4H, -ArH), 7.60 (s, 2H, -ArH), 7.81 (s, 2H, -ArH, core), 7.83 (s, 1H, -ArH, core), and 8.14 (s, 2H, -triazoleH). ¹³C{¹H} NMR (100MHz, CDCl₃): δ (ppm) 33.2, 53.8, 79.3, 82.1, 120.3, 122.7, 125.3, 126.4, 131.7, 134.8, 136.0, 139.3, and 147.4. HRMS (ES): Theoretical M_w⁺ = 580.10 g/mol. Found M_w⁺ = 581.09 g/mol.

Synthesis of compound (7): To a solution of **6a** (112 mg, 0.093 mmol), NaN₃ (30 mg, 0.46 mmol) was added. The reaction mixture was left to stir at room temperature for 1h. The solution was extracted with ethylacetate (3x50ml), and the organic phase was washed with brine (3x70mL). It was dried over MgSO₄ and followed by removal of the solvent. The product was flushed through a short silica-gel column with ethyl acetate/hexanes (1:10) to yield a white solid. (96 mg, 89%). ¹H NMR (300MHz, CDCl₃): δ (ppm) 1.11 (br. s, 84H, -Si(C₃H₇)), 4.44 (s, 2H, -CH₂N₃), 5.51 (s, 4H, -CH₂Ar), 7.38 (s, 4H, -ArH), 7.54 (s, 2H, -ArH), 7.78 (s, 2H, -ArH), 7.80 (s, 2H, -triazoleH), and 8.14 (s, 1H, -ArH). ¹³C{¹H} NMR (75 MHz, CDCl₃): δ (ppm) 11.5, 18.9, 53.9, 54.7, 93.1, 105.2, 120.2, 122.9, 125.2, 131.8, 134.9, 135.9, 137.2, and 147.7. HRMS (ES): Theoretical M_w⁺ = 1168.73 g/mol. Found M_w⁺ = 1168.54 g/mol.

Synthesis of generation dendrimer 1 (8a): 1,3,5-triethynylbenzene (**TEB**) (80 mg, 0.53 mmol) and compound **4** (0.986 g, 2.0 mmol) were dissolved in 3 mL of DMF, followed by addition of sodium ascorbate (79 mg, 0.40 mmol). An aqueous solution (1 mL) of CuSO₄·5H₂O (50 mg, 0.20 mmol) was added

dropwise to the solution. The solution was left to stir for 30 minutes, and then THF (3 mL) was added to the solution mixture. The reaction mixture was left to stir overnight at room temperature. THF was then evaporated, and the remaining solution was extracted with ethyl acetate (3x30mL), and then the organic layer was extracted with brine (3x50mL). It was dried over MgSO₄, and the solvent was evaporated. Silica-gel column chromatography was used to remove any excess of the starting material (compound **4**) using ethyl acetate/hexane (1:20). The product was flushed through the column with ethyl acetate/hexane (1:5). The solvent was evaporated to yield the product as a yellowish white solid (0.83g, 96.1%). ¹H NMR (400 MHz, CDCl₃): δ (ppm) 1.12 (br. s, 126H, -Si(C₃H₇), 5.51 (s, 6H, -CH₂Ar), 7.39 (s, 6H, ArH), 7.55 (s, 3H, ArH), 7.88 (s, 3H, ArH), and 8.25 (s, 3H, triazoleH). ¹³C{¹H} NMR (100 MHz, CDCl₃): δ (ppm) 11.2, 18.7, 53.7, 92.8, 105.0, 120.2, 122.3, 124.9, 131.5, 134.6, 135.7, and 147.6. HRMS (ES): Theoretical M_w⁺ = 1631.04 g/mol. Found M_w⁺ = 1631.11 g/mol.

Synthesis of generation dendrimer 1 with terminal acetylenes (8b): To a solution of generation dendrimer **1 8a** (0.389 g, 0.24 mmol) in THF (3mL) in a dry ice/acetone bath, a solution of Bu₄NF (1.72 mL, 1M solution in THF, 1.72 mmol) was added in a dropwise fashion. The reaction mixture was allowed to warm to room temperature and left to stir overnight. The solvent was removed under vacuum and the residue was extracted with ethyl acetate. The extract was then dried over MgSO₄, and solvent was evaporated. The product was washed with ether to yield a white powder (0.158g, 94.9%). ¹H NMR (400 MHz, CDCl₃): δ (ppm) 3.11 (s, 6H, -CCH), 5.54 (s, 2H, -CH₂Ar), 7.40 (s, 6H, ArH), 7.59 (s, 3H, ArH), 7.87 (s, 3H, ArH), and 8.23 (s, 3H, triazoleH). ¹³C{¹H} NMR (100 MHz, CDCl₃): δ (ppm) 53.4, 79.1, 81.7, 120.3, 122.5, 123.6, 131.5, 131.7, 135.2, 135.9, and 147.7. HRMS (ES): Theoretical M_w⁺ = 694.24 g/mol. Found M_w⁺ = 694.13 g/mol.

Divergent synthesis of protected dendrimer generation 2 (9a): Dendrimer generation 1 (**8b**) (0.195 g, 0.28 mmol) and compound **4** (0.999 g, 2.03 mmol) were dissolved in 3 mL of DMF, followed by addition of sodium ascorbate (0.119 g, 0.60 mmol). An aqueous solution (1 mL) of CuSO₄·5H₂O (75 mg, 0.30 mmol) was added dropwise to the solution. The solution was left to stir for 30 minutes, and then THF (3 mL) was added to the solution mixture. The reaction mixture was left to stir for 48h at room temperature. THF was then evaporated, and the remaining solution was extracted with ethyl acetate (3x30mL), and then the organic layer was extracted with brine (3x50mL). Organic layer was then dried over MgSO₄, and the solvent was evaporated. The product was flushed down a short silica-gel column with hexanes. The solvent was evaporated to yield the product as a yellowish white solid (0.92g, 90.3%). The excess of the starting material (compound **4**) was then removed using ethyl acetate/hexane (1:20).

Convergent synthesis of protected dendrimer generation 2 (9a): TEB (20 mg, 0.13 mmol) and compound **7** (0.5 g, 0.43 mmol) were dissolved in 3 ml of DMF, followed by addition of sodium ascorbate (34 mg, 0.17 mmol). An aqueous solution (1 mL) of CuSO₄ (21 mg, 0.086 mmol) was added dropwise to the solution. The solution was left to stir for 30 minutes, and then THF (3mL) was added to the solution mixture. The reaction mixture was left to stir for 48h at 40°C. THF was then evaporated, and the remaining solution was extracted with ethyl acetate (3x30mL), and then the organic layer was extracted with brine (3x50mL). It was then dried over MgSO₄, and the solvent was evaporated. The product was flushed down a short silica-gel column with hexanes. The solvent was evaporated to yield the product as a yellowish white solid (0.423g, 89.1%). The excess of the starting material compound **7** was then removed using ethyl acetate/hexane (1:10).

¹H NMR (400 MHz, CDCl₃): δ (ppm) 1.09 (br. s, 252 H, Si(C₃H₇)), 5.49 (s, 12H, -CH₂), 5.61 (s, 6H, -CH₂, core), 7.37 (s, 12H, -ArH), 7.52 (s, 6H, -ArH), 7.80 (s, 6H, -ArH), 7.81 (s, 6H, -ArH, from DG1), 7.88 (s, 3H, -ArH), 8.17 (s, 3H,

triazole), and 8.23 (s, 3H, triazole, core). $^{13}\text{C}\{^1\text{H}\}$ NMR (75 MHz, CDCl_3): δ (ppm) 11.2, 18.9, 54.0, 93.7, 105.3, 120.2, 125.1, 125.3, 132.0, 132.4, 134.9, 136.3, and 147.7. MALDI: Theoretical $M_w + \text{Li}^+ = 3661.22$ g/mol. Found $M_w + \text{Li}^+ = 3661.31$ g/mol.

Synthesis of dendrimer generation 2 (9b): To a solution of protected dendrimer generation 2 (9a) (0.328 g, 0.090 mmol) in THF (3 mL) in a dry ice/acetone bath, a solution of Bu_4NF (1.29 mL, 1M solution in THF, 1.29 mmol) was added in a dropwise fashion. The reaction mixture was allowed to warm to room temperature and left to stir overnight. The solvent was removed under vacuum, and the product was washed with H_2O , then with ether to yield a brownish white powder (0.144g, 88.7%). ^1H NMR (400 MHz, DMSO-d_6): δ (ppm) 4.29 (s, 12H, -CCH), 5.65 (s, 12H, - CH_2Ar), 5.75 (s, 6H, - CH_2Ar , core), 7.48 (s, 12H, ArH), 7.50 (s, 6H, ArH), 7.85 (s, 6H, ArH, from DG1), 8.27 (s, 3H, ArH), 8.30 (s, 3H, ArH, core), 8.72 (s, 6H, triazole), and 8.81 (s, 3H, triazole, core). $^{13}\text{C}\{^1\text{H}\}$ NMR (100 MHz, $(\text{CD}_3)_2\text{SO}$): δ (ppm) 52.4, 82.3, 82.8, 122.8, 123.2, 124.8, 132.2, 134.6, 137.7, 137.8, 146.5 and 146.7. MALDI: Theoretical $M_w^+ = 1800.62$ g/mol. Found $M_w^+ = 1800.51$ g/mol.

4.5 References

-
- ¹ (a) Langereis, S.; Dirksen, A.; Hackeng, T. M.; van Genderena, M. H. P.; Meijer, E. W. *New J. Chem.* **2007**, *31*, 1152. (b) Svenson, S.; Tomalia, D. A. *Advanced Drug Delivery Reviews* **2005**, *57*, 2106. (c) Islam, M.; Majoros, I. J.; Baker Jr, J. R. *J Chromat. B Analyt. Technol. Biomed. Life Sci.* **2005**, *21*, 822. (d) Gillies, E. R.; Dy, E.; Fréchet, J. M. J.; Szoka, F. C. *Molecular Pharmaceutics* **2004**, *2(5)*, 129.
- ² (a) Grayson, S. M.; Fréchet, J. M. J. *Chem. Rev.* **2001**, *101*, 3819. (b) Gossage, R. A.; van de Kuil, L. A.; van Koten, G. *Acc. Chem. Res.* **1998**, *31*, 423. (c) Majoral, J.-P.; Caminade, A.-M. *Chem. Rev.* **1999**, *99(30)*, 845. (d) Newkome, G. R.; Moorefield, C. N.; He, E. *Chem. Rev.* **1999**, 1689.

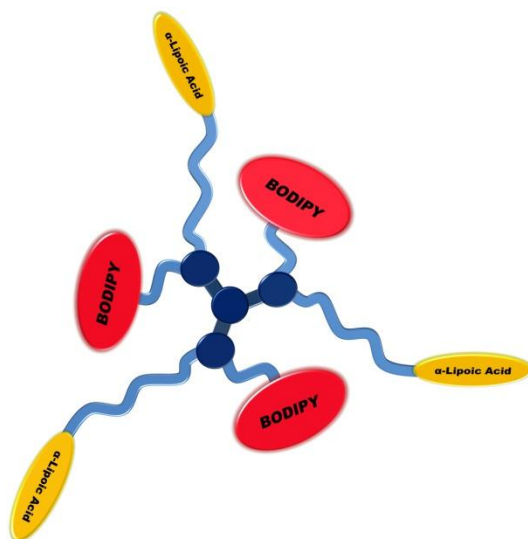
³ (a) Kolb, H. C.; Finn, M. G.; Sharpless, K. B. *Angew. Chem. Int. Ed.* **2001**, *40*, 2004. (b) Wu, , C. J. Hawker, A. Scheel, B. Voit, J. Pyun, J. M. J. Fréchet, K. B. Sharpless, V. V. Fokin, P. ; Feldman, A. K. ; Nugent, A. K.; Hawker, C. J.; Scheel, A.; Voit, B.; Pyun, J.; Fréchet, J. M. J.; Sharpless, K. B.; Fokin, V. V. *Angew. Chem. Int. Ed.* **2004**, *43*, 3928. (c) Franc, G.; Kakkar, A. *Chem. Comm.* **2008**, 5267. (d) Carlmark, A.; Hawker, C.; Hult, A.; Malkoch, M. *Chem. Soc. Rev.* **2009**, *38*, 352.

⁴ (a) Wu, P.; Malkoch, M.; Hunt, J. N.; Vestberg, R.; Kaltgrad, E.; Finn, M. G.; Fokin, , V. V.; Sharpless , K. B.; Hawker, C. J. *Chem. Commun.* **2005**, 5775. (b) Gopin, A.; Ebner, S.; Attali, B.; Shabat, D. *Bioconjugate Chem.* **2006**, *17*, 1432. (c) Parrish, B.; Emrick, T. *Bioconjugate Chem.* **2007**, *18*, 263. (d) Ornelas , C.; Ruiz Aranzaes, J.; Cloutet, E.; Alves, S.; Astruc, D. *Angew. Chem. Int. Ed.* **2007**, *46*, 872. (e) Kolb, H. C.; Sharpless, K. B. *DDT* **2003**, *8(24)*, 1128.

⁵ (a) Goodwin, A. P.; Lam, S. S.; Fréchet, J. M. J. *J. Am. Chem. Soc.* **2007**, *129*, 6994. (b) Gillies, E. R.; Fréchet, J. M. J. *J. Am. Chem. Soc.* **2002**, *124*, 14137.

Chapter 5

Multi-tasking with Single Scaffold Dendrimers for Targeting Sub-Cellular Microenvironment



This chapter highlights the importance of introducing orthogonal functionalities into the same dendrimer scaffold for applications in biology and medicine. These multi-tasking dendrimers are now easily accessible using the building blocks and their "click" chemistry developed in chapter 4. Their potential in drug delivery is elaborated by covalently linking a dye and a drug, and examining their entry into human cells in detail.

Reproduced in part with permission from:

Hourani R., Jain M., Maysinger D., & Kakkar A., **2009**, submitted for publication.

Unpublished work copyright, 2009.

5.1 Introduction

Dendrimers are monodisperse and hyperbranched macromolecules whose unique architecture and properties can be tailored for specific applications.¹ However, introducing multiple functionalities into a single dendrimer scaffold for performing complementary biological tasks has presented significant synthetic challenges.² We address this problem with an efficient iterative methodology, using Cu(I) catalyzed “click” chemistry³ constructing bifunctional dendrimers that can carry out combined imaging and drug delivery functions. Multi-tasking efficiency of these nanotools containing covalently linked imaging BODIPY dye and a therapeutic agent, α -lipoic acid, in targeting intracellular lipid droplets was demonstrated. They do not induce marked metabolic abnormalities in primary human liver cells, and they distribute differently from the free dye and drug. Thus, the design and construction of orthogonally functionalized dendrimers for synergistic effects can now be easily carried out with this versatile approach which is widely applicable for theragnostics combining different imaging agents and therapeutics.

The fabrication of multifunctional biocompatible materials with a high degree of order at the molecular level constitutes a key to the future of biotechnology.⁴ Much remains to be done to develop efficient physiologically or therapeutically active nanostructures to not only transport biologically active cargo across cell membranes, but also ensure delivery to specific intracellular locations. Macromolecular architectures with well defined particle size and shape are of eminent interest for biomedical applications such as the delivery of therapeutics and tissue imaging. Bioactive molecules including imaging probes and therapeutic drugs can either be encapsulated inside polymeric micelles⁵ and dendrimers,⁶ or covalently attached to polymers or dendritic macromolecules⁷ to provide enhanced stability and control over the amount to be transported, and its final destination.

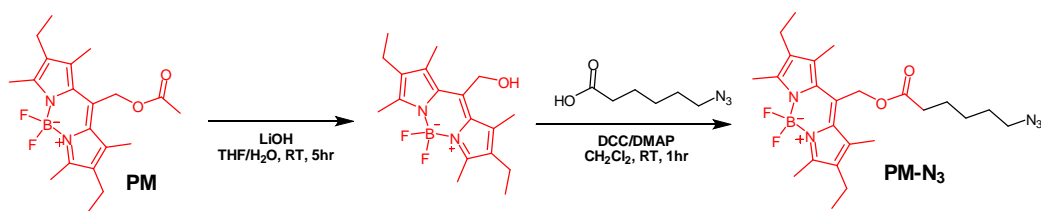
A significant issue related to the biomedical applications of dendrimers pertains to their cytotoxicity,^{8,9} and the need for versatile, clean, and high yield chemistry under mild conditions with essentially no side products, continues to

be the key tenet and a topical area of research.¹⁰ In 2001, Sharpless and coworkers introduced what is now well known as “click” chemistry which includes the Cu(I)-catalyzed cycloaddition between primary alkynes and azides (CuAAC).³ The latter has been demonstrated to be a very useful tool for the construction of a variety of macromolecules including dendrimers,¹¹ and it has led to unprecedented yields under some of the mildest reaction conditions desirable for bioconjugates and drug discovery.¹² Another challenge in the development of dendrimers for applications in medicine is to incorporate important tasks including solubility, targeting, imaging and therapeutic delivery in the same dendrimer scaffold. In a typical dendrimer, the peripheral groups are generally similar, and it is synthetically difficult to functionalize them asymmetrically.¹³ By using the “click” chemistry approach, we demonstrate here how these tree-like structures can be decorated with diverse peripheral groups such as a fluorescent dye (BODIPY) useful for organelle imaging, and therapeutic (α -lipoic acid) moieties, that can be directed towards lipid droplets.

Considerable effort has been made in the past to develop controlled and targeted drug delivery systems that can enter cellular organelles such as nuclei and mitochondria.¹⁴ The branched dendrimer nanodelivery system described here is the first one to simultaneously direct a drug and a fluorophore to lipid droplets. These are phylogenetically well preserved cellular organelles, and have been neglected for a while as “boring and passive” lipid blobs.¹⁵⁻¹⁷ In non-adipocytes they are small and mobile and can interact with other compartments.¹⁸ Excess lipid accumulation in non-adipose tissue is associated with pancreatic disorders related to diabetes, heart failure, infectious and neoplastic conditions. Lipid droplets have recently gained popularity as “inflammatory organelles” of particular interest in these pathologies.¹⁹ Lipid droplets play a crucial role in lipid metabolism and might have a much broader repertoire of “tasks” such as managing the availability of proteins and serve as generic sites of protein sequestration. This suggests a wide and diverse role of lipid droplets possibly involved in inactivation of proteins, prevention of protein aggregation and localized delivery of signalling molecules.²⁰

5.2 Results and discussion

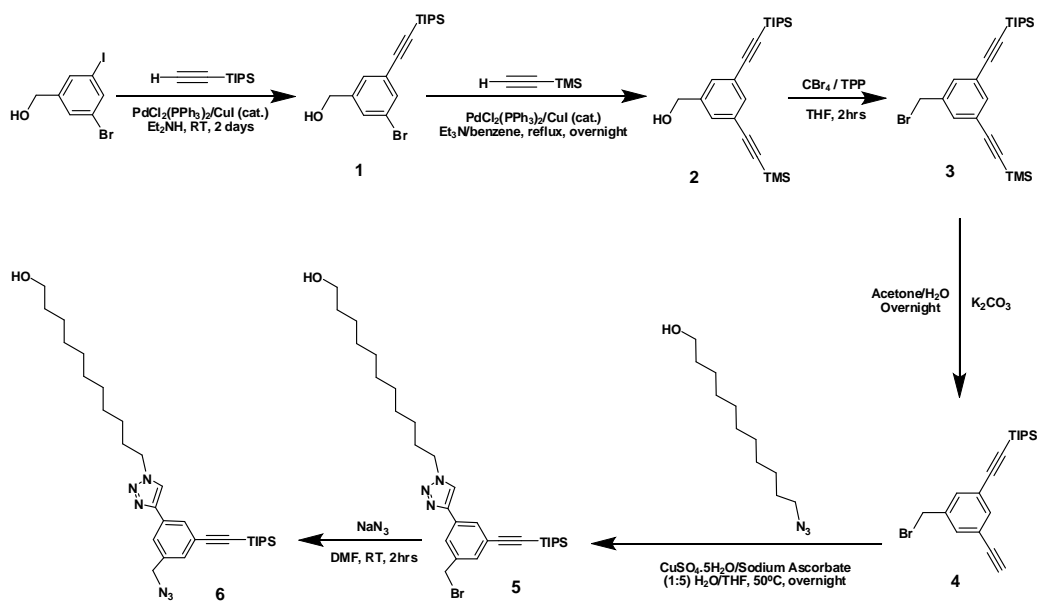
α -Lipoic acid (LA) is an essential cofactor for many enzymes, particularly in aerobic metabolism.²¹ It is readily taken up by cells and reduced to its potent dithiol form, dihydrolipoate, much of which is rapidly effluxed out from cells. We envisioned that by linking lipoic acid to a dendrimer, its intracellular retention could be increased, thereby providing an enhanced effectiveness with smaller therapeutic doses. BODIPY PM605 (lipophilic fluorophore, dipyrromethene boron difluoride, abbreviated here as PM) is an efficient and photostable laser red dye that has characteristic narrow absorption and emission bands in the visible region of the spectrum with high fluorescence quantum yields. It readily diffuses into cells and accumulates in lipid bodies, but rapidly bleaches upon multiple exposures to light. We anticipated that its photostability could be improved by attaching it to a dendrimer. PM has not been previously employed for labelling dendrimers or for tracking their subcellular distribution. For covalently linking the PM dye, it was functionalized with an azide group (PM-N₃), and this modification involved the formation of an ester linkage between the alcohol form of the dye with 6-azido-hexanoic acid (Scheme 5.1).



Scheme 5.1 The synthesis of the azide functionalized red BODIPY dye (PM-N₃) using the alcohol form of the commercial PM605 dye (PM) and 6-azidohexanoic acid.

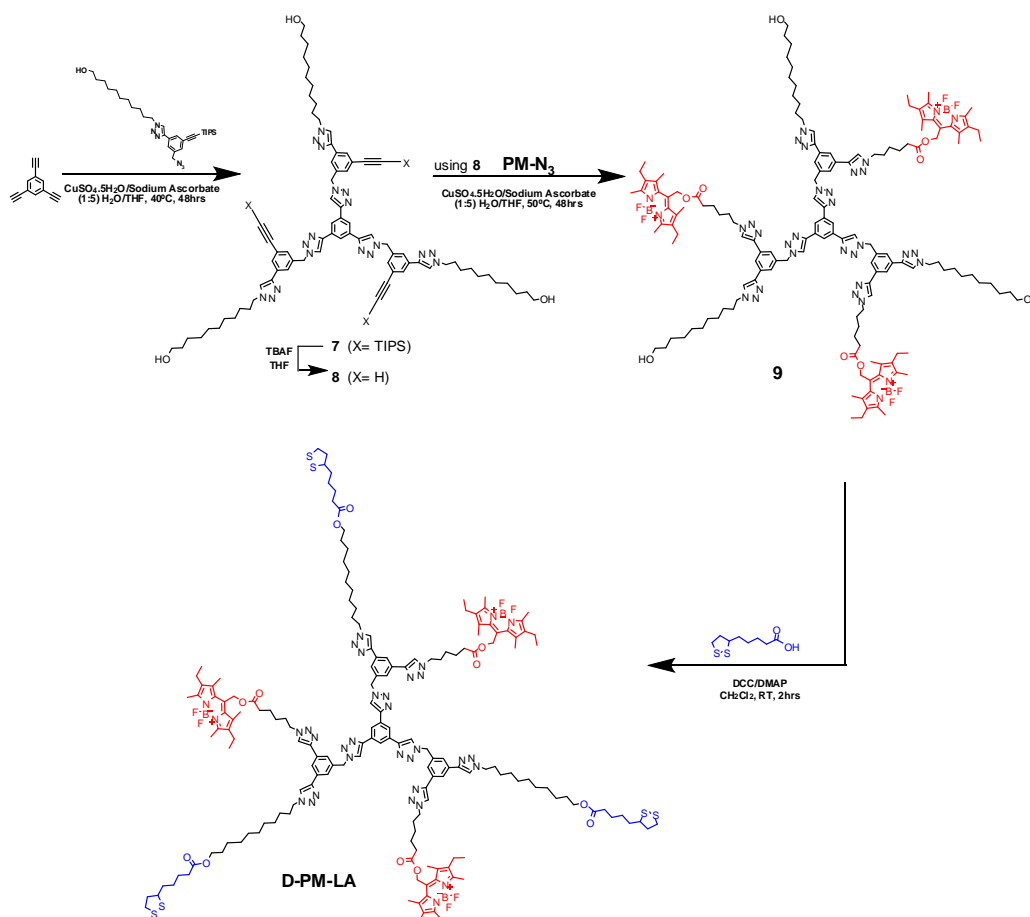
The synthetically tailored linkage of PM and α -lipoic acid to the same assembly was made possible via the design and synthesis of an ABB' building block that facilitates performing Cu^I catalyzed “click” reactions in a sequential manner (Scheme 5.2). This, to our knowledge, is the first building block of its

kind that allows construction of multivalent dendrimers using simple “click” chemistry. It contains two acetylenes (BB’) protected with two different groups (trimethylsilyl (TMS)- and triisopropylsilyl (TIPS)), which are individually removed when desired. It was constructed starting from 3-bromo-5-iodobenzylalcohol, and performing Sonogashira coupling to introduce triisopropylacetylene at the iodo position at room temperature (compound 1), and the substitution of bromo group with trimethylsilylacetylene under reflux (compound 2). It was subsequently followed by bromination of the benzylalcohol (compound 3), and a mild deprotection procedure to eliminate the trimethylsilyl (TMS) group (compound 4). The resulting compound is a highly versatile unit that can carry multiple functionalities on it, or introduce them on the dendritic macromolecule at a later stage. We used its free acetylene arm to click a long chain alcohol upon reaction with 11-azido-undecan-1-ol (compound 5) that was subsequently used to covalently link α -lipoic acid. The benzyl bromide was then activated using a simple azidation process (compound 6).



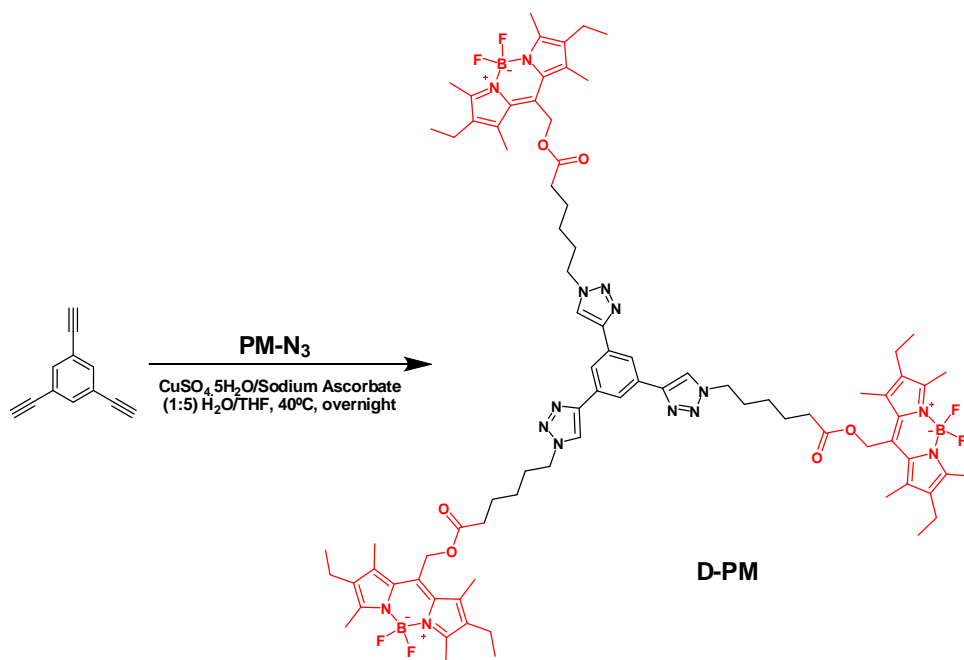
Scheme 5.2 Synthetic scheme for the ABB' building block, and its functionalization with 11-Azido-undecan-1-ol, and the azide moiety.

The resulting compound 6 was then “clicked” to the triethynylbenzene core (compound 7), followed by deprotection of triisopropyl-acetylene groups (compound 8), as shown in **Scheme 5.3**. The corresponding free acetylene centers were then clicked with the azide-functionalized PM-N₃ dye (compound 9). The hydroxyl terminated arms were then reacted with α -lipoic acid using a simple and quantitative esterification reaction to obtain the desired bifunctional dendrimer (D-PM-LA). Our methodology demonstrates that click chemistry provides an effective way of generating previously allusive asymmetrically functionalized dendrimers in excellent yields.



Scheme 5.3 Synthesis of bifunctional dendrimer (D-PM-LA) with PM dye and α -lipoic acid at the periphery.

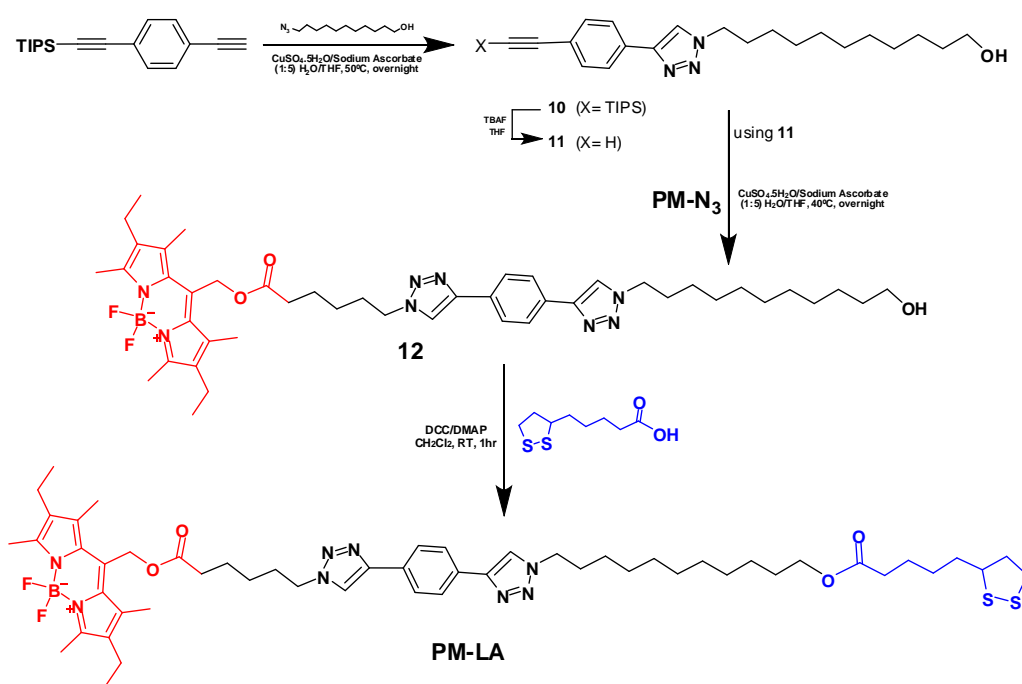
The synthetic goals of this study included examining the role of hyperbranched structure on the internalization process. For this purpose, we synthesized the monofunctional dendrimer (D-PM), as shown in **Scheme 5.4**, by “clicking” three azide terminated PM-N₃ dye molecules to the 1,3,5-triethynylbenzene (TEB) core.



Scheme 5.4 Synthesis of D-PM by the reaction of three PM-N₃ dye molecules with a three arm core (1,3,5-triethynylbenzene) (TEB).

As we had anticipated that the structure of the carrier may influence its overall behaviour, and the linear analogue of the dendrimer containing the dye and drug was expected to show different internalization and intracellular localization than the dye molecule, without marked cytotoxicity similar to the larger dendritic macromolecules. The linear carrier containing the PM dye and α -lipoic acid (PM-LA), shown in **Scheme 5.5**, was constructed using (4-ethynylphenylethynyl)-triisopropyl-silane as the central unit on which two CuAAC click reactions were carried out in sequence. The free acetylene arm of (4-ethynylphenylethynyl)-triisopropyl-silane was first functionalized with a long alkane chain alcohol using 11-azido-undecan-1-ol. Upon subsequent de-protection, the

other acetylene unit was made available for the second click reaction with PM-N₃. The free primary alcohol was subsequently used for attaching α -lipoic acid through a simple and quantitative esterification reaction.



Scheme 5.5 Synthetic scheme for the linear analog (PM-LA) containing covalently linked PM dye and α -lipoic acid.

Detailed pharmacological studies were carried out to study and compare the internalization, cytotoxicity, and the therapeutic (cytoprotection) properties of the bifunctional dendrimer (D-PM-LA), its linear analog (PM-LA), and the dendrimer containing the PM dyes alone (D-PM) (**Figure 5.1**). It is worth mentioning here that the chemical modification of the dye (PM) and its subsequent attachment to the dendrimers and the linear analogue did not alter its photophysical properties. As shown in **Figure 5.2**, the absorption and emission spectra of the commercial dye (PM) and the bifunctional dendrimer (D-PM-LA) overlap. The spectra of the other dye-containing compounds, azide-functionalized dye (PM-N₃), linear analog containing the dye and lipoic acid (PM-LA), dendrimer with three PM dye molecules (D-PM), showed similar

absorption and emission characteristics. A typical λ_{max} (absorption) was found at 545 nm, and λ_{max} (emission) at 559 nm in *p*-dioxane.

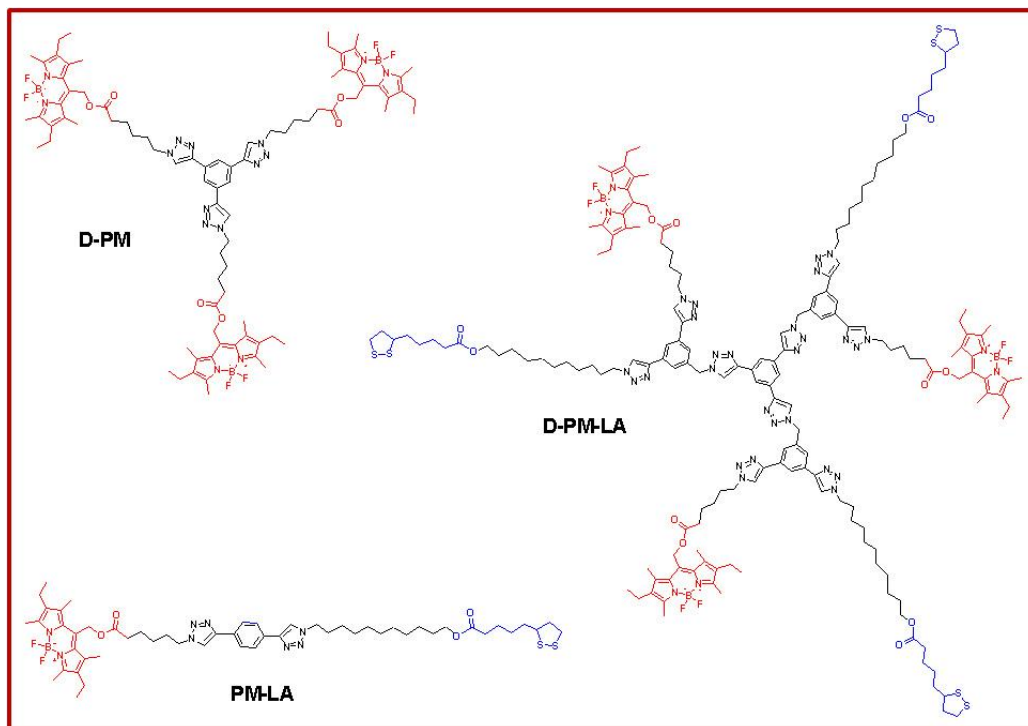


Figure 5.1 Structures of dendrimers containing the red BODIPY dye (D-PM), BODIPY dye and the lipionic acid (D-PM-LA), and its linear analogue (PM-LA).

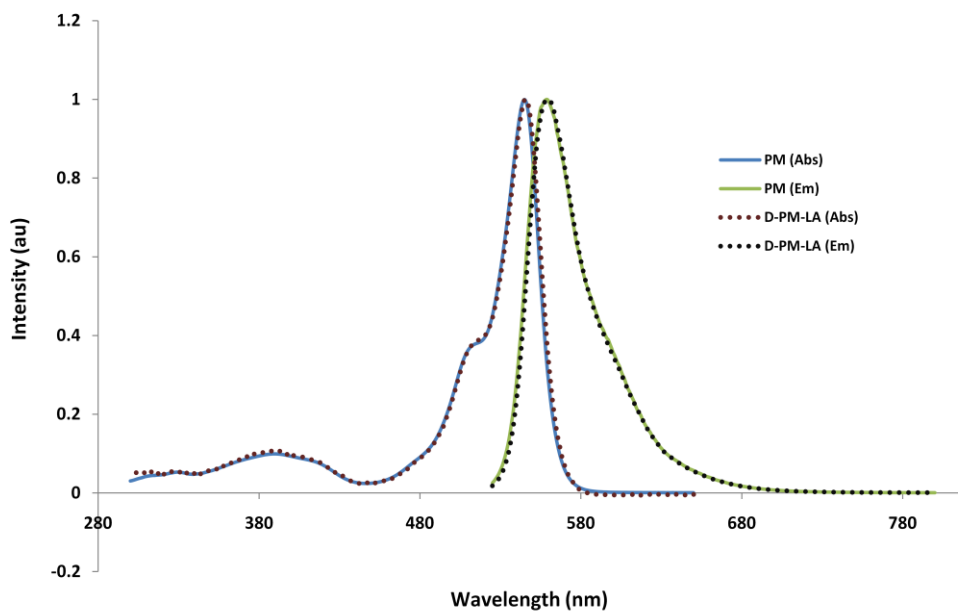


Figure 5.2 The absorption and emission spectra of the commercial PM605 red BODIPY dye (PM), and the bifunctional dendrimer (D-PM-LA).

We first assessed whether the carriers reported here can gain entry into cells (**Figure 5.3a**), and if they exert any cytotoxicity in human cells in culture. We demonstrate that they are internalized by the cells, however, the quantity and rate of entry varies significantly for each compound, as observed within a 24 hour time period (**Figure 5.3b**). The free PM dye rapidly entered the cells and reached a maximum intracellular fluorescence within an hour before gradually decreasing to approximately 11% of its initial value. The dendrimer containing dye molecules (D-PM) was also rapidly internalized by the cells, however to a lesser degree and with slower kinetics. After one hour of incubation with the dendrimer, the intracellular fluorescence was about 20% of total initial concentration. The mean fluorescence intensities were significantly higher in cells exposed to the bifunctional dendrimer incorporating both LA and dye (D-PM-LA), as well as the dendrimer containing the dye alone (D-PM), after 24 and 48 hours of incubation, in comparison to the free dye or the linear analog (PM-LA) (**Figure 5.3b**).

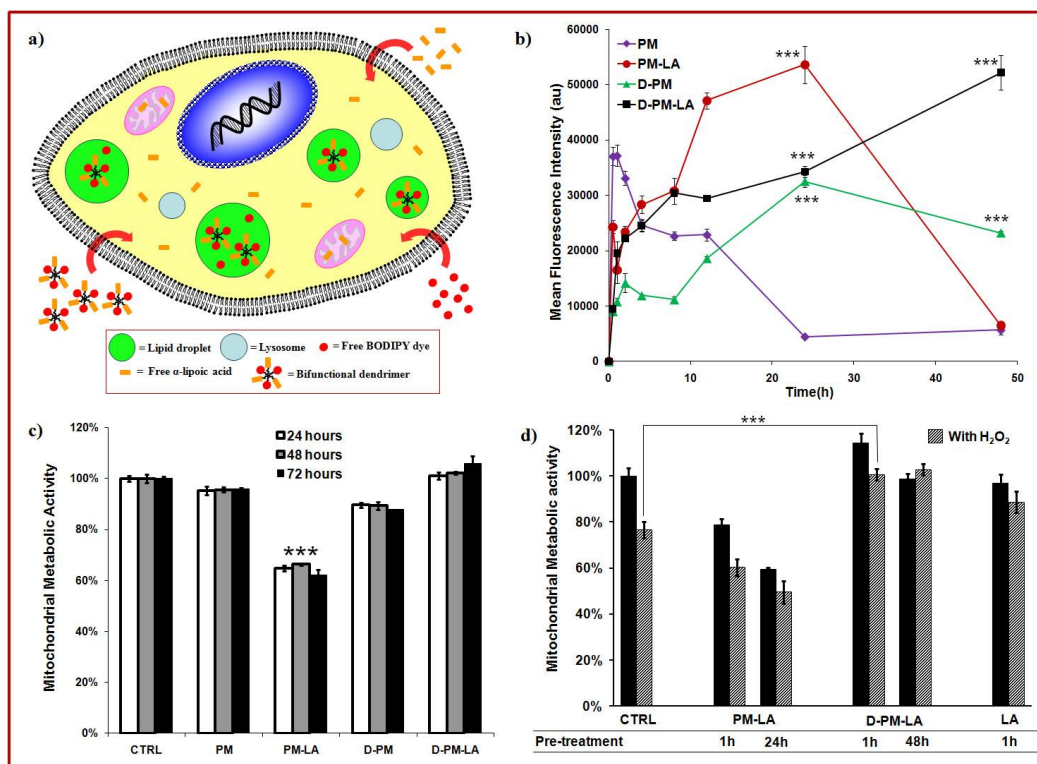


Figure 5.3 Cellular internalization, distribution, cytotoxicity, and cytoprotectivity of the linear and dendritic compounds; **a)** Subcellular

compartments and anticipated distribution of free lipoic acid, free BODIPY (PM) dye and the bifunctional dendrimers. **b)** Time course of cellular internalization of the dendrimers (D-PM, D-PM-LA), linear compound (PM-LA) and free dye (PM) were evaluated over 48 hours. Hepatocyte cells were treated with equimolar concentrations (1 μ M) of red BODIPY (PM) dye, and of all four compounds. Spectrofluorometric measurements of intracellular fluorescence show significant differences in the internalization kinetics. Intracellular fluorescence intensities of PM-LA, D-PM and D-PM-LA were found to be significantly different from the free dye (PM), ($***p<0.0001$) after 24 hours of incubation. After 48 hours, only the two dendrimers showed statistically significant differences from the free dye (PM), ($***p<0.0001$). **c)** Mitochondrial metabolic activity of cells was assessed via the MTT assay. Note that the linear PM-LA reduced mitochondrial metabolic activity after 24 hours, 48 hours and 72 hours of incubation, ($***p<0.0001$). **d)** Cytoprotective effect of PM-LA and D-PM-LA in cells exposed to H₂O₂; Each compound was preincubated with the cells for either 1 hour or the optimal time required to ensure maximal cellular uptake (as determined in 2b: 24 hours for PM-LA, and 48 hours for D-PM-LA). Cells were preincubated with LA, linear PM-LA or D-PM-LA in equimolar concentrations (5.6 μ M) for 1 hour. The linear compound regardless of incubation time was not protective, but rather significantly cytotoxic ($p<0.0001$) and further enhanced the cytotoxicity obtained with H₂O₂ insult ($p<0.01$), whereas D-PM-LA was cytoprotective ($***p<0.0001$).

Linear and dendritic compounds functionalized with PM (in 100 nM – 10 μ M concentration) did not markedly reduce mitochondrial metabolic activity or alter cell morphology of the human cell lines when examined for up to 24 hours. The mitochondrial metabolic activity assessed as the oxidation of a tetrazolium salt, MTT and formazan generation did not decrease even after 72 hours upon exposure to these compounds (in 1 μ M concentration) (**Figure 5.3c**). The only significant reduction in mitochondrial metabolic activity occurring at all three time intervals (24 hours, 48 hours and 72 hours) was induced by the linear

analog PM-LA, and was possibly due to i) high intracellular PM-LA concentrations achieved within 10-20 minutes; ii) diffusion and damage to mitochondrial membranes; and iii) reduction in membrane potential. The fact that dendrimers functionalized with the dye (D-PM) and the dye plus α -lipoic acid (D-PM-LA) are not toxic, is noteworthy. It suggests that the “click” methodology reported here for designing dendrimers can enable functionalization of their backbones with numerous other therapeutic agents without compromising cell viability.

The therapeutic potential of the LA containing dendrimer D-PM-LA, and the linear analog PM-LA, was evaluated for cytoprotectivity against H_2O_2 insult in human breast cancer (MCF-7) cells (**Figure 5.3d**).²² The linear compound did not exert any cytoprotective effects but rather decreased mitochondrial metabolic activity, and even further enhanced H_2O_2 induced cytotoxicity. This detrimental effect was significant when PM-LA was pre-incubated with the cells for one hour or 24 hours (as per the time required for maximal internalization (**Figure 5.3c**)). Conversely, D-PM-LA after both 1 hour and 48hours of pre-incubation was completely able to protect cells against H_2O_2 cytotoxicity (** $p < 0.0001$). Free LA at equimolar concentrations was only able to partially protect cells from the oxidative stress (** $p < 0.01$). These results imply that LA may be therapeutically effective at reduced concentrations when bound to the dendrimers, perhaps due to the greater retention time permitted by the dendritic structure.

Since most of the cell labelling protocols call for short times of exposure to the fluorophore, and our initial internalization experiments showed a rapid increase in fluorescence intensities in the treated cells, we assessed the fluorophore entry by fluorescence microscopy (**Figure 5.4**). The imaging of single cells clearly supported the spectrofluorometric measurements, and showed that the PM dye, and the covalently linked linear and dendritic molecules are internalized at different rates, and also that their subcellular distribution patterns are different.

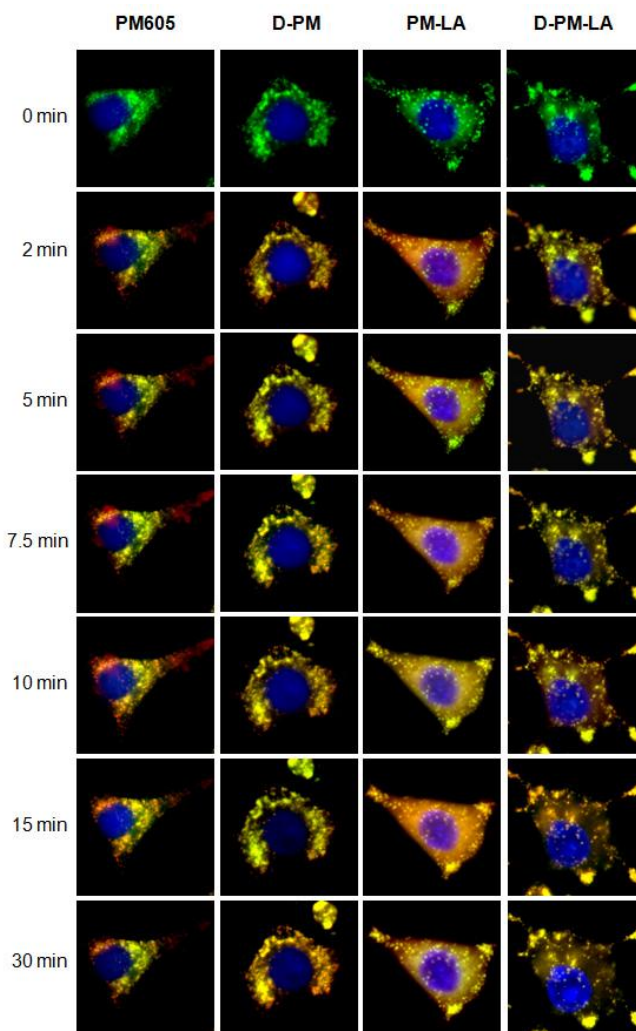


Figure 5.4 Time course of cellular uptake and subcellular distribution of dendrimers, PM-linear analog and PM alone. Human hepatocytes were seeded in 24 well plates (Sarstedt, Montreal) at a density of 25000 cells/well. The nuclei and lipid droplets of the cells were stained first with fluorescently labelling dyes, Hoechst 33342 (10 μ M for 30 minutes) (Invitrogen, Mississauga) and green BODIPY 495/503 (20 μ M for 10 minutes) (Invitrogen, Mississauga), respectively; and imaged using fluorescent microscopy at a magnification of 40X. Subsequently the dendrimers, PM-LA or PM (at a concentration of 1 μ M of the free dye) alone were added to the cells, and a time course was begun to monitor the gradual increase and localization of fluorescence. Note that the free dye PM rapidly entered the cell upon two minute incubation, but was most concentrated at the periphery of the cell whereas after 30 min it was mostly

found in the perinuclear region suggesting gradual co-localization of the PM dye with the lipid droplets. The dendrimer, D-PM was also rapidly taken up by the cell, after two minutes, though to a much lesser degree than the free dye. The dendrimers, within 2 minutes of incubation, showed distinct punctate formations which appeared to co-localize with lipid droplet co-labelling (BODIPY 495/503) suggesting dendrimer co-localization with lipid droplets.. The linear analog containing LA, PM-LA rapidly entered the cell though initially appeared highly diffuse throughout the cell; gradually the linear analog appeared to localize with the lipid droplets. The LA containing dendrimers, D-PM-LA, was also rapidly internalized within the cell, and almost immediately visible as puncta that overlaid completely with the green BODIPY, producing a yellow appearance of the lipid droplets and indicating co-localization of the dendrimers with the lipid droplets. Though the dendrimers fluorescence within the cell increased during the 30 minutes, the pattern of dendrimer distribution was similar to that at the earlier time points.

Images acquired using fluorescent microscopy indicated that the red PM and the green BODIPY dyes were at least partially co-localizing in lipid droplets, as shown by the yellow fluorescent signal from the overlaid red and green fluorescence (**Figure 5.4**). In the case of D-PM, the yellow fluorescence was almost immediately detectable suggesting that some molecules could be associated with lipid bodies. However, some red fluorescence did not overlay with the green, hinting at an alternate site also being occupied by the dendrimer. For the bifunctional compounds, the addition of lipoic acid in the linear compound (PM-LA) seemed to promote the appearance of yellow puncta, rendering them visible as early as 7.5 minutes post-treatment. For the bifunctional dendrimer (D-PM-LA), the yellow fluorescent signal was most intense and clearly detectable as early as five minutes post-treatment (**Figure 5.4**).

Since the results from fluorescence microscopy indicated punctate subcellular distribution of dendrimers and dyes, it was necessary to assess their localization more precisely. Thus, confocal microscopy was employed and z-

stacks were collected from individual cells (**Figure 5.5**). Results from these studies confirmed the differences in the extent of localization between PM, D-PM, PM-LA, or D-PM-LA. The free fluorophore PM was seen in some but not all lipid droplets, PM-LA showed a larger extent of co-localization, followed by D-PM, whereas the bifunctional dendrimer D-PM-LA was fully co-localized with the lipid droplets labelled with BODIPY 493/503 (**Figure 5.5a**). Additional organelles analyses using confocal microscopy were subsequently performed after labelling mitochondria with Mitotracker deep red 633 (**Figure 5.5b**). Results from these studies clearly showed that fluorescent dendrimers co-localize with lipid droplets but not mitochondria within 10 minutes (**Fig. 5.5**). Fluorescence patterns of dendrimers containing dye alone are markedly different from those of free dyes labelling lipid droplets. PM does not enter acidic organelles but is detectable in lipid droplets, and it is faintly diffused in the cytoplasm. The model therapeutic compound, lipoic acid, diffuses within the cell but when covalently bound to the dendrimer, it follows the route and pattern of distribution of its carrier (the dendrimer). It has been suggested that dendrimers can enter cells by a variety of routes depending on their surface properties. Regardless of the mode of internalization, these nanostructures can enter the cells relatively easily and introduce their cargo to the cytosol.

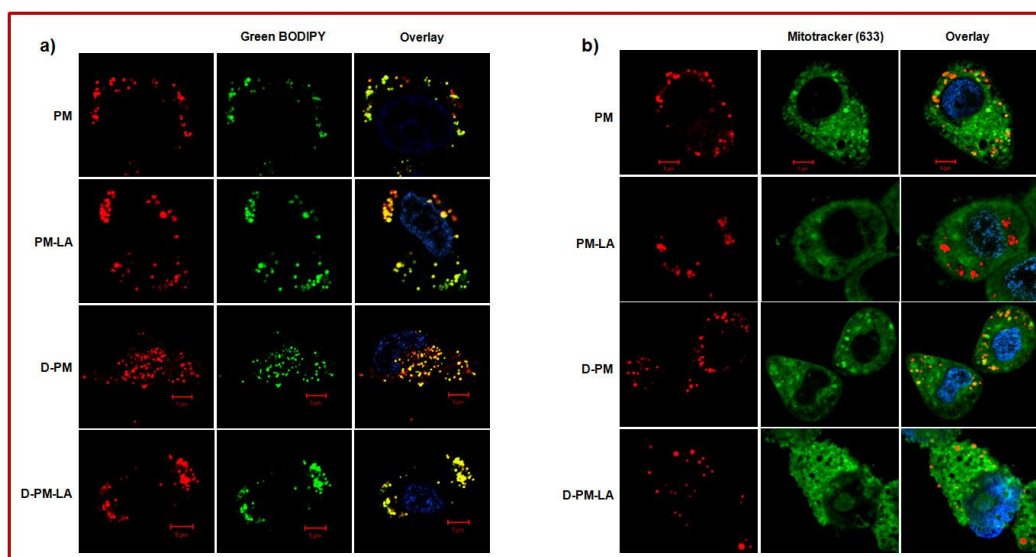


Figure 5.5 Intracellular localization of fluorescent linear and dendritic structures; **a)** Confocal photomicrographs of primary human hepatocytes

stained with the blue fluorescent nuclear dye, Hoechst 33342 (10 μ M, 1h; λ_{ex} 350 nm, λ_{em} 461 nm) and the lipid droplets labeled with BODIPY 493/503 (20 μ M, 10minutes; λ_{ex} 493 nm, λ_{em} 503 nm). Images were acquired using Zeiss LSM 510 microscope. Note marked co-localization between lipid droplets and bifunctional dendrimer (D-PM-LA). **b)** Confocal micrographs of cells labelled with MitoTracker Deep Red 633 (1 μ M, 1 min; λ_{ex} 644 nm, λ_{em} 665 nm) and exposed to dendrimers, the linear analog, (PM-LA) and free dye (PM) for 10 minutes. Note the absence of co-localization between the compounds and mitochondria.

5.3 Conclusions

We conclude that dendritic macromolecules functionalized with two key components for developing efficient materials for biomedical applications, are easily accessible using “click” chemistry. These multifunctional dendrimers which are biocompatible and could carry inhibitors of lipid synthesis or storage, and interfere with sequestration or synthesis of specific lipid droplet-associated proteins, could provide clinically useful “nano-regulators” of cellular lipid homeostasis. Since lipid bodies may function as specialized intracellular sites of signalling engaged in lipotoxicity and inflammatory¹⁹ processes ranging from allergy to infections,²³ cancer,²⁴ diabetes²⁵ and atherosclerosis, approaches to inhibit lipid accumulation is of significant therapeutic value. For instance, aspirin and other non-steroidal anti-inflammatory drugs (NSAID) inhibit lipid droplet formation *in vivo* and *in vitro*,²⁶ however, these drugs as well as lipoic acid have a broad distribution,²⁷ if not incorporated in any nano-delivery system. In this study we have demonstrated that the synthetic methodology developed here, is versatile and widely applicable, and could be used for linking other drugs e.g. regulators of lipid synthesizing enzymes which could be useful in reducing the long-term consequences of lipotoxicity. Moreover, in analogy to recently suggested use of multi-peptides, arising problem with regulating glycemia and obesity at the same time, might be tackled with “clicked” multifunctional dendrimers presented here.

5.4 Methods

Spectrophotometric measurements of the internalized free BODIPY and labelled dendrimers. Cells were seeded at a concentration of 150000 cells/well in a 24well (Sarstedt). Prior to the addition of fluorescent dyes the media was changed to serum free RPMI 1640. Cells were treated with various forms of the red fluorescent BODIPY dye (free dye, linear analogs and dendrimers), and allowed to incubate for several subsequent hours as indicated in the Figure 5.3. Upon termination of the incubation period media from the cells was aspirated and the cells were gently rinsed with PBS. DMSO was next added to each well and pipetted in triplicate to a black 96-well plate (Costar). Red fluorescence of the samples was then measured using a BMG spectrofluorometer.

Confocal laser scanning microscopy. Confocal laser scanning microscopy was carried out using a Zeiss LSM 510 microscope equipped with the following lasers: (i) HeNe LASOS LGK 7786 P/Power supply 7460 A: 543 nm, 1 mW, (ii) Argon LASOS LGK 7812 ML-1/LGN: 458, 488, 514 nm, 25 mW, Laser class 3D and (iii) Titanium:Sapphire The Coherent Mira Model 900-F Laser tunable from 710 to 1000 nm for two photon Microscopy set to pulse at 800 nm. Cells for imaging were grown on 8-well chambers (Lab-Tek, Nalge Nunc International, Rochester, NY, USA). Prior to staining cells, cell media was changed to serum free and fluorescent organelle dyes were added to. Lipid bodies were stained with green BODIPY (Invitrogen) (20 μ M, 10 min; λ_{ex} 644 nm, λ_{em} 665 nm), mitochondria were stained with MitoTracker Deep Red 633 (1 μ M, 1 min; λ_{ex} 644 nm, λ_{em} 665 nm), but then pseudo colored green, and nuclei with Hoechst 33342 (Invitrogen) (10 μ M, 1h; λ_{ex} 350 nm, λ_{em} 461 nm). Red BODIPY, linearized Red BODIPY and dendrimers with red BODIPY were added to designated wells and the cells were incubated for 10 minutes. Before imaging cells were washed with PBS or with serum-free medium. No background fluorescence of cells was detected under the settings used.

Cell culture. Primary human hepatocyte cells (Celprogen, USA) were cultured in media Human Hepatocyte Complete growth media purchased from Celprogen, containing 10% serum and supplemented with antibiotics. The cells were maintained at 37°C (5% CO₂) in a humidified atmosphere. Normal hepatocyte culture media contained phenol red, however, during experimentation cells were switched to serum free, phenol red free, RPMI 1640 (Invitrogen, Canada), supplemented with 1% streptomycin and penicillin (Invitrogen, Canada). For spectrofluorometric, cytotoxicity and fluorescent microscopy experiments the cells were seeded in 24 well plates (Sarstedt, Montreal, QC, Canada) at densities varying between 15000 – 150000 cells/well. Human hepatocytes were switched from their serum containing media to serum free RPMI 1640, one hour prior to treatments. Dendrimers and other compounds were incubated with cells between two minutes to 72 hours. MCF-7 cells were maintained in 10% FBS (Invitrogen, Canada), RPMI 1640, supplemented with 1% streptomycin and penicillin and placed at 37°C (5% CO₂) in a humidified atmosphere. For experimental purposes cells were counted and seeded onto 24 well plates at densities varying between 25000 and 200000 cells per well.

MTT assay and trypan blue exclusion assay. Colorimetric MTT (3-(4,5-dimethylthiazol-2-yl)-2,5-diphenyl tetrazolium bromide, Sigma) assays were performed to assess cell viability. After 24, 48 and 72 hour treatments (see treatment details above), media was removed and replaced with serum-free media (500 µL/well). 50 µL of an MTT stock solution (12 µM) was added to each well and cells were then incubated for one hour at 37°C. Following the incubation, the media was removed, and cells and formazan were dissolved with dimethyl-sulfoxide (DMSO, Sigma). Absorbance was measured at 595 nm using a Benchmark microplate reader (Bio-Rad, Mississauga, ON, Canada). All measurements were done in triplicates in three or more independent experiments. Additional cell viability assays, including cell counting using the trypan blue exclusion assay, confirmed that the results obtained from the MTT assays, thus allowing for correlation of MTT results and cytotoxicity.

Fluorescent microscopy. Human hepatocytes were seeded on 24 well plates at a density of 25000cells/well. Prior to fluorescent labeling the medium was changed to serum free, phenol red free, RPMI 1640 media. Cells were stained first with green BODIPY (BODIPY 493/503, 20 μ M, 10 minutes), to label the lipid bodies and Hoechst 33342 (10 μ M for 30 minutes) to label the nucleus. The cells were then rinsed and an initial image was captured. The fluorescent red BODIPY dye, either in its free, linearized or dendrimer-associated form was added to the cells, and images were captured at time intervals as indicated over a thirty minute time period. The images were taken using a Leica fluorescent microscope and processed using Leica image analysis software.

5.5 Experimental section

Copper(II) sulfate pentahydrate ($\text{CuSO}_4 \cdot 5\text{H}_2\text{O}$) (>98.0%), sodium ascorbate (NaAsc) (crystalline) (98%), tetrabutylammonium fluoride (Bu_4NF) (1.0 M in THF), tetrabromomethane (CBr_4) (99%), K_2CO_3 , Cu(I), Bis(triphenylphosphine)palladium(II) dichloride [$\text{PdCl}_2(\text{PPh}_3)_2$], triphenylphosphine (TPP), 6-Bromohexanoic acid (97%), 11-Bromo-1-undecanol (98%), α -Lipoic acid (>99%), *N,N'*-Dicyclohexylcarbodiimide (DCC) (99%), 4-(dimethylamino)pyridine (DMAP) (99%), and sodium azide (NaN_3) (>99.5%) were purchased from Sigma-Aldrich Canada, and used as received. (Triisopropylsilyl)acetylene, and (trimethylsilyl)acetylene were purchased from Oakwood Products, Inc., and used as purchased. 8-Acetoxyethyl-2,6-diethyl-1,3,5,7-tetramethyl pyrromethene fluoroborate (PM605) was purchased from Exciton Inc, and used as received. Tetrahydrofuran (THF) was dried over sieves, and Diethylamine (DEA), triethylamine (NEt_3) were distilled over KOH. All other solvents were used as received in their anhydrous forms.

NMR spectra were measured on a 270, 300, or 400MHz (as specified) spectrometer at ambient temperatures. The chemical shifts in ppm are reported relative to tetramethylsilane as an internal standard for ^1H and $^{13}\text{C}\{^1\text{H}\}$ NMR spectra. Mass spectra were recorded on Thermo Scientific Orbitrap mass analyzer (ES) and Kratos MS25 (EI) mass spectrometers, and MALDI-TOF spectra on Autoflex III Mass Spectrometer (Bruker) using LiBr-dithranol as the matrix. UV-Vis spectra were recorded on a Cary 5000 UV-Vis-NIR Spectrophotometer with a resolution of less than 2 nm using quartz cuvettes. Fluorescence measurements were performed on Fluoromax-2 fluorimeter.

1,3,5-Triethynylbenzene (**TEB**), (4-Ethynyl-phenylethynyl)-triisopropyl-silane, 11-Azido-undecan-1-ol, 6-Azido-hexanoic acid, 3-bromo-5-iodo benzyl alcohol, 8-Hydroxymethyl-2,6-diethyl -1,3,5,7-tetramethyl pyrromethene fluoroborate (**BODIPY-OH**) were synthesized by adaptation of the previously published procedure as follows:

1,3,5-Triethynylbenzene (TEB): Weber, E.; Hedur, M.; Koepp, E.; Orlia, W.; Czugler, M. *J. Chem. Soc., Perkin Trans. 2*, **1988**, 1251.

^1H NMR (400 MHz, CDCl_3): δ (ppm) 3.11 (s, 3H, -ArCCH), 7.57 (s, 3H, ArH).

(4-Ethynyl-phenylethynyl)-triisopropyl-silane: Lavastre, O.; Ollivier, L.; Dixneuf, P. H.; Sibandhit, S. *Tetrahedron*, **1996**, 52, 5495.

^1H NMR (270 MHz, CDCl_3): δ (ppm) 1.13 (br. s, 21H, -Si(C₃H₇)), 3.16 (s, 1H, -CCH), 7.44 (d, 4H, ArH).

11-Azido-undecan-1-ol: Lin Y.; Tsai S.; Yu S. J.; *J. Org. Chem.* **2008**, 73, 4920.

^1H NMR (400 MHz, CDCl_3): δ (ppm) 1.20-1.33 (m, 14H, -CH₂-), 1.55 (m, 4H, -CH₂CH₂OH), 3.21 (t, 2H, -CH₂OH), 3.57 (t, 2H, -CH₂-N₃).

6-Azido-hexanoic acid: Parrish B.; Emrick T.; *Bioconjugate Chem.*, **2007**, 18 (1), 263.

^1H NMR (400 MHz, CDCl_3): δ (ppm) 1.40 (m, 2H, $-\text{CH}_2-$), 1.57-1.70 (m, 4H, $-\text{CH}_2-$), 2.35 (t, 2H, $-\text{CH}_2\text{COOH}$), 3.29 (t, 2H, $-\text{CH}_2\text{N}_3$), 11.70 (br. s, 1H, $-\text{COOH}$); $^{13}\text{C}\{^1\text{H}\}$ NMR (100 MHz, CDCl_3): δ 24.1, 26.1, 28.5, 51.1, 179.5.

3-bromo-5-iodo benzyl alcohol: This compound was obtained from its carboxylic acid form using a literature procedure: Lehmann U.; Schlüter A. D.; *Eur. J. Org. Chem.* **2000**, 3483.

8-Hydroxymethyl-2,6-diethyl-1,3,5,7-tetramethyl pyrromethene

fluoroborate (BODIPY-OH): This compound was obtained from its carboxylic acid form: Oleynik P.; Ishihara Y.; Cosa C.; *J. Am. Chem. Soc.* **2007**, *129*, 1842.

^1H NMR (400 MHz, CDCl_3): δ (ppm) 1.05 (t, 6H, $-\text{ArCH}_2\text{CH}_3$), 2.25 (s, 6H, $-\text{ArCH}_3$), 2.39 (q, 4H, $-\text{ArCH}_2\text{CH}_3$), 2.43 (s, 6H, $-\text{ArCH}_3$), 2.50 (s, 6H, $-\text{ArCH}_3$), and 4.92 (d, 2H, $-\text{ArCH}_2\text{OH}$).

Synthesis of PM-N₃: To a solution of **BODIPY-OH** (300 mg, 0.898 mmol), 6-azidohexanoic acid (282 mg, 1.80 mmol), and DMAP (13.5 mg) in dichloromethane (DCM) (10 mL), DCC (365.5 mg, 1.8 mmol) were added, and the solution was stirred at room temperature for 1 hour. It was then filtered, and the solid was washed with more DCM (30 mL), and the filtrate was washed with a saturated solution of NaHCO_3 (3x100mL), dried with MgSO_4 . The solvent was then evaporated, and the residue was flushed on a silica column using DCM. The solvent was evaporated again to yield a dark purple solid (401mg, 94.4%). ^1H NMR (400 MHz, CDCl_3): δ (ppm) 1.05 (t, 6H, $-\text{ArCH}_2\text{CH}_3$), 1.41 (m, 2H, $-\text{OOCCH}_2\text{CH}_2-$), 1.61 (m, 2H, $-\text{CH}_2\text{CH}_2\text{CH}_2\text{N}_3$), 1.69 (m, 2H, $-\text{CH}_2\text{CH}_2\text{N}_3$), 2.25 (s, 6H, $-\text{ArCH}_3$), 2.38 (t, 2H, $-\text{OOCCH}_2-$), 2.40 (q, 4H, $-\text{ArCH}_2\text{CH}_3$), 2.51 (s, 6H, $-\text{ArCH}_3$), 3.27 (t, 2H, $-\text{CH}_2\text{N}_3$), and 5.32 (s, 2H, $-\text{ArCH}_2\text{OOCCH}_2-$); $^{13}\text{C}\{^1\text{H}\}$ NMR (75 MHz, CDCl_3): δ 12.8, 12.9, 14.9, 17.4, 24.7, 26.5, 28.7, 34.1, 51.4, 58.5, 131.8, 132.5, 133.8, 136.7, 155.2, 173.3. HRMS (ESI): Theoretical $M_w + \text{Na}^+ = 496.28$ g/mol. Found $M_w + \text{Na}^+ = 496.27$ g/mol.

Synthesis of 3-bromo-5-(triisopropylsilylethynyl)benzyl alcohol (1): To a solution of 3-bromo-5-iodobenzyl alcohol (5g, 16 mmol) in diethylamine (150 mL), triisopropylsilylacetylene (3.80 g, 20.8 mmol) and catalytic amounts (ca. 5 mol%) of [PdCl₂(PPh₃)₂], and CuI were added. The reaction mixture was stirred for 2 days at room temperature. The solvent was then evaporated and the residue was extracted with diethyl ether. The extract was dried over MgSO₄ and the solvent was evaporated again. The product was purified by silica-gel column chromatography with 1:20 (ethylacetate : hexane). The solvent was removed under vacuum to yield a pale yellow oil (4.64 g, 79.1%). ¹H NMR (300 MHz, CDCl₃): δ (ppm) 1.12 (br. s, 21H, -Si(C₃H₇)), 4.63 (d, 2H, -ArCH₂OH), 7.38 (d, 1H, ArH), 7.45 (s, 1H, ArH), 7.52 (s, 1H, ArH); ¹³C{¹H} NMR (75 MHz, CDCl₃): δ (ppm) 11.5, 18.9, 64.3, 92.7, 105.4, 122.4, 125.7, 129.0, 130.0, 133.9, and 143.1. HRMS (EI): Theoretical M_w = 366.10 g/mol. Found M_w = 366.10 g/mol.

Synthesis of 3-(triisopropylsilylethynyl)-5-trimethylsilylethynylbenzyl alcohol (2): To a solution of 3-bromo-5-isopropylsilylethynylbenzyl alcohol (1) (4.46 g, 12.2 mmol) and trimethylsilylacetylene (3.58 g, 36.5 mmol) in benzene (70 mL) and triethylamine (130 mL), catalytic amounts (ca. 5 mol%) of [PdCl₂(PPh₃)₂] and CuI were added. The reaction mixture was stirred overnight under reflux. The solvent was then evaporated and the residue was extracted with diethyl ether. The extract was dried over MgSO₄ and the solvent was evaporated again. The product was purified by silica-gel column chromatography with 1:20 (ethylacetate : hexane). The solvent was removed under vacuum to yield a pale yellow oil (4.23 g, 90.4%). ¹H NMR (300 MHz, CDCl₃): δ (ppm) 0.23 (s, 9H; SiCH₃), 1.12 (br. s, 21H, -Si(C₃H₇)), 4.63 (d, 2H, -ArCH₂OH), 7.41 (s, 2H, ArH), 7.50 (s, 1H, ArH); ¹³C{¹H} NMR (100 MHz, CDCl₃): δ (ppm) 0.1, 11.2, 18.6, 64.4, 91.5, 95.0, 103.9, 105.8, 123.5, 123.9, 130.0, 130.2, 134.4, and 141.1. HRMS (ESI): Theoretical M_w⁺ = 385.23 g/mol. Found M_w⁺ = 385.32 g/mol.

Synthesis of 3-(triisopropylsilylethynyl)-5-trimethylsilylethynylbenzyl bromide (3): To a stirring solution of 3-(triisopropylsilylethynyl)-5-

trimethylsilylethynyl) benzyl alcohol (**2**) (3.99 g, 10.4 mmol) and carbon tetrabromide (4.48 g, 13.5 mmol) in THF (40mL) in an ice bath, TPP (3.55g, 13.5mmol) was added slowly in many portions. After 15 minutes, the ice bath was removed, and the reaction mixture was left to stir at room temperature for 2 hours. The reaction was then quenched with water and THF was evaporated. The aqueous phase was then extracted with DCM (3x50 mL) and dried over MgSO₄. The product was purified by column chromatography using 1:20 (ethylacetate : hexane) mixture. The solvent was evaporated to yield the product as a pale yellow oil (4.57 g, 98.6%). ¹H NMR (300 MHz, CDCl₃): δ (ppm) 0.24 (s, 9H; SiCH₃), 1.12 (br. s, 21H, -Si(C₃H₇)), 4.39 (s, 2H, -ArCH₂Br), 7.42 (s, 1H, ArH), 7.43 (s, 1H, ArH), 7.50 (s, 1H, ArH); ¹³C{¹H} NMR (75 MHz, CDCl₃): δ 0.1, 11.5, 18.9, 32.2, 92.3, 95.8, 103.6, 105.8, 124.2, 124.5, 132.4, 132.5, 135.4, and 138.3. HRMS (EI): Theoretical M_w = 446.15 g/mol. Found M_w = 446.10 g/mol.

Synthesis of 3-(triisopropylsilylethynyl)-5-ethynylbenzyl bromide (4): To a solution of 3-(triisopropylsilylethynyl)-5-trimethylsilylethynyl)benzyl bromide (**3**) (4.50 g, 10.1 mmol) in acetone (100 mL), an aqueous solution of K₂CO₃ (20 mL; 3.48 g, 25.2 mmol) was added. The reaction mixture was stirred overnight at room temperature. Acetone was then evaporated and the residue was extracted with ethyl acetate. The extract was dried over MgSO₄, and solvent was evaporated. The product was then purified by silica column chromatography using ethylacetate/hexane (1:1) mixture to yield a yellowish oil which solidifies upon standing (3.51g, 93.1%). ¹H NMR (400 MHz, CDCl₃): δ (ppm) 1.13 (br. s, 21H, -Si(C₃H₇)), 3.10 (s, 1H, ArCCH), 4.40 (s, 2H, -ArCH₂Br), 7.46 (s, 2H, ArH), 7.52 (s, 1H, ArH); ¹³C{¹H} NMR (100 MHz, CDCl₃): δ (ppm) 11.2, 18.7, 31.8, 78.3, 82.1, 92.4, 105.2, 122.9, 124.5, 132.4, 132.6, 135.4, and 138.2. HRMS (EI): Theoretical Mw= 374.11 g/mol, found Mw= 374.10 g/mol.

Synthesis of compound (5): Compound **4** (500 mg, 1.34 mmol) and 11-Azido-undecan-1-ol (314 mg, 1.47 mmol) were dissolved in 5 mL of THF followed by addition of sodium ascorbate (198 mg, 0.51 mmol). An aqueous solution (1 mL) of CuSO₄·5H₂O (64 mg, 0.26 mmol) was added dropwise to the solution which

was left to stir overnight at 40°C. THF was then evaporated, and the remaining solution was extracted with DCM (3x30 mL), and dried over MgSO₄. The solvent was evaporated, and the crude product was then purified by flash chromatography eluting the product with EthAc/Hex (1:2). The solvent was evaporated to yield the product as yellowish oil (683 mg, 87%). ¹H NMR (400 MHz, CDCl₃): δ (ppm) 1.13 (br. s, 21H, -Si(C₃H₇)), 1.25-1.34 (m, 14H, -CH₂-), 1.55 (m, 2H, -CH₂CH₂OH), 1.94 (m, 2H, -CH₂CH₂-triazole), 3.63 (t, 2H, -CH₂OH), 4.39 (t, 2H, -CH₂-triazole), 4.48 (s, 2H, -ArCH₂Br), 7.45 (s, 1H, ArH), 7.79 (s, 1H, triazoleH), 7.84 (s, 1H, ArH), 7.85 (s, 1H, ArH); ¹³C{¹H} NMR (100 MHz, CDCl₃): δ 11.3, 18.7, 25.7, 26.4, 28.9, 29.3, 29.4, 29.5, 30.3, 32.4, 32.8, 50.5, 63.0, 91.7, 105.9, 119.8, 124.7, 126.2, 129.0, 131.5, 131.9, 138.2, and 146.4. HRMS (EI): Theoretical M_w+Na⁺ = 610.29 g/mol. Found M_w+Na⁺ = 610.10 g/mol.

Synthesis of compound (6): To a solution of compound (5) (336 g, 0.57 mmol) in DMF (10 mL), NaN₃ (186 mg, 2.86 mmol) was added. The reaction mixture was left to stir at room temperature for 1 hour. The solution was extracted with ethyl acetate (3x20 ml). The organic phase was then washed with brine (3x40mL), and dried overwith MgSO₄, followed by removal of the solvent. The product was flushed over a short silica-gel column with EthAc/Hex (1:3) to yield a pale yellow oil (303 mg, 96.5%). ¹H NMR (400 MHz, CDCl₃): δ (ppm) 1.14 (br. s, 21H, -Si(C₃H₇)), 1.25-1.34 (m, 14H, -CH₂-), 1.55 (m, 2H, -CH₂CH₂OH), 1.95 (m, 2H, -CH₂CH₂-triazole), 3.63 (t, 2H, -CH₂OH), 4.40 (t, 2H, -CH₂-triazole), 4.38 (s, 2H, -ArCH₂N₃), 7.39 (s, 1H, ArH), 7.78 (s, 1H, ArH), 7.80 (s, 1H, triazoleH), and 7.86 (s, 1H, ArH) ppm; ¹³C{¹H} NMR (100 MHz, CDCl₃): δ (ppm) 11.3, 18.7, 25.7, 26.4, 28.9, 29.3, 29.4, 29.5, 30.3, 32.8, 50.5, 54.3, 63.0, 91.8, 106.0, 119.9, 124.7, 125.1, 128.9, 131.1, 131.4, 136.3, and 146.5. HRMS (EI): Theoretical M_w⁺ = 551.38 g/mol. Found M_w⁺ = 551.40 g/mol.

Synthesis of compound (7): TEB (50 mg, 0.33 mmol) and compound 6 (605 mg, 1.10 mmol) were dissolved in 10mL of THF followed by addition of sodium ascorbate (87 mg, 0.44 mmol). An aqueous solution (2 mL) of CuSO₄.5H₂O (55

mg, 0.22 mmol) was added dropwise to the solution, and it was left to stir for 48 hours at 40°C. THF was then evaporated, and the remaining solution was extracted with ethyl acetate (3x40 mL), and dried over MgSO₄. The solvent was evaporated, and the crude product was then purified by flash chromatography eluting the product with ethyl acetate. The solvent was evaporated to yield the product as a white solid (546 mg, 91%). ¹H NMR (400 MHz, CDCl₃): δ (ppm) 1.11 (br. s, 63H, -Si(C₃H₇)), 1.21-1.34 (m, 42H, -CH₂-), 1.52 (m, 6H, -CH₂CH₂OH), 1.90 (m, 6H, -CH₂CH₂-triazole), 3.60 (t, 6H, -CH₂OH), 4.36 (t, 6H, -CH₂CH₂-triazole), 5.56 (s, 6H, -ArCH₂-triazole), 7.42 (s, 3H, ArH), 7.73 (s, 3H, triazoleH), 7.83 (s, 3H, ArH), 7.86 (s, 3H, ArH), 7.96 (s, 3H, ArH, core), and 8.16 (s, 3H, triazoleH, core); ¹³C{¹H} NMR (100 MHz, CDCl₃): δ (ppm) 11.3, 18.7, 25.7, 26.4, 28.9, 29.2, 29.3, 29.3, 29.4, 30.2, 32.8, 50.5, 53.9, 62.9, 92.4, 105.6, 120.2, 120.3, 122.3, 125.2, 129.6, 131.2, 131.5, 132.0, 135.2, 146.1, and 147.5. MALDI: Theoretical M_w⁺ = 1825.19 g/mol. Found M_w⁺ = 1825.24 g/mol.

Synthesis of compound (8): To a solution of compound **7** (400 mg, 0.22 mmol) in THF (10 mL) in a dry ice/acetone bath, a solution of Bu₄NF (0.79 mL (1M solution in THF, 0.79 mmol) was added in a dropwise fashion. The reaction mixture was allowed to warm to room temperature and left to stir overnight. The solvent was removed under vacuum and the residue was the residue was extracted with ethyl acetate (3x30 mL). The extract was then dried over MgSO₄, and solvent was evaporated. The product was washed with ether to yield a white solid (258 mg, 88.1%). ¹H NMR (400 MHz, CDCl₃): δ (ppm) 1.21-1.34 (m, 42H, -CH₂-), 1.52 (m, 6H, -CH₂CH₂OH), 1.90 (m, 6H, -CH₂CH₂-triazole), 2.16 (s, 3H, -CH₂OH), 3.11 (s, 3H, ArCCH), 3.60 (m, 6H, -CH₂OH), 4.36 (t, 6H, -CH₂CH₂-triazole), 5.56 (s, 6H, -ArCH₂-triazole), 7.36 (s, 3H, ArH), 7.79 (s, 3H, triazoleH), 7.82 (s, 3H, ArH), 7.86 (s, 3H, ArH), 7.93 (s, 3H, ArH, core), and 8.15(s, 3H, triazoleH, core); ¹³C{¹H} NMR (100 MHz, CDCl₃): δ 25.7, 26.4, 28.9, 29.2, 29.2, 29.3, 29.3, 29.4, 30.2, 32.8, 50.5, 53.8, 62.9, 78.7, 82.4, 120.2, 120.4, 122.3, 123.8, 125.6, 129.5, 131.0, 131.5, 132.1, 135.5, 145.9, and 147.5

ppm. HRMS (EI): Theoretical $M_w+Na^+ = 1356.72$ g/mol. Found $M_w+Na^+ = 1356.78$ g/mol.

Synthesis of compound (9): Compound **8** (140 mg, 0.105 mmol) and PM-N₃ (164 mg, 0.35 mmol) were dissolved in 10 mL of THF followed by addition of sodium ascorbate (55 mg, 0.28 mmol). An aqueous solution (2 mL) of CuSO₄·5H₂O (35 mg, 0.14 mmol) was added dropwise to the solution. The solution was left to stir for 48 hours at 50°C. THF was then evaporated, and the remaining solution was extracted with DCM (3x20 mL), dried over MgSO₄. The solvent was evaporated, and the crude product was then purified by flash chromatography eluting the product with MeOH/DCM (1:15). The solvent was evaporated to yield the product as dark red solid (254 mg, 87.9%). ¹H NMR (400 MHz, CDCl₃): δ (ppm) 0.98 (t, 18H, -ArCH₂CH₃), 1.17-1.40 (m, 48H, -CH₂-), 1.49 (m, 6H, -CH₂CH₂OH), 1.67 (m, 6H, -CH₂CH₂CH₂-triazole), 1.80-1.95 (m, 12H, -CH₂CH₂-triazole), 2.18 (s, 18H, -ArCH₃), 2.24-2.38 (m, 18H, -CH₂-), 2.46 (s, 18H, -ArCH₃), 3.58 (m, 6H, -CH₂OH), 4.31 (t, 12H, -CH₂CH₂-triazole), 5.25 (s, 6H, -ArCH₂OOCCH₂-), 5.52 (s, 6H, -ArCH₂-triazole), 7.71 (s, 3H, ArH), 7.73 (s, 3H, triazoleH), 7.85 (s, 3H, ArH, core), 7.90 (s, 6H, ArH), 8.03 (s, 3H, triazoleH, BODIPY arm), and 8.23(s, 3H, triazoleH, core); ¹³C{¹H} NMR (100 MHz, CDCl₃): δ 12.6, 12.7, 14.7, 17.1, 24.2, 25.7, 25.9, 26.3, 28.8, 29.2, 29.2, 29.3, 29.4, 29.9, 30.1, 32.7, 33.6, 50.1, 50.5, 54.0, 58.2, 62.8, 120.5, 122.0, 122.9, 124.7, 131.4, 131.5, 132.2, 132.3, 133.6, 136.0, 136.5, 146.4, 146.5, 147.3, 154.9 and 172.9. HRMS (EI): Theoretical $M_w^+ = 2753.62$ g/mol. Found $M_w^+ = 2753.66$ g/mol.

Synthesis of D-PM-LA: To a solution of compound **9** (107 mg, 0.039 mmol), lipoic acid (27 mg, 0.13 mmol), and DMAP (5 mg) in DCM (10 mL), DCC (54 mg, 0.26 mmol) was added, and the solution was stirred at room temperature for 2 hours. It was filtered, and the solid was washed with more DCM (10 mL), and the filtrate was washed with a saturated solution of NaHCO₃ (3x30 mL), dried over MgSO₄. The solvent was then evaporated, and the residue was flushed on a silica column using MeOH/DCM (1:20). The solvent was evaporated again to

yield a purple solid (120 mg, 93%). ^1H NMR (400 MHz, CDCl_3): δ (ppm) 0.99 (t, 18H, $-\text{ArCH}_2\text{CH}_3$), 1.17-1.55 (m, 54H, $-\text{CH}_2-$), 1.55-1.80 (m, 24H, $-\text{CH}_2-$), 1.80-1.95 (m, 12H, $-\text{CH}_2\text{CH}_2$ -triazole), 2.19 (s, 18H, $-\text{ArCH}_3$), 2.24-2.38 (m, 30H, $-\text{CH}_2-$), 2.47 (s, 18H, $-\text{ArCH}_3$), 3.10 (m, 6H, $-\text{CH}_2\text{CH}_2\text{SS}-$), 3.55 (m, 3H, $-\text{CH}_2\text{CH}_1(\text{S}-)\text{CH}_2-$), 4.04 (t, 6H, $-\text{CH}_2\text{CH}_2\text{OOCCH}_2-$), 4.37 (t, 12H, $-\text{CH}_2\text{CH}_2$ -triazole), 5.27 (s, 6H, $-\text{ArCH}_2\text{OOCCH}_2-$), 5.61 (s, 6H, $-\text{ArCH}_2$ -triazole), 7.76 (s, 3H, ArH), 7.79 (s, 3H, triazoleH), 7.90 (s, 9H, ArH), 8.15 (s, 3H, triazoleH, BODIPY arm), and 8.30 (s, 3H, triazoleH, core); $^{13}\text{C}\{^1\text{H}\}$ NMR (100 MHz, CDCl_3): δ 12.6, 12.7, 14.7, 17.1, 24.2, 24.7, 24.9, 25.6, 25.9, 26.5, 28.6, 28.8, 29.0, 29.2, 29.3, 29.4, 29.9, 30.3, 33.6, 33.9, 34.1, 34.6, 38.5, 40.2, 50.1, 50.5, 53.5, 54.1, 56.4, 58.2, 64.5, 120.3, 120.4, 122.2, 123.0, 124.7, 124.8, 131.6, 132.2, 132.3, 132.4, 133.6, 135.9, 136.5, 146.5, 146.6, 147.4, 154.9, 172.9, and 173.6. HRMS (EI): Theoretical $M_w + \text{Na}^+ = 3339.75$ g/mol. Found $M_w + \text{Na}^+ = 3339.75$ g/mol.

Synthesis of D-PM: TEB (10 mg, 0.067 mmol) and PM- N_3 (114 mg, 0.24 mmol) were dissolved in 5 mL of THF followed by addition of sodium ascorbate (16 mg, 0.081 mmol). An aqueous solution (1 mL) of $\text{CuSO}_4 \cdot 5\text{H}_2\text{O}$ (10 mg, 0.040 mmol) was added dropwise to the solution. It was left to stir overnight at 40°C , and THF was then evaporated. The remaining solution was extracted with DCM (3X15mL), and dried over MgSO_4 . The solvent was evaporated, and the crude product was then purified by flash chromatography eluting the product with MeOH/DCM (1:10). The solvent was evaporated to yield the product as a purple powder (94 mg, 89.9%). ^1H NMR (400 MHz, CDCl_3): δ (ppm) 1.02 (t, 18H, $-\text{ArCH}_2\text{CH}_3$), 1.40 (m, 6H, $-\text{OOCCH}_2\text{CH}_2-$), 1.73 (m, 6H, $-\text{CH}_2\text{CH}_2\text{CH}_2$ -triazole), 1.98 (m, 6H, $-\text{CH}_2\text{CH}_2$ -triazole), 2.23 (s, 18H, $-\text{ArCH}_3$), 2.36 (t, 6H, $-\text{OOCCH}_2-$), 2.41 (q, 12H, $-\text{ArCH}_2\text{CH}_3$), 2.49 (s, 18H, $-\text{ArCH}_3$), 4.41 (t, 6H, $-\text{CH}_2$ -triazole), 5.31 (s, 6H, $-\text{ArCH}_2\text{OOCCH}_2-$), 7.97 (s, 3H, ArH), and 8.31 (s, 3H, triazoleH); $^{13}\text{C}\{^1\text{H}\}$ NMR (75 MHz, CDCl_3): δ 12.8, 12.9, 14.9, 17.3, 24.4, 26.2, 30.2, 33.9, 50.3, 58.5, 120.4, 122.4, 131.8, 132.0, 132.4, 133.8, 136.7,

147.4, 155.2, 173.1. HRMS (ESI): Theoretical $M_w + Na^+ = 1592.88$ g/mol. Found $M_w + Na^+ = 1592.92$ g/mol.

Synthesis of compound (10): 4-Ethynyl-phenylethynyl)-triisopropyl-silane (150 mg, 0.53 mmol) and 11-Azido-undecan-1-ol (125 mg, 0.59 mmol) were dissolved in 5 mL of THF followed by addition of sodium ascorbate (42 mg, 0.21 mmol). An aqueous solution (1 mL) of $CuSO_4 \cdot 5H_2O$ (26 mg, 0.11 mmol) was added dropwise to the solution. The solution was left to stir overnight at 40°C. THF was then evaporated, and the remaining solution was extracted with ethyl acetate (3x20mL), and dried over $MgSO_4$. The solvent was evaporated, and the crude product was then purified by flash chromatography eluting the product with EthAc/Hex (1:3). The solvent was evaporated to yield the product as yellowish oil (223mg, 84.8%). 1H NMR (400 MHz, $CDCl_3$): δ (ppm) 1.13 (br. s, 21H, - $Si(C_3H_7)_3$), 1.23-1.33(m, 12H, - CH_2 -), 1.55 (m, 2H, - CH_2CH_2OH), 1.63 (m, 2H, - $CH_2CH_2CH_2$ -triazole), 1.93 (m, 2H, - CH_2CH_2 -triazole), 2.16 (s, 1H, - CH_3OH), 3.63 (t, 2H, - CH_2OH), 4.38 (t, 2H, - CH_2 -triazole), 7.51 (d, 2H, ArH), 7.75 (s, 1H, triazoleH), 7.76 (d, 2H, ArH); $^{13}C\{^1H\}$ NMR (100 MHz, $CDCl_3$): δ 11.3, 18.7, 25.7, 26.4, 28.9, 29.3, 29.4, 29.5, 30.3, 32.8, 50.5, 63.0, 91.4, 106.9, 119.7, 123.1, 125.3, 130.5, 132.5, and 147.4. MALDI: Theoretical $M_w^+ = 496.36$ g/mol. Found $M_w^+ = 496.19$ g/mol.

Synthesis of compound (11): To a solution of compound **10** (195 mg, 0.39 mmol) in THF (5 mL) in a dry ice/acetone bath, a solution of Bu_4NF (0.47 mL (1M solution in THF, 0.47 mmol) was added in a dropwise fashion. The reaction mixture was allowed to warm to room temperature and left to stir overnight. The solvent was removed under vacuum and the residue was extracted with ethyl acetate (3x20 mL). The extract was then dried over $MgSO_4$, and solvent was evaporated. The product was washed with ether to yield a white solid (125 mg, 93.6%). 1H NMR (400 MHz, $CDCl_3$): δ (ppm) 1.26-1.34 (m, 12H, - CH_2 -), 1.55 (m, 2H, - CH_2CH_2OH), 1.57 (m, 2H, - $CH_2CH_2CH_2$ -triazole), 1.94 (m, 2H, - CH_2CH_2 -triazole), 2.16 (s, 1H, - CH_3OH), 3.13 (s, 1H, -CCH), 3.63 (t, 2H, - CH_2OH), 4.40 (t, 2H, - CH_2 -triazole), 7.54 (d, 2H, ArH), 7.76 (s, 1H, triazoleH),

7.78 (d, 2H, ArH); $^{13}\text{C}\{^1\text{H}\}$ NMR (100 MHz, CDCl_3): δ (ppm) 25.7, 26.4, 28.9, 29.3, 29.4, 29.5, 30.3, 32.8, 50.5, 63.0, 77.9, 83.5, 119.7, 121.6, 125.5, 131.1, 132.6, and 147.4. HRMS (ESI): Theoretical $M_w^+ = 340.23$ g/mol. Found $M_w^+ = 340.24$ g/mol.

Synthesis of compound (12): Compound **11** (104 mg, 0.31 mmol) and **PM-N₃** (160 mg, 0.34 mmol) were dissolved in 5 mL of THF followed by addition of sodium ascorbate (25 mg, 0.12 mmol). An aqueous solution (1 mL) of $\text{CuSO}_4 \cdot 5\text{H}_2\text{O}$ (15 mg, 0.062 mmol) was added dropwise to the solution. The solution was left to stir overnight at 40°C. THF was then evaporated, and the remaining solution was extracted with DCM (3x20 mL), and dried over MgSO_4 . The solvent was evaporated, and the crude product was then purified by flash chromatography eluting the product with MeOH/DCM (1:20). The solvent was evaporated to yield the product as purple solid (221 mg, 88.9%). ^1H NMR (400 MHz, CDCl_3): δ (ppm) 1.01 (t, 6H, -ArCH₂CH₃), 1.22-1.41 (m, 14H, -CH₂-), 1.53 (m, 2H, -CH₂CH₂OH), 1.68 (m, 4H, -CH₂CH₂CH₂-triazole), 1.92 (m, 4H, -CH₂CH₂-triazole), 2.15 (s, 1H, -CH₃OH), 2.20 (s, 6H, -ArCH₃), 2.36 (t, 2H, -OOCCH₂-), 2.38 (q, 4H, -ArCH₂CH₃), 2.48 (s, 6H, -ArCH₃), 3.60 (t, 2H, -CH₂OH), 4.37 (t, 4H, -CH₂-triazole), 5.29 (s, 2H, -ArCH₂OOCCH₂-), 7.79 (s, 2H, triazoleH), 7.86 (s, 4H, ArH); $^{13}\text{C}\{^1\text{H}\}$ NMR (100 MHz, CDCl_3): δ 12.6, 12.7, 14.7, 17.1, 24.2, 24.9, 25.6, 25.7, 25.9, 26.4, 28.9, 29.3, 29.4, 29.5, 29.9, 30.3, 32.8, 33.7, 33.9, 49.0, 50.0, 50.4, 53.5, 58.2, 62.9, 119.6, 119.7, 126.0, 130.2, 130.4, 131.5, 132.2, 133.6, 136.5, 147.2, 147.3, 155.0, and 172.9. MALDI: Theoretical $M_w + \text{Na}^+ = 835.51$ g/mol. Found $M_w + \text{Na}^+ = 835.31$ g/mol.

Synthesis of PM-LA: To a solution of compound **12** (100 mg, 0.123 mmol), lipoic acid (27.9 mg, 0.135 mmol), and DMAP (3 mg) in DCM (10 mL), DCC (27.9 mg, 0.135 mmol) was added, and the solution was stirred at room temperature for 1 hour. The solution was filtered, the solid was washed with more DCM (5 mL), and the filtrate was washed with a saturated solution of NaHCO_3 (3x15 mL), and dried over MgSO_4 . The solvent was then evaporated, and the residue was flushed on a silica column using MeOH/DCM (1:20). The

solvent was evaporated again to yield a dark purple solid (112 mg, 91.1%). ¹H NMR (400 MHz, CDCl₃): δ (ppm) 1.03 (t, 6H, -ArCH₂CH₃), 1.23-1.56 (m, 18H, -CH₂-), 1.58-1.73 (m, 6H, -CH₂-), 1.87-1.98 (m, 6H, -CH₂-), 2.22 (s, 6H, -ArCH₃), 2.30 (t, 4H, -OOCCH₂-), 2.38 (q, 4H, -ArCH₂CH₃), 2.45 (m, 2H, -CH₁CH₂CH₂SS-), 2.49 (s, 6H, -ArCH₃), 3.10 (m, 2H, -CH₂CH₂SS-), 3.56 (m, 1H, -CH₂CH₁(S-)CH₂-), 4.05 (t, 2H, -CH₂CH₂OOCCH₂-), 4.40 (t, 4H, -CH₂-triazole), 5.29 (s, 2H, -ArCH₂OOCCH₂-), 7.79 (s, 2H, triazoleH), 7.89 (s, 4H, ArH); ¹³C{¹H} NMR (100 MHz, CDCl₃): δ 12.6, 12.7, 14.7, 17.1, 24.2, 24.7, 24.9, 25.9, 26.0, 26.5, 28.8, 29.0, 29.2, 29.3, 29.4, 29.5, 30.0, 30.4, 33.7, 34.1, 34.6, 38.5, 40.2, 50.0, 50.5, 56.4, 58.3, 64.5, 119.5, 119.6, 126.1, 130.3, 130.4, 131.5, 132.2, 133.6, 136.4, 147.3, 147.4, 155.0, 172.9, and 173.6. HRMS (ESI): Theoretical M_w+Na⁺ = 1039.54 g/mol. Found M_w+Na⁺ = 1039.52 g/mol.

5.6 References

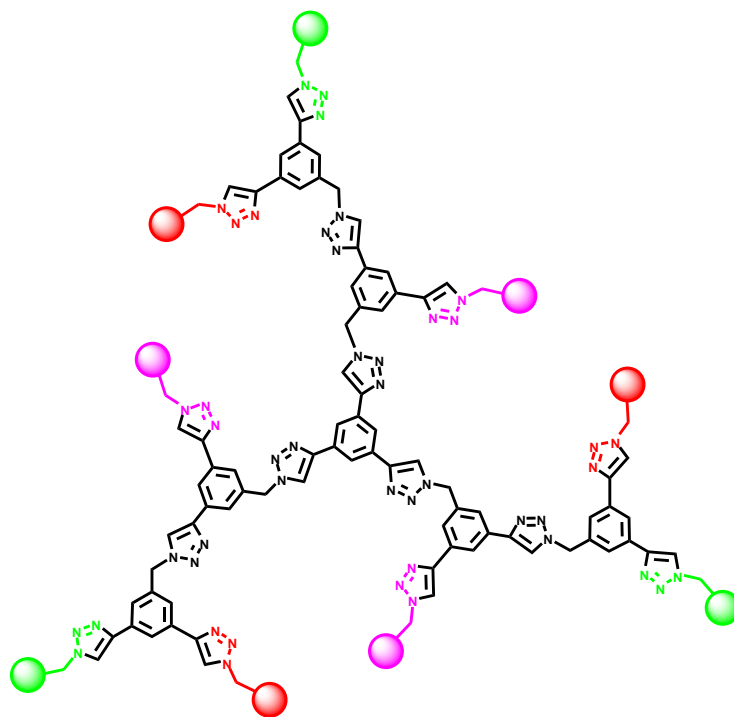
1. Tomalia, D.A., & Fréchet, J.M. Discovery of dendrimers and dendritic polymers: A brief historical perspective. *Journal of Polymer Science Part A: Polymer Chemistry* **40**, 2719-2728 (2002).
2. Goodwin, A.P., Lam, S.S. & Fréchet, J.M. Rapid, efficient synthesis of heterobifunctional biodegradable dendrimers. *Journal of the American Chemical Society* **129**, 6994-6995 (2007).
3. Kolb, H.C., Finn, M.G. & Sharpless, K.B. Click Chemistry: Diverse Chemical Function from a Few Good Reactions. *Angewandte Chemie (International ed)* **40**, 2004-2021 (2001).
4. Lee, C.C., MacKay, J.A., Fréchet, J.M. & Szoka, F.C. Designing dendrimers for biological applications. *Nature biotechnology* **23**, 1517-1526 (2005).
5. Savic, R., Eisenberg, A. & Maysinger, D. Block copolymer micelles as delivery vehicles of hydrophobic drugs: micelle-cell interactions. *Journal of drug targeting* **14**, 343-355 (2006).
6. Liu, M., Kono, K. & Fréchet, J.M. Water-soluble dendritic unimolecular micelles: their potential as drug delivery agents. *J Control Release* **65**, 121-131 (2000).

7. Gillies, E.R., Dy, E., Fréchet, J.M. & Szoka, F.C. Biological evaluation of polyester dendrimer: poly(ethylene oxide) "bow-tie" hybrids with tunable molecular weight and architecture. *Molecular pharmaceutics* **2**, 129-138 (2005).
8. Duncan, R. & Izzo, L. Dendrimer biocompatibility and toxicity. *Advanced drug delivery reviews* **57**, 2215-2237 (2005).
9. Shaunak, S. et al. Polyvalent dendrimer glucosamine conjugates prevent scar tissue formation. *Nature biotechnology* **22**, 977-984 (2004).
10. Svenson, S. & Tomalia, D.A. Dendrimers in biomedical applications--reflections on the field. *Advanced drug delivery reviews* **57**, 2106-2129 (2005).
11. DeForest, C.A., Polizzotti, B.D. & Anseth, K.S. Sequential click reactions for synthesizing and patterning three-dimensional cell microenvironments. *Nature materials* **8**, 659-664 (2009).
12. Wu, P. et al. Efficiency and fidelity in a click-chemistry route to triazole dendrimers by the copper(i)-catalyzed ligation of azides and alkynes. *Angewandte Chemie (International ed)* **43**, 3928-3932 (2004).
13. Thomas, T.P. et al. Targeting and inhibition of cell growth by an engineered dendritic nanodevice. *Journal of medicinal chemistry* **48**, 3729-3735 (2005).
14. Yousif, L.F., Stewart, K.M. & Kelley, S.O. Targeting mitochondria with organelle-specific compounds: strategies and applications. *Chembiochem* **10**, 1939-1950 (2009).
15. Martin, S. & Parton, R.G. Lipid droplets: a unified view of a dynamic organelle. *Nature reviews* **7**, 373-378 (2006).
16. Urahama, Y. et al. Lipid droplet-associated proteins protect renal tubular cells from fatty acid-induced apoptosis. *The American journal of pathology* **173**, 1286-1294 (2008).
17. Thiele, C. & Spandl, J. Cell biology of lipid droplets. *Current opinion in cell biology* **20**, 378-385 (2008).

18. Bickel, P.E., Tansey, J.T. & Welte, M.A. PAT proteins, an ancient family of lipid droplet proteins that regulate cellular lipid stores. *Biochimica et biophysica acta* **1791**, 419-440 (2009).
19. Bozza, P.T., Magalhaes, K.G. & Weller, P.F. Leukocyte lipid bodies - Biogenesis and functions in inflammation. *Biochimica et biophysica acta* **1791**, 540-551 (2009).
20. Murphy, S., Martin, S. & Parton, R.G. Lipid droplet-organelle interactions; sharing the fats. *Biochimica et biophysica acta* **1791**, 441-447 (2009).
21. Bolognesi, M.L., Minarini, A., Tumiatti, V. & Melchiorre, C. Lipoic acid, a lead structure for multi-target-directed drugs for neurodegeneration. *Mini reviews in medicinal chemistry* **6**, 1269-1274 (2006).
22. Lee, B.W. et al. Dose-related cytoprotective effect of alpha-lipoic acid on hydrogen peroxide-induced oxidative stress to pancreatic beta cells. *Free radical research* **43**, 68-77 (2009).
23. Ohshiro, T., Namatame, I., Lee, E.W., Kawagishi, H. & Tomoda, H. Molecular target of decursins in the inhibition of lipid droplet accumulation in macrophages. *Biological & pharmaceutical bulletin* **29**, 981-984 (2006).
24. Accioly, M.T. et al. Lipid bodies are reservoirs of cyclooxygenase-2 and sites of prostaglandin-E2 synthesis in colon cancer cells. *Cancer research* **68**, 1732-1740 (2008).
25. Le Lay, S. & Dugail, I. Connecting lipid droplet biology and the metabolic syndrome. *Progress in lipid research* **48**, 191-195 (2009).
26. Zentella de Pina, M. et al. Inhibition of cAMP-dependent protein kinase A: a novel cyclo-oxygenase-independent effect of non-steroidal anti-inflammatory drugs in adipocytes. *Autonomic & autacoid pharmacology* **27**, 85-92 (2007).
27. Totskii, V.N. [Mechanisms and ways of regulation of lipoic acid penetration into biological structures]. *Biokhimiia (Moscow, Russia)* **41**, 1094-1105 (1976).

Chapter 6

Conclusions, Contributions to Original Knowledge, and Suggestions for Future Work



6.1 Conclusions and contribution to general knowledge

Dendrimers continue to be in the forefront of research due to the significant potential demonstrated by these monodisperse macromolecules in a variety of disciplines. This thesis has provided a summary account of the research carried out in this field. It has also established that a combination of experimental design with theoretical evaluation is essential in understanding structure property relationships in these macromolecules, and in facilitating their entry into real life applications. For understanding the three dimensional structure of these macromolecules, we developed a general theoretical molecular modelling technique using ordinary computers. This technique revealed detailed structural information related to the size, shape, and the structural evolution of 3,5-dihydroxybenzyl alcohol (DHBA) and 1,3,5-triethynylbenzene (TEB) based dendrimers. In addition, it demonstrated the effect of using different linkers and building units on the developing 3D structure. This structural evaluation plays a pivotal role in practical applications related to molecular encapsulation in the internal cavities, selective catalysis, and the transport through biological barriers and membranes. The modelling strategy developed here can be applied to different types of macromolecules in varied disciplines as a reliable and powerful technique to reveal structural details.

We subsequently developed an efficient and reliable inorganic synthetic route to construct rigid-rod type dendrimers using dimethyldiaminostannanes to link 1,3,5-triethynylbenzene (TEB) molecules, in quantitative yields, and without the need for exhaustive purification steps. The inorganic entities in the dendritic framework, especially trimethylstannanes at the terminus, were shown to act as electron donors, similar to organic donors such as methoxy groups. This played a significant role in enhancing photophysical properties of these dendrimers. Furthermore, we demonstrated the possibility of replacing the inorganic Sn moieties in the backbone of these dendrimers with Pt-based metallic centers without the addition of any external catalyst that is generally needed in the synthesis of such organometallic dendrimers. It is a versatile methodology that can be applied to other macromolecular systems, to incorporate active transition

metal centers in dendritic macromolecules for a diverse range of applications including catalysis.

In an attempt to streamline the synthesis of dendrimers using an efficient methodology that could eventually lead to multifunctional dendrimers, we designed versatile organic building blocks containing azide and alkyne terminated arms, suitable for inclusion into Cu(I) catalyzed alkyne azide cycloaddition (CuAAC) “click” reactions. The acetylene arms were protected with triisopropylsilyl (TIPS) groups, and were used to construct a small library of dendritic structures containing 4, 6, and 12 acetylene groups at the periphery. The synthesis of these compounds was achieved in quantitative yields with minimal number of purification steps. The versatility of these building blocks can be taken advantage of in scaling up the synthesis to gram scale, and with different types of molecules that contain azide or alkyne terminal units. The acetylene terminated molecules can be used to functionalize them with desired targets including drug molecules, fluorescent dyes, catalysts, solubilising polymers etc.

In order to demonstrate the versatility of our above mentioned building block methodology in the synthesis of dendrimers for pharmacological applications, we constructed a multifunctional dendrimer for targeted drug delivery. Multiple functions were introduced into the same dendritic scaffold by introducing two acetylene arms protected with different groups (trimethylsilyl (TMS), and triisopropylsilyl (TIPS)) into the design of our building blocks. This allows iterative and orthogonal deprotection and functionalization. We used this unit to synthesize a dendrimer that contains a fluorescent dye (BODIPY), and therapeutic drug (α -lipoic acid) at the peripheries, using “click” chemistry with almost quantitative yields and minimal purification steps. The *in vitro* pharmacological studies showed that these dendrimers display no apparent cytotoxic effect in two different types of human cells. The latter is a fascinating discovery since it implies that the dendritic backbone, which is similar to that of the dendritic frameworks constructed with the first building block, is suitable for use in biomedical applications. The bifunctional dendrimers showed

cytoprotective activity in the cells due to the effect of the α -lipoic acid, and the presence of the BODIPY dye allowed us to monitor the internalization process and final localization of this vehicle into the lipid droplets. This is the first study of its kind to demonstrate delivery of therapeutic drugs in a monitored fashion to lipid droplets using dendrimers. This synthesis and design can be used as a general technique to incorporate multiple functionalities including solubilizing agents, targeting molecules, and other therapeutic drugs into the same dendritic structure.

6.2 Suggestions for future work

The lack of cytotoxicity of the dendritic backbone of dendrimers synthesized using CuAAC “click” chemistry has great potential for designing a variety of other multifunctional dendrimers for targeted delivery to tumor tissue or intracellular organelles.

6.2.1 Using the acetylene-terminated dendrimers as unimolecular micelles

The dendritic frameworks described in chapter 4 constitute a platform for designing unimolecular micelles by grafting water-solubilizing linear polymer chains such as poly(ethylene glycol) (PEG). This design will simply require functionalization of one end of the PEG chain with an azide using well-established literature procedure, and then anchoring those chains at the periphery of the frameworks in the same fashion described in this thesis using “click” reactions. These systems would have the capability to encapsulate hydrophobic drug molecules inside their hydrophobic core, while the PEG chains at the periphery provides solubility in aqueous media, for potential applications in drug delivery (**Figure 6.1**). Modifying the size of the PEG chains can also introduce different delivery paths by changing the size of the vehicle, especially for targeting tumor tissues.

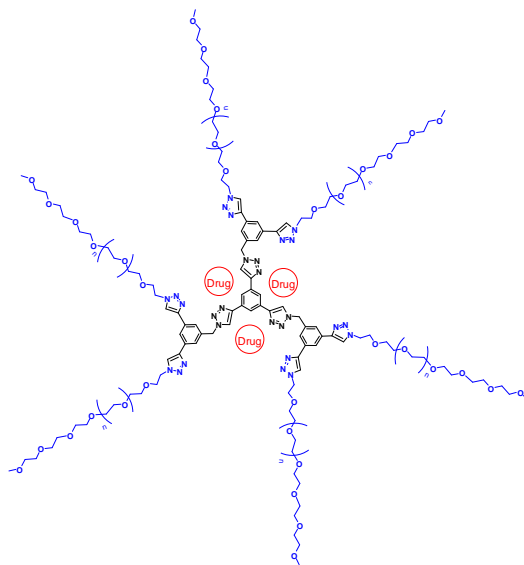


Figure 6.1 Dendritic unimolecular micelles.

6.2.2 Using the acetylene-terminated dendrimers as frameworks for larger multifunctional dendrimers

In a similar fashion as described in chapter 5 of this thesis for the synthesis of bifunctional dendrimer, larger bifunctional systems can be made available. The methodology to achieve this relies on using any of the acetylene terminated frameworks with 4, 6, or 12 arms as a core instead of the TEB smaller unit. This will help introduce higher number of drug molecules into the system for more enhanced therapeutic effects. Moreover, it could change the delivery path and enable targeting of different cytoplasmic organelles.

6.2.3 Incorporating solubilizing agents and other therapeutic molecules

The synthetic methodology used in this thesis can be used to attach different types of therapeutic drugs that are more specific for lipids such as non-steroidal anti-inflammatory drugs (NSAID) for precise localization within the lipid droplets. These therapeutic drugs can be attached in combination with BODIPY or other laser dyes for tracking purposes. On the other hand, solubilizing agents such as PEG chains can also be introduced in combination with hydrophobic therapeutic drugs to provide solubility and to amplify the effect of the drug (**Figure 6.2**).

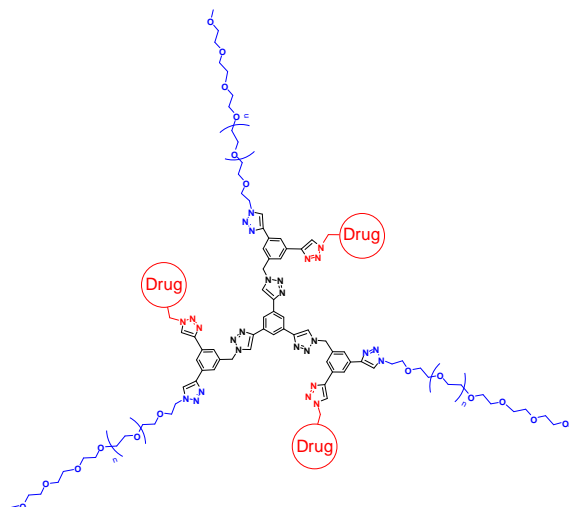


Figure 6.2 Covalent attachment of drugs and solubilizing polymers to the dendrimer.

6.2.4 Incorporating solubilizing agents, therapeutic molecules and Imaging dye

Using the same synthetic methodology in chapter 5, a third functionality can be incorporated by reintroducing the bifunctional building block onto the dendrimer after the attachment of only one functional molecule. This can introduce solubilizing polymers with therapeutic drugs, while allowing imaging at the same time (**Figure 6.3**).

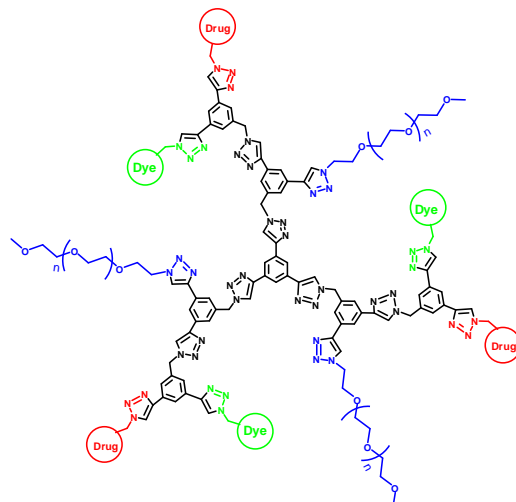


Figure 6.3 covalent attachments of drugs, dyes and solubilizing polymers to the dendrimer.

Appendix I

Theoretical Investigation of 3,5-Dihydroxybenzyl Alcohol Based Dendrimer Generations 1–5 Using Molecular Mechanics (MM+) Method and the PM3 Semi-Empirical Molecular Orbital Theory

This Appendix provides details for the theoretical calculations and results in Chapter 2.

Reproduced in part with permission from:

Hourani R., Kakkar A., and Whitehead M. A., *J. Mol. Struct., (Theochem.)*,
2007, 807, 101.

Copyright, 2009, Elsevier B. V.

Theoretical investigation of 3,5-Dihydroxybenzylalcohol Based Dendrimer Generations 1-5 Using Molecular Mechanics (MM+) Method and the PM3 Semi-Empirical Molecular Orbital Theory.

Rami Hourani, Ashok Kakkar*, and M. A. Whitehead*

Department of Chemistry, McGill University, 801 Sherbrooke Street West, Montreal, Quebec, H3A 2K6, Canada.

Abstract

The structures of 3,5-dihydroxybenzyl alcohol (DHBA) based dendrimer generations 1 to 5 (DG1-5) were optimized using the Molecular Mechanics, MM+ method. The PM3 Semi-Empirical Molecular Orbital Theory was used to optimize the structures of DHBA-based dendrimer generations 1 to 3 (DG1-3). By comparing the results, it was established that the MM+ molecular modelling results for DG1-3 had identical conformations to the PM3 global minimum structures, and therefore were reliable and predictive for DG4 and 5 structures. Single Point PM3 calculations were performed on MM+ optimized DG4 and 5 structures, and the energies and wave functions obtained. The peripheral molecular wave functions of DG1-5 are reactive, and were found to be a degenerate set with the similar eigenvalues. The reactivities of the peripheral orbitals allow the synthesis of larger generations. However, the structures start to close up on each other and the steric hindrance prevents the formation of larger generations than DG5, in agreement with the experiment. The bond lengths, shapes, sizes of the DG1-5 structures and the size of the internal cavities in the 3D structures were obtained.

Keywords: Dendrimers, 3,5-dihydroxybenzyl alcohol (DHBA), Molecular Mechanics, Semi-Empirical Molecular Orbital Theory, Optimization.

Introduction

Dendrimers constitute a fascinating area in nanotechnology. Their distinct structure and properties can be manipulated in various ways to make use of such nanostructures in a variety of applications.¹⁻⁵ Most of the work was devoted to developing synthetic techniques to prepare those interesting macromolecules via a very controlled fashion using organic, inorganic, and/or organometallic routes.⁶⁻¹⁰ However, understanding their actual shape and size, the environment of their cavities, and their intermolecular association, is still required.¹¹⁻¹⁵ Determining the 3-dimensional structure of the dendrimers is an important step in predicting their conformations in the preferred media, and exploring their potential applications in catalysis, drug delivery, photonics etc. Recently, theoretical and molecular modelling investigations of dendrimers have given more details about their chemical and physical properties to allow for their practical applications.¹⁶⁻¹⁸ For example, pharmaceutical applications of dendrimers requires a knowledge of the size of the internal cavities of the dendrimers to allow a guest (drug) molecule to fit in.¹⁹ It is also important to know details about the environment in these cavities, and the orientation of the surrounding branches around them. This constitutes one of the main requirements for designing a suitable drug delivery vehicle.²⁰ At the same time, molecular modelling provides information about the overall size of a dendrimer, its three dimensional orientation in space, and the reactivities of the peripheral chemical groups.¹⁶

We have already published preliminary general theoretical results about the structures of 3,5-dihydroxybenzyl alcohol (DHBA)-based dendrimers.¹⁶ In this paper, we expand our investigation of the structures of DHBA-based dendrimers using the Molecular Mechanics (MM+) method, and the PM3 Semi-Empirical Molecular Orbital Theory.²¹ Determining of the most stable structure, at its lowest energy, provides vital information about the size, shape, and spatial orientations of dendrimers. The Delocalized Molecular Orbitals (DLMOs) in these dendrimers can also be examined, which gives information about their electronic structures and reactivities. These properties are important, because they govern the size of

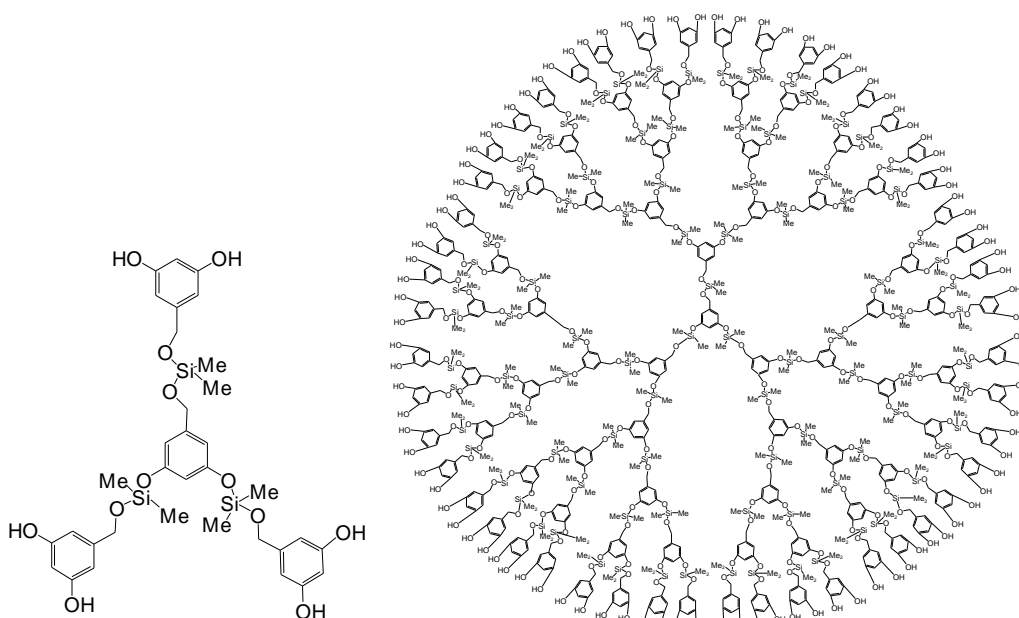
molecules, which can be encapsulated into the internal cavities, as well as the ability of dendrimers to go through different barriers in different media.

Theoretical methods

Because dendrimers are macromolecules which increase size upon addition of each generation, it is necessary to choose a theoretical method capable of geometric characterization of such large structures. Initially, the Molecular Mechanics method with the MM+ force field was used to perform the calculations. The geometry optimization was carried out using the Polak–Ribiere conjugate gradient, set to terminate at an RMS gradient of $0.01 \text{ kcal } \text{Å}^{-1} \text{ mol}^{-1}$. Secondly, the Semi-Empirical Parametrization Model 3 (PM3) Molecular Orbital Method, developed by Stewart,^{22,23} was used with the Gaussian98 program.²⁴ Semi-Empirical optimizations were carried out under standard convergence criteria (max force = 4.5×10^{-4} hartrees bohr⁻¹; RMS force = 3.0×10^{-4} hartrees bohr⁻¹; max displacement = 1.8×10^{-3} Å ; RMS displacement = 1.2×10^{-3} Å). PM3 was chosen because it is a robust, accurate, Semi-Empirical Theory, which always parallels experiment and is consequently predictive.^{25–28} It is a particularly advantageous method to obtain conformational and chemical information about dendrimers.

The molecules were initially drawn in the HyperChem Visualizer program,²⁹ and optimized using molecular mechanics with MM+ force field, followed by the Gaussian98 program²⁴ to optimize the PM3 structures. The conformations of the dendrimers were found by varying all torsional axes to discover the minimum global energy conformation, which was 8–9 kcal more stable than any other conformer. This minimum was established both by using the program in the PM3 Gaussian package, and also established independently using the Tree Branch Method.³⁰ DHBA-based dendrimers (**Figure 1** shows generations 1 and 5) have recently become available in large quantities,³¹ and their synthesis is based on a simple and highly versatile methodology using acid–base hydrolytic chemistry of commercially available reagents: 3,5-dihydroxybenzyl alcohol and $\text{Me}_2\text{Si}(\text{NMe}_2)_2$.

Figure 1: Dendrimer generations 1 and 5 (DG1 and 5) of DHBA-based dendrimers.³¹



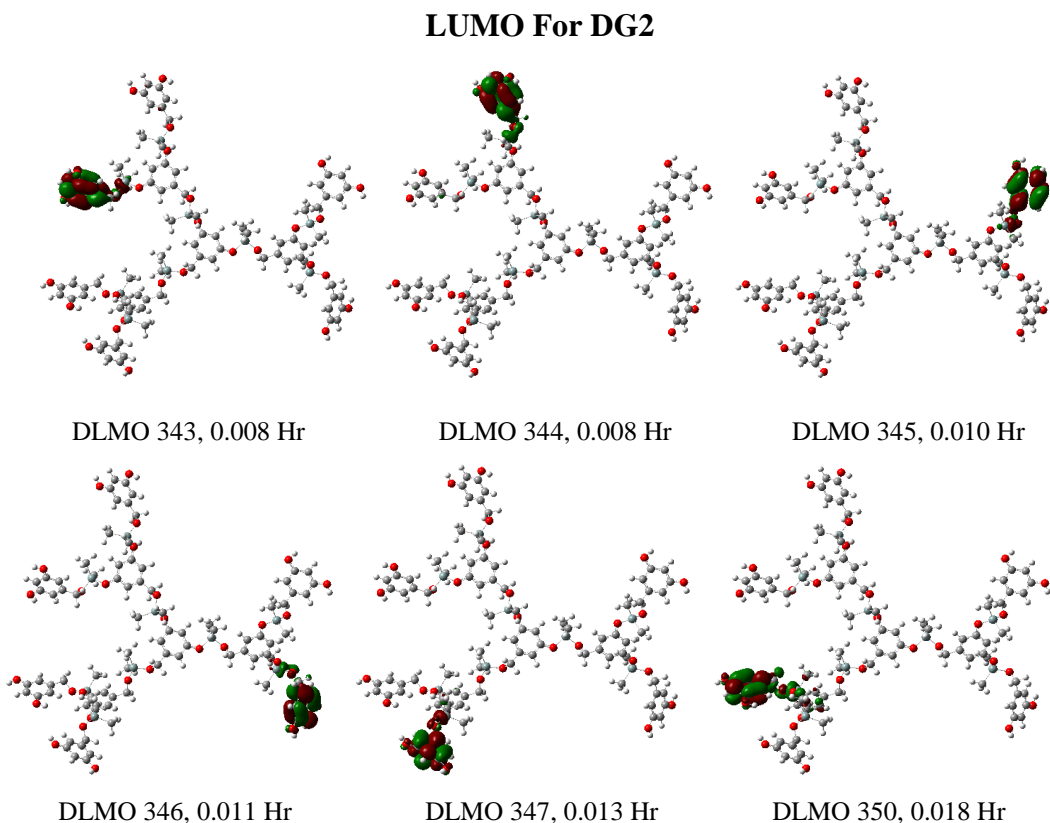
It is important to note that the core molecule of these dendrimers has one branch with an extra CH₂ group as shown in the structure of DG1 of **Figure 1**. This branch will be non-degenerate with the other two branches, which are also not exactly degenerate because of that asymmetry as will be shown later using the Molecular Orbitals of the dendrimers.

For the PM3 calculations, the core molecule, 3,5-dihydroxybenzyl alcohol (DHBA), and the linker bis(dimethylamino)-dimethyl silane (Me₂Si(NMe₂)₂) were geometrically optimized. The optimized core molecule was then linked to three Me₂Si(NMe₂) molecules by forming O–Si bonds to give a branched structure. The energetically most stable branched structure was found by re-optimizing the total system by rotating about the CH₂ group of the core, and then rotating the Me₂Si(NMe₂) around their linkages to the core, followed by the optimization of the whole system. Three additional 3,5-dihydroxybenzyl alcohol molecules were linked to the Me₂Si(NMe₂) branches by forming Si–O bonds at the end of each branch and removing HNMe₂ to give the first dendrimer generation (DG1). In a similar manner, the second and third dendrimer generations (DG2 and DG3) were built and optimized. Initially, the DG(n-1) generation was frozen while DG(n) was optimized.

The system was then re-optimized with the DG(n-1) unfrozen, and the results were unchanged. As the dendrimer generations number increases, it becomes difficult to study them using PM3, since the surface to be searched for various conformations becomes too large.

Dendrimer generations 1–5 were optimized in a similar fashion by the Molecular Mechanics MM+ in the HyperChem visualizer program.²⁹ By comparison of the results, it was established that the MM+ Molecular Modelling results for DG1–3 were almost identical in conformation to the PM3 global minimum structures, and should consequently prove reliable and predictive for the DG4 and 5 conformations. Furthermore, PM3 single point calculations, using the HyperChem visualizer program, on DG4 and 5 gave identical Delocalised Molecular Orbitals (DLMO) on the periphery atoms to those found by PM3 in DG1–3. In order to compare PM3 energies from the same program, PM3 single point calculations, using the Gaussian98 program, were performed on DG4, but it was impossible to be completed for DG5 using ordinary computers, since it required a large memory. The energies are discussed later on in this paper. **Figure 2** shows the lowest unoccupied molecular orbitals (LUMO) for DG2, which are almost identical to those we showed previously for DG1,¹⁶ and to those in DG3-5 in terms of their locations on the periphery and their energies. Therefore, we can safely conclude that these DLMO do not change as the dendrimer generation number increases, but they obviously multiply in number rapidly as the dendrimer grows. This shows that DHBA-based dendrimers would behave in a similar manner, and the reactions that take place at all stages in forming the dendrimers are identical. The DLMOs of DG3-5 are not shown because there are too many of them to be presented in this paper.

Figure 2: The lowest unoccupied molecular orbitals (LUMO) of DG2 along with their numbers and energies.



Because of the asymmetry caused by the presence of an extra CH_2 group in the structure of the core molecule (DHBA), these DLMOs are not degenerate, but very close in energy, well separated, and orthogonal to other Molecular Orbitals.

Since the dendrimers gradually bend to form more spherical shape, the branches get closer to each other and start overlapping. It was impossible to optimize dendrimer generations larger than DG5. This is in agreement with the fact that DG6 could not be synthesized experimentally.³¹

Results and Discussion

Energies and Bond lengths of dendrimer generations 1-5

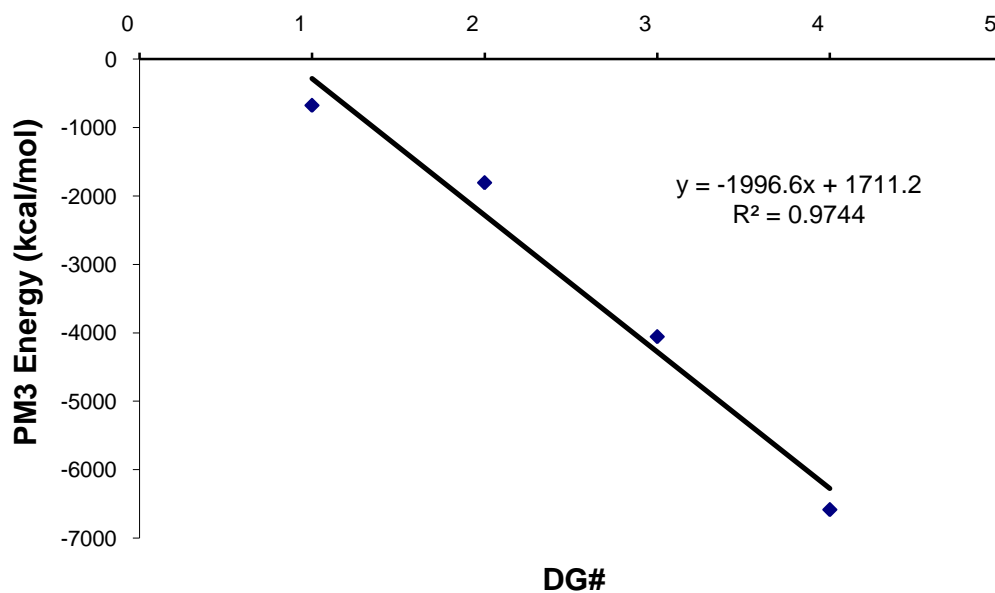
The energies obtained from MM+ and PM3 for the global energy conformations of DG1-5 are summarized in **Table 1**.

Table 1: Optimized conformational energies of DG1-5 using PM3 and MM+ methods: PM3 energies are heats of formation, and MM+ are arbitrary energies in kcal/mol.²⁹

Dendrimer Generation #	Energy (kcal/mol)	
	MM+	PM3
1	0.57	-676.8
2	10.76	-1806.4
3	14.76	-4055.9
4	302.9	-6582.4
5	394.48	-8271.8

The MM+ energies are conformational energies, and they are not related to heats of formation nor to total energies as computed by semi-empirical, PM3, and ab initio methods. They do not have any physical meaning. However, these energies do include the effect of strained bond lengths and angles, and therefore have units of kcal/mol because the force constants used are in these units. Therefore, they can be used to relate different dendrimers, and compare the difference in energy between different conformations of the same dendrimer.²⁹ The conformations from both MM+ and PM3 were identical for DG1-3. Consequently, it was assumed that the MM+ conformation of DG4 and 5 can be used for single point calculations using the PM3 method using the Gaussian98 program, and the energy value for DG5 was obtained from the linear relationship between the PM3 energies and the dendrimer generation number for DG1-4 as shown in **Figure 3**.

Figure 3: The relationship between the dendrimer generation numbers and their corresponding PM3 energies.



The graph shows a fairly linear relationship based on the R^2 value, so it is safe to assume that the extrapolated energy value for DG5 is very close to that of the global minimum.

The bond lengths between the atoms of each structure were also measured and found to be consistent in all the dendrimer generations. The bond length ranges for all structures are summarized in **Table 2**.

Table 2: Summary of bond lengths values in dendrimer generations 1-5.

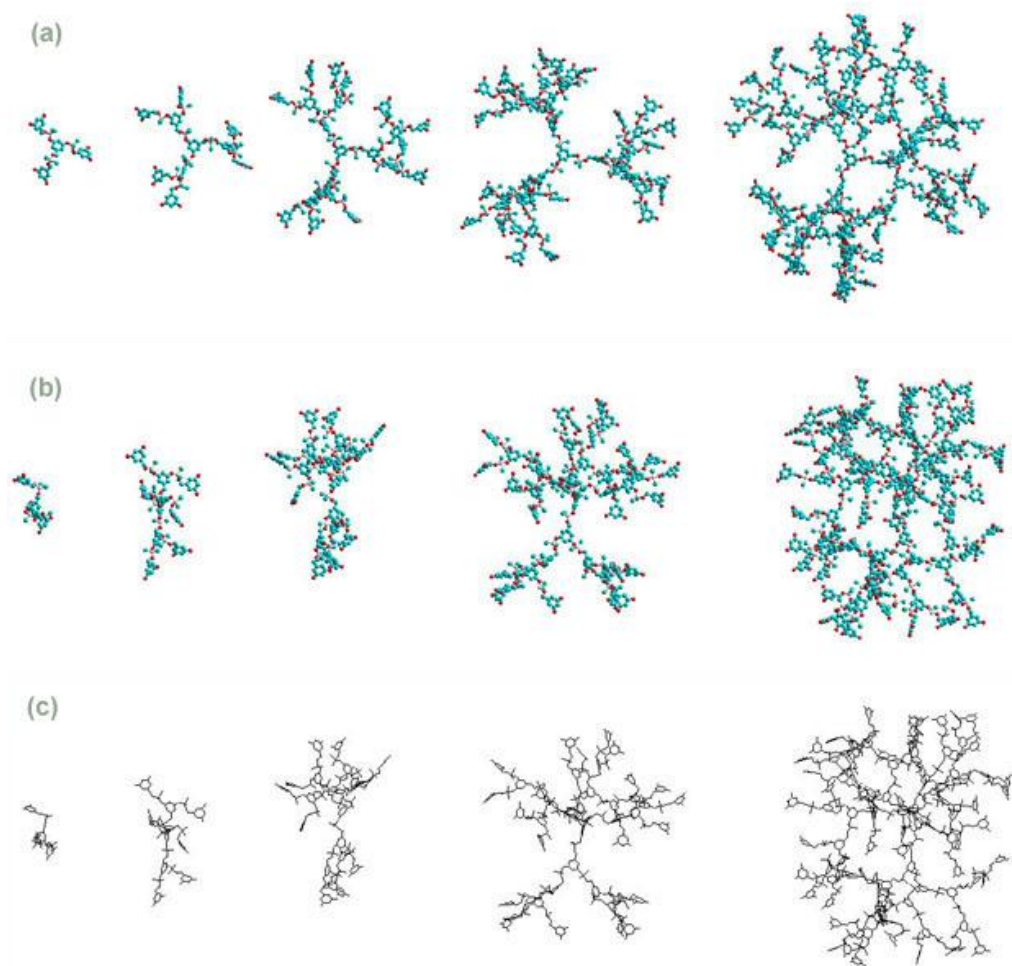
Bond Type	Bond length (Å)
C-C (benzene ring)	1.38-1.41
C-O (phenolic)	1.35-1.36
C-C (benzylic)	1.50-1.51
O-Si	1.70-1.71
C-O (benzylic)	1.38-1.39
O-H (peripheral)	0.95

The interesting aspect of the bond lengths is that while C-C bonds always remain fairly constant if single, the C-O, Si-O, and O-H bonds usually reflect the molecular chemistry changes. Here, all the bond lengths are constant supporting the molecular orbitals results, and showing that the dendrimers are additive and each added unit is orthogonal to the previous dendrimer.

Shapes of dendrimer generations 1-5

The shapes of dendrimer generations 1-5 are shown in **Figure 4**. The structures with the lowest energies were obtained by rotating several bonds in the dendrimers to obtain a more symmetric structure with the least number of unbonded atoms close to each other in MM+. Dendrimer generations 1-3 were then optimized using the PM3 method to give identical structures as from the MM+ method. The structures of dendrimer generations 4 and 5 were obtained from the MM+ calculations. It was assumed that these structures would be very close to those expected when optimized using the PM3 method.

Figure 4: The optimized structures of dendrimer generation 1-5 using the molecular modelling MM+ method shown as (a) sticks and balls of flat dendrimers (b) sticks and balls of side view of dendrimers (c) sticks of side view of dendrimers to show clearly the development of the globular shape as the dendrimer generation increases.



Dendrimer generation 1 (DG1) is an open and planar structure, with the three branches around the core arranged to give the least steric interaction between the branches. The spaces between the branches do not have any particular shape or size, and encapsulation of guest molecules is going to be difficult without the formation of aggregates of the dendrimers. The structure of DG2 is slightly less planar and the branches bend away from the plane but do not give any recognizable internal cavity. Dendrimer generation 3 (DG3) is even more non-planar, but still does not create any recognizable cavities. In contrast, the

optimized structures of DG4 and DG5 both have a three dimensional globular structure, with well-defined internal cavities. The change in the 3D structure between DG1 to DG5 shows a clear progress in forming internal cavities in these dendrimers, with increasing rigidity and more globular structure.

The peripheral hydroxyl groups in DG4 and DG5 become much more dense on the surface than DG1-3, consequently, they can form a larger number of hydrogen bonds. This was demonstrated experimentally because the critical aggregation concentration (*cac*) of DG1-3 was found to be around 3.7mg mL^{-1} , while DG4 and DG5 formed aggregates even at much lower concentrations as low as 0.1mg mL^{-1}

1 31,32

Sizes of the dendrimer generations 1-5 and their internal cavities

The relative diameters of DG1-5 were obtained by measuring the distance between several pairs of peripheral atoms on opposite sides of the dendrimers as shown in **Figure 5** for DG1-3. A summary of the relative diameters of DG1-3 calculated using MM+ and PM3, and those of DG4-5 obtained using MM+ are shown in **Table 3**. The limits in **Table 3** are the minimum and maximum measured distances because the dendrimers are not symmetric.

Figure 5: DG1, DG2, and DG3 structures with their relative sizes (diameters).

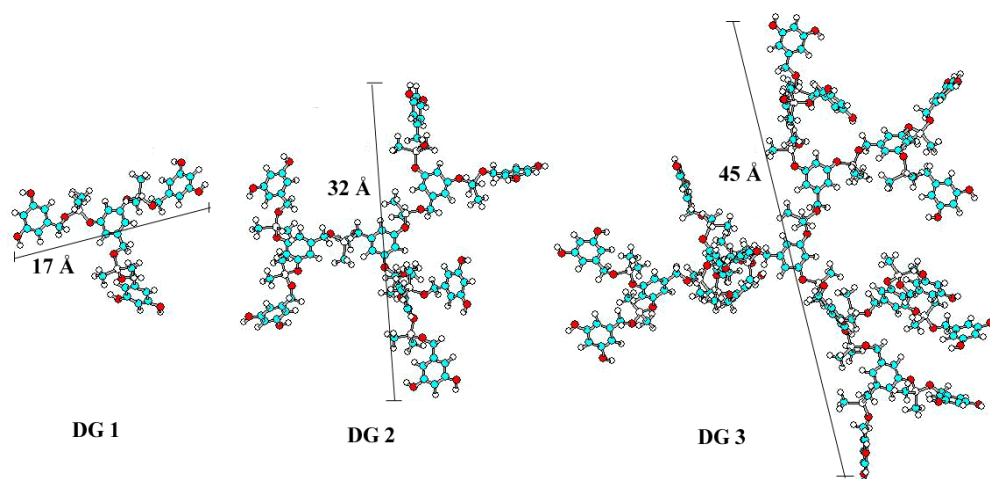


Table 3: Summary of relative sizes of DG1-5 determined by MM+ and PM3 methods.¹⁶

Dendrimer Generation	Diameter (Å)
1	16-19
2	28-35
3	43-47
4	58-67
5	62-75

The maximum, minimum, and average of the diameters of DG1-5 were plotted against the dendrimer generation number previously.¹⁶ The onset of the globular structure was shown by the decrease in the rate of increase of the diameter.

The sizes of the internal cavities of DG4 and 5 were estimated from the MM+ calculations, and found to be in the range of 24-35 Å. The size of a guest molecule can be chosen to match that of the internal cavities in these dendrimers as it has been shown experimentally with disperse red 1 (DR1) dye as a guest molecule.¹⁶ The relative sizes of the guest molecule and the cavity show that.

Conclusions

Theoretical calculations using the Molecular Mechanics (MM+) method and the Semi-Empirical (PM3) Molecular Orbital Theory have been shown very useful to obtain important information about 3,5-dihydroxybenzylalcohol (DHBA) based dendrimers. The optimizations revealed the overall sizes of these dendrimers, which ranged between 16-75 Å for generations 1-5 respectively. The calculations gave information about the development of the three dimensional structure of these dendrimers from generation 1 to 5. Generations 4 and 5 are globular in shape with well-defined internal cavities that can be used as a guest-host system. Beyond DG5, the area for additional bonding is constricted by steric

hindrance, which prevents the making and optimization of larger generations. The dimensions of the internal cavities in DG4 and five are between 24-35 Å, which is a suitable size for various small drugs and catalysts. The theoretical methods used in this paper, and the technique used to optimize such macromolecules using ordinary computers, has given clear information about the shape, size, energy, molecular orbitals, and explained the inability to make higher dendrimer generations after a certain limit. This useful information can be applied to other types of dendrimers and macromolecules.

Acknowledgements

The authors thank NSERC of Canada, FQRNT (Quebec, Canada), the Centre for Self-Assembled Chemical Structures (FQRNT), and Sigma Xi for financial assistance.

References

1. R. van Heerbeek, P.C.J. Kamer, P.W.N.M. van Leeuwen, J.N.H. Reek, *Chem. Rev.*, **2002**, 102, 3717.
2. A. Andronov, J.M.J. Fréchet, *Chem. Commun.*, **2000**, 1701.
3. D. Astruc, F. Chardac, *Chem. Rev.*, **2001**, 101, 2991.
4. F. Vögtle, *Topics Curr. Chem.*, **1998**, 197, 7.
5. Lupton, J.M.; Samuel, I.D.W.; Burn, P.L.; Mukamel, S. *Journal of Chemical Physics* **2002**, 116(2), 455.
6. Vögtle F., Gestermann S., Hesse R., Schwierz H., and Windisch B., *Prog Polym. Sci.* **2000**, 25, 987.
7. Grayson S. M. and Fréchet J. M. J., *Chem. Rev.*, **2001**, 101, 3819.
8. Tomalia D. A., Naylor A., and Goddard W. A., *Angew. Chem. Int. Ed. Engl.*, **1990**, 29, 138.
9. Majoral J.-P., and Caminade A. M., *Chem. Rev.*, **1999**, 99, 845.
10. Fischer M., and Vögtle F., *Angew. Chem. Int. Ed. Engl.*, **1999**, 38, 884.

11. Zhang, X.; Haxton, K.J.; Ropartz, L.; Cole-Hamilton, D.J.; Morris, R.E. *J. Chem. Soc., Dalton Trans.* **2001**, 3261.
12. Herrmann, A.; Weil, T.; Sinigersky, V.; Wiesler, U-M.; Vosch, T.; Hofkens, J.; Schryver, F.C.D.; Mullen, K. *Chem. Eur. J.* **2001**, 7(22), 4844.
13. Govorun, E.N.; Zeldovich, K.B.; Khokhloy, A.R. *Macromol. Theory Simul.* **2003**, 12, 705.
14. Striegel, A.M.; Plattner, R.D.; Willett, J.L. *Anal. Chem.* **1999**, 71, 978.
15. Pricl, S.; Fermeglia, M.; Ferrone, M.; Asquini, A. *Carbon* **2003**, 41, 2269.
16. Hourani R., Kakkar, A.K.; M. A. Whitehead, *J. Mater. Chem*, **2005**, 15, 2106.
17. Evangelista-Lara A., Guadarrama P., *Int. J. Quan. Chem.*, **2005**,103, 460.
18. Likos C. N., Rosenfeldt S., Dingenouts N., Ballauff M., Lindner P., Werner N., and Vögtle F., *J. Chem. Phys.*, **2002**,117(4), 1869.
19. Patri A. K., Majoros I. J., and Baker J. R.,*Current Opinion in Chemical Biology*, **2002**, 6, 466.
20. Liu M., Kono K., Fréchet J. M. J., *J. Controlled Release*, **2000**, 65, 121.
21. Segal, G.A., *Semiempirical Methods of Electronic Structure Calculation, Part A: Techniques*, University of Southern California, Los Angeles, 1997.
22. Stewart, J.J.P., *J. Comp. Chem.* **1989**, 10(2), 209.
23. Stewart, J.J.P., *J. Comp. Chem.* **1989**, 10(2), 221.
24. Gaussian 98W (Revision A.5), M.J. Frisch, G.W. Trucks, H.B. Schlegel, G.E. Scuseria, M.A. Robb, J.R. Cheeseman, V.G. Zakrzewski, J.A. Montgomery, R.E. Stratmann, J.C. Burant, S. Dapprich, J.M. Millam, A.D. Daniels, K.N. Kudin, M.C. Strain, O. Farkas, J. Tomasi, V. Barone, M. Cossi, R. Cammi, B. Mennucci, C. Pomelli, C. Adamo, S. Clifford, J. Ochterski, G.A. Petersson, P.Y. Ayala, Q. Cui, K. Morokuma, D.K. Malick, A.D. Rabuck, K. Raghavachari, J.B. Foresman, J. Cioslowski, J.V. Ortiz, B.B. Stefanov, G. Liu, A. Liashenko, P. Piskorz, I. Komaromi, R. Gomperts, R.L. Martin, D.J. Fox, T. Keith, M.A. Al-Laham, C.Y.

- Peng, A. Nanayakkara, C. Gonzalez, M. Challacombe, P.M.W. Gill, B.G. Johnson, W. Chen, M.W. Wong, J.L. Andres, M. Head-Gordon, E.S. Replogle, J.A. Pople, Gaussian, Inc., Pittsburgh, PA, **1998**.
25. Dickie A., Kakkar A. K. and Whitehead M. A., *Langmuir*, **2002**, 18, 5657.
26. Rakotondradany F., Whitehead M. A., Lebuis A. and Sleiman H. F., *Chem.–Eur. J.*, **2003**, 9, 4771.
27. Charbonneau P., Jean-Claude B. and Whitehead M. A., *J. Mol. Struct. (THEOCHEM)*, **2001**, 574, 85.
28. Malardier-Jugroot C., Spivey A. C. and Whitehead M. A., *J. Mol. Struct. (THEOCHEM)*, **2003**, 623, 263.
29. HyperChem release 5.11. For Windows molecular modeling system, Hypercube Inc., 419 Philip Street, Waterloo, Ont., Canada N2L 3X2, **1999**.
30. Villamagna F. and Whitehead M. A., *J. Chem. Soc., Faraday Trans.*, **1994**, 90, 1, 47.
31. Bourrier, O.; Kakkar, A.K. *J. Mater. Chem.* **2003**, 13, 1306.
32. Bourrier, O.; Butlin, J.; Hourani, R.; Kakkar, A.K. *Inorg. Chim. Acta* **2004**, 357, 3836, special issue in honor of Tobin J. Marks.